Berichte
zur Polar-
und Meeresforschung

597
2009

Reports
on Polar and Marine Research

The Expedition of the Research Vessel "Polarstern" to the Arctic in 2008 (ARK-XXIII/3)

Edited by
Wilfried Jokat
with contributions of the participants

HELMHOLTZ
GEMEINSCHAFT

ALFRED-WEGENER-INSTITUT FÜR
POLAR- UND MEERESFORSCHUNG
In der Helmholtz-Gemeinschaft
D-27570 BREMERHAVEN
Bundesrepublik Deutschland

ISSN 1866-3192

Hinweis

Die Berichte zur Polar- und Meeresforschung werden vom Alfred-Wegener-Institut für Polar-und Meeresforschung in Bremerhaven* in unregelmäßiger Abfolge herausgegeben.

Sie enthalten Beschreibungen und Ergebnisse der vom Institut (AWI) oder mit seiner Unterstützung durchgeführten Forschungsarbeiten in den Polargebieten und in den Meeren.

Es werden veröffentlicht:

— Expeditionsberichte (inkl. Stationslisten und Routenkarten)

— Expeditionsergebnisse (inkl. Dissertationen)

— wissenschaftliche Ergebnisse der Antarktis-Stationen und anderer Forschungs-Stationen des AWI

— Berichte wissenschaftlicher Tagungen

Die Beiträge geben nicht notwendigerweise die Auffassung des Instituts wieder.

Notice

The Reports on Polar and Marine Research are issued by the Alfred Wegener Institute for Polar and Marine Research in Bremerhaven*, Federal Republic of Germany. They appear in irregular intervals.

They contain descriptions and results of investigations in polar regions and in the seas either conducted by the Institute (AWI) or with its support.

The following items are published:

— expedition reports (incl. station lists and route maps)

— expedition results (incl. Ph.D. theses)

— scientific results of the Antarctic stations and of other AWI research stations

— reports on scientific meetings

The papers contained in the Reports do not necessarily reflect the opinion of the Institute.

The „Berichte zur Polar- und Meeresforschung”
continue the former „Berichte zur Polarforschung”

* Anschrift / Address

Alfred-Wegener-Institut
Für Polar- und Meeresforschung
D-27570 Bremerhaven
Germany
www.awi.de

Editor in charge:
Dr. Horst Bornemann

Assistant editor:
Birgit Chiaventone

Die "Berichte zur Polar- und Meeresforschung" (ISSN 1866-3192) werden ab 2008 ausschließlich als Open-Access-Publikation herausgegeben (URL: http://epic.awi.de).

Since 2008 the "Reports on Polar and Marine Research" (ISSN 1866-3192) are only available as web based open-access-publications (URL: http://epic.awi.de)

The Expedition of the Research Vessel "Polarstern" to the Arctic in 2008 (ARK-XXIII/3)

Edited by
Wilfried Jokat
with contributions of the participants

Please cite or link this publication using the identifier hdl:10013/epic.33317 or http://hdl.handle.net/10013/epic.33317

ISSN 1866-3192

ARK-XXIII/3

12 August 2008 - 17 Oktober 2008

Reykjavík - Bremerhaven

Fahrtleiter / Chief Scientist
Wilfried Jokat

Koordinator / Coordinator
Eberhard Fahrbach

CONTENTS

1. ZUSAMMENFASSUNG UND FAHRTVERLAUF

Wilfried Jokat
Alfred-Wegener-Institut, Bremerhaven

Die 23. Arktisexpedition des Forschungsschiffes *Polarstern* begann am 12. August in Rejkjavik (Island) und endete am 17. Oktober 2008 in Bremerhaven. Das Schiff legte auf dieser Expedition 10.800 sm (20.000 km) zurück. An Bord befanden sich 43 Mannschaftsmitglieder und bis zu 47 WissenschaftlerInnen aus Belgien, Deutschland, Frankreich, Japan, Kanada, Korea, Niederlanden, Russland und den USA.

Klares Ziel dieser Expedition war es, belastbare geowissenschafltiche Daten zu erheben, die Informationen über die ältere geologische Geschichte und die jüngere Vereisungsgeschichte des ostsibirischen Schelfs zu erhalten. Im Gegensatz zu anderen Regionen der Arktis beruhen die aktuellen Modellvorstellungen auf nur wenigen verlässlichen geowissenschaftlichen Fakten.

Daher standen u.a. sediment-akustische (Parasound) Profilfahrten und detaillierte Beprobungen und Untersuchungen von Sedimenten vom ostsibirischen Kontinentalrand und über den Mendelejew-Rücken im Vordergrund. Mittels Parasound-Vermessung wurden große Rutschmassen in den oberflächennahen Sedimentpaketen vom ostsibirischen Kontinentalrand entdeckt. Diese lassen sich im Untersuchungsgebiet nur durch großräumige Vereisungen in Ostsibirien erklären, wie sie bisher für die jüngere geologische Geschichte nicht bekannt waren. In Ergänzung hierzu zeigen allerdings seismische Daten, dass das ostsibirische Schelf in den letzten 3 Millionen Jahren nur während weniger Eiszeiten von einem Eisschild bedeckt war. Die Schelfgebiete von Ostgrönland bzw. der Antarktis wurden in diesem Zeitraum wesentlich stärker durch Eisschilde erodiert.

Vom Kanada-Becken über den Mendelejew-Rücken bis ins Makarow-Becken konnten auf einem über 1200 km langen Transekt Sedimentkerne höchster Qualität gezogen werden. Zwischen den geologischen Stationen wurden seismische Mehrkanal-Daten mit einem 300 m langen Streamer und einem 33 ltr. Airgun Array erhoben. Diese Daten haben ebenfalls eine hervorragende Qualität. Sie zeigen den Verlauf des akustischen Basements entlang des gesamten Transektes. Ein Erosionshorizont, der bei der Trennung des Lomonossow-Rückens vom sibirischen Schelf gebildet wurde, lässt sich durch das gesamte Makarow-Becken verfolgen. Damit ist eine relative Datierung des Beckens möglich. Es muss deutlich älter als 60 Millionen Jahre sein. Die seismischen Daten zeigen deutliche Hinweise auf starke Umlagerungsprozesse in den Tiefseesedimenten entlang dieses Erosionshorizontes. In dieser geologischen Phase sind entweder die bodennahen Strömungen sehr stark gewesen oder der Meeresspiegel im Arktischen Ozean war erheblich niedriger als heute. Viele Modellvorstellungen über die Entwicklung des Arktischen Ozeans müssen aufgrund der neuen Daten revidiert werden.

Ozeanographische Programme untersuchten die Verbreitung, Zirkulation und Vermischung der verschiedenen Wassermassen sowie deren Umwandlung durch Einflüsse an der Ozeanoberfläche, wie z.B. Eisbildung. Zur Erfassung von langen Zeitreihen zur Zirkulation von Meereis im Arktischen Ozean wurde nicht nur vom Schiff aus gemessen, sondern es wurden auch mehrere autonome Beobachtungsbojen auf Eisschollen installiert. XCTD-Messungen wurden überwiegend entlang der seismischen Profile durchgeführt, um die Wassermassenverteilung entlang des Kontinentrandes zu bestimmen.

Biologische Untersuchungen hatten zum Ziel das Vorkommen der Ruderfußkrebsart *Oithona similis* im Arktischen Ozean zu bestimmen. Dieser kleine Krebs ist ein wichtiger Bestandteil des Nahrungsnetzes im Arktischen Ozean. Er ernährt sich u.a. von kleineren Algen und Tieren und dient z.B. Fischlarven als Nahrung. Für dieses Projekt wurden an 21 Stationen Proben mit einem Multinetz, welches 5 unabhängig voneinander schließbare Netze besitzt, sowie Wasserproben aus der CTD genommen. Die Auswertung der Proben bezüglich Morphologie und Genetik erfolgt im Alfred-Wegener-Institut in Bremerhaven. Ein weiteres biologisches Programm hatte zum Ziel, die Verteilung von Vögeln, Robben, Walen und Eisbären entlang unserer Route zu erfassen. Eine nahezu kontinuierliche bathymetrische Vermessung des Meeresbodens, ein Pollenprojekt sowie ein Wasserbeprobungsprogramm rundeten unser wissenschaftliches Programm ab.

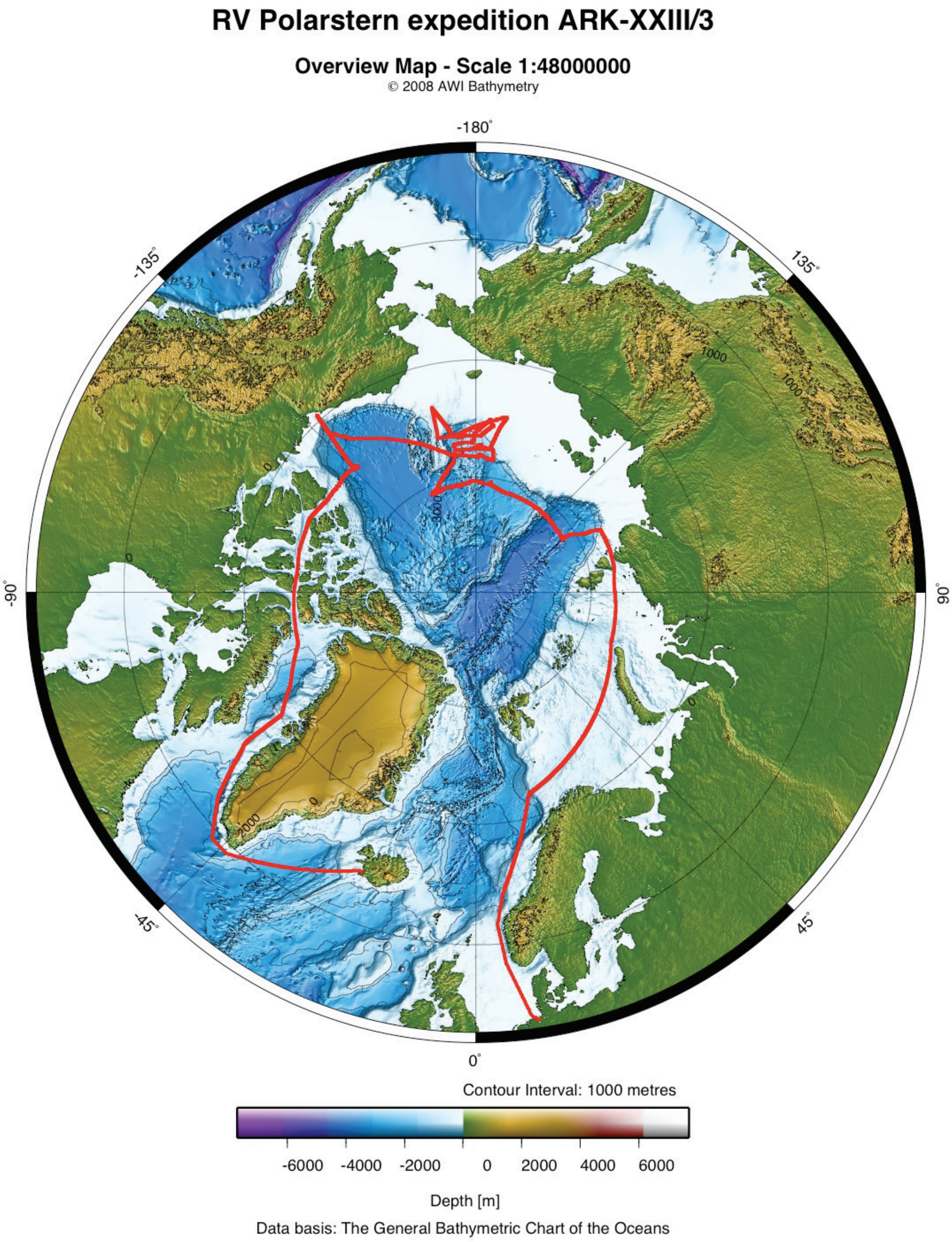

Abb. 1.1: Kurskarte der Polarstern Reise ARK-XXIII/3
Fig. 1.1: Cruise track of Polarstern during the expedition ARK-XXIII/3

ITINERARY AND SUMMARY

The 23rd Arctic expedition of *Polarstern* started on 12 August in Reykjavík (Iceland) and terminated on 17 October 2009 in Bremerhaven. The entire cruise track had a length of 10,800 nm (20,000 km). In total 43 crew members and up to 47 scientists from Belgium, Germany, France, Japan, Canada, Korea, Netherlands, Russia and the USA joined the cruise.

The main objective of this expedition was to gather sound geoscientific data for better characterizing the older geological history as well as the younger glacial history of the East Siberian margin. In contrast to other areas in the Arctic the current knowledge on the above issues are based on an extremely poor data base.

One focus was to gather new sedimentary material by gravity coring across the East Siberian margin and the Mendeleev Ridge. The Parasound echosounder data imaged large debris floes in shallow part of the sedimentary column. The large-scale sediment transport can only be explained by a significant glaciation of the East Siberian shelf, which was so far unknown. In addition, seismic multichannel seismic data show that the East Siberian shelf was not heavily eroded by large ice shields in the last 3 Myr. The seismic signature is quite different compared to the strongly eroded shelves of East Greenland and Antarctica. An almost 1,200 km long transect along 81°N from the Canada Basin to the Amundsen Basin provided a unique opportunity to gain sediment cores from the different basins and the Mendeleev Ridge. In between the geological stations seismic data were acquired with a 300 m long streamer and an 33 litre airgun array. The data have an excellent quality. They imaged the shape of the acoustic basement along the entire transect. An erosional unconformity, which marks the break-up of the Lomonosov Ridge from the Siberian shelves can be traced across the entire Makarov Basin, and allows a relative dating. The Makarov Basin has to be significantly older than 60 Myr. Furthermore, the seismic data show strong evidence for strong erosion/transport of deep sea sediments along this unconformity. Thus, either strong bottom currents were present or the sea level was significantly lower than today in the Arctic Ocean. A number of geodynamic models have to be revised taking the new data into account.

Oceanographic investigations gathered new information on the distribution of the water masses in the Arctic Ocean and their changes due to surface processes, like e.g. sea ice formation. To gain long time series on the oceanographic processes in the Arctic four oceanographic buoy arrays were deployed on ice floes. In addition 23 CTD casts were taken along the Canada/Amundsen Basin transect. During seismic profiling most of the XCTD measurements were taken to map the water mass distribution across the margin. Biological investigations were concentrated to determine the abundance of the cyclopoid copepods *Oithona similes*. In total 21 multinet casts were taken in the different basins and across the Mendeleev Ridge. Continuous observation of birds and marine mammals, pollen and continuous water sampling with the onboard pumping system, and bathymetric mapping supplemented the scientific programme.

2. WEATHER CONDITIONS

Manfred Gebauer, Hartmut Sonnabend
Deutscher Wetterdienst, Hamburg

Polarstern left Reykjavík on 12 August heading southwest, while there was a weak low in the area between Iceland and the south-eastern part of Greenland. In the beginning the weather was smooth and the wind blew with 3 to 4 Bft from south to southeast. Finally, near Kap Farvel, the wind got stronger with 6 to 7 Bft, when the ship surrounded Kap Farvel und was sailing north-westward entering the Labrador Sea. A new low was getting closer from Labrador and the wind direction changed from southerly to north-easterly and northerly directions, blowing with 3 to 5 Bft.

The ship crossed the northern parts of the Labrador Sea, finally Davis Strait and Baffin Bay. When the ship entered the Northwest Passage on 20 August, the wind force increased to 6 to 7 Bft, blowing from astern. Prevailing weather conditions were grey and low clouds with occasional drizzle, temperatures hardly above 0 °C.

The ship proceeded on its way to the end of the Northwest Passage. From now on it was sometimes foggy and mostly cold with temperatures below -2 °C. Entering the main area of research north of the Bering Strait near 80° N, the weather was dominated by an extensive high between 80° N and the North Pole, and also sometimes by small low pressure systems moving from the East Siberian Sea north-eastwards. Very often it was foggy, sometimes with freezing drizzle, sometimes there was snowfall with temperatures a little bit below 0 °C (Fig. 5). Mostly the wind was not very strong. Finally, the high-pressure system approached the East Siberian coast, but the weather conditions did not change significantly. During this cruise the weather conditions included fog or low clouds with intermediate freezing drizzle or snowfall for more than 60 % of the research time (Figs. 1, 2).

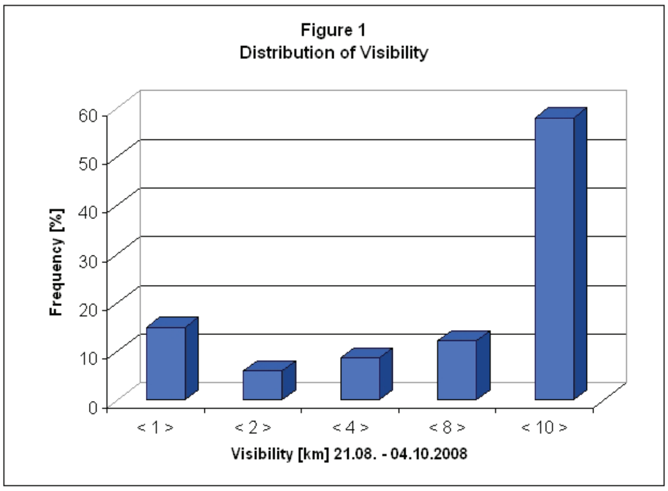

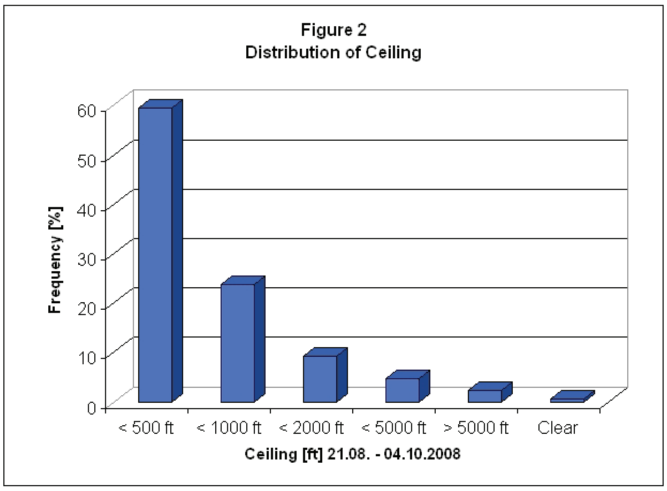

During the last days of September, the temperatures decreased to -5 to -15 °C, when very cold air moved to the ship from the east, induced by a high over the Beaufort Sea. The influence of these low temperatures lasted until the end of the research work on 6 October (Fig. 5).

The high dominated the weather in the Beaufort Sea and later near the North Pole for a long time. Although some low-pressure systems were passing, the temperatures increased only for a short time to -5 to -2 °C. The wind blew mostly from south-easterly directions with wind force 2 to 5 Bft (Fig. 3, 4), sometimes turning out the outdoor scientific work rather unpleasant.

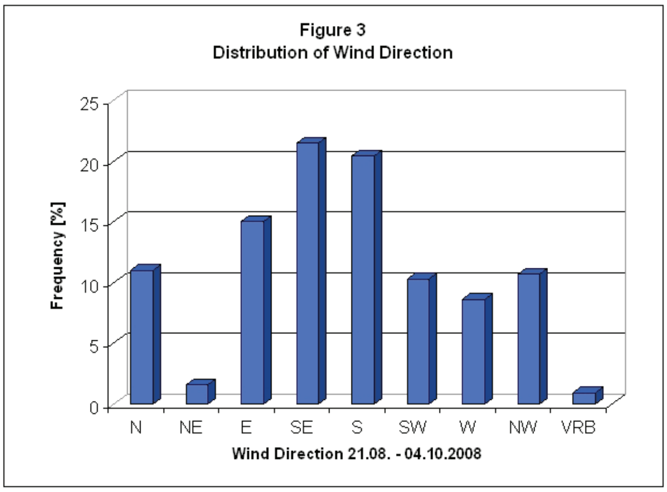

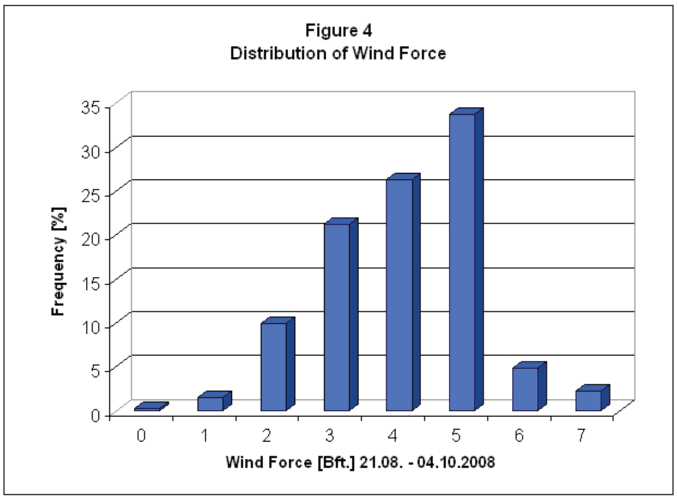

Finally the ship made headway westwards, and between the high over the area near Canada and a low near Severnaya Zemlya, the wind force improved to 6 Bft for a few days.

In the beginning of October the research work was finished, and the ship began its journey home. On the way through the Northeast Passage, the Kara Sea and the Barents Sea the weather was mostly rather calm.

However, when the ship reached the last scientific station at the Haakon Mosby Mud Volcano, weather conditions began to change. Intensive lows arrived on the way from the Irminger See and Iceland north-eastwards. From now on during the way home along the Norwegian coast and across the North Sea, several stormy lows had to come through.

The ship arrived in Bremerhaven on 17 October.

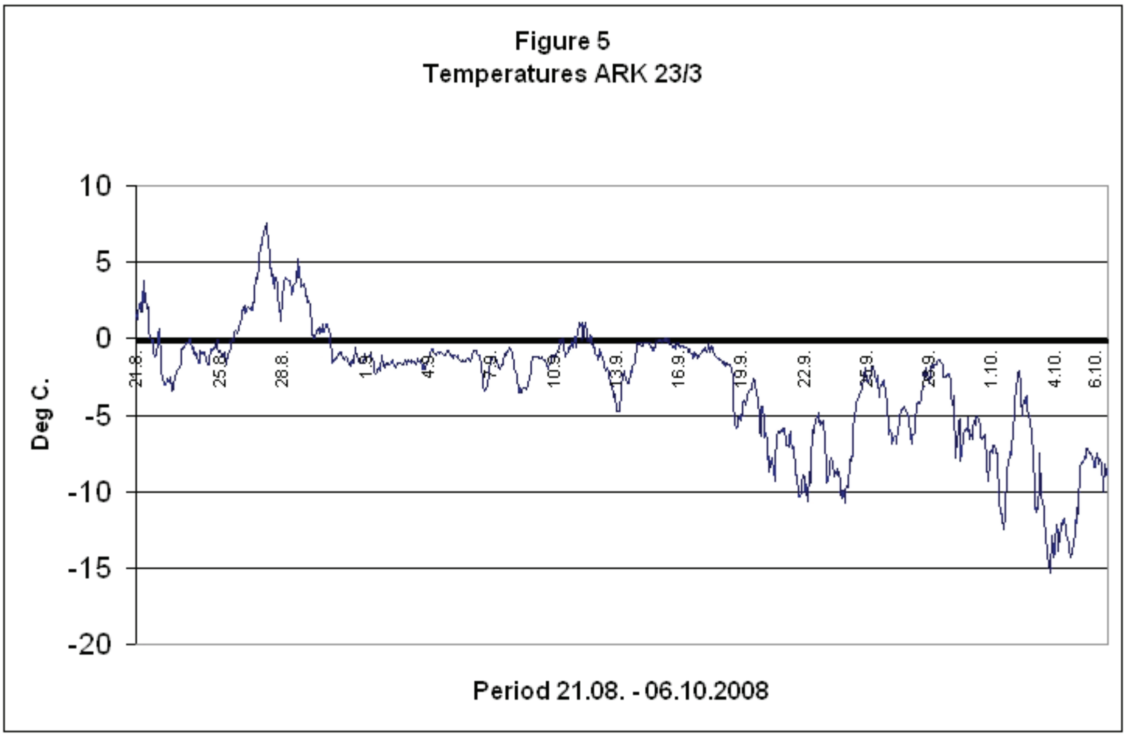

Figure 5
Temperatures ARK 23/3

3. MARINE GEOLOGY

3.1 Introduction and background

Rüdiger Stein, Jens Matthiessen, Frank Niessen
Alfred-Wegener-Institut, Bremerhaven

The overall goals of the marine-geological research programme included (1) high-resolution studies of changes in paleoclimate, paleoceanic circulation, paleoproductivity, and sea-ice distribution in the central Arctic Ocean and at the adjacent continental margin during Late Quaternary times, and (2) the long-term history of the Mesozoic and Cenozoic Arctic Ocean and its environmental evolution from a warm to an ice-covered polar ocean. In areas such as the Alpha-Mendeleev Ridge, pre-Quaternary sediments are cropping out, which could even be cored with coring gears aboard *Polarstern,* and which would allow to study the Mesozoic/Tertiary history of the (pre-glacial) Arctic Ocean. Unfortunately, areas where pre-Quaternary sediments are cropping out could not be identified. Thus, our studies will concentrate on theme (1) of our original research programme.

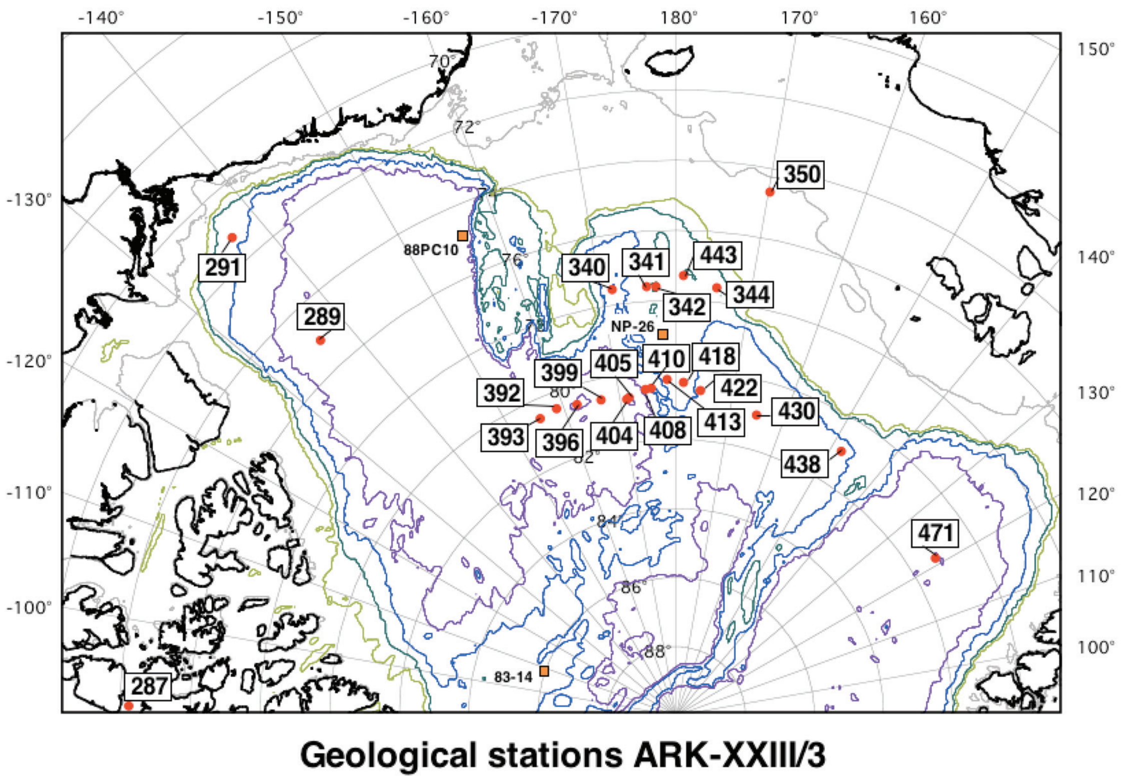

Fig. 6: Map showing the location of geological stations carried out during expedition ARK-XXIII/3. In addition, locations of cores 88PC10, NP-26, and CESAR 83-14 are shown.

During expedition ARK-XXIII/3 we focussed our station work on two main transects (Fig. 6): Transect 1 (along about 77°40'N) from the Chukchi Abyssal Plain across the southern Mendeleev Ridge towards the East Siberian Continental Margin, and Transect 2 (along about 80°30'N) from the Canada Basin across the central Mendeleev Ridge towards the Makarov Basin. In addition, geological station work was done at single stations in Barrow Strait, in the Canada Basin off McClure Strait, on the Mackenzie slope, in the Makarov Basin, on the eastern slope of southern Lomonosov Ridge, and in a central rift valley of Gakkel Ridge (Fig. 6). Coring was carried out using the Kastenlot (KAL), gravity corer (SL), giant box corer (GKG), and multicorer (MUC) (see Chapter 3.4 for details). Coring positions were collected carefully using detailed Hydrosweep bathymetric mapping and sub-bottom Parasound profiling systems (see Chapter 3.2 for details) to avoid areas of sediment re-deposition (turbidites and slumps) and erosion. Shipboard analyses performed on the sediment cores are described in Chapter 3.4. Preliminary results of these shipboard analyses are presented in the following chapters.

Later shore-based studies of the ARK-XXIII/3 sediments will concentrate on several major objectives:

Stratigraphic analyses of the sediment sequences

As basis for all further reconstructions of paleoenvironmental changes, a stratigraphic framework as precise as possible will be established. Starting with the lithostratigraphy and core logging records already obtained onboard *Polarstern*, this work will continue by shore-based studies including magnetostratigraphy, oxygen and carbon stable isotopes, absolute age dating, biostratigraphy, natural radionuclides (^{10}Be, ^{234}Th), magnetic susceptibility, cyclostratigraphy (manganese cycles, physical properties, XRF scanning), and correlation to other existing (dated) Arctic Ocean records.

Terrigenous sediment supply

The terrigenous sediment supply into the Arctic Ocean is controlled by river discharge, oceanic currents, sea-ice (and iceberg) transport, down-slope transport, and eolian input. Most of these mechanisms also influence biological processes in the water column as well as at the sea floor (i.e., surface-water productivity, particle fluxes through the water column, benthic activities at the sea floor, organic carbon export and burial, etc.).

The research will concentrate on the quantification, characterization and variability of terrigenous sediment supply to the Alpha-Mendeleev Ridge and adjacent continental margin areas. This study will allow estimates of chemical and sedimentary budgets, identifications of main source areas and major transport processes, and reconstructions of oceanic currents. Of major interest is a detailed sedimentological, geochemical, petrographical, mineralogical, and micropaleontological study of surface sediments and sediment cores. Methods should include determinations of grain size, petrography of coarse fraction, clay minerals, heavy minerals, major, minor, trace and rare earth elements, organic carbon fractions, and physical properties. Mapping of sediment echotypes from Parasound profiles will allow an extrapolation of point information from core data into spatial facies pattern.

Analytical techniques to be used include X-ray diffraction (XRD), X-ray fluorescence (XRF), inductivity-coupled plasma mass spectrometry (ICP-MS), and microscopy of coarse fraction. Furthermore, MSCL-logging and XRF-scanning records will be determined.

Geochemical and micropaleontological tracers: Organic-carbon flux and water-mass characteristics

One of the major goals is to quantify the flux of organic carbon and to characterize the mechanisms controlling organic carbon deposition and their changes through Quaternary times. Here, the oxygenation of water masses, surface-water productivity, surface-water temperature, sea-ice cover, and terrigenous input are of special interest. Analytical techniques to be used include LECO ($CaCO_3$, TOC, C/N), Rock-Eval pyrolysis, gas chromatography (GC), gas chromatography/mass spectrometry (GC/MS), and high-performance liquid chromatography/mass spectrometry (HPLC/MS), XRF, ICP-MS, and microscopy as well as XRF scanning.

Of major interest are:

- to determine the amount, composition, and maturity of the organic carbon fraction, i.e., (sub-) recent marine and terrigenous organic carbon, reworked fossil material (coals), using organic-geochemical bulk parameters (TOC, C/N, HI values), biomarkers (e.g., n-alkanes, sterols, GDGTs, BIT index), maceral assemblages, and stable carbon isotopes of organic matter;
- to quantify the flux of marine and terrigenous organic carbon (accumulation rates), its change through space and time and its relationship to changes in sea-ice distribution and paleoclimate;
- to estimate the (paleo-) productivity from various productivity proxies: marine organic-carbon flux, biomarker composition (e.g., n-alkanes, sterols, fatty acids, alkenones, etc.); stable carbon and nitrogen isotopes of organic matter; barium; biogenic opal; diatom and dinoflagellate assemblages;
- to reconstruct sea-surface temperature and sea-ice cover from biomarker composition (alkenones, TEX 86; HBIs, IP25);
- to reconstruct water-mass oxygenation using organic carbon/sulfur and organic carbon/iron/sulfur relationships, redox-sensitive trace elements (e.g., Mo, V, U. Ag, Cd, Zn, Re), and specific biomarkers (isorenieratane);
- to compare the records from the East Siberian continental margin and the Mendeleev Ridge with similar data sets from the eastern central Arctic and Eurasian continental margin areas.

Foraminifers and stable isotopes
The distribution and variability of planktonic and benthic foraminifers and their stable isotope signal will be determined to reconstruct changes in paleo-environment such as water mass properties, surface-water productivity etc. through time.

Palynological proxies
The temporal distribution of organic-walled microfossils (dinoflagellate cysts, acritarchs, freshwater algae) will be used to establish a biostratigraphic framework of Neogene to Mesozoic sediments and to provide information on sea-surface conditions through time.

Pore-water (geo-) chemistry
Pore waters of marine sediments give valuable information about biogeochemical processes related to the early diagenetic degradation of organic matter. As these processes can potentially alter the geochemical and geophysical characteristics of a sediment, and can have an impact on preservation of certain microfossils as well, their study is of broad interest. In particular, for detailed investigation of the Quaternary manganese cycles known to occur in Arctic sediments, it is necessary to decipher the redox zonation of the upper sediment column through combined solid phase and pore water analyses. For this purpose, a pore water programme was conducted onboard *Polarstern* (in addition to later shore-based inorganic-geochemical sediment analyses) (see Chapter 3.7 for details).

3.2. Marine sediment echosounding using Parasound

Frank Niessen, Jens Matthiessen
Alfred-Wegener-Institut, Bremerhaven

Scientific Objectives

Bottom and sub-bottom reflection patterns obtained by Parasound characterize the uppermost sediments of the Arctic Ocean in terms of their acoustic behaviour down to about 100 m below the sea floor. This can be used to study depositional environments of unknown areas on larger scales in terms of space and time, of which the uppermost sediments may also be sampled. The objectives of sediment echosounding during ARK-XXIII/3 were:

- to provide the data base for an acoustic facies interpretation indicative for different sedimentary environments,
- to obtain different pattern of high-resolution acoustic stratigraphy useful for lateral correlation over shorter and longer distances thereby aiding correlation of sediment cores retrieved during the cruise,
- to select coring stations based on acoustic pattern and backscatter, and
- to provide a high-resolution supplement for the uppermost sections of seismic profiles recorded during the cruise.

Technical aspects and modes of operation

The Deep Sea Sediment Echo Sounder Parasound (ATLAS HYDROGRAPHIC, Bremen, Germany) was upgraded from DS II to DS III-P70 during the shipyard stay of *Polarstern* in Bremerhaven in May 2007. This upgrade included a complete installation of new hardware and software, and replaced the original system installed on *Polarstern* in 1989 (e.g. Spiess 1992). Between June 2007 and May 2008, three sea-trial phases including final software updating and testing at sea, as well as one expedition using the new system in preliminary mode were carried out before this cruise (Klages & Thiede in prep., Schauer 2008, Schiel 2009, Macke 2009). During ARK-XXIII/3 all new functions of the new system were available, and operation was tested under full Arctic expedition conditions.

An overview about the basic system set up of “Parasound DS III-P70” is given by Niessen et al. (in Klages & Thiede in prep.). A brief description of additional options offered by DS III-P70 including data examples is given by Niessen et al. (in Schiel 2009). The results of the final sea trial are described by Niessen et al. (in Macke 2009).

The hull-mounted Parasound system generates two primary frequencies selectable between 18 and 23.5 kHz transmitting in a narrow beam of 4° at high power. As a result of the non-linear acoustic behaviour of water, the so-called “Parametric Effect”, two secondary harmonic frequencies are generated of which one is the difference (e.g. 4 kHz) and the other the sum (e.g. 40 kHz) of the two primary frequencies, respectively. As a result of the longer wavelength, the difference parametric frequency allows sub-bottom penetration up to 200 m (depending on sediment conditions) with a vertical resolution of ca. 30 cm. The primary advantage of parametric echosounders is based on the fact that the sediment-penetrating pulse is generated within the narrow beam of the primary frequencies, thereby providing a very high lateral resolution compared to conventional 4 kHz-systems.

Parasound DS III-P70 is controlled by two different operator software packages plus server software running in the background. These processes are running simultaneously on a PC under Windows XP. (i) ATLAS HYDROMAP CONTROL is used to run the system by an operator. The selected modes of operation, sounding options and ranges used during the cruise are summarized in Tab. 1. A list of abbreviations is given at the end of this chapter. (ii) ATLAS PARASTORE-3 is used by the operator for on-line visualization (processing) of received data on PC screen, for data storage and printing. It can also be used for replaying of recorded data, post-processing and further data storage in different output formats (PS3 and/or SEG-Y). For any further details the reader is referred to the operator manuals of Atlas Hydromap Control and Atlas Parastore, and some basic descriptions given by Niessen et al. (in Schiel 2009).

Tab. 1: Settings of ATLAS HYDROMAP CONTROL for operating Parasound during cruise ARK-XXIII/3

Used Settings	Selected Options	Selected Ranges
Mode of Operation	P-SBP/SBES	PHF, (SHF), SLF
Frequency	PHF	18.75 kHz
	SHF	(41.66 kHz)
	SLF	4.166 kHz
Pulselength	No. of Periods	2
	Length	0.5 ms
Transmission Source Level	Transmission Power	100%
	Transmission Voltage	159 V
Beam Steering	none	
Mode of Transmisson	Single Pulse	
	Quasi-Equidistant	Interval 400-1200 ms
	Pulse Train	for testing only
Pulse Type	Continuous Wave	
Pulse Shape	Rectangular	
Receiver Band Width	Output Sample Rate (OSR)	6.1 kHz
	Band Width (% of OSR)	66%
Reception Shading	none	
System Depth Source	Fix Min/Max Depth Limit	Manual
		Other (DWS)
		Atlas Parastore
Water Velocity	C-Mean	Manual 1500 m/s
	C-Keel	System C-keel
Data Recording	PHF	Full Profile
	SLF	Full Profile

From the operational point of view, the hardware installed on *Polarstern* was only slightly modified from the previous DS2 system (Niessen et al. in Stein 2005) and now consists of the following units:

1. User interface in form of an Operator PC containing the control software ATLAS HYDROMAP SERVER, ATLAS HYDROMAP CONTROL, and the data acquisition software ATLAS PARASTORE-3.
2. Two colour printers HP Deskjet 5652 for printing of echograms and online status (navigation, depth and Parasound settings).
3. Data Storage PC for data management, recording and data replay in off-line mode.
4. Spare PC of the Operator PC as hardware backup but fully installed in the winch control room in order to provide track plot and single trace information for station work.
5. Flat-Screen Monitor for duplication of echogram information of the Operator PC on the bridge.

With installation of Parasound DS III-P70 the PCs were upgraded with new motherboards and hard discs. The DESO-25 printer as a slave is no longer available.

Data acquisition and management

During ARK-XXIII/3 digital data acquisition and storage were switched on in the Irminger Basin on 13 August at 15:27 UTC, and was switched off after the last station at the Gakkel Ridge on 3 October at 11:04 UTC. Acquisition included PHF and SLF data during the entire cruise, and SHF data at the beginning of the cruise for test purposes only. Both PHF and SLF traces were visualized as online profiles on screen. SLF profiles (100 m or 200 m depth windows) and online status (120 s intervals) were printed on A4 pages.

For the entire period above and simultaneously with sounding five different types of data files were stored on hard disc:

- PHF data in ASD format
- SLF data in ASD format
- SLF data in PS3 format
- Navigation data and general Parasound settings (60s intervals) in ASCII format
- Auxiliary data about ATLAS PARASTORE 3 settings in ASCII format

In total 20 system crashes were observed during the cruise. 15 crashes affected ATLAS PARASTORE-3 only. The first and third crash were caused by a failure of ATLAS HYDROMAP CONTROL and ATLAS HYDROMAP SERVER, respectively. In only one case a failure in the transceiver cabinets caused a complete shut down and restart of the entire system. All crashes caused some loss of data, which lasted from about 30 minutes, in case of a full restart, to only a few minutes for crashes caused by ATLAS PARASTORE-3. A more detailed description about the observed problems is provided by the authors to Laeisz Shipping Company, and may be available on request.

All ASD data are automatically packed into “cabinet files” by Atlas software. The files are named according to date and time of recording (containing about five minutes of acquired data per file). The data have been sorted by the operator into folders according to data type and recording dates (0 to 24 hours UTC), copied to the storage PC via LAN and checked for completeness and readability (ATLAS PARASTORE-3 in replay mode, selectively only). Once checked, the data folders were copied to the *Polarstern* mass storage for daily back ups and final transfer into the AWI database after the end of cruise. In total 208 folders of data with a total volume of 385.1 GB were transferred.

During the entire period of acquisition the system was operator controlled (watch keeping). Book keeping was carried out including basic Parasound system settings, some navigation information, various kinds of remarks as well as a low-resolution hand-drawn bathymetry plot with preliminary data interpretation of SLF online profiles, which provides an overview about echo types and specific findings during the cruise.

Time windows with data of specific interest (e.g. geological situations at or near stations, special observations, key examples for different types of facies or stratigraphy) were selected and replayed during the cruise using optimal settings of ATLAS PARASTORE-3.

Examples of recorded data along the cruise track near geological stations

In the area of the Northwest Passage, between Lancaster Sound and M'Clure Strait, Parasound shows the typical thin sediment cover of a terrain formerly covered by thick ice during the LGM. Typically, up to four units can be identified in sub-bottom profiles: an acoustically transparent Holocene cover (i, not present in the entire area) is overlying a few meters of well stratified sediments (ii), which is found on top of glacial till (iii). In places, sedimentary bedrock was acoustically penetrated as lowermost unit (iv). In the Barrow Strait, based on information from a previous Canadian cruise, a coring station (PS72/287) was selected according to Parasound (Fig. 7) in order to penetrate through the Holocene into the lower well-stratified unit, which has not been previously sampled.

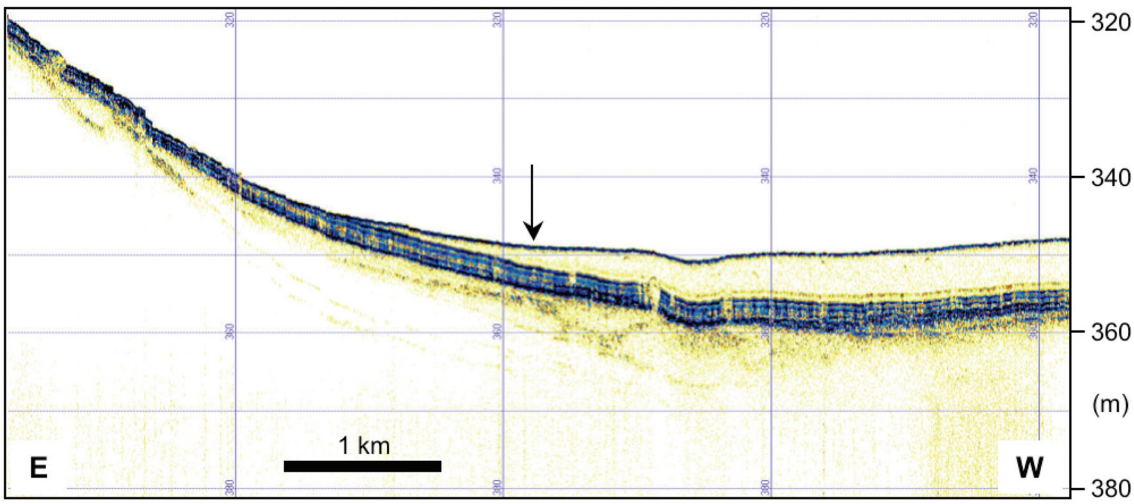

Fig. 7: Parasound example from the Barrow Strait (Northwest Passage). Position of coring location PS72/287 is marked with an arrow.

In the Chukchi Abyssal Plain (Fig. 8) a typical pelagic type of strata was sampled using a Kastenlot (PS72/340). Parasound exhibits well-stratified sediments draping sub-bottom topography with constant (or nearly constant) thickness. There is a two-fold increase in acoustic backscatter towards the top. A distinctly strong reflector is visible between 8 and 10 mbsf.

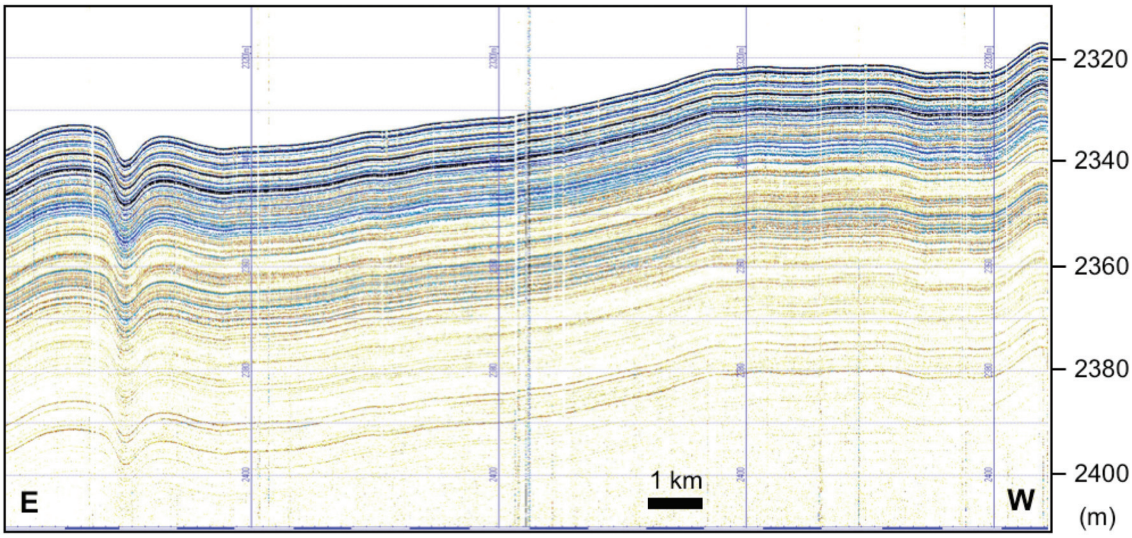

Fig. 8: Parasound example from the Chukchi Abyssal Plain. Coring location PS72/340 is on left end of the profile. Data processing: negative flank suppressed

On the Arlis Plateau, near coring station PS72/343, pelagic type of sediments are intercalated with two relatively thick isolated debris flows. The latter are of transparent acoustic character and show clear indication of erosion at the base. Like in Fig. 9, backscatter increase in the top 20 m of pelagic sediments. However, between the Chukchi Abyssal Plain and the Arlis Plateau, a direct correlation of the strata based on Parasound reflectors is not yet possible at the present level of investigation.

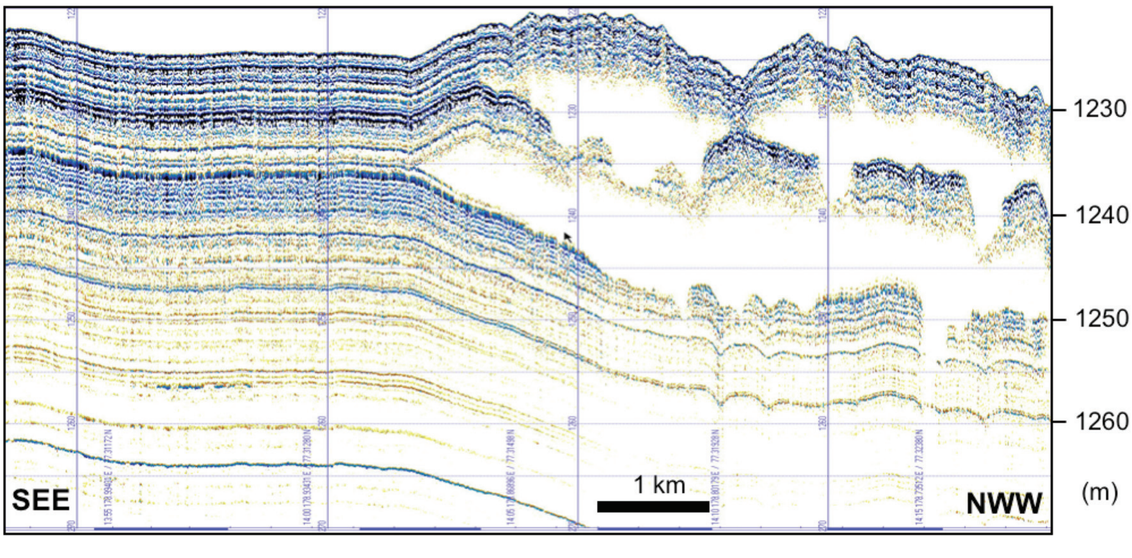

Fig. 9: Parasound example from the Arlis Plateau. Coring location PS72/343 is on left end of the profile. Data processing: negative flank suppressed

For coring station PS72/392, at the eastern edge of the Mendeleev Abyssal Plain, a short Parasound Profile is presented only because most of the data recorded in the area are noisy as an effect of heavy ice conditions during cruising. Nevertheless, the example given in Fig. 10 is representative for a larger area of undisturbed pelagic sedimentation. Once again, backscatter increase is observed in the top 20 m of the sediment column. Typical for the area is the topmost unit of about 3 m in thickness of which the reflection amplitudes are extremely strong.

At the most distal end of the Canada Abyssal Plain, near coring station PS27/393, the well-stratified sequence abruptly pinches out towards the steep wall of a seamount (Fig. 10, right panel). The geometry is typical for distal turbidites, of which the density currents were likely originated at the Arctic continental slope of the North American Continent.

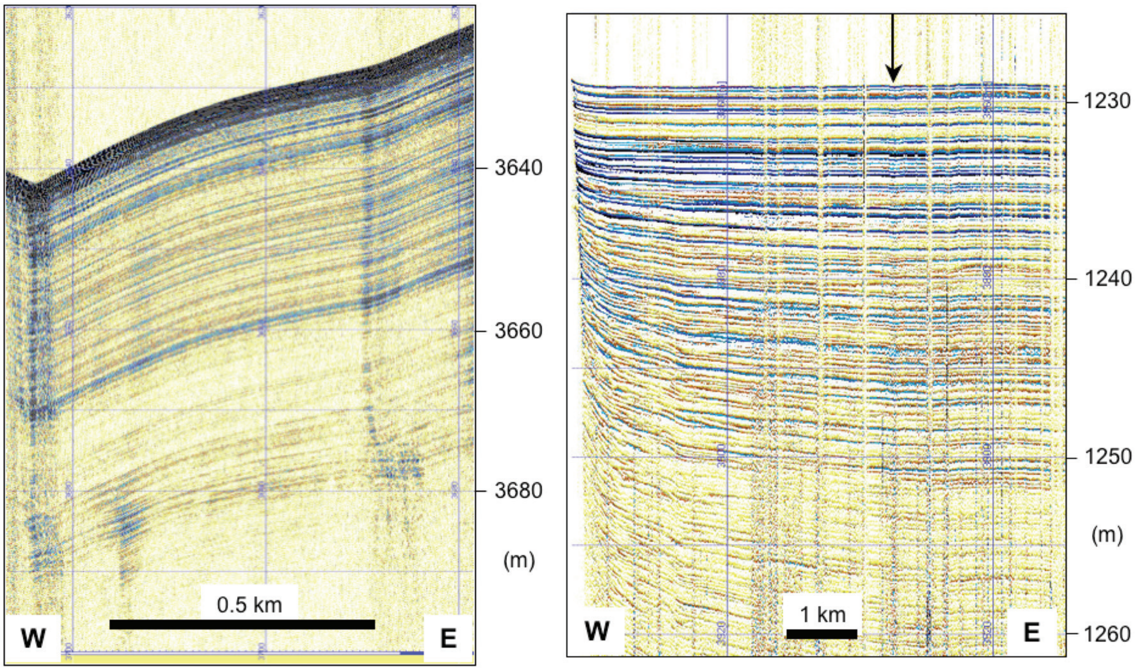

Fig. 10: Left: Parasound example from the eastern end of the Mendeleev Abyssal Plain as drifting on coring location PS72/329. Right: Parasound example from the Canada Abyssal Plain. Coring position PS72/393 is marked with an arrow. Data processing: negative flank suppressed, two traces stacked to one.

A typical sequence from top of the Mendeleev Ridge (Fig. 11) exhibits the acoustic geometry of a drape suggesting pelagic sedimentation. The increase of backscatter towards the top is slightly more complex than at the other locations presented above. It is clearly visible that the resolution of distinct reflectors is lost in the top 10 m of the sequence. Also, the strong backscatter becomes more diffuse, although the thickness of this unit remains constant regardless of sub-bottom topography. This acoustic character is more abundant in the shallower parts of Mendeleev Ridge whereas in the deeper parts reflectors are visible in the top 10 m of the profiles. The example exhibits the geological situation at station PS72/410.

The Parasound example from the Makarov Abyssal Plain (Fig. 11) near station PS72/430 exhibits well-stratified sediments characterized by a more or less regular pattern of sub-parallel reflectors. Because the area is largely flat it is hard to interpret different proportions of pelagic types of sediments and turbidites, which may also be present at the location. A weak increase of backscatter in the top 20 m of the sediment column is somewhat similar to the situation observed in the Chukchi Abyssal Plain. Once again, a direct correlation of reflectors is not possible at the present level of investigation.

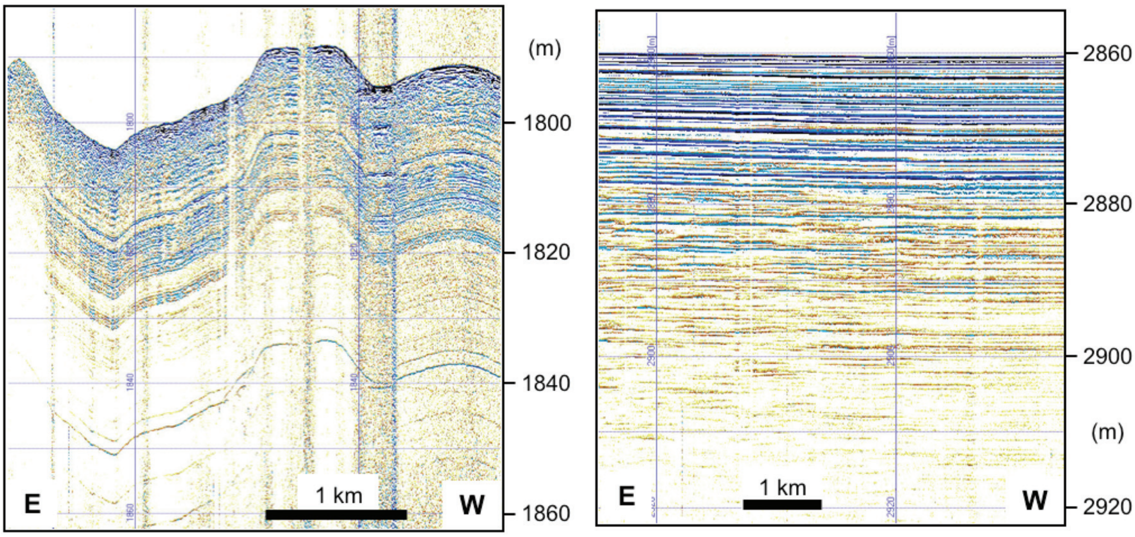

Fig. 11: Left: Parasound example from the top area of the Mendeleev Ridge. Coring location PS72/410 is at right end of the profile. Data processing: negative flank suppressed. Right: Parasound example from the Makarov Abyssal Plain. Coring location PS72/430 is at right end of the profile. Data processing: negative flank suppressed, two traces stacked to one.

List of abbreviations

ASD	Atlas Sounding Data
DWS	Deep Water System (Simrad Echosounder)
mbsf	Meters below Sea Floor
PHF	Primary High Frequency
P-SBP	Parametric Sub-bottom Profiling
PS3	Export format of Parasound data
SBES	Single-Beam Echo-Sounder
SHF	Secondary High Frequency
SLF	Secondary Low Frequency

References

ATLAS Hydrographic (2007): ATLAS HYDROMAP CONTROL Operator Manual. Doc.-Id.: ED 1060 G 312, File: ED-1060-G-312_ V5-0. Edition: 04.2007. ATLAS HYDROGRAPHIC, Bremen, Germany.

ATLAS Hydrographic (2007): ATLAS PARASTORE-3 Operator Manual. Doc. Id.: ED 6006 G 212:/ Version: 4.0 / Edition: 05/2007. ATLAS HYDROGRAPHIC, Bremen, Germany.

Klages M. & Thiede J. (in prep.).- The expeditions ARKTIS-XXII/1a-c of the research vessel "Polarstern" in 2007 / Ed. by Michael Klages and Jörn Thiede with contributions of the participants. Reports on Polar and Marine Research.

Macke A. (2009): The Expedition of the Research Vessel Polarstern to the Antarctic in 2008 (ANT-XXIV/4), Reports on Polar and Marine Research, Alfred Wegener Institute for Polar and Marine Research, Bremerhaven, 591, 64 pp.

Schauer, U. (2008): The Expedition ARKTIS-XXII/2 of the Research Vessel Polarstern in 2007, Reports on Polar and Marine Research, Alfred Wegener Institute for Polar and Marine Research, Bremerhaven, 579, 264 pp.

Schiel, S. (2009:) The Expedition of the Research Vessel Polarstern to the Antarctic in 2007 (ANT-XXIV/1), 592, 114 pp.

Spiess V. (1992): Digitale Sedimentechographie - Neue Wege zu einer hochauflösenden Akustostratigraphie. Berichte aus dem Fachbereich Geowissenschaften der Universität Bremen, Nr.35, 199pp.

Stein R. (2005). The Expedition ARKTIS-XX/2 of "Polarstern" in 2004, Reports on Polar Research, Alfred Wegener Institute for Polar and Marine Research, Bremerhaven, 517, 188pp.

3.3 Physical properties and core logging

3.3.1 Multi-sensor core logging

Frank Niessen[1)], David Poggemann[2)], Isabell Schulte-Loh[1)]

[1)] Alfred-Wegener-Institut, Bremerhaven
[2)] IFM-Geomar, Kiel

Introduction

Whole-core physical properties provide initial core characterization with a very high vertical resolution. Physical properties can be used to define and interpret stratigraphical patterns, including a comparison with lithology and other properties such as shear strength or data obtained from sediment color scanning. Together with other data down-core pattern of physical properties provide a powerful tool for lateral core correlation. The latter is beyond the scope of this report and will be carried out after the cruise. Physical properties are also useful to link the cores to high-resolution echosounding profiles obtained by Parasound, thereby aiding the projection of core data from a single spot into larger spatial and temporal scales.

Work at sea

Measurements in the ship laboratory included non-destructive, continuous determinations of wet bulk density (WBD), P-wave velocity (Vp) and magnetic susceptibility (MS) at 10 mm intervals on all cores obtained during the cruise. The Multi Sensor Core Logger (MSCL, GEOTEK Ltd., UK) was used to measure core temperature, core diameter, P-wave travel time, gamma-ray attenuation and MS. The technical specifications of the MSCL system are summarized in Tab. 2. The principle of logging cores is described in more detail in previous *Polarstern* cruise reports. The orientation of the P-wave and gamma sensors was horizontal. Gravity cores (SL) were measured in coring liners including end caps, whereas Kastenlot (KAL) cores were measured in sub-cores retrieved from the original core using length-wise open transparent plastic boxes of 1,000 mm length and variable cross section.

Geometry: In order to convert raw data to density, velocity and volume susceptibility the geometry of the cores must be determined. Whereas for the calculation of density and velocity the core diameter (SL) and core width (KAL), are directly measured at the position of the Vp transducers, volume susceptibility is calculated from the cross section of the core as outlined below. The distance between the Vp transducers were calibrated using plastic cylinders of known geometry. SL core diameters range from 119.65 to 120.4 mm with a standard deviation of 0.022 and a mean diameter of 120.07 mm. Hand-measured heights of KAL sub-cores range from 70.3 to 73.35 mm with a standard deviation of 0.0815 and a mean height of 71.89 mm. Mean KAL sub-core widths per box are more variable and range from 66.9 to 81.0 mm.

WBD: For both gravity and Kastenlot cores, WBD was determined from attenuation of a gamma-ray beam transmitted from a radioactive source (^{137}Cs). A beam collimator of 5 mm was used and the beam was focused through the core-centre into a gamma detector. To calculate density from gamma counts, Geotek-MSCL software was used (www.geotek.co.uk), which applies a 2nd order polynomial function to describe the relationship between the natural logarithm of gamma counts per second and the product of density and thickness of the measured material. For calibration the three constants of the equation are determined empirically for each day by logging a standard core consisting of different proportions of aluminium and water as described in Best & Gunn (1999).

V_p: Whole-core P-wave velocities were calculated from the core diameter and travel time after subtraction of the P-wave travel time through the core liner wall (SL) or box wall (KAL), transducer, electronic delay, and detection offset between the first arrival and second zero-crossing of the received waveform, where the travel time can be best detected. This travel-time offset was determined using a SL-liner or KAL-box filled with water (V_p = 1481 m/s). P-wave velocities (V_p) were normalized to 20°C using the temperature logs. Core temperature was measured by a calibrated PT-100 sensor placed into the sediments near the end of each core section:

$$V_p = V_{pm} + 3 * (20 - t_m) \qquad \text{(iii)}$$

where V_{pm} = P-wave velocity at measured temperature;
t_m = measured temperature.

MS on whole cores was measured in terms of SI units, using Bartington MS-2 meter loop sensors of 140 mm internal diameter. The sensor was calibrated by Bartington and data output is MS. The meter was set to zero 150 mm before the core reached the MS sensor. After removing the last section of a core from the track, a zero-reading of the MS-2 meter was used to monitor sensor drift. Assuming linear drift with core depth a drift correction was applied. In order to calculate volume-specific susceptibility data are corrected for loop-sensor and core diameter as follows:

$$\text{MS } (10^{-5}\text{ SI}) = \text{measured value } (10^{-5}\text{ SI}) / \text{K-rel} \quad \text{(i)}$$

K-rel is a sensor-specific correction calculated from the diameter of the core over the diameter of the loop sensor as outlined in the Geotek MSCL manual (www.geotec.co.uk). We have used the empirical relationship of relative response to varying core and loop diameters outlined in the MSCL-Manual (www.geotec.co.uk):

$$K\text{-rel} = 4.8566(d/D)^2 - 3.0163(d/D) + 0.6448$$

D is the diameter of the MS-2 meter core loop (140 mm) and d (d_{KAL} or d_{SL}) is the diameter of the core. For KAL-cores, the rectangular cross section of the core was equalized to a size-equivalent circular section, of which a fictive core diameter was calculated as input parameter for loop-sensor correction coefficient:

$$d_{KAL} = 2 \sqrt{a * b / \pi}$$

For the height of KAL-cores (a) we used the average value of 71.89 mm (see Geometry above). The width of KAL-cores (b) was measured at each logging interval by the MSCL. The variation of SL-core diameters were determined as being very small (see above) so that d_{SL} was set to the mean value of 120.07 mm.

In addition, for a higher resolution, MS on split cores was measured using the MS-2 meter point sensor. Drift corrections were applied in a similar way as for loop-sensor described above. In general, the correlation of loop sensor and point sensor MS is good. However, a perfect correlation cannot be expected because the loop data is obtained from a larger core volume as the point data so that data from different material is compared. Also the effect of clasts in the core is more pronounced in loop data than in point data, because clasts may have been removed after splitting or are not directly measured with the point sensor. For this reason it is not straight forward to calculate volume-specific susceptibility from point-sensor data. We have used two correlations of volume-specific MS with point-sensor MS for one SL-core and one KAL-core, respectively to offer an approximation for data conversion using empirical linear regressions according to Fig. 12. One has to bear in mind that the range of measured MS on cores retrieved during the cruise is relative small in amplitude (in particular in KAL-cores, Fig. 12) so that these algorithms should not be used as general relationships to correct point-sensor data from other cores.

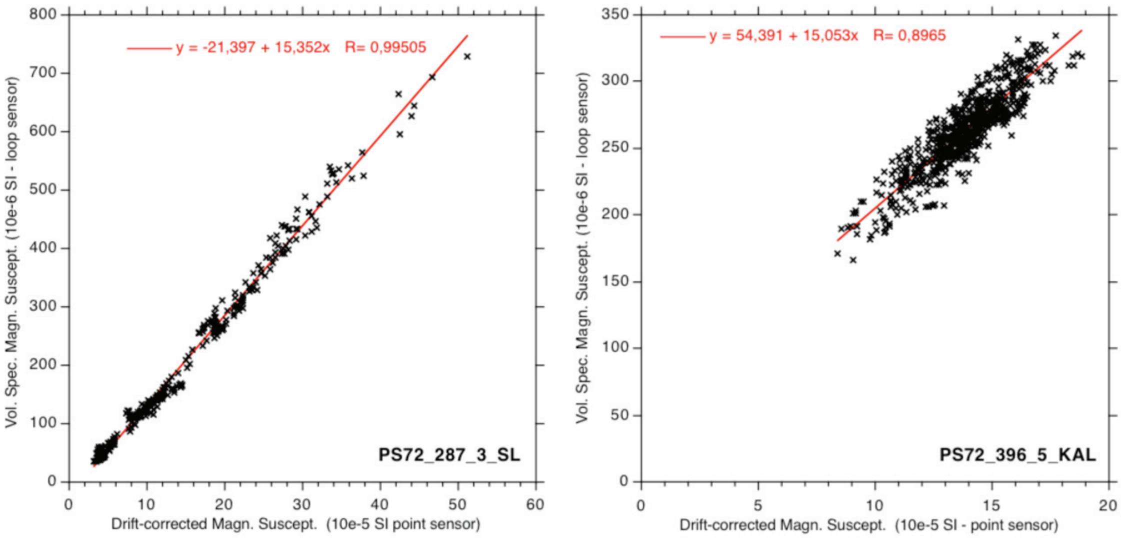

Fig. 12: Correlation of MS data measured with a loop sensor and converted to volume-specific MS with MS data measured with a point sensor.

The data of WBD, Vp and volume-specific MS (loop-sensor) as a function of core depth of all cores are presented as plots in the appendix of this report.

Reference

Best, A. I., Gunn, D.E. (1999) Calibration of marine sediment core loggers for quantitative acoustic impedance studies. Marine Geology, 160, 137-146

Tab. 2: Technical specifications of the GEOTEK MSCL14n

P-wave velocity and core diameter Plate-transducer diameter: 4 cm Transmitter pulse frequency: 500 kHz Pulse repetition rate: 1 kHz Received pulse resolution: 50 ns Gate: 5000 Delay: 0 ms
Density Gamma ray source: Cs-137 (1983) Activity: 356 MBq Energy: 0.662 MeV Collimator diameter: 5.0 mm Gamma detector: Gammasearch2, Model SD302D, Ser. Nr. 3043 , John Count Scientific Ltd., 10 s counting time
Magnetic susceptibility Loop sensor: BARTINGTON MS-2C Loop sensor diameter: 14 cm Point sensor: BARTINGTON MS-2F Alternating field frequency: 565 Hz, counting time 10 s, precision 0.1 * 10^{-5} (SI) Magnetic field intensity: ca. 80 A/m RMS Krel: 1.63 (SL, 12 cm core-ø), variable for KAL counting time 10 s

3.3.2 Spectral photometry

Michael Schreck[1)], Evgenia Bazhenova[1,2)], Sebastian Eckert[3)], Christian März[3)], Jens Matthiessen[1)], Rüdiger Stein[1)]

[1)] Alfred-Wegener Institut, Bremerhaven
[2)] State University, St. Petersburg
[3)] Institute for Chemistry and Biology, Oldenburg

The spectral reflectance was measured on freshly split core surfaces that were covered with transparent wrap („Frischhaltefolie TOPPITS" Melitta, Minden, Germany) with a hand held spectrophotometer (Minolta CM 2002, lens diameter 8 mm, field of view Ø 0.8 cm) at wave lengths from 400 to 700 nm (10 nm steps), connected to a MACINTOSH Powerbook 5300C. Output files are the L*a*b* colour space that is also referred to as CIELAB space (Commission Internationale de l´Éclairage L*a*b colour space 1976), the chroma, hue and value of the Munsell Colour Chart, the percentage value of the spectrum at 10 nm steps from 400 to 700 nm, and the colour values x, y and z that are defined according to the RGB colours (CIE 1931). Lightness L* (grey scale) is recorded from 0 % (black) to 100 % (white), the red-green colour space a* from -4 (green) to 16 (red), and the yellow-blue colour space b* from 0 (blue) to 40 (yellow).

Every core section was measured at centimetre intervals separately, and a white calibration first without and then with transparent wrap was conducted before and after each core section to identify a possible drift of the spectrophotometer measurements.

The raw spectral photometer data were stored as .txt files, then converted into Excel files (.xls) and processed and edited for each core separately in Excel sheets. Obvious outliers e.g. due to uneven core surfaces as noted while measuring were deleted from the data set. After final editing all data will be deposited separately for each sediment core under the respective station and gear number in the data bank Pangaea (WDC-mare).

Most box cores, gravity cores and Kastenlot cores were scanned until the MAC Powerbook crashed. Cores from Sites 408, 413, 422, 430, 438, 471 will be scanned after the cruise in Bremerhaven.

Here we shortly present the colour reflectance measurement record of Kastenlot core PS 72/340-5 as an example for Transect 1 (Fig. 13).

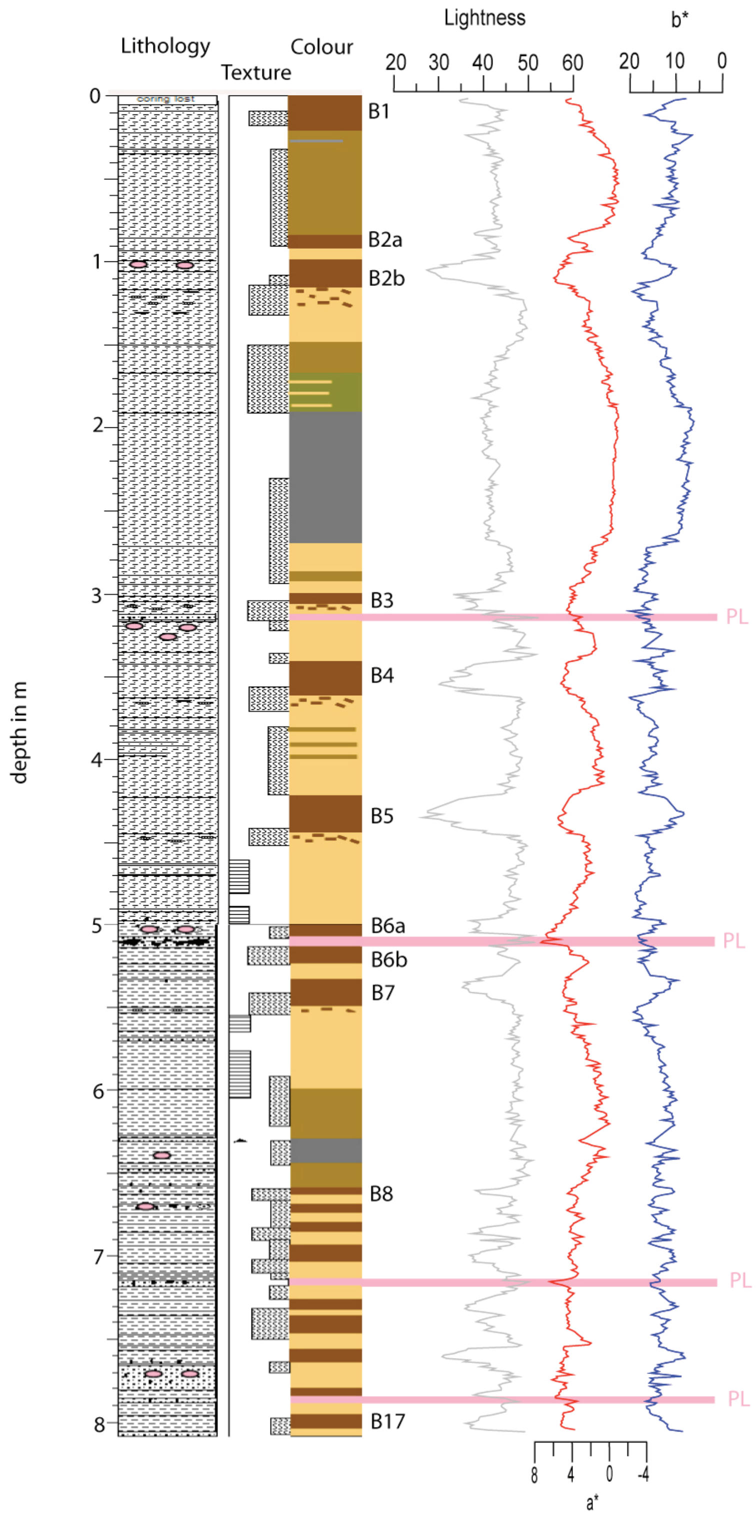

Fig. 13: Results of colour scanning and correlation with lithological core description sedimentary sequence of Core PS72/340-5

The cyclic alternation of very dark greyish brown (10YR 3/2) and light olive brown (2.5Y 5/3 to 2.5Y 5/4) sediment units was also documented in the L-a*-b* space of the colour reflectance measurements. The very dark greyish brown layers are characterized by relatively low grey-scale values (lightness) corresponding to higher values in a* and lower values in b* space. The yellowish brown layers are reflected by higher lightness values, lower a* and higher b* values. Similar patterns of cyclic alteration can be easily identified in the other cores of Transect 1 (PS 72/340 – 344).

According to Clark et al. (1980) an important stratigraphic feature for the correlation of sediment cores from the western Arctic Ocean are the so-called „pinkish-white“ layers. Their typical spectral-photometric characteristic can also be identified by using the colour reflectance measurements. The four clearly developed pinkish layers of Kastenlot PS72/340-5 are characterized by maximum peaks in the lightness record and a* and b* values which are more influenced by red and yellow components, respectively.

The major lithological change at about 5 mbsf is not reflected in the spectral photometric data. Nonetheless the colour reflectance measurements can be used for a first tentative correlation of the sediment cores throughout Transect 1.

3.3.3 Shear strength measurements

Bernhard. Naafs[1)], David Poggemann[2)], Juliane Müller[1)], Evgenia Bazhenova[1,3)]

[1)] Alfred-Wegener-Institut, Bremerhaven
[2)] IFM-Geomar, Kiel
[3)] State University, St. Petersburg

Undrained shear strength was measured with a hand held shear vane, equipped with a 19 mm blade (Geotechnics, Auckland, New Zealand). The used Geovane GEO 709 device was calibrated on August 30, 2006. The measurements were conducted on selected Kastenlot and gravity cores (PS72/287-3, 340-5, 342-1, 343-1, 344-3 and 350-2) at irregular intervals in the centre of the split cores. Depending on the shear strength of the sediment, the device depicts a division between 0 and 140. A calibration chart provided by the company was used to convert the shear strength divisions into undrained vane shear strength (in kPa). The shear strength curves of most measured sediment cores indicate normal consolidation (Fig. 14). However, cores PS72/342-1 and PS72/350-2 show sharp increases in shear strength (Fig. 15), which can be attributed to major lithological changes within the sediment cores, e.g. the presence of debris flows. All data will be deposited separately for each sediment core under the respective station and gear number in the data bank Pangaea (WDC-mare).

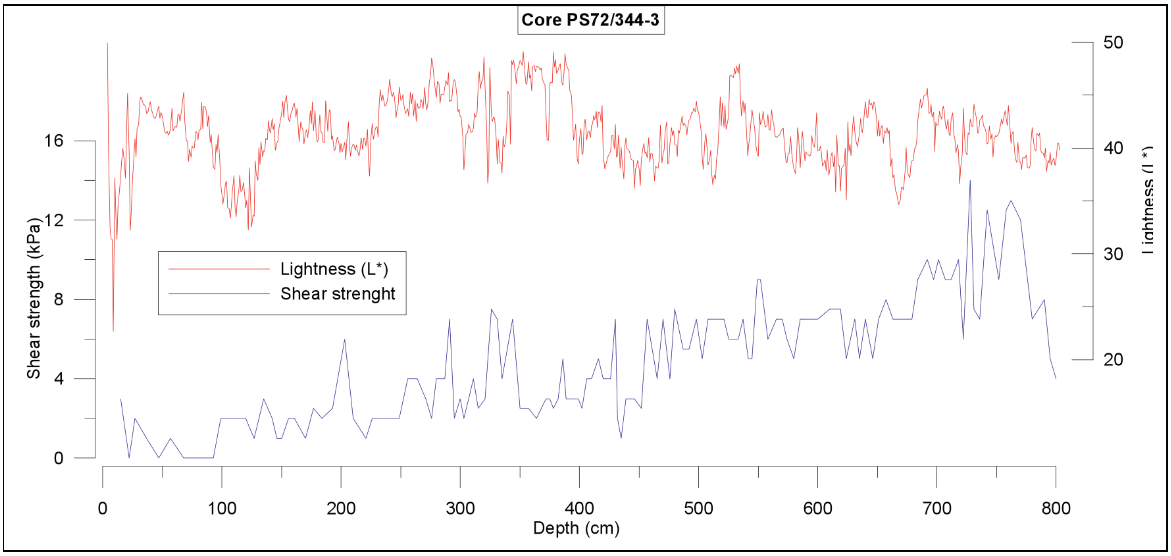

Fig. 14: Shear strength of core PS72/344-3 from the Arctic Ocean plotted together with the lightness record of the same core. The gradual increase in shear strength is typical for normal consolidation processes.

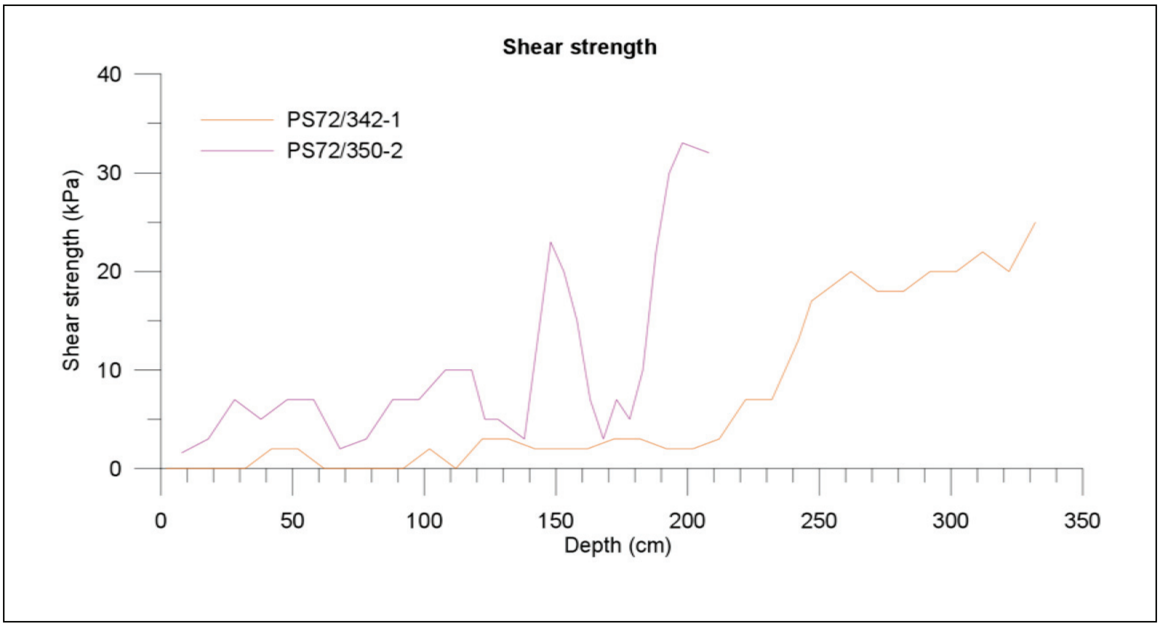

Fig. 15: Shear strength of core PS72/342-1 and PS72/350-2 from the Arctic Ocean. Both cores show a rapid increase in shear strength, caused by changes in lithology.

3.4 Geological sampling, description, and methods applied

Juliane Müller[1)], Evgenia Bazhenova[1,2)], Sebastian Eckert[3)], Alexey Krylov[4)], Norbert Lensch[1)], Christian März[3)], Jens Matthiessen[1)], Bernhard Naafs[1)], Seung-Il Nam[5)], Frank Niessen[1)], Christelle Not[6)], David Poggemann[7)], Michael Schreck[1)], Isabell Schulte-Loh[1)], Rüdiger Stein[1)]

[1)] Alfred-Wegener-Institut, Bremerhaven
[2)] State University, St. Petersburg
[3)] Institute of Chemistry and Biology, Oldenburg
[4)] VNIIO, St. Petersburg
[5)] Korea Institute of Geoscience, Seoul
[6)] University of Quebec, Montreal
[7)] IFM-Geomar, Kiel

In total, geological coring was carried out at 23 stations, using the Giant Box Corer (GKG), Multicorer (MUC), Gravity Corer (SL), and/or Kastenlot Corer (KAL) (Tab. 3). In addition, the Multicorer was run four times at Station PS72/478 in the Haakon Mosby Mud Volcano (Tab. 3).

Surface and near-surface sediment sampling was carried out by using a Giant Box Corer and a Multicorer. The Giant Box Corer (weight of ca. 500 kg; volume of sample 50*50*60 cm; manufactured by Fa. Wuttke, Henstedt-Ulzburg, Germany) was successfully used 21 times at 21 stations. Two times there was no recovery due to technical problems. From the Box Corer surface sediments and usually two archive tubes (diameter 12 cm) were taken. Usually both archive tubes were logged (MSCL, see Chapter 3.3.).The following samples were obtained from the surface sediments:

10x10 cm^2 (100 cm^3) Foraminifera (IfM-GEOMAR)
10x10 cm^2 (100 cm^3) Benthic Foraminifera (AWI)
10x10 cm^2 (100 cm^3) Sedimentology (AWI)
10x10 cm^2 (100 cm^3) Micropaleontology (KIGAM)
10x10 cm^2 (100 cm^3) Palynomorphs (GEOTOP, Canada)

Tab. 3: Locations and gears of geological stations

Station	Gear	Latitude	Longitude	Water Depth [m]
PS72/287-1	GKG	74° 15.96' N	90° 59.15' W	352.7
PS72/287-2	MUC	74° 15.96' N	90° 59.19' W	353.1
PS72/287-3	GC	74° 15.96' N	90° 59.12' W	352.8
PS72/287-4	GC	74° 15.97' N	90° 59.10' W	352.5
PS72/289-1	GKG	75° 6.73' N	136° 34.67' W	3532
PS72/289-2	KAL	75° 7.14' N	136° 35.07' W	3534
PS72/291-1	GKG	71° 16.17' N	137° 10.80' W	1550
PS72/291-2	KAL	71° 16.22' N	137° 10.82' W	1549
PS72/340-3	GKG	77° 35.42' N	171° 32.56' W	2344
PS72/340-4	MUC	77° 35.96' N	171° 31.69' W	2348
PS72/340-5	KAL	77° 36.31' N	171° 29.09' W	2349
PS72/341-3	GKG	77° 36.44' N	176° 7.37' W	1386
PS72/341-4	MUC	77° 37.06' N	176° 8.35' W	1409
PS72/341-5	KAL	77° 36.11' N	176° 6.23' W	1368
PS72/342-1	GC	77° 36.01' N	177° 20.62' W	819.8
PS72/343-1	GC	77° 18.33' N	179° 2.99' E	1227
PS72/343-2	GC	77° 18.33' N	179° 2.73' E	1225
PS72/343-3	GKG	77° 18.34' N	179° 2.92' E	1227
PS72/343-4	MUC	77° 18.37' N	179° 2.65' E	1226
PS72/344-1	GKG	77° 36.02' N	174° 32.49' E	1262
PS72/344-2	MUC	77° 36.23' N	174° 32.87' E	1262
PS72/344-3	KAL	77° 36.62' N	174° 32.37' E	1257
PS72/350-2	GC	74° 40.20' N	169° 50.26' E	61.1
PS72/350-3	GKG	74° 40.20' N	169° 50.28' E	60
PS72/392-4	GC	80° 28.31' N	158° 50.86' W	3632
PS72/392-5	GC	80° 27.81' N	158° 49.75' W	3624
PS72/392-6	GKG	80° 28.42' N	158° 50.83' W	3637
PS72/393-3	GKG	80° 43.08' N	155° 31.90' W	3882
PS72/393-4	GC	80° 43.14' N	155° 32.32' W	3880
PS72/396-3	GKG	80° 35.17' N	162° 22.57' W	2733
PS72/396-4	MUC	80° 35.07' N	162° 20.07' W	2727
PS72/396-5	KAL	80° 34.74' N	162° 19.01' W	2722
PS72/399-3	GKG	80° 38.48' N	166° 42.99' W	3375
PS72/399-4	GC	80° 39.18' N	166° 45.81' W	3376
PS72/404-3	GKG	80° 45.39' N	171° 09.69' W	2182
PS72/404-4	GC	80° 45.29' N	171° 09.63' W	2181
PS72/405-1	GC	80° 42.05' N	171° 37.29' W	2873
PS72/405-2	GC	80° 42.30' N	171° 38.45' W	2782
PS72/408-3	GKG	80° 32.92' N	174° 40.17' W	2576
PS72/408-4	MUC	80° 32.94' N	174° 40.41' W	2576.7
PS72/408-5	GC	80° 33.11' N	174° 41.77' W	2583.4
PS72/410-1	GKG	80° 30.37' N	175° 44.38' W	1802
PS72/410-2	MUC	80° 30.89' N	175° 44.27' W	1816
PS72/410-3	KAL	80° 31.29' N	175° 43.49' W	1847
PS72/413-3	GKG	80° 16.49' N	178° 31.29' W	1261
PS72/413-4	MUC	80° 16.93' N	178° 30.27' W	1267
PS72/413-5	GC	80° 17.25' N	178° 29.27' W	1273
PS72/418-5	GKG	80° 23.54' N	178° 49.00' E	2045
PS72/418-6	MUC	80° 23.68' N	178° 50.29' E	2045
PS72/418-7	GC	80° 23.92' N	178° 51.34' E	2043
PS72/422-3	GKG	80° 33.08' N	175° 44.75' E	2547
PS72/422-4	MUC	80° 32.88' N	175° 44.37' E	2545
PS72/422-5	KAL	80° 32.68' N	175° 44.63' E	2536
PS72/430-3	GKG	81° 02.29' N	164° 45.59' E	2874
PS72/430-4	GC	81° 03.37' N	164° 43.72' E	2874
PS72/438-3	GKG	80° 58.94 ' N	148° 59.04' E	2468
PS72/438-4	GC	80° 58.96 ' N	148° 00.82' E	2474
PS72/471-4	GKG	81° 14.00' N	121° 17.45' E	4120
PS72/471-5	GC	81° 13.82' N	121° 18.42' E	4049
PS72/472-1	DRG_C	81° 12.76' N	121° 25.87' E	3257
PS72/478-1	MUC	72° 00.34' N	14° 43.13' E	1286.8
PS72/478-2	MUC	72° 00.28' N	14° 43.08' E	1289.4
PS72/478-3	MUC	72° 00.24' N	14° 43.10' E	1287.4
PS72/478-4	MUC	72° 00.27' N	14° 43.09' E	1286

The standard 8-tubes-version Multicorer (manufactured by Fa. Wuttke, Henstedt-Ulzburg, Germany) with an inner tube diameter of 10 cm was used. The penetration weight was always 250 kg. The Multicorer was successfully used 13 times at 12 stations, and usually recovered undisturbed surface sediments and overlying bottom water. In general, the Multicorer cores were sampled in slices of 1 cm throughout the whole core for the following investigations:

1 core	Sedimentology (AWI)
1 core	Archive (AWI)
1 core	Radioactive Isotopes (GEOTOP, Montréal, Canada)
1 core	Organic Geochemistry (AWI)
2 cores	Inorganic Geochemistry (ICBM Oldenburg)
2 cores	Micropaleontology (AWI, only uppermost 10 cm))

Surface water- and sediment samples (50 ml, 15 cm^3) for microbiological investigations (E. Helmke, AWI) have been taken from the archive or inorganic geochemistry tubes. Sampling of long sediment cores Long sediment cores were taken by a Gravity Corer and a Kastenlot. The Gravity Corer (GC or "Schwerelot", SL) has a penetration weight of 1.5 t. It was successfully used with variable barrel lengths of 3, 5 or 10 m at 15 stations (19 cores; see Tab. 4 for details). The recovery of the gravity corer varied between 2.16 and 7.55 m, the penetration between 2.5 and 10 m (Tab. 4).

Tab. 4: Gravity and Kastenlot cores from expedition ARK-XXIII/3 with penetration and recovery values

Station	Gear	Penetration (cm)	Recovery (cm)	
PS72/287-3	SL-10	550	463	
PS72/287-4	SL-10	550	433	
PS72/289-2	KAL	0	0	
PS72/291-2	KAL	1000	850	
PS72/340-5	KAL	900	830	
PS72/341-5	KAL	400	329	
PS72/342-1	SL-5	400	340	
PS72/343-1	SL-10	1000	712	
PS72/343-2	SL-10	1000	749	
PS72/344-3	KAL	900	823	
PS72/350-2	SL-3	250	216	
PS72/392-4	SL-10	1000	568	
PS72/392-5	SL-10	900	615	
PS72/393-4	SL-10	1000	556	
PS72/396-5	KAL	850	791	
PS72/399-4	SL-10	900	571	
PS72/404-4	SL-10	900	562	
PS72/405-1	SL-3	400	300	(overpenetration)
PS72/405-2	SL-3	400	300	(overpenetration)
PS72/408-5	SL-10	900	633	
PS72/410-3	KAL	850	780	
PS72/413-5	SL-10	950	644	
PS72/418-7	SL-10	950	688	
PS72/422-5	KAL	830	815	
PS72/430-4	SL-10	750	445	
PS72/438-4	SL-10	950	755	
PS72/471-5	SL-5	550	498	(overpenetration)

The Kastenlot (Kögler, 1963), a Gravity Corer with a rectangular cross section of 30 x 30 cm, has a penetration weight of 3.5 t and a core box segment sized 30 x 30 x 575 cm (manufactured by Hydrowerkstätten Kiel). The length of the Kastenlot boxes used was 11.75 m plus about 30 cm for the core catcher. The great advantage of the Kastenlot is a wall-thickness of the barrel of only 2 mm. Because of the great cross-sectional area (900 cm^2) and the small thickness of the barrels, the quality of the cores was generally excellent. The Kastenlot was successfully used at 7 stations. The recovery of the Kastenlot cores varied between 3.29 and 8.50 m (Tab. 4, Fig. 16). All Kastenlot sediments were stored in plastic boxes (100 x 12 and 100 x 8 cm) for the following investigations:

Series I Archive
Series II MSCL-logging
Series III Sedimentology I
Series IV Organic Geochemistry Series V Sedimentology II

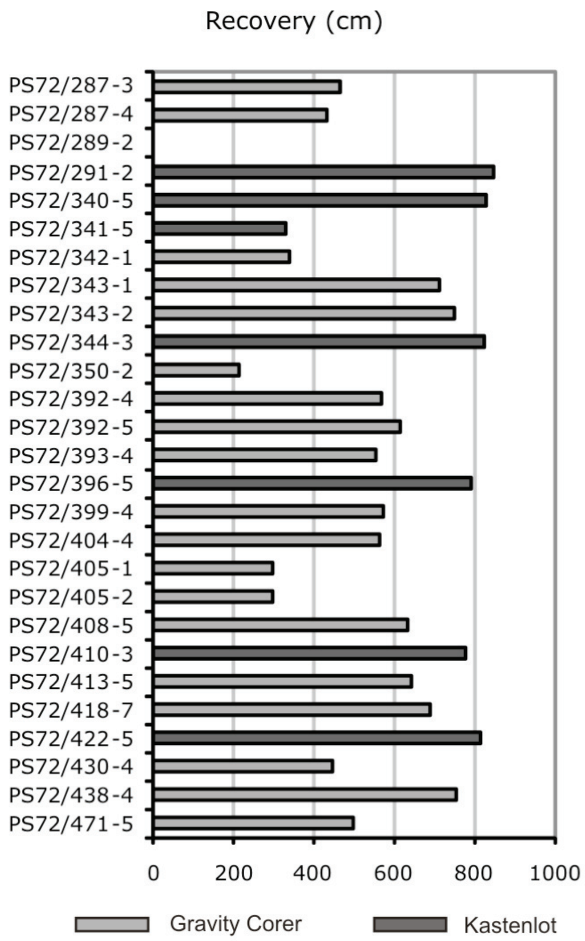

Fig. 16: Recovery of the gravity and Kastenlot cores (in cm). For location of cores see Fig. 6.

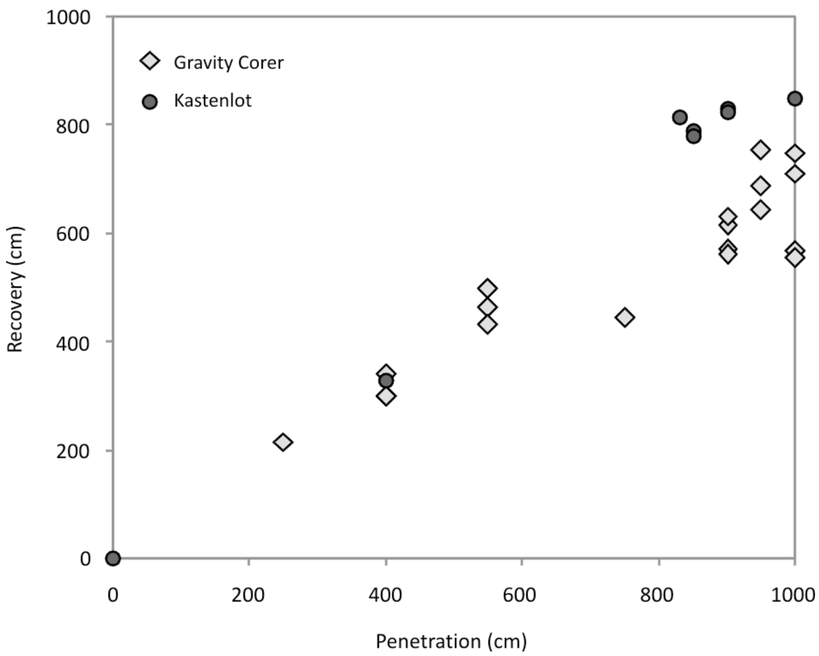

Fig. 17: Penetration (cm) vs. recovery (cm) of the gravity and Kastenlot cores

All gravity cores were logged before they were opened whereas plastic boxes of the Kastenlot cores were logged after sampling (MSCL; Chapter 3.3). Most gravity cores and all Kastenlot cores were opened and described (see Chapter 3.6. and Annex). Sediment slabs were taken from all opened cores for X-ray photography. Tab. 5 gives an overview of the geological work that has been done on board.

Sampling of crystalline basement

In order to collect samples from outcropping crystalline basement at the Gakkel Ridge a dredge (chain bag, see Fig. 18) was successfully used at station PS72/472-1 (81° 12.76' N, 121° 25.87' E to 81° 12.15' N, 121° 31.26' E, 3,257 - 2,474 m water depth). The chain bag is 0.95 x 0.35 x 0.40 m large and has a weight of 100 kg. The rope length during dredging was three times the water depth.

The collected stones were most likely porphyritic and varied in size and composition, some of them were covered by a black layer (possibly Fe-Mn-crusts). Identification and quantification will take place in the home laboratories.

Fig. 18: Dredge containing stones collected at station PS72/472-1 during Polarstern cruise ARK-XXIII/3

Tab. 5: Overview of geological methods that have been applied during the Expedition ARK-XXIII/3

station/gear	photography	x-ray slabs	x-radiographics	x-ray IRD counts	colour scanning	shear strength	foram. sieving	smear slides
PS72/287-1 GKG	x	x	x	x				
PS72/287-3 GC	x	x	x	x	x	x	x	x
PS72/287-4 GC								
PS72/289-1 GKG	x	x	x	x	x		x	
PS72/289-2 KAL	x	x	x	x				
PS72/291-1 GKG	x	x	x	x			x	
PS72/291-2 KAL	x	x	x	x	x		x	x
PS72/340-3 GKG	x	x	x	x				
PS72/340-5 KAL	x	x	x	x	x	x	x	x
PS72/341-3 GKG	x	x	x	x	x			
PS72/341-5 KAL	x	x	x	x	x		x	
PS72/342-1 GC	x	x	x	x	x	x		x
PS72/343-1 GC	x	x	x	x	x	x		
PS72/343-2 GC	x	x	x	x	x			
PS72/343-3 GKG	x	x	x	x	x			
PS72/344-1 GKG	x	x	x	x	x		x	
PS72/344-3 KAL	x	x	x	x	x	x		x
PS72/350-2 GC	x	x	x	x	x	x		
PS72/350-3 GKG	x	x	x	x	x		x	
PS72/392-4 GC	x	x	x	x				
PS72/392-5 GC	x	x	x	x	x	x		x
PS72/392-6 GKG	x	x	x	x	x		x	
PS72/393-3 GKG	x	x	x	x	x			
PS72/393-4 GC	x	x	x	x	x			
PS72/396-3 GKG	x	x	x	x	x		x	
PS72/396-5 KAL	x	x	x	x	x		x	x
PS72/399-3 GKG	x	x	x	x	x			
PS72/399-4 GC	x	x	x	x	x			
PS72/404-3 GKG	x	x	x	x	x			
PS72/404-4 GC	x	x	x	x	x			
PS72/405-1 GC	x	x	x	x				
PS72/405-2 GC	x	x	x	x				
PS72/408-3 GKG	x	x	x	x	x			
PS72/408-5 GC	x	x	x	x				
PS72/410-1 GKG	x	x	x	x	x			
PS72/410-3 KAL	x	x	x	x	x		x	
PS72/413-3 GKG	x	x	x	x	x			
PS72/413-5 GC	x	x	x	x				
PS72/418-5 GKG	x	x	x	x	x			
PS72/418-7 GC	x	x	x	x	x			
PS72/422-3 GKG	x	x	x	x	x			
PS72/422-5 KAL	x	x	x	x			x	x
PS72/430-3 GKG	x	x	x	x				
PS72/430-4 GC	x	x	x	x				
PS72/438-3 GKG	x	x	x	x	x			
PS72/438-4 GC	x	x	x					
PS72/471-4 GKG	x	x	x					
PS72/471-5 GC	x	x	x					

3.5 Characteristics of surface sediments

Evgenia Bazhenova[1,2], Christelle Not[3], Alexey Krylov[4], Seung-Il Nam[5], Jens Matthiessen[1]

[1] Alfred-Wegener-Institut, Bremerhaven
[2] State University, St. Petersburg
[3] University of Quebec, Montreal
[4] VNIIO, St. Petersburg
[5] Korea Institute of Geoscience, Seoul

During the ARK-XXIII/3 expedition surface sediments were taken by the giant box corer (GKG) at 20 geological stations from water depths between 61 and 4,073 m (for locations see Fig. 6). Recovery of the GKG cores ranges between 36 and 54 cm. Sediments from 18 box cores were mostly undisturbed while the very water-saturated sediments from cores PS 72/ 393-3 and PS 72/ 471-4 were strongly disturbed (see Tab. 6).

Photographs of all GKGs and sub-cores were taken. Lithology was preliminary described visually for all box cores. Colour of surface sediments (0 - 1 cm) and cores was described using Munsell Soil Colour Chart (1954). The colour of cores was additionally logged at 1 cm intervals using a Minolta Spectrophotometer (Minolta CM 2002, Chapter 3.3). Measurements of wet bulk density, P-wave velocity and magnetic susceptibility were performed on unsplit subcores at 1 cm intervals using GEOTEK Multi Sensor Core Logger (MSCL-14, Chapter 3.3). X-radiography was carried out to investigate sedimentary structures and to estimate the ice-rafted debris (IRD) contents larger than 2 mm (Chapter 3.6).

The characteristics of surface sediments (0 - 1 cm) recovered by GKG are summarized in Tab. 7. Surface sediments from the Canadian Basin locations are represented by olive to brown sandy mud. Surface sediments from the southern Mendeleev Ridge locations are represented by dark yellowish brown sandy mud, the amount of gravel decreases to the west (with decreasing water depth). Surface sediments from the Mendeleev Ridge locations are dominated by dark brown sandy mud and silty clay, the amount of gravel increases to the west (with decreasing depth).

Tab. 6: Characteristics of surface sediments recovered by large box corer (GKG) during ARK-XXIII/3 expedition

Core ID (GKG)	Location	Water depth (m)	Core length (cm)	Colour and lithology	Remarks
PS 72/ 287-1	Barrow Strait	337	33	Olive sandy mud	Starfish
PS 72/ 289-1	Canadian Basin	2179	40	Dark olive brown sandy mud	Bioturbated
PS 72/ 291-1	Mackenzie Slope	1502	42	Dark brown mud	Insignificant admixture of sand
PS 72/ 340-3	Southern Mendeleev Ridge	2298	41	Brown sandy mud	Some dropstones (ø up to 1 cm)
PS 72/ 341-3	Southern Mendeleev Ridge	1339	48	Dark yellowish brown sandy mud	Some dropstones (ø up to 1,5 cm); Hydrozoa; polychets; shell detritus
PS 72/ 343-3	Southern Mendeleev Ridge	1193	40	Dark yellowish brown sandy mud	Valves of Brachiopoda; polychets
PS 72/ 344-1	Southern Mendeleev Ridge	1224	54	Dark yellowish brown sandy mud	Bioturbated, polychets
PS 72/ 350-3	East Siberian Shelf	61	46	Brown mud	Insignificant admixture of sand
PS 72/ 392-6	Mendeleev Ridge	3582	44	Dark yellowish brown sandy mud	Valves of Brachiopoda, Bivalvia; Foraminifera
PS 72/ 393-3	Mendeleev Ridge	3880	36	Brown sandy mud	Very soft sediment; some shells
PS 72/ 396-3	Mendeleev Ridge	2663	39	Dark yellowish brown gravelly sandy mud	Many dropstones (ø up to 15 cm); Hydrozoa; worms
PS 72/ 399-3	Mendeleev Ridge	3375	43	Dark brown sandy mud	Bioturbated, polychets
PS 72/ 404-3	Mendeleev Ridge	2182	37	Dark brown sandy silty clay	Some dropstones (ø up to 2 cm); valve of Bivalvia; Foraminifera; polychets
PS 72/ 408-3	Mendeleev Ridge	2576	42	Dark brown sandy mud	Some dropstones (ø up to 4 cm); valves of Brachiopoda, Bivalvia; polychets, traces of worms
PS 72/ 410-1	Mendeleev Ridge	1808	38	Dark brown gravelly sandy silty clay	Many dropstones (ø up to 3 cm); some valves
PS 72/ 413-3	Mendeleev Ridge	1264	38	Dark yellowish brown gravelly sandy mud	Many dropstones (ø up to 3 cm); valves of Brachiopoda, Bivalvia; shell detritus
PS 72/ 418-5	Mendeleev Ridge	2046	50	Dark brown mud	Bioturbated, some valves (Cephalopoda), insignificant admixture of sand
PS 72/ 422-3	Mendeleev Ridge	2546	40	Dark brown sandy mud	Bioturbated, some valves (Bivalvia)
PS 72/ 430-3	Makarov Basin	2875	36	Dark brown sandy mud	Bioturbated, some valves
PS 72/ 438-3	Lomonosov Ridge	2472	39	Dark brown mud	Insignificant admixture of sand
PS 72/ 471-4	Gakkel Ridge	4073	-	Dark brown sandy silty clay	Some dropstones; coring disturbed

Surface sediments were sampled using 100 ml boxes. Coarse fraction (> 63 μm) was isolated by means of wet sieving. Results of preliminary coarse-fraction analysis are summarized in Tab. 7. Mineralogical composition of surface samples is plotted in Fig. 19 (Transect 1 from the southern Mendeleev Ridge locations) and in Fig. 20 (Transect 2 from the Mendeleev Ridge locations). The abiogenic fraction (mainly represented by quartz and feldspar with a certain amount of mica, terrigenous carbonate and heavy minerals) is almost absent at the deep-sea locations (cores PS

72/ 289-1 and PS 72/393-3). The highest content of minerals is observed at the shallow-water location on the East Siberian shelf (core PS 72/350-3), probably reflecting high terrigenous input from the shelf. Rock fragments are most abundant at slopes (locations in the Mendeleev Ridge area and on the Canadian shelf).

Tab. 7: General mineralogical and biogenic composition of surface sediments (0-1 cm) based on coarse-fraction (> 63μm) analysis

Station	PS72/ 341-3	PS72/ 438-3	PS72/ 399-3	PS72/ 396-3	PS72/ 410-1	PS72/ 413-3	PS72/ 340-3	PS72/ 343-3	PS72/ 291-1	PS72/ 408-3	PS72/ 422-3	PS72/ 418-5	PS72/ 414-3	PS72/ 289-1	PS72/ 350-3	PS72/ 413-3	PS72/ 393-3	PS72/ 430-3	PS72/ 344-1
Component																			
Quartz+Feldspar	4	4	3	5	4	2	3	4	5	2	3	3	4	2	5	3	-	3	5
RockFragments	-	-	-	-	-	2	2	-	2	3	1	1	1	-	-	2	-	-	-
Mica	-	1	1	-	1	1	1	1	1	-	1	1	1	-	2	1	-	1	2
Terr.Carbonate	3	1	3	3	3	3	3	2	2	2	2	3	3	-	3	3	-	-	3
HeavyMinerals	1	2	2	2	1	1	1	2	1	1	2	2	2	1	3	2	-	1	2
PlanktonicForams	5	4	5	4	5	5	5	4	4	5	5	5	5	5	1	5	5	5	4
BenthicForams	1	3	1	1	1	3	3	2	4	1	3	3	2	1	3	3	-	2	3
Diatoms	2	1	-	-	-	2	-	2	-	-	-	1	-	1	3	1	1	-	3
SpongeSpicules	3	4	4	3	1	3	3	3	1	2	1	3	2	2	-	3	3	2	2
Brachiopoda	2	1	-	-	1	2	-	-	-	-	-	-	-	-	3	1	-	-	-
Bivalvia	1	1	-	-	-	1	-	-	-	-	-	-	-	-	-	-	-	1	-
Polychets	1	-	-	-	-	1	1	-	-	-	-	-	-	-	-	1	-	-	-
ShellFragments	3	3	2	2	3	3	2	4	2	3	2	1	3	-	3	4	-	2	3
Cephalopoda	-	-	-	-	1	-	-	-	-	-	-	-	-	-	-	1	-	-	-
Bryozoa	-	-	-	-	-	1	-	1	-	-	-	-	-	-	-	-	-	-	1
Ostracoda	-	-	-	-	-	-	-	-	-	-	-	-	-	-	3	-	-	-	2

Results of onboard preliminary coarse fraction analysis:
- none; 1 very rare; 2 rare; 3 common; 4 abundant; 5 dominant.

The biogenic fraction dominates the majority of samples (Figs. 19, 20). It mainly consists of planktic foraminifers (*Neogloboquadrina pachyderma*) except for the shallow-water location on the East Siberian shelf (core PS 72/350-3). Benthic foraminifers are represented by a few species, common in the surface sediments except for the deep-sea location in the Chukchi Basin (core PS 72/393-3). The highest contents of diatoms are observed in the southern Mendeleev Ridge area (core PS 72/344-1) and at the shallow-water location on the East Siberian shelf (core PS 72/350-3), reflecting either high silica input from the shelf or better preservation. At the same locations some ostracod fragments were found. Sponge spicules were found in all the samples except for the shallow-water location on the East Siberian shelf (core PS 72/350-3). Shell fragments are common in all surface sediments except for the locations in the Makarov Basin (core PS 72/430-3) and in the Lomonosov Ridge area (core PS 72/438-3). Bivalves occur in the surface sediments from the Canadian Basin (core PS 72/291-1 and PS 72/289-1).

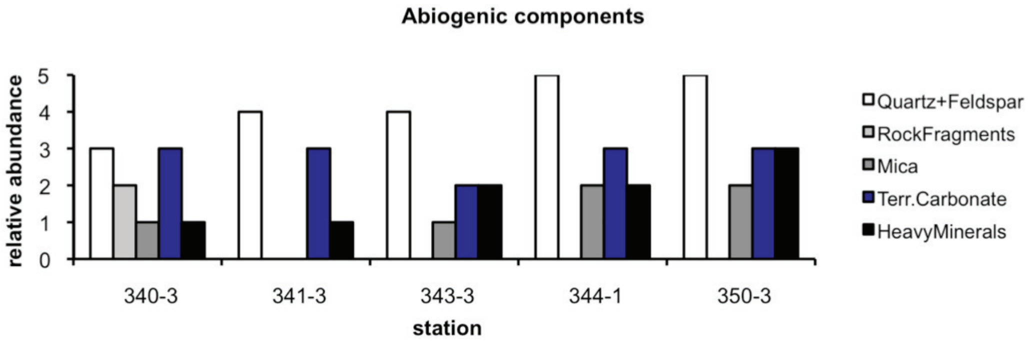

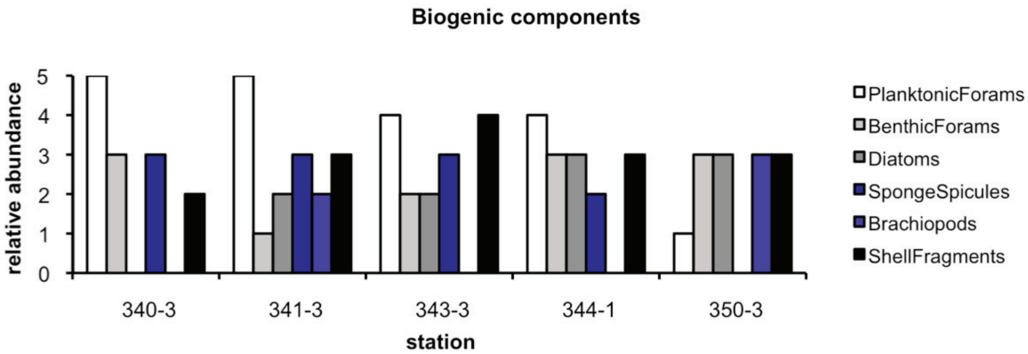

Fig. 19: Plot of abundance of abiogenic and biogenic components in the surface samples as based on coarse –fraction analysis (southern Mendeleev Ridge)

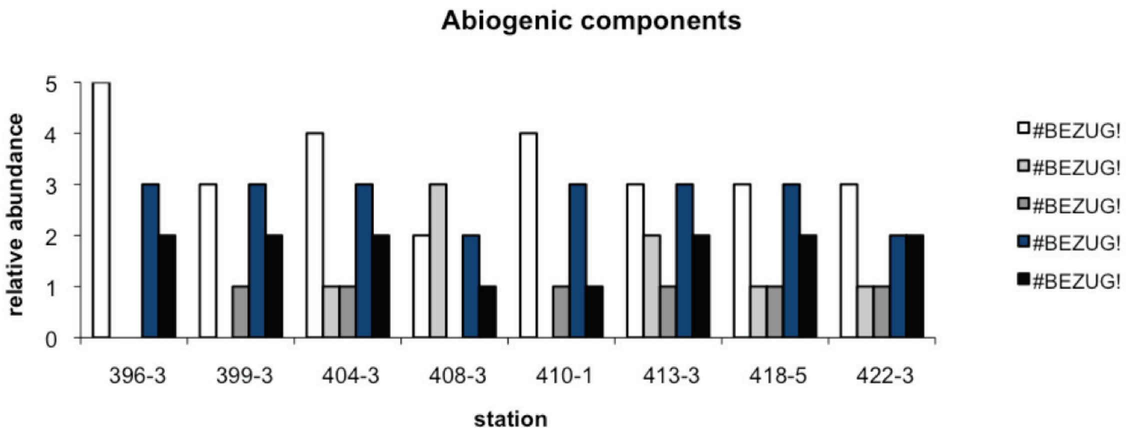

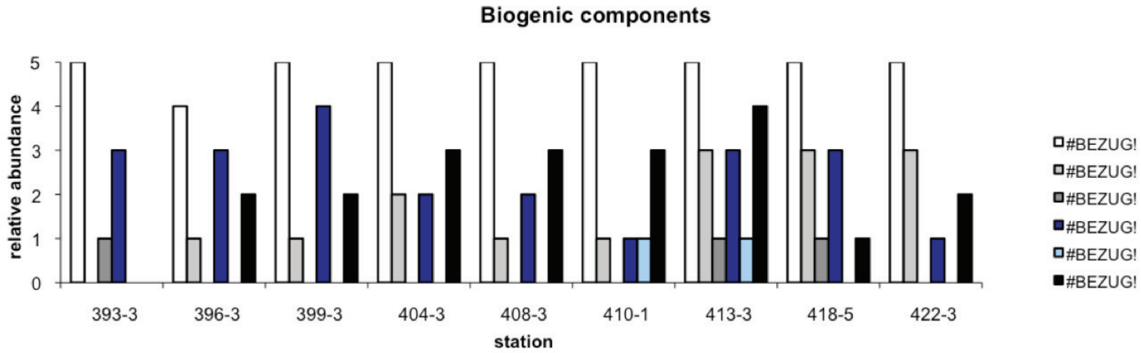

Fig. 20: Plot of abundance of abiogenic and biogenic components in the surface samples as based on coarse –fraction analysis (Mendeleev Ridge)

3.6 Characteristics of ARK-XXIII/3 sediment cores

3.6.1 Photographs of sediment cores

Christelle Not[1)], Juliane Müller[2)]

[1)] University of Quebec, Montreal
[2)]Alfred-Wegener-Institut, Bremerhaven

Core photographs are a good complement of the core description. They allow a good representation of the different colours, structures and cycles present along the core. Two different patterns have been used for the photography. For the GKG, photographs of the fresh sediment surface and of the box corer profile have been taken using a Nikon Coolpix P80 (zoom 27 - 486 mm). Furthermore some GKG boxes have been photographed like the long cores. The long core (SL and KAL) photographs have been done using the photographic system present on-board (Fig. 21) with a Olympus E-10 (lens diameter 62 mm, zoom 9 - 36 mm). Two different light intensities have been used during taking pictures, named as full and half. These two intensities give different information about the core. In general, the half intensity shows the colour of the sediment, and the full light gives a better view of the structure present in the sediment. During the cruise pictures of different quality have been produced. Figure 22 presents two examples of photos taken by the photographic system on-board. The upper part shows a bad picture, with red tendency and reflection whereas the lower part presents a good photo of the core. The difference between the two pictures is summarized by the identification of point where a particular attention is required (see Fig. 21):

- the support orientation
- the room light intensity
- the spot orientation
- the choice of the light intensity

For example, the room light (covered with aluminium paper for the good picture) and the orientation of the spots can create reflections on the sediment.

All the digital images are organized separately for each sediment core under the respective station and gear number in the data bank Pangaea (WDC-mare).

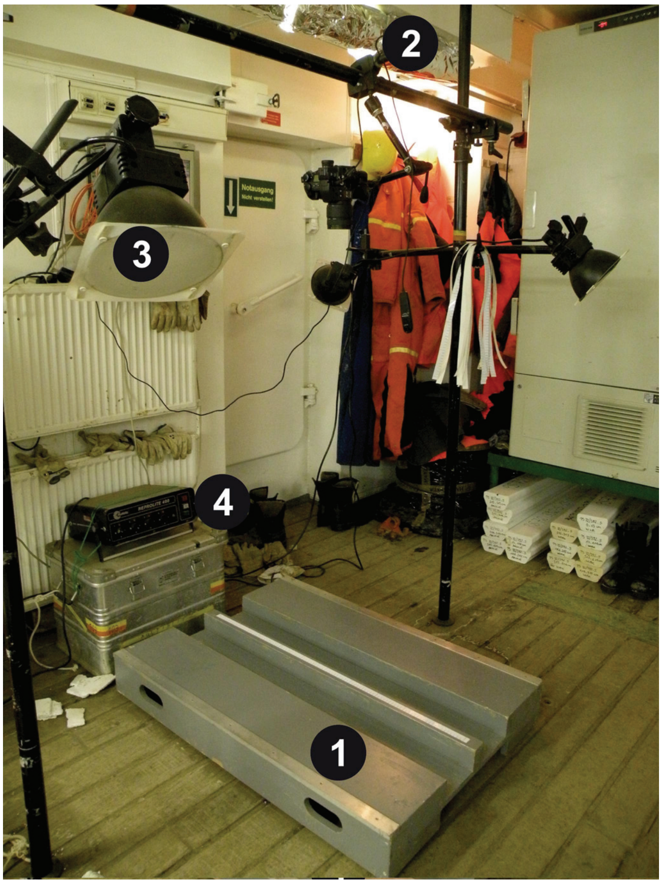

Fig. 21: On-board photography system. Numbers label the different parts where particular attention is required. 1 the support orientation. 2 the room light intensity. 3 spot orientation. 4 spot light intensity control.

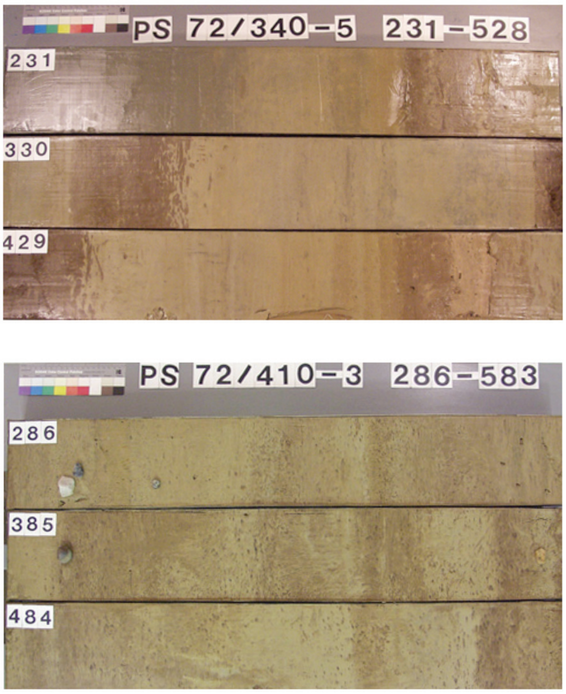

Fig. 22: Two examples of pictures from KAL. The upper part shows a bad photo of the core PS72/340-5 231 to 528 cm and the lower part shows a good photo of the core PS72/410-3 286 to 583 cm.

3.6.2 X-Ray photography: Sediment structures and IRD content

Jens Matthiessen[1], Bernhard Naafs[1], Evgenia Bazhenova[1,2], Christian März[3], Christelle Not[4], Michael Schreck[1]

[1] Alfred-Wegener-Institut, Bremerhaven
[2] State University, St. Petersburg
[3] Institute for Chemistry and Biology, Oldenburg
[4] University of Quebec, Montreal

Sediment slabs (250 x 100 x 8 mm) from almost every sediment core (GKG, SL, KAL) were prepared for x-radiography. Plastic slabs (252 x 103 x 12 mm) were slowly pushed into the scraped and smoothed sediment surface and carefully removed. These slabs were sealed in a plastic cover and the air was evacuated to stabilize the slabs. The slabs were placed on 100 x 300 mm large film stripes (Industrial X-Ray Film Agfa-Gevaert Structurix D4 FW 30 x 40) in a cabinet x-ray system (Hewlett-Packard Faxitron Series) and were exposed on the average for 6 minutes at 40 kV. Films were developed for 3 minutes (Agfa-Gevaert Developer Structurix G 128), washed for 1 minute and then fixed for 3 minutes (Agfa-Gevaert Fixing Bath Structurix G335). After washing in a water bath for 10 minutes the film negatives were dried and finally stored in a transparent cover.

An initial analysis of the negatives was conducted on a light table to study sedimentary structures and to count gravel particles (> 2 mm). The number of gravel particles in fields of 100 x 10 x 10 mm is routinely used as a measure of ice-rafted debris (IRD) and is tabulated as number of particles/10 ccm (Grobe 1987). Gravel particles in the studied cores generally have an angular shape indicating a glacial origin. The x-ray negatives will be scanned at AWI and after a final quality control all images and the gravel counts will be stored separately for each sediment core under the respective station and gear number in the data bank Pangaea (WDC-mare).

X-radiograph analyses confirm the visual core descriptions indicating that the sediments have a siliclastic composition. Biogenic particles (e.g. foraminifers, remains of molluscs) were rarely seen on the negatives, whereas bioturbation suggests a significant activity of bottom-living organisms that were not preserved in the sediments. The majority of the recovered long sediment cores (Fig. 6) can be grouped into four geographic areas: 1) Canada Basin, 2) Siberian continental slope, 3) Mendeleev Abyssal Plain and eastern Mendeleev Ridge, and 4) western Mendeleev Ridge and Makarov Basin. The single sediment cores from the Northwest Passage (PS72/289) and the East Siberian Shelf (PS72/350) are not considered here. The major sedimentary facies types are shortly described and a full facies analysis will be conducted after the expedition at AWI (Matthiessen et al. 2009). The term mud is used for silty clays to clayey silts that cannot be distinguished on x-radiographs.

a. Canada Basin (PS72/291-1, PS72/393-4)
The sediments generally consist of stratified to massive muds. Sediments are partly laminated (lamination on sub-mm scale) or comprise fining upward sequences grading from silts with sharp, partly erosional basal contacts into muds. Cross-bedding and load casts occur occasionally. These sediments may be interpreted as distal turbidites and/or contourites. Bioturbation and IRD is restricted to a few distinct layers of muds to sandy muds representing glaciomarine deposition (Fig. 23).

b. Siberian Continental Slope (Transect 1: PS72/340-5 to PS72/344-3)
The sediment cores are located along a transect across the Mendeleev Ridge located at the lower continental slope. The sediments consist of an alternation of stratified to massive muds, bioturbated muds with variable gravel and sand contents, and diamictons. IRD occurs in the diamictons, in distinct layers or is scattered throughout the bioturbated intervals. The distribution is not related to a common colour facies but is enriched in most brown layers (including the pink layers) that are regularly distributed in the sediment cores (Fig. 23). Stratified muds are almost free of IRD and have partly a distinct sub-mm scale lamination or comprise fining-upward sequences. Stratified and massive muds are generally more abundant in the eastern part of the transect. These sediments were generally deposited in a glacio-marine setting with IRD-rich layers probably representing de-glacial sequences and/or sea ice/iceberg melting events. The massive to stratified muds at the continental slope might have been caused by melt water discharge, nepheloid layer transport, and/or bottom-current induced sedimentation.

c. Mendeleev Abyssal Plain and eastern Mendeleev Ridge (Transect 2: PS72/392 – PS72/413)
The sediment cores of the deep-sea transect from the Nautilus Basin to the Mendeleev Ridge comprise two distinct units. The upper unit (down to 200 - 400 cm core depth) consists of alternating bioturbated to stratified muds to sandy muds and sandy diamictons with common to abundant IRD partly enriched in distinct layers and diamictons of variable colour (Fig. 24). Fining-upward sequences grade from sandy muds into muds. Contacts are distinctly gradational or sharp. These sediments are of glaciomarine origin with a strong contribution of sediments from melting sea ice

and/or icebergs. The lower unit differs in consisting of monotonous bioturbated muds which are almost free of IRD. Sandier layers are rare. A deposition in a glaciomarine setting is likely with possible minor contribution of iceberg-rafted sediments.

d. Western Mendeleev Ridge and Makarov Basin (Transect 2: PS72/418- PS72/430)
These sediment cores from the western half of the northern transect do not show such a clear subdivision as the cores from the eastern half. These cores are generally characterized by an alternation of bioturbated muds with variable IRD contents, either scattered in beds or enriched in distinct layers, and massive to stratified muds. These muds often show wavy to erosional contacts and stratification is caused by lamination, fining upward sequences, ripple marks and cross-bedding. Occasionally gravity flow structures and load casts have been observed. The structures indicate transport by currents and/or mass flows (distal turbidites, contourites) while the bioturbated muds represent glacio-marine sedimentation with a variable supply of IRD from icebergs/sea ice.

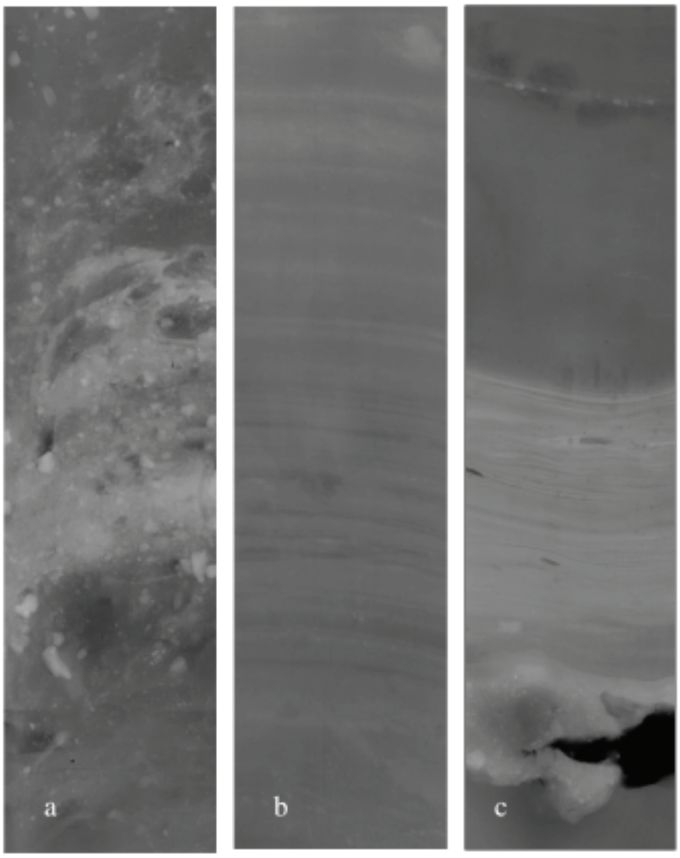

Fig. 23: X-radiographs from selected core intervals

a. *Brown and light reddish brown („pinkish“) silty diamicton (498-513 cm) in sediment core PS72/340-5.*
b. *Laminated sediments in sediment core PS72/340-5 (450-466 cm).*
c. *Diamicton, massive muds, and current-transported silts in sediment core PS72/393-4 (393-419 cm).*

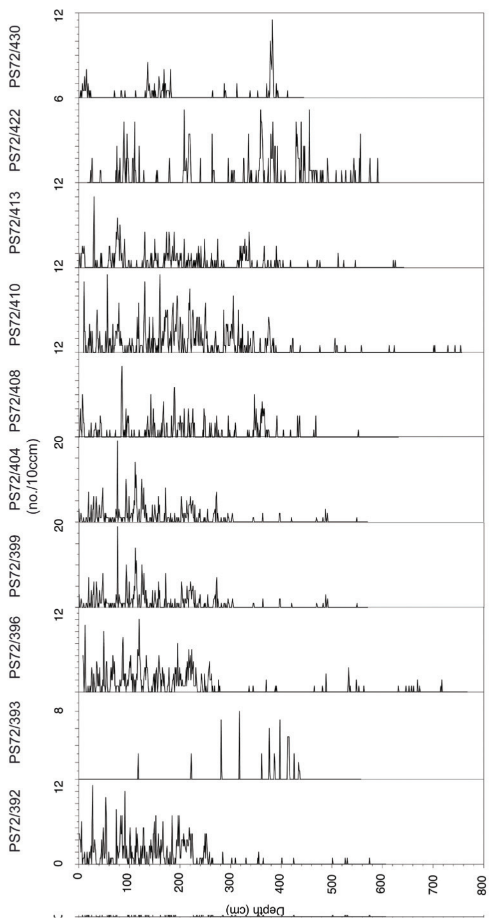

Fig. 24: IRD records of sediment cores from the northern transect

3.6.3 Results of smear-slide analysis

Alexey Krylov
Viniio, St. Petersburg

Onboard *Polarstern* a selected set of sediment cores was sampled for smear-slide analyses. These sediment cores are located in Barrow Strait (PS72/287-3), at the Mackenzie Slope (PS72/291-2), on the southern Mendeleev Ridge (PS72/340-5, PS72/342-1 and PS72/344-3) and on the Northern Mendeleev Ridge (PS72/392-5, PS72/396-5 and PS72/422-5) (for location of the cores see Fig. 6). A total of 150 smear-slides were investigated under the light microscope. Smear-slides description was performed for rough evaluation of grain-size composition, preliminary determination of mineralogical composition and content of biogenic components (foraminifers, coccoliths, diatoms, sponge spicules).

Based on smear-slide analyses, the main minerals are quartz, terrigeneous carbonates (mainly dolomite) and clay minerals. The contents of feldspar, mica, Fe-hydroxides and heavy minerals are usually less than 10%. The heavy minerals are presented by clinopyroxene, hornblende, epidote, garnets, zircon, and black ores. The results of smear-slide description are shown in Fig. 25 to 29 and in the appendix (App. 4.2 Tab. 1 – 8).

15 smear-slides were examined in Core PS72/287-3 (Fig. 25; App. 4.2 Tab. 1). The sediments in this core are characterized by elevated contents of terrigeneous

carbonates and quartz. The amount of terrigeneous carbonates strongly increased below 290 cmbsf; close to this boundary the main lithological change is also observed. The main biogenic components are represented by diatoms and foraminifers. The clay-sized particles are predominant in the sediments.

8 smear-slides were taken from Core PS72/291-2 in the uppermost 150 cm (App. 4.2 Tab. 2). The main components are clay minerals, quartz and terrigenous carbonates. The sediments are composed of silty clay.

42 smear-slides were taken from Core PS72/340-5 between 7 and 807 cmbsf (Fig. 26; App. 4.2 Tab. 3). The 7 “pinkish” layers observed in this core are characterized by elevated concentration of dolomite and sand. Interestingly, biogenic components were observed in the “brown” layers almost through out the whole section until 760 (coccoliths) and 800 (foraminifers) cmbsf. However, the abundance of coccoliths must be checked onshore by a specialist.

The sediments in Core PS72/342-1 are silty clays or sand-bearing silty clays (Fig. 27; App. 4.2 Tab. 4). Quartz and feldspar slightly increase from the top to bottom, whereas terrigenious carbonates show the opposite trend. The elevated contents of coccoliths and foraminifers in the brownish layers between 130 and 180 cmbsf may represent MIS 3.3.

Only 6 smear-slides were taken from the upper 3 m of Core PS72/344-3 (App. 4.2 Tab. 5). These sediments are represented by silty clay. The main components are clay minerals and quartz. Concentration of dolomite is low (1-4%) with one exception at 290 cmbsf (15%).

Core PS72/392-5 (Clark’s key site FL-224) was investigated in detail (26 smear-slides, Fig. 28; Tab. App. 4.2 Tab. 6). The sediments are represented by silty clay and sand-bearing silty clay. Several “white” and “pinkish” layers are mainly composed of dolomite. The amount of dolomite is strongly decreased at about 240 cmbsf coinciding with the boundary between lithological unit I and II. Foraminifers and coccoliths are observed only in the uppermost 180 cmbsf.

Core PS72/396-5 is located relatively close to Clark’s key site. Dolomite is abundant in the “white” and “pinkish” layers in the uppermost 160 cm but disappear at approximately 230 cmbsf. Several peaks of foraminifers and coccoliths are observed in the upper 200 cm. The elevated concentrations of quartz and feldspar usually coincide with sandy layers (Fig. 29; App. 4.2 Tab. 7).

13 smear-slides were taken from the uppermost 362 cm of Core PS72/422-5 (App. 4.2 Tab. 8). The sediments are mainly composed of silty clay. Elevated concentrations of dolomite are observed in the “pinkish” layers at 93 and 220 cmbsf (45 and 50% respectively). In the other layers clay minerals and quartz are the most abundant components (more than 10%). Biogenic components are very rare in this core.

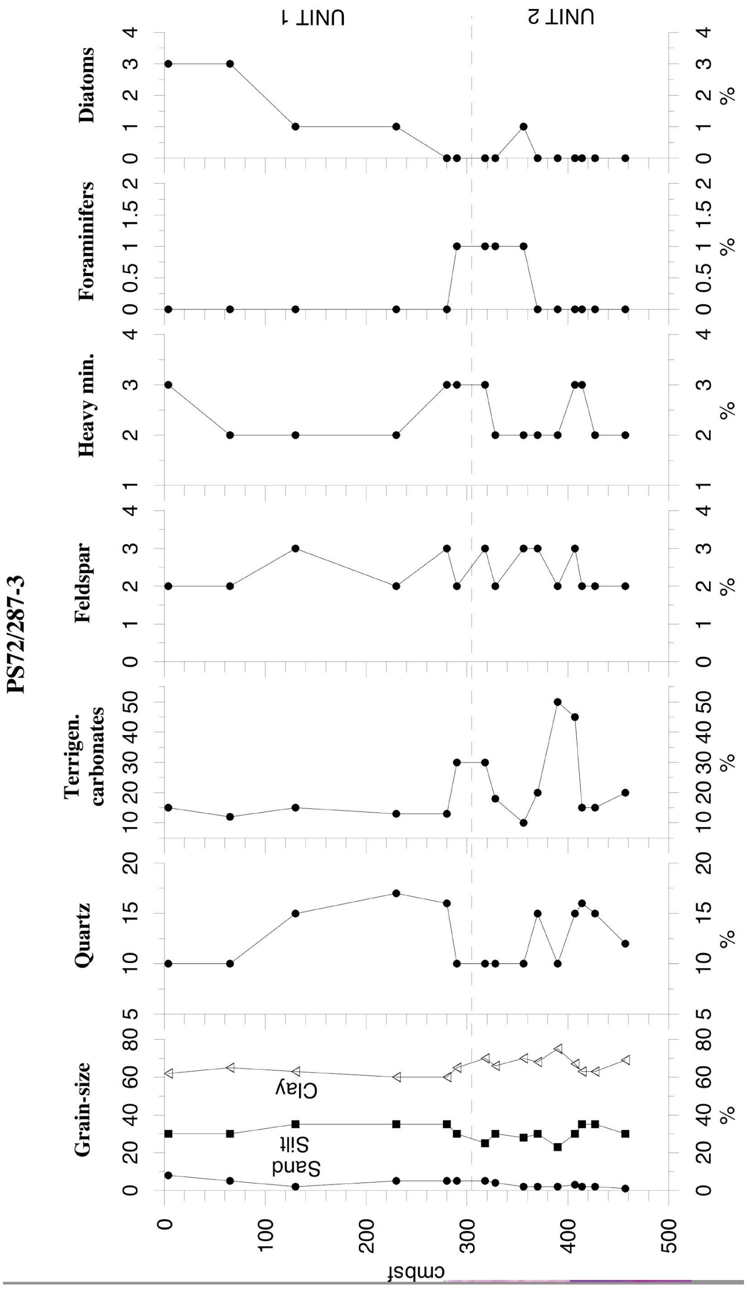

Fig. 25: Grain-size and composition of Core PS72/287-3, based on smear-slide estimates

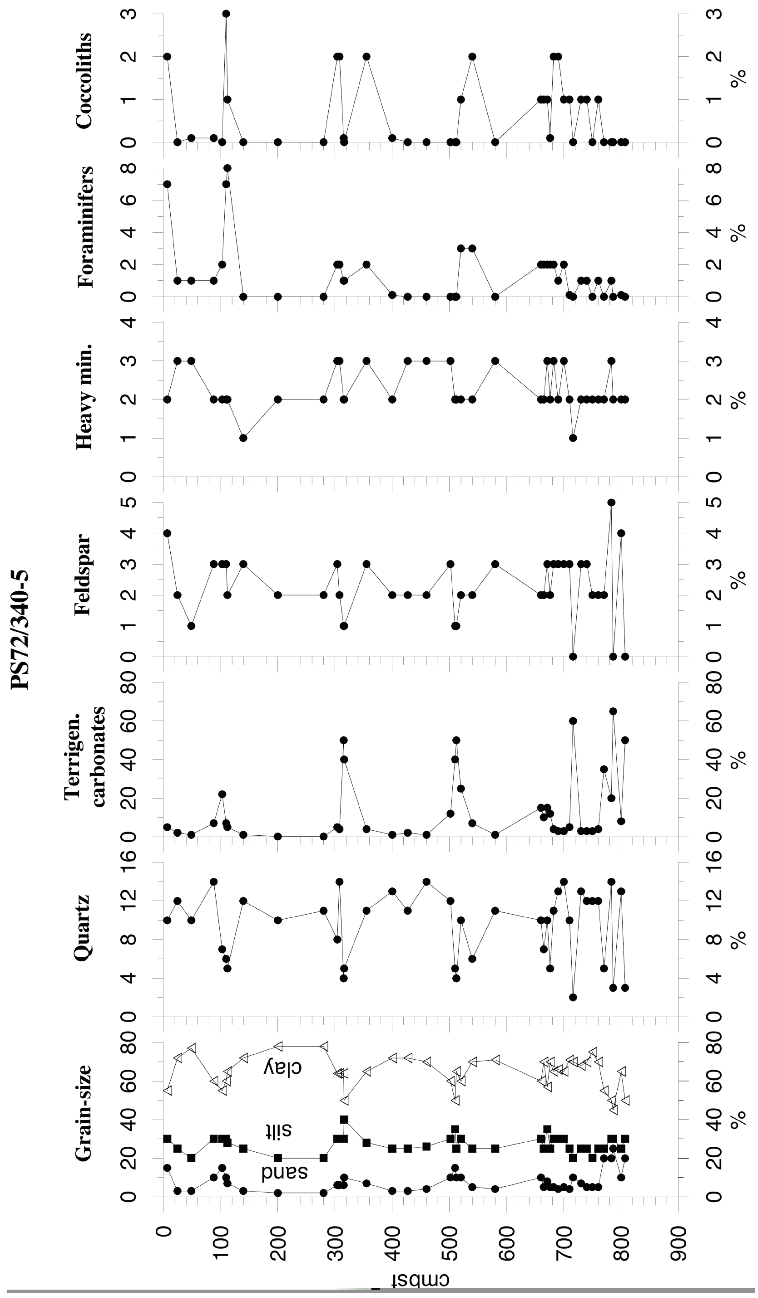

Fig. 26: Grain-size and composition of Core PS72/340-5, based on smear-slide estimates

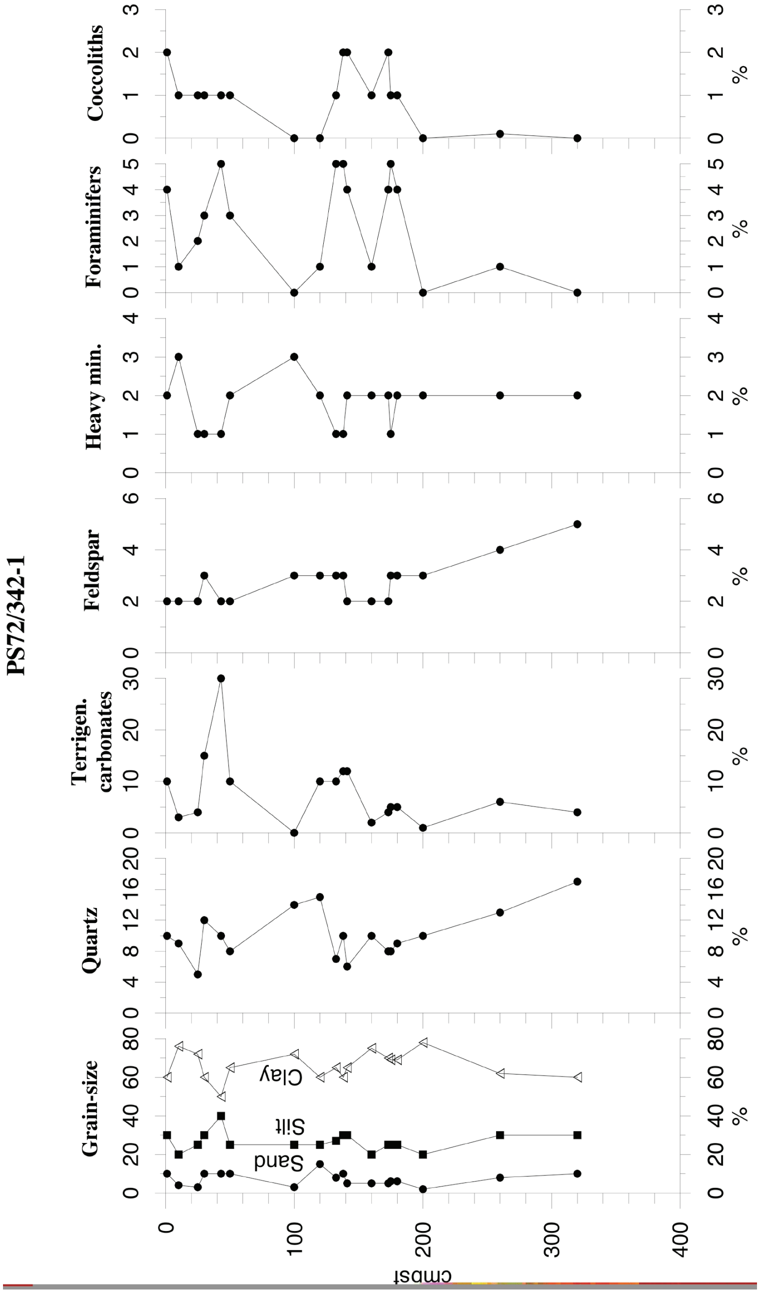

Fig. 27: Grain-size and composition of Core PS72/342-1, based on smear-slide estimates

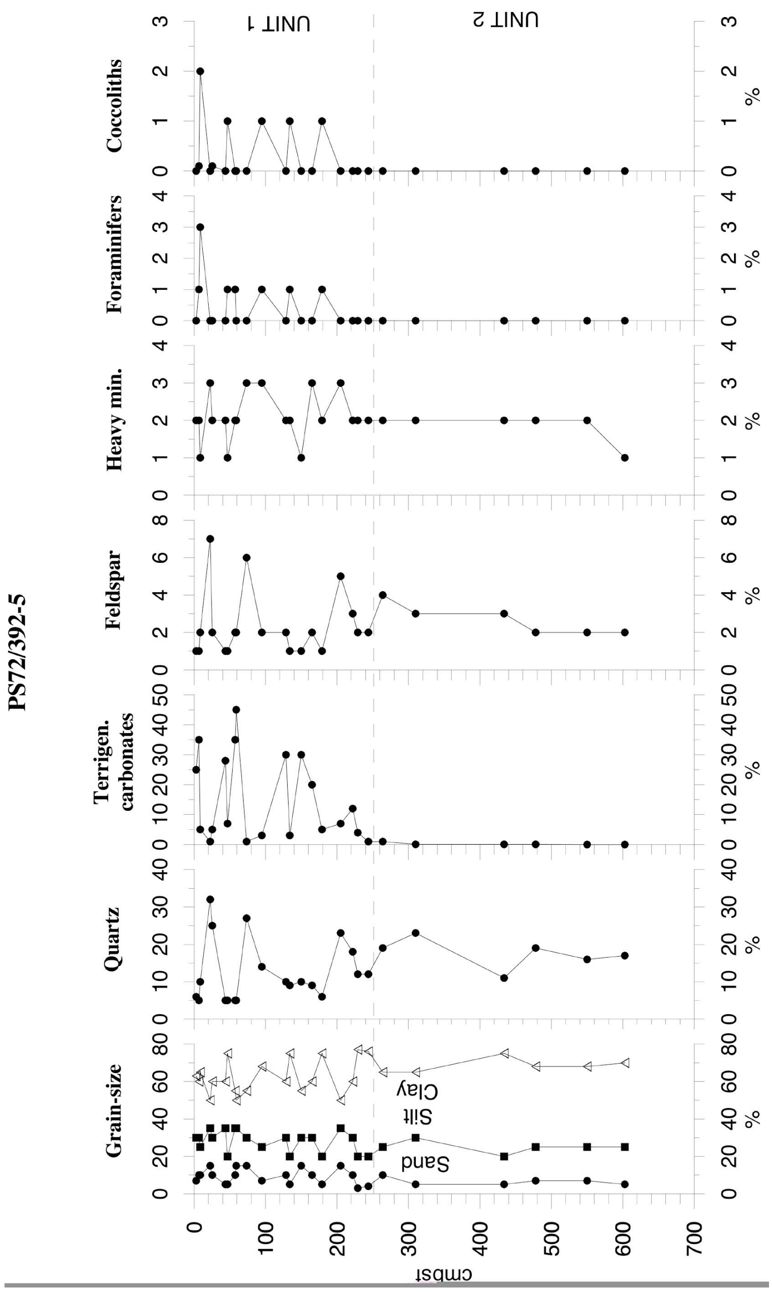

Fig. 28: Grain-size and composition of Core PS72/392-5, based on smear-slide estimates

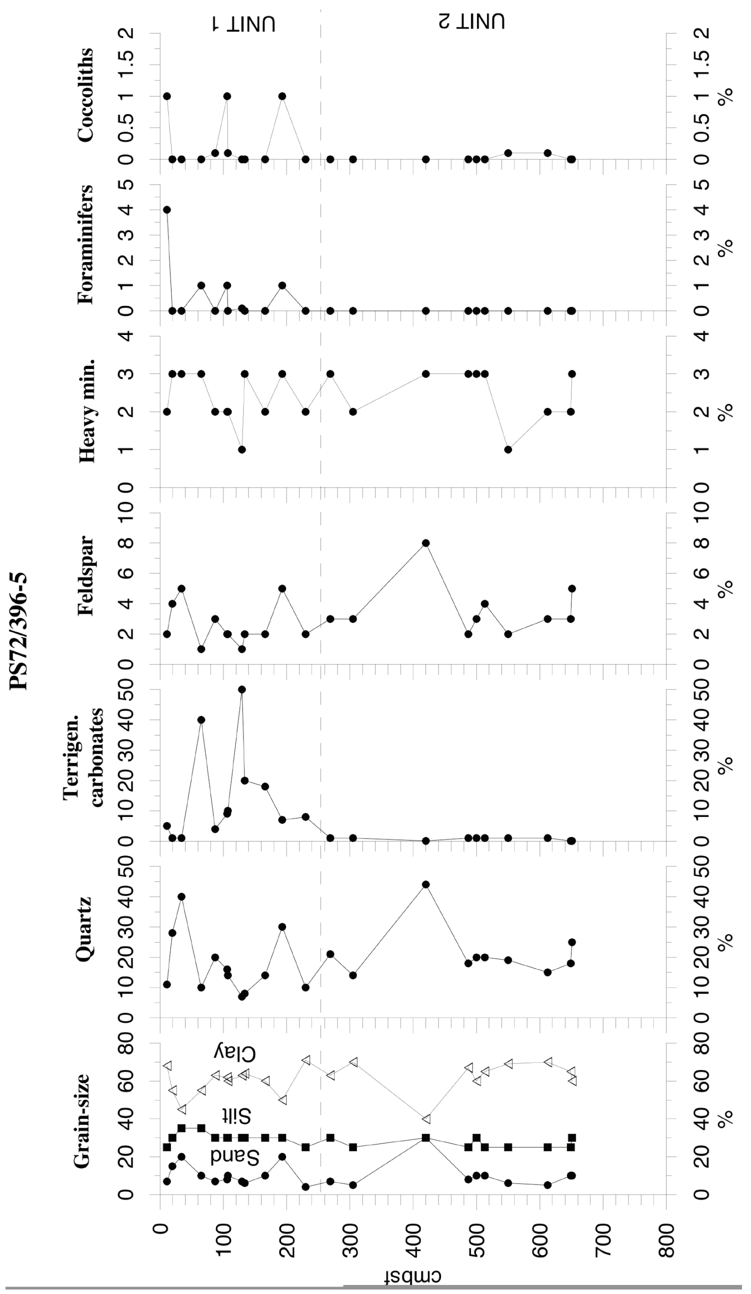

Fig. 29: Grain-size and composition of Core PS72/396-5, based on smear-slide estimates

3.6.4 Results of coarse fraction analysis

Seung-Il Nam
Korean Institute for Geoscience, Seoul

In order to estimate the abundance of sediment components within the sand fraction onboard *Polarstern*, large amounts of sediment samples were taken from 5 Kastenlot cores recovered from the southern and northern transects across the Mendeleev Ridge. The samples were wet-sieved with a mesh of 63 μm to separate the coarse fraction (> 63 μm) from the silt and clay fractions. The coarse fraction was dried at 60°C, and then was sieved with a mesh of 125 μm to separate the coarse sand and gravel fractions of >125 µm from the fine sand fraction of <125 µm. Furthermore, the coarse fractions of >125 µm were sieved with a mesh of 500 µm to separate the coarse sand and gravel of >500 µm. The composition of the fractions between 125 µm and 500 µm was estimated using a binocular microscope. In addition to the coarse fraction analysis, about 15 specimens of planktonic foraminifera *N. pachyderma* sin. were picked from the 125 - 250 µm subfraction for stable oxygen and carbon isotope analysis which will be done at the Alfred Wegener Institute for Polar and Marine Research. The composition of the coarse fraction between 125 µm and 500 µm was estimated on the basis of five simple categories (0-5). The abundance of each component was simply expressed in the five criteria of 0 to 5 (0, absent; 1 very rare; 2, rare; 3, common; 4, abundant; 5, dominant).

According to the semi-quantitative estimation, the sediment components of 125 µm to 500 µm can be simply classified into siliciclastic (terrigenous), biogenic and authigenic components. The siliciclastic components are mainly composed of quartz, feldspar, rock fragment, mica, carbonate/dolomite, basalt and heavy minerals. The biogenic components consist mostly of planktonic and benthic (calcareous and agglutinated) foraminifera, ostracoda, mollusca and biogenic opal such as radiolarian, diatoms and sponge spicules. The authigenic component consists mainly of micro-manganese nodules.

Preliminary results from Transect 1 across Mendeleev Ridge

The preliminary results are shown in Fig. 30 and 31. In most sediment samples of the two cores PS72/340-5 and PS72/341-5, the dominant siliciclastic components are quartz and feldspar, while common to minor amounts of rock fragments, terrigenous carbonate, basalt, mica and heavy minerals occurred throughout the core. In contrast, the biogenic components are mostly dominated by planktonic foraminifera with an almost monospecific assemblage of *N. pachyderma* sin.. *N. pachyderma* dex. (subpolar species) together with other subpolar species like as *G. quinqueloba, G. bulloides* is also present, but with small amounts which is generally evidence of relatively increased sea surface temperature due to advection of the North Atlantic Surface Water into the Arctic Ocean mostly during the interglacial periods. Therefore, most intervals with dominant planktonic and benthic foraminifera might be tentatively interpreted as interglacial periods (MIS 7, 5.5 and Holocene). During these intervals, *N. pachyderma* dex. may be common. In addition, agglutinated foraminifera are present with small amounts. Sponge spicules as dominant biogenic biosilceous component mostly occurred throughout core PS72/341-5. In the same core, ostracoda and mollusca are also observed. The micro-manganese nodules mostly occurred in the brown coloured layers with a high variability from being absent to dominant in core PS72/340-5. However, in core PS72/341-5 the micro-manganese nodules occurred with relatively low amounts.

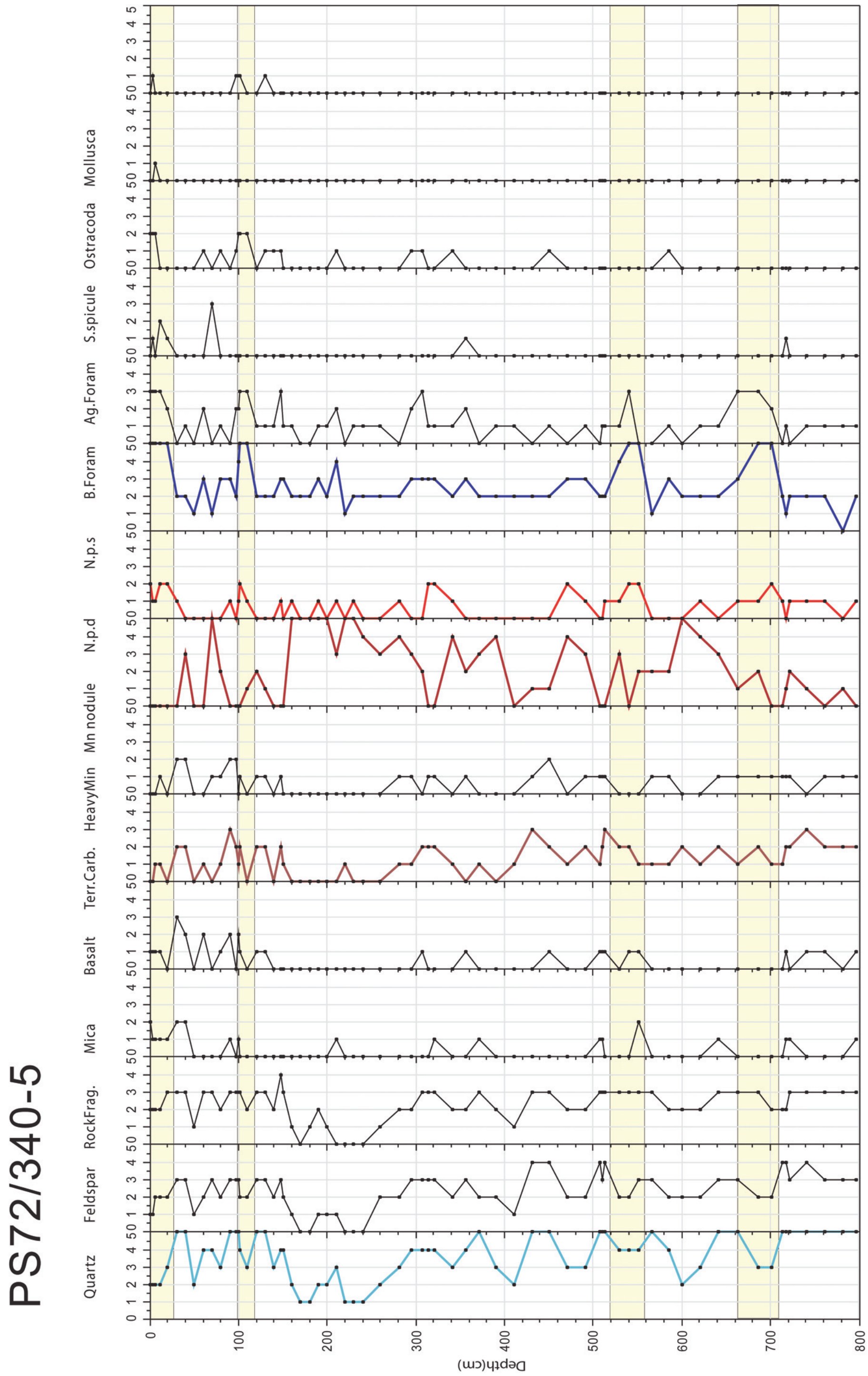

Fig. 30: Down-core variations in siliciclastic, biogenic and authigenic sediment components estimated from the coarse sand fraction between 125 µm and 500 µm of core PS72/340-5. Note that scales from 0 to 5 indicate relative abundance of each component (0, absent; 1, very rare; 2, rare, 3, common; 4, abundant; 5, dominant). Shadow area indicates intervals with high amounts of foraminiferal tests within the sediment cores.

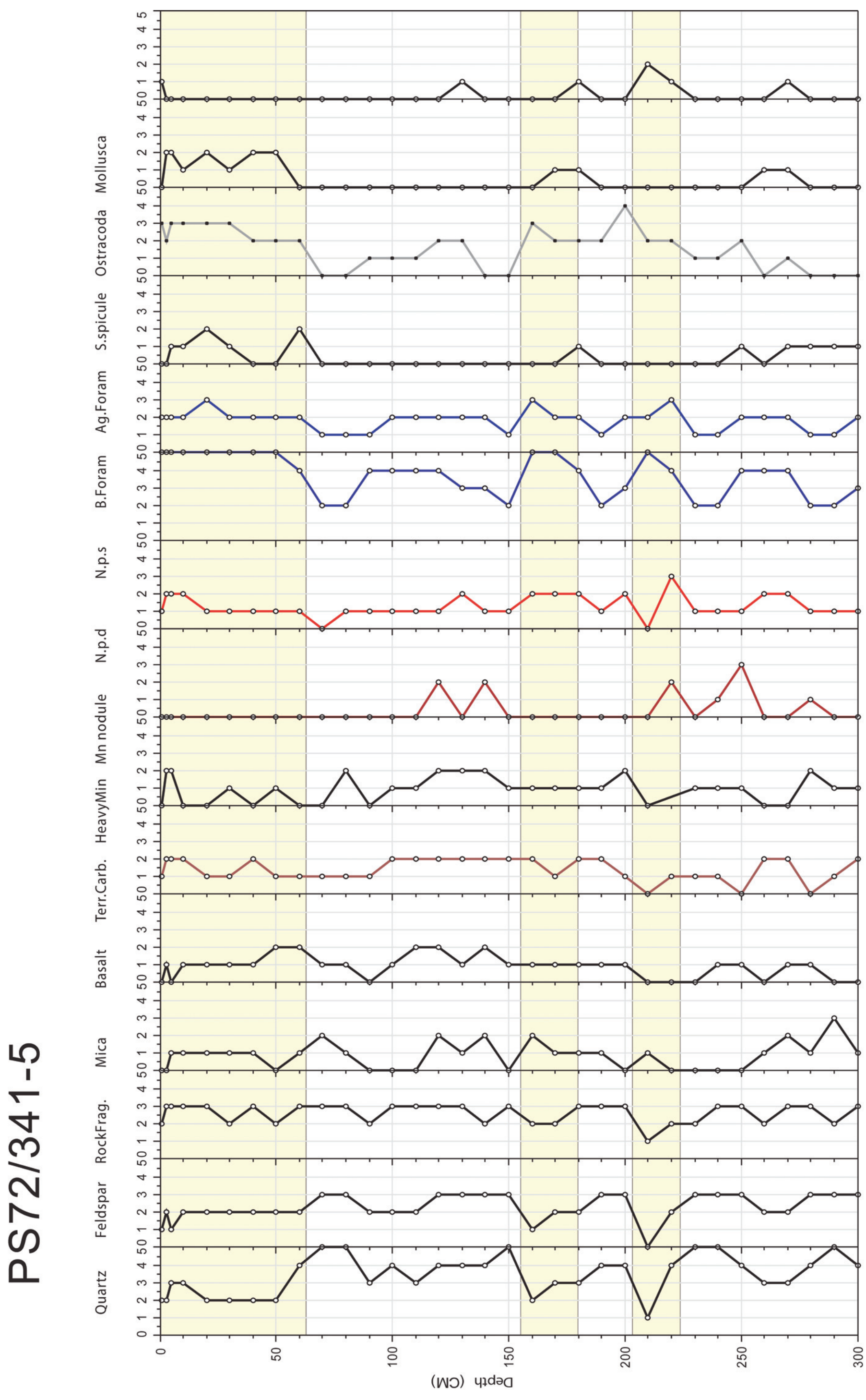

Fig. 31: Down-core variations in siliciclastic, biogenic and authigenic sediment components estimated from the coarse sand fraction between 125 µm and 500 µm of core PS72/341-5. Note that scales from 0 to 5 indicate relative abundance of each component (0, absent; 1, very rare; 2, rare, 3, common; 4, abundant; 5, dominant).
Shadow area indicates intervals with high amounts of foraminiferal tests within the sediment cores.

Preliminary results from Transect 2 across Mendeleev Ridge

Terrigenous components in core PS72/396-5 are characterized by predominance of quartz and relatively high amounts of feldspar and mica as well as minor amounts of rock fragments, carbonate, heavy minerals and basalt (Fig. 32). In particular, it is interesting to note that mica with golden colours occurred with high amounts in the intervals from the bottom to 295 cm in core depth. Similar to the cores from the Transect 1, monospecific planktonic foraminifera assemblages of *N. pachyderma* sin. are the most dominant biogenic component while calcareous benthic foraminifera are rare to common. However, calcareous planktonic and benthic foraminifera are restricted to the upper 2 m, while rare agglutinated benthic foraminifera occurred below 4 m core depth. Similar to the foraminiferal occurrence, few sponge spicules occur in the upper 2 m. The micro-manganese nodules show high fluctuations varying from being absent to abundant. Interestingly, similar patterns with fluctuations in abundance of foraminiferal tests, micro-manganese nodules and mica with golden colours are also observed in the other two cores PS72/410-3 and PS72/422-5. In particular, the abrupt occurrence of calcareous foraminiferal tests together with sponge spicules at about 2 m core depth might be correlated with the same patterns in the other cores PS72/410-3 and PS72/422-5.

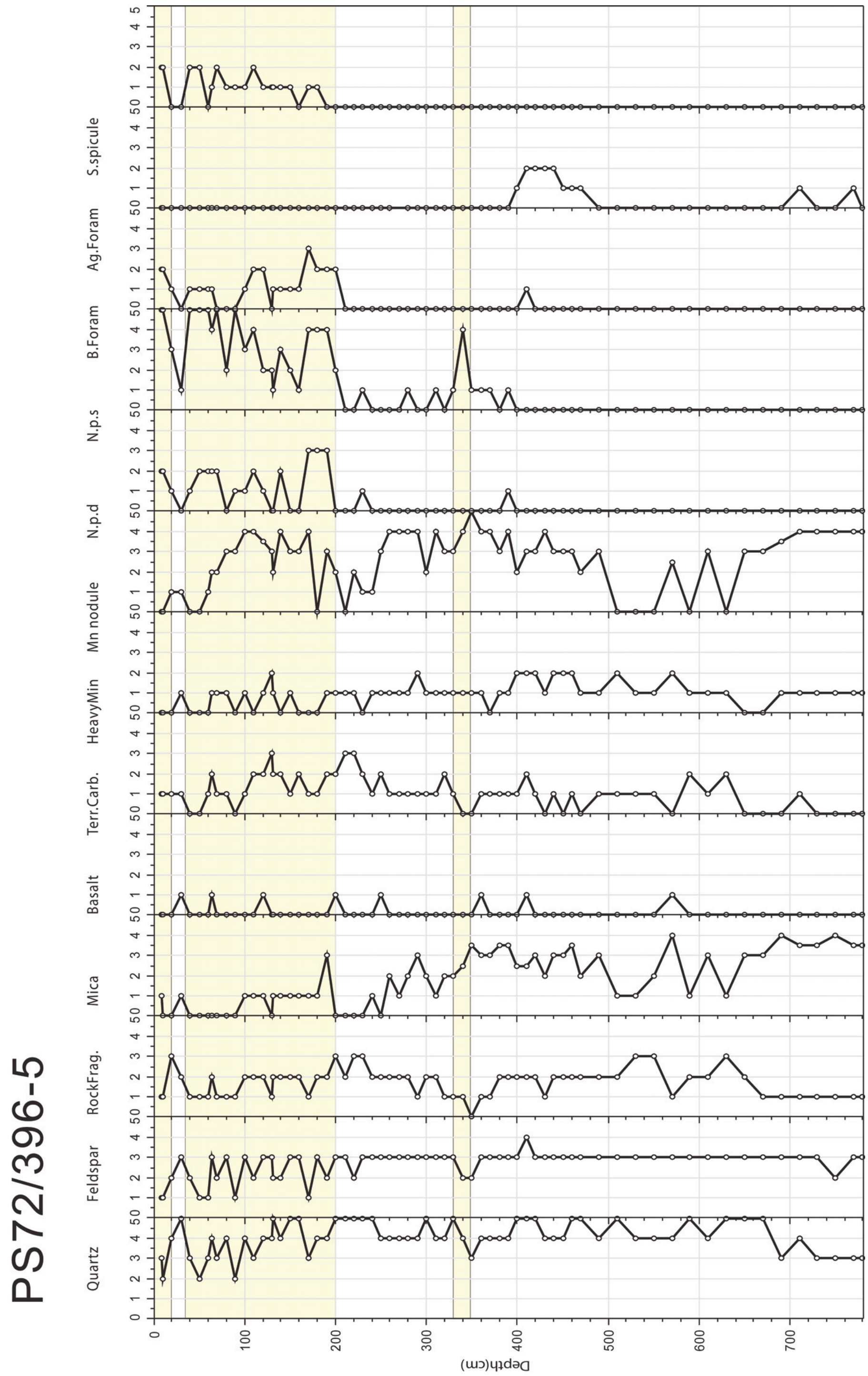

Fig. 32: Down-core variations in siliciclastic, biogenic and authigenic sediment components estimated from the coarse sand fraction between 125 µm and 500 µm of core PS72/396-5. Note that scales from 0 to 5 indicate relative abundance of each component (0, absent; 1, very rare; 2, rare, 3, common; 4, abundant; 5, dominant).
Shadow area indicates intervals with high amounts of foraminiferal tests within the sediment cores.

3.6.5 Occurrence of dropstones

Alexey Krylov
VINIIO, St. Petersburg

436 large-sized stones (> 1 cm) were collected during description and sampling of the sediments cored by Gravity Corer (21 stones), Kastenlot (89 stones), Multicorer (17 stones) and Box Corer (309 stones). A list of the stones, their sizes and preliminary identifications are shown in the Annex (App. 4.3). The occurrence of stones in cores PS72/287-3, PS72/340-5, PS72/396-5, PS72/410-3 and PS72/422-5 is shown in Fig. 33.

Stones are mainly composed of carbonates (dolomite) and to a lesser degree of sandstones. Igneous rocks (granites, diorites, and basalts), chert and schist are infrequent. Concentration of carbonates decrease to the Lomonosov Ridge. In order to reconstruct the source areas of the stones more accurately, thin sections will be made from selected stones for petrographic analysis during a shore-based study.

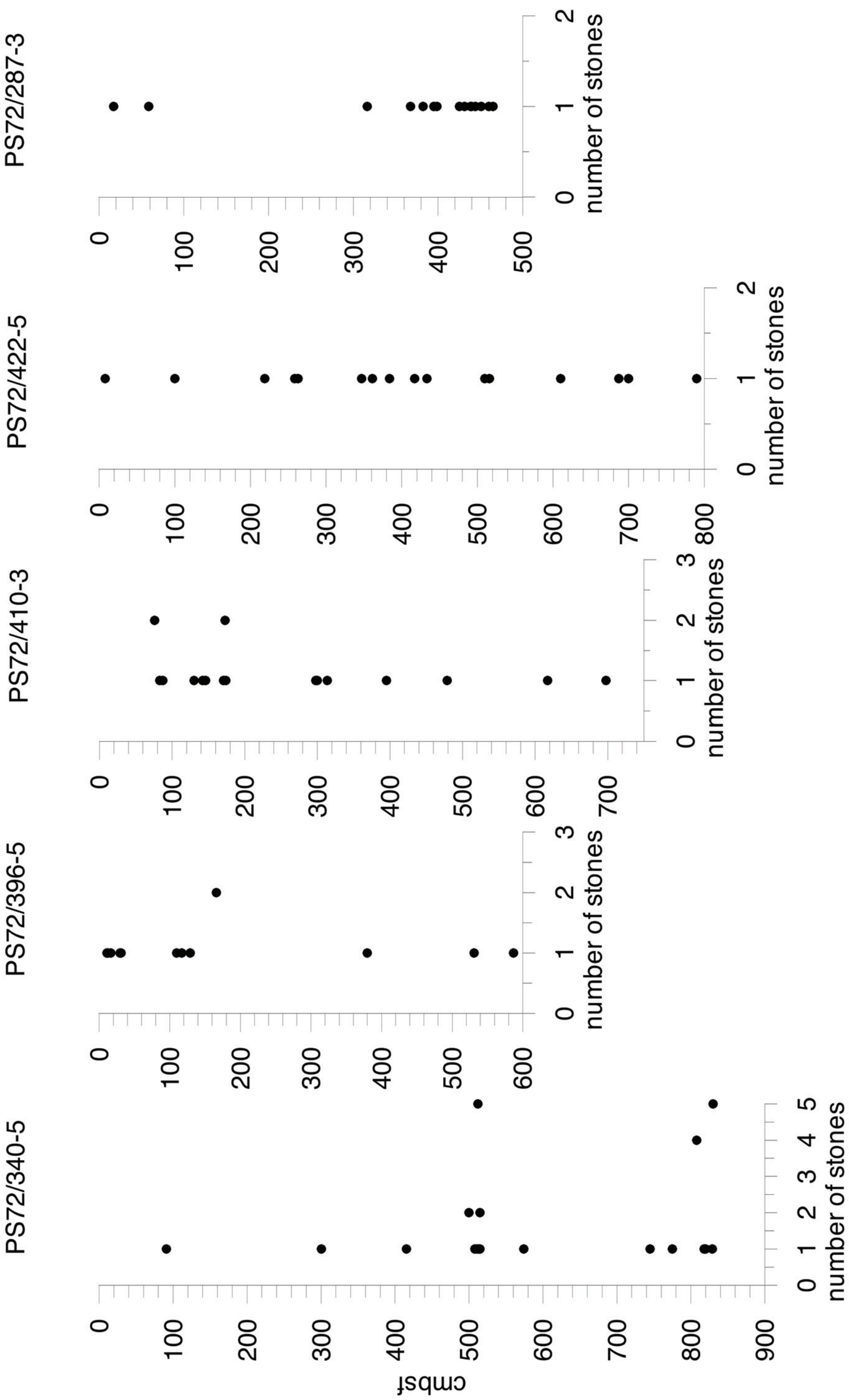

Fig. 33: Occurrence of stones in selected ARK-XXIII/3 sediment cores

3.6.6 Main lithologies and lithostratigraphy of ARK-XXIII/3 sediment cores

Rüdiger Stein[1)], Alexey Krylov[2)], Jens Matthiessen[1)], Seung-Il Nam[3)], Frank Niessen[1)] and the ARK-XXIII/3 Geoscientific Party

[1)] Alfred-Wegener-Institut, Bremerhaven
[2)] VINIIO, St. Petersburg
[3)] Korean Institute for Geoscience, Seoul

During the *Polarstern* Expedition ARK-XXIII/3, sediment cores were taken at 15 stations in total (see Chapter 3.4 for details). In the following, the main lithologies of the recovered sediments from selected areas are described and some preliminary interpretations are given:

(1) Barrow Strait / Northwest Passage
(2) Mackenzie continental slope and central Canada Basin
(3) Transect 1; southern Mendeleev Ridge (77°40' N)
(4) Transect 2; central Mendeleev Ridge (80°30' N)

The detailed lithological core descriptions of all Kastenlot and gravity cores are shown in the appendix.

Barrow Strait / Northwest Passage

Core PS72/287-3 SL (74°15.95'N, 90°59.09'W; water depth 337 m) was recovered in Barrow Strait in the Canadian Arctic Archipelago (see Fig. 6 for location). The 463 cm long sedimentary section can be divided into two lithological units. Unit I (0 – 3.12 m) is mainly composed of olive brown (upper 33 cm) and olive gray to (dark) grayish brown, partly bioturbated silty clay to sandy silty clay. Ice-rafted debris (IRD) > 2 mm (as counted in X-Ray photographs) only occur in minor amounts, with minimum values (almost absence) between about 100 and 250 cm and increasing number in the uppermost 70 cm. Shell debris was found at 74, 103 - 105, and 141-142 cm, and large (about 3 cm in length) well preserved gastropods were found at 43 - 45 and 165 - 165 cm. Larger dropstones are very rare in Unit I. Unit II (312 - 463 cm) dominantly consists of grayish brown, light grayish brown, and light gray to gray sandy silty clay and silty clay with common occurrence of dropstones. The occurrence of dropstones ranging in size from 0.5 to 7 cm in diameter, is the main difference to Unit I. Dropstones are especially enriched between 378 and 399 cm, between 412 and 428 cm, and in the lowermost part of the core, classifying the sediment as diamicton. The intervals with highest amounts pf large-sized dropstones are also characterized by maximum numbers of IRD > 2 mm (Fig. 34). Furthermore, maxima in IRD and dropstones coincide with maxima in wet bulk density and – although not always – in magnetic susceptibility (Fig. 34).

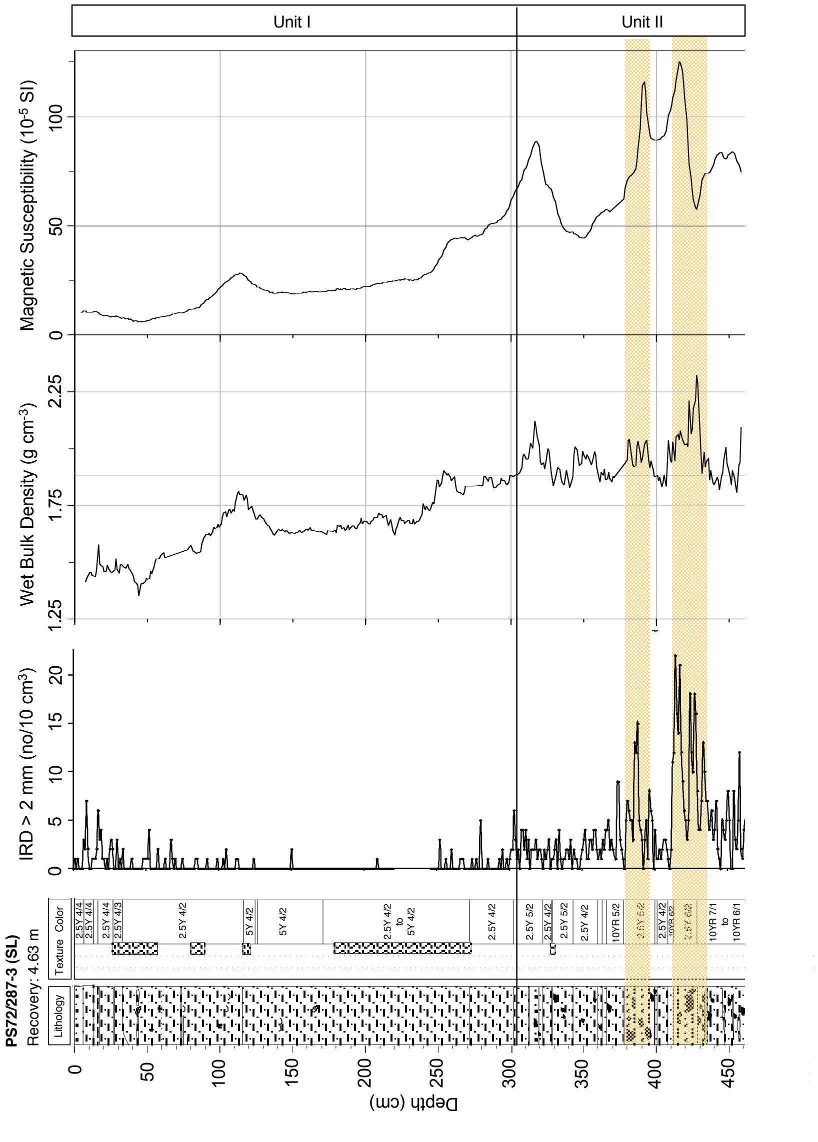

Fig. 34: Lithology, amount of IRD >2 mm (counting in X-Ray photographs), and wet bulk density and magnetic susceptibility from multi-sensor core logging of Core PS72/287-2.

Unit II probably represent the final stage of the last glaciation and/or the deglacial period. An extended ice sheet and its subsequent decay resulted in the formation of diamictons and large input of IRD at the core location (Fig. 35). Unit I represents the post-glacial Holocene time interval when seasonally open-marine conditions were predominant. The elevated IRD values in the uppermost part of the record suggesting increased IRD input due to an advance of glaciers on the surrounding islands (e.g. Devon Island), may correlate with the late Holocene neo-glaciation. During this time period, i.e., during the last about 3000 yrs. BP, also an advance of glaciers in western Norway was recorded (Nesje et al., 2001).

Mackenzie continental slope and central Canada Basin

At two locations from the Canada Basin (Cores PS72/291-2 and PS72/393-4; see Fig. 6 for location), sediments were recovered which totally differ from the sediments recovered at all other stations during the ARK-XXIII/3 expedition. Whereas the latter mainly represent undisturbed pelagic sedimentation (see below), the sediments of the Canada Basin cores are mainly composed of distal fine-grained turbidites.

Core PS72/291-2 (Mackenzie slope/southern Canada Basin; 71°16.18'N, 137°10.82'W; 1502 m of water depth) consists of two lithological units. Unit I (0 – 152 cm) is characterized by three different types of sediment facies. Facies 1 is a bioturbated brown, greyish brown, and olive brown silty clay (representing pelagic sedimentation); Facies 2 (90 – 99 cm and 141 – 150 cm) is a dark greyish brown to greyish brown silty clay to sandy silty clay with abundant reddish brown („pinkish") lenses/clasts and dropstones, and Facies 3 is characterized by dark grey to dark greyish brown laminated fine-grained (silty clay to clay; some sand) sediments. Unit II mainly consists of dark greyish brown, very dark grey to dark olive grey clay, intercalated with thin coarser-grained (silty) layers (fining-upward cycles). Occasionally, small pinkish grey lenses occur (Fig. 35).

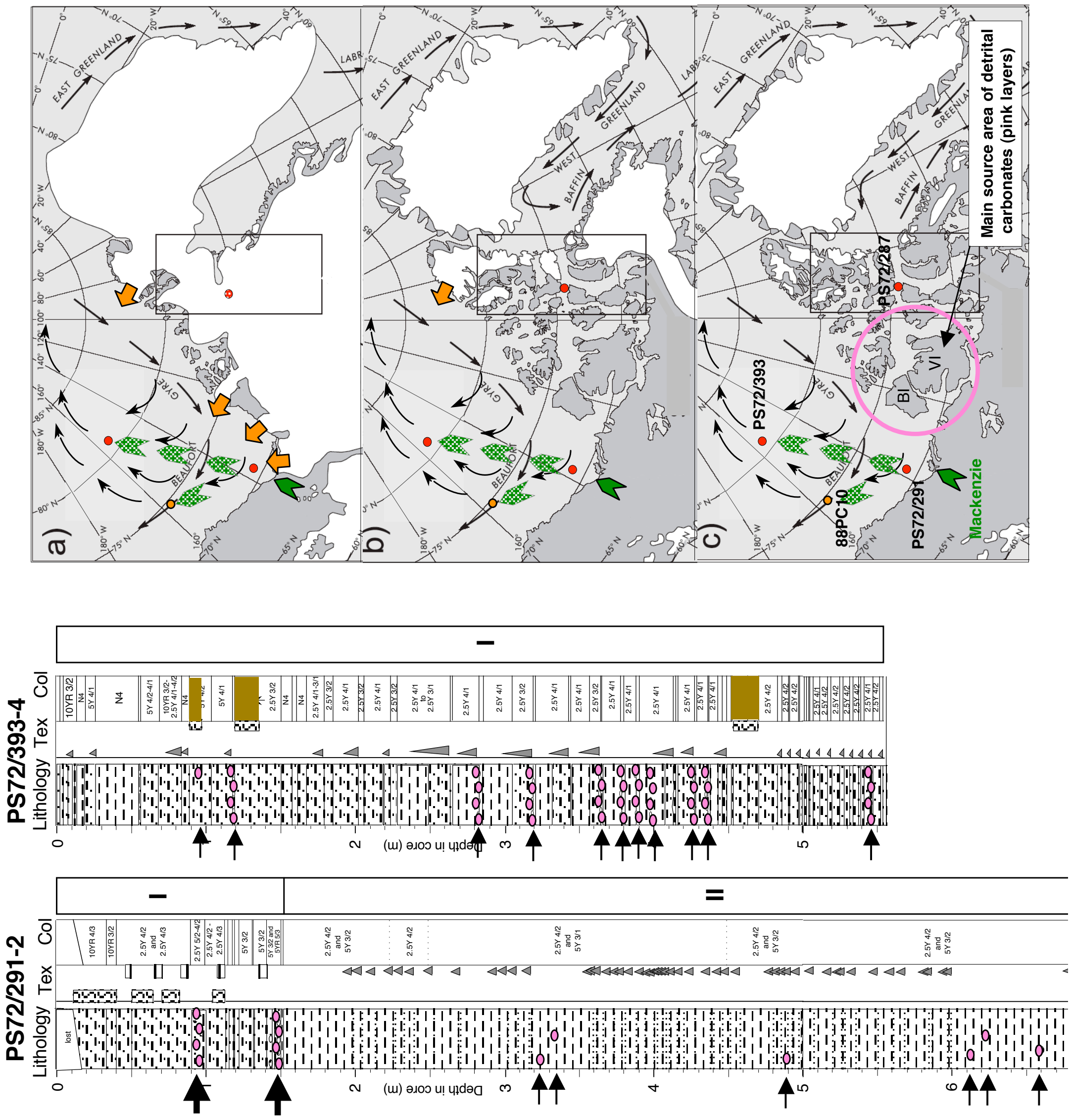

Fig. 35: Lithologies of cores PS72/291-2 and PS72/393-4

The sediments recovered at Core PS72/393-4 (central Canada Basin north of the Chukchi Borderland; 80°43.37'N, 155°32.81'W; 3801 m of water depth) are mainly composed of dark grey and (dark) greyish brown silty clay to clay alternations representing fining-upward cycles, and intercalated dark olive brown silty clay horizons. Occasionally, light grey to very pale brown and pinkish lenses/clasts occur on top of the dark olive brown horizons (Fig. 35). Bioturbated intervals are very rare (90 - 97, 119 - 135, and 450 - 470 cm core depth).

In both cores, the dominantly dark grey to dark greyish brown silty clay to clay (fining-upward) cycles are interpreted as distal turbidites related to short-term periods of increased suspended matter supply by the Mackenzie river. A similar sediment facies also interpreted as distal turbidites with a Mackenzie source, was described from Core 88PC10 located in the Canada Abyssal Plain close to Northwind Ridge (Grantz et al.; 1996; see Fig. 6 for location).

A second important process of sediment transport towards the locations of Cores PS72/291-2 and PS72/393-4 seems to be ice rafting. Phases of increased IRD input are reflected in the intervals characterized by a more coarse-grained facies with enrichment of pale brown and pinkish lenses/clasts (Fig. 35). This very specific lithology can be related to a restricted source area in the Canadian Arctic (Bank Island, Victoria Island; Fig. 35) where Paleozoic carbonates (dolomite) are cropping out (e.g., Bischof and Darby, 1997; Phillips and Grantz, 2001; Polyak et al., 2004), and it can be interpreted as pulses of increased iceberg discharge due to the disintegration of extended Canadian glacial ice sheets.

Transect 1; southern Mendeleev Ridge transect (77°40' N)

Five sediment cores (PS72/340-5, PS72/341-5, PS72/342-1, PS72/343-2, and PS72/344-3) were recovered on a transect from the Chukchi Abyssal Plain across the southern Mendeleev Ridge toward the East Siberian continental margin (Fig. 36). The sediments of these cores are characterized by prominent changes in sediment colour, grain-size, sediment composition, and degree of bioturbation (Fig. 37).

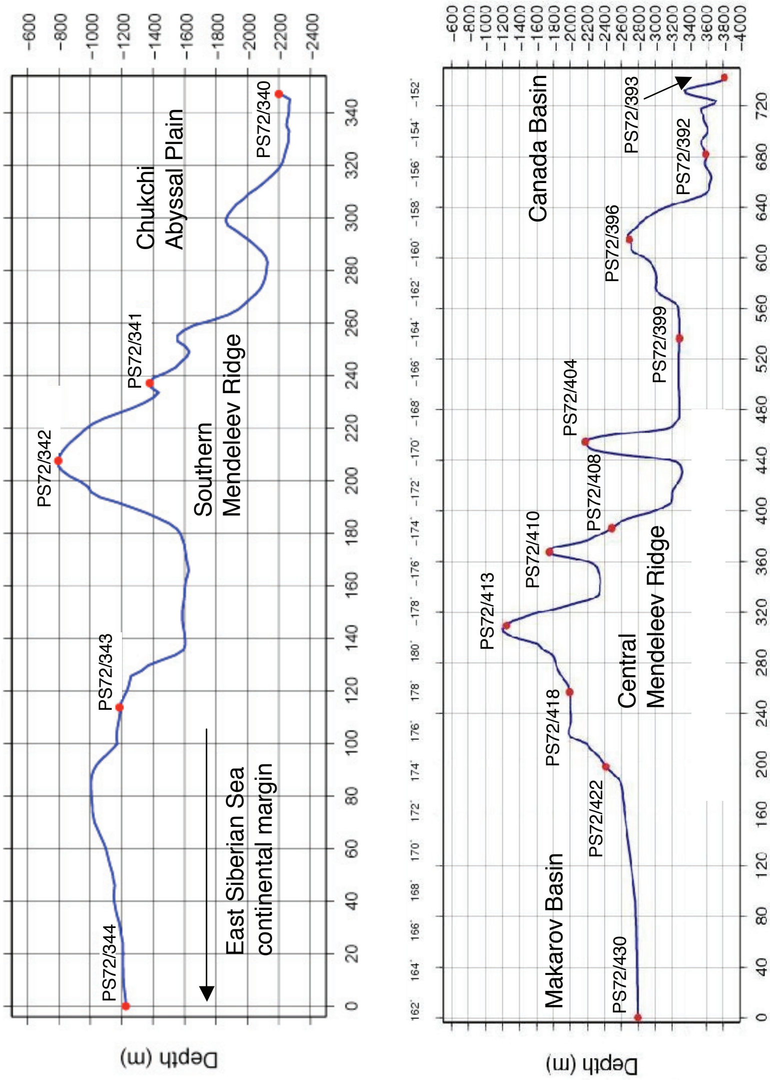

Fig. 36: Bathymetric profiles across the (a) southern and (b) central Mendeleev Ridge

Looking at the lithology of Core PS72/340-5 in more detail, the following types of sediment facies can be distinguished (Fig. 37): Interval I (0-167 cm) is mainly composed of dark grayish brown, dark brown and brown silty clay and light olive brown silty clay, with variable degree of bioturbation. Interval II (167-272 cm) consists of olive gray to dark gray silty clay. Interval III (272 – base of core) contains alternations of dark brown to brown silty clay and light olive brown silty clay. Between 380 and 420 cm and, especially, between 630 and 644 cm also dark gray colours occur. At 498-513 cm, 714-718 cm, and 785-787 cm, prominent horizons of light reddish brown („pinkish“) sandy silty clay intervals with several dropstones (diamictons) were found. In the first horizons dropstones (dolomite) may reach a size of up to 10 cm in diameter (Fig. 38). These „pinkish“ horizons are important lithostratigraphic marker horizons (see below, central Mendeleev Ridge transect, for some more details). In addition to the prominent pinkish layers, small pinkish lenses were found at 102 - 103 cm, 321 - 326 cm, 637 - 639 cm, 670 - 671 cm, 680 - 686 cm, 771 - 772 cm, and 775 - 776 cm.

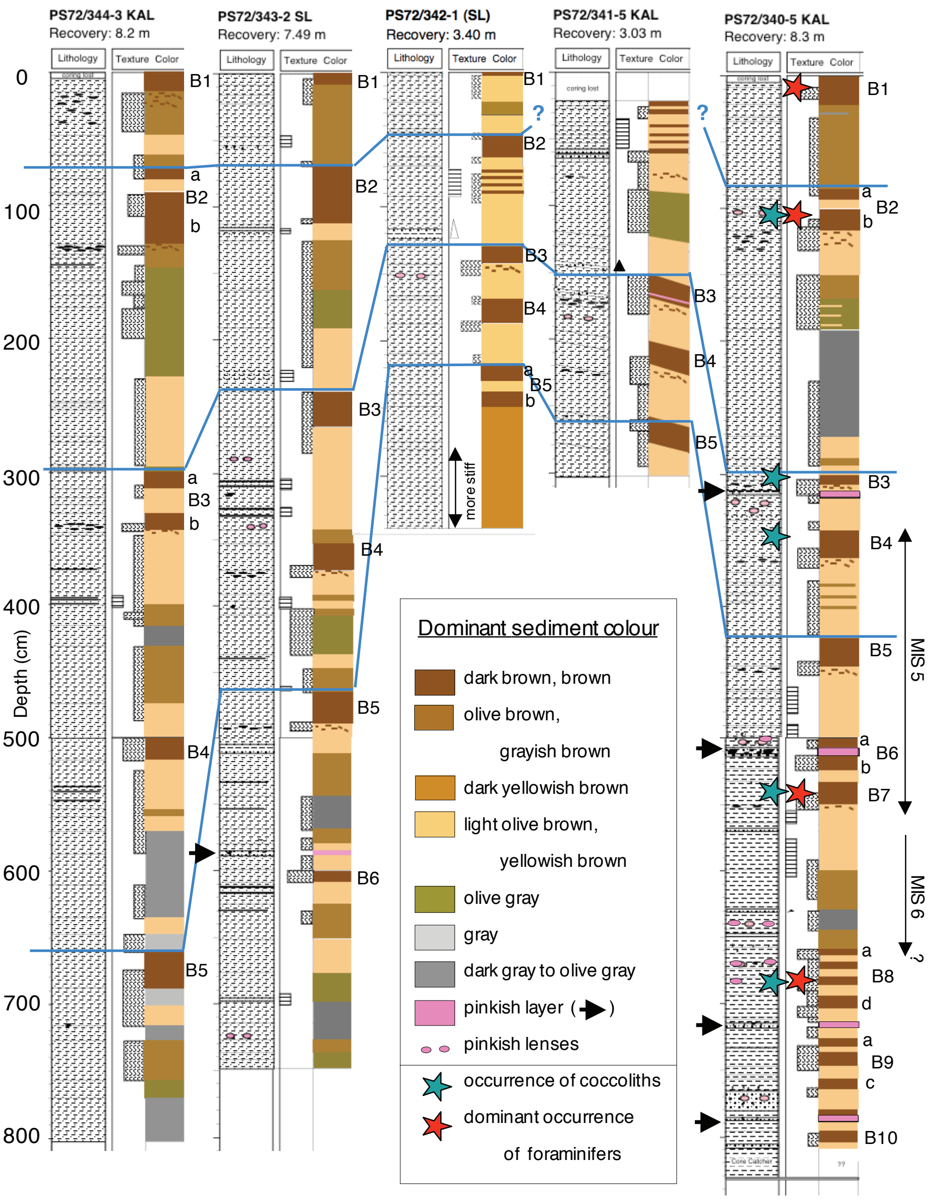

Fig. 37: Simplified summary of lithologies and main sediment colours determined in the sediment cores across the southern Mendeleev Ridge. Main brown to dark brown intervals (B1 to B6) and pink layers were used to obtain a preliminary age model (c.f., Polyak et al., 2004; Darby et al., 2006). Occurrence of coccoliths and foraminifers is indicated by asterisks.

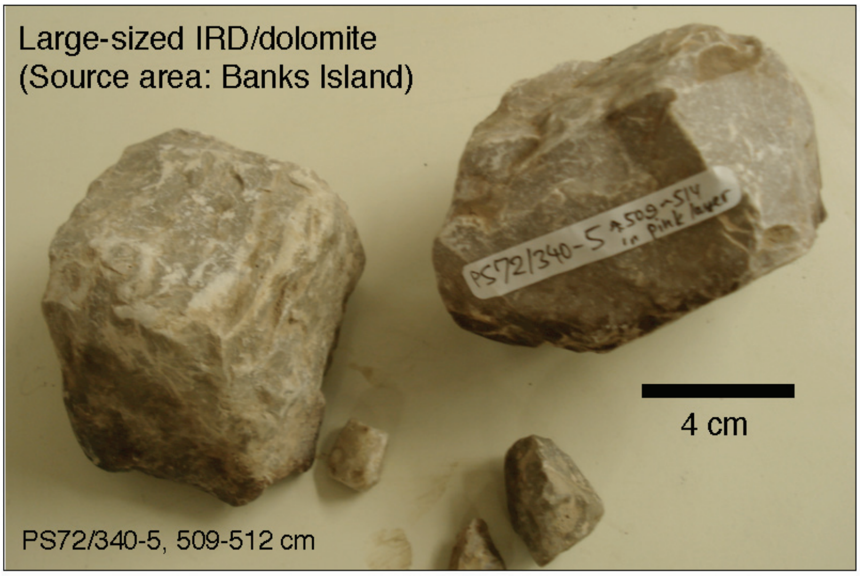

Fig. 38: Large-sized dropstones (dolomite) from the pink layer (498-513 cmbsf) in Core PS72/340-5

Using the upper seven, most prominent dark brown intervals (B1 to B7), it seems to be possible to correlate the five cores across the southern Lomonosov Ridge (Fig. 37). This correlation is also supported by colour scanning records (i.e., lightness and red values). Furthermore, from the correlation of Core PS72/340-5 with near-by Core NP-26-5/32, a preliminary age model can be obtained. Following Polyak et al. (2004) and Darby et al. (2006), the brown to dark brown intervals mainly represent interglacial (interstadial) time intervals, with the upper seven brown intervals representing the time interval of marine oxygen isotope (MIS) stages MIS 1 to 5. Based on this age model and its extrapolation, Core PS72/340-5 probably contains MIS 1 to MIS 10, cores PS72/343-2 and PS72/344-3 probably reach MIS 6. The identification of MIS 5.5 (brown interval B7) and MIS 7 in the record of Core PS72/340-5 is supported by the dominance of planktonic foraminifers in the coarse fraction and the occurrence of coccoliths in smear slides. Thus, the most prominent pinkish intervals recovered at Core PS72/340-5 and characterized by high numbers of dolomitic IRD/dropstones, are related to increased IRD supply due to extended glaciations in Arctic Canada during MIS 5.4, MIS 8, and MIS 10. For the upper about five meter of Core PS72/340-5 (i.e., B1 to B7 or MIS1 to MIS 5), an average linear sedimentation rate of about 4 cm/ky was calculated. Further shore-based studies, however, are needed to prove this preliminary age model and interpretation.

Transect 2; Central Mendeleev Ridge (80°30' N)

On a 700 km long transect at about 80° 30' N from the Canada Basin across the central Mendeleev Ridge into the Makarov Basin 12 sediment cores were retrieved (see Fig. 36 for location). Except for Core PS72/393-4 (see above), the predominent lithology of all the sediment cores is silty clay (to sandy silty clay) of brown to dark brown, light to dark yellowish brown, and light olive brown colours (Fig. 39; see appendix for detailed description of all cores). In the upper about 0.7 to about 4 m of most of the cores, more sandy intervals, dropstones, and mud clasts occur. The most prominent features of all cores are colour cycles of brown to dark brown and light olive brown to yellowish brown sediments occurring down to the bottom of the cores. Most of the sediments are slightly to strongly bioturbated. Furthermore, specific marker horizons (i.e., pink-white and white layers; see above) could be identified in all these cores. In general, the sedimentary sequences can be divided into two main units. Unit I is composed of alternations of silty clays and more sandy intervals, partly with mud clasts and dropstones whereas Unit II is mainly composed of fine-grained sediments (silty clays) with brown/light olive brown colour cycles (Fig. 39).

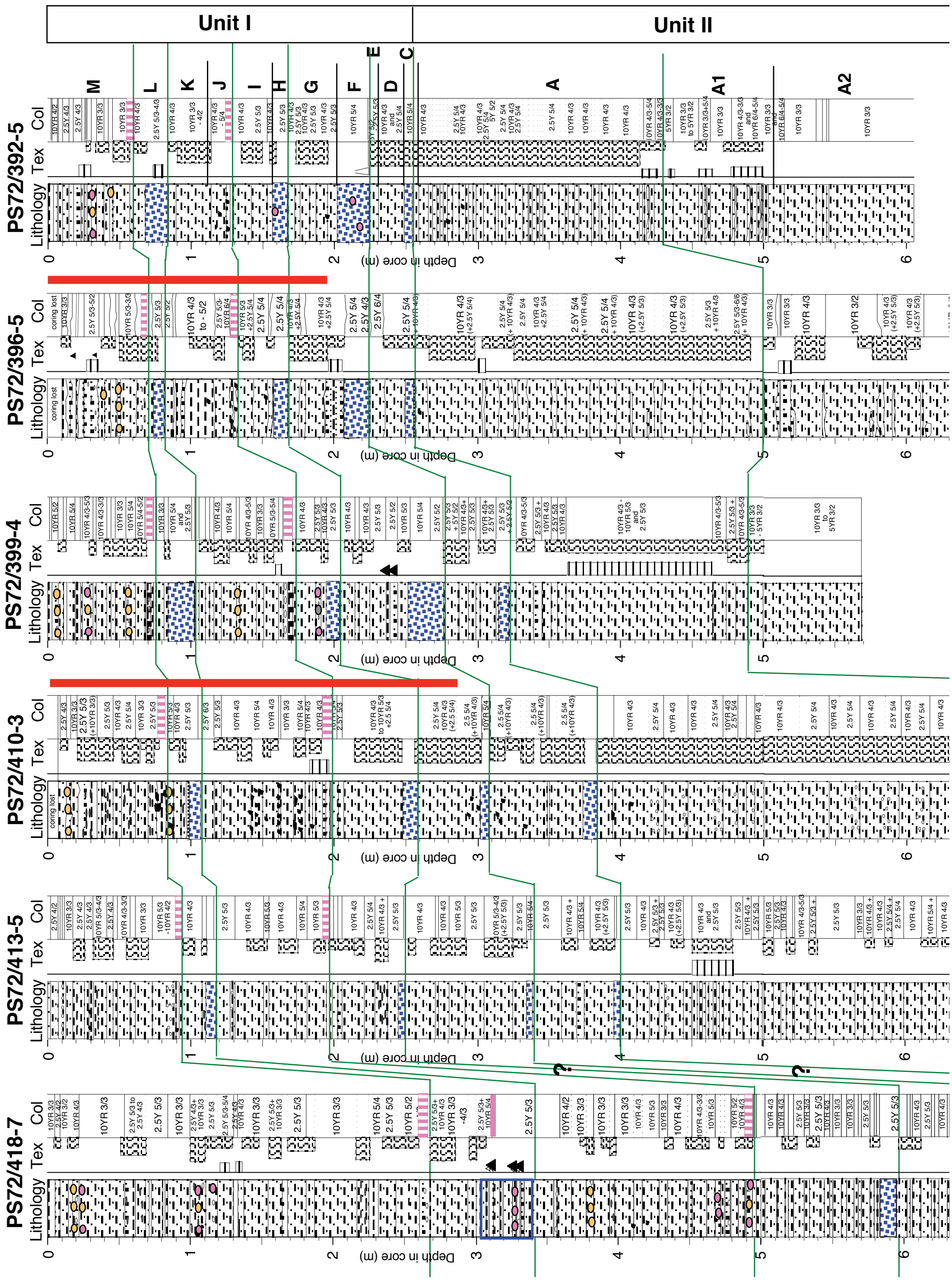

Fig. 39: Main lithologies of selected sediment cores across the central Mendeleev Ridge (for core location on transect see Fig. 36). Occurrence of pink layers and sandy intervals are highlighted. Furthermore, standard lithological units A to M of Clark et al. (1980) are shown.

Based on the visual core description, the standard lithological units A to M developed by Clark et al. (1980) using several hundred of short sediments cores collected from Ice Island T-3 (or Fletcher's Ice Island) in the Amerasia Basin, could also be identified in the ARK-XXIII/3 sediment cores from the central Mendeleev Ridge transect (Fig. 39). Following Clark et al. (1980), the content of sand-sized material (enriched in units C, F, H, J, L, and parts of M) and the pink-white layers were considered to be the key sedimentary characteristic used for correlation of these lithostratigraphic units. In our cores, this lithostratigraphic correlation is supported by the (dominant) occurrence of planktonic foraminifers in the coarse fraction of samples from units M to G (Cores PS72/410-3 and PS72/396-5). In 1985, Clark's lithostratigraphic succession with units A to M was expanded by three new lithostratigraphic units A1, A2, and A3 recovered in CESAR Core 83-14 (Mudie and Blasco, 1985; for location of core see Fig. 6). In some cores (e.g., PS72/392-5, PS72/396-5, and PS72/399-4), these lower lithostratigraphic units were also recovered. In general, there is an increase in sedimentation rate from the Canada Basin across the Mendeleev Ridge toward the Makarov Basin (Fig. 37). More details about the lithostratigraphy of the ARK-XXIII/3 sediment cores are described in Stein et al. (2009b).

Core PS72/392-2 is a re-coring of Clark's key Core FL-224, which will allow to re-study the „old" core using standard methods, such as photography, visual core description, coarse fraction analysis, stable oxygen and carbon isotopes on foraminifers, paleomagnetic data, but also MSCL logging, colour and XRF scanning etc. This will give the unique possibility for correlation of sediment cores and development of a stratigraphic framework throughout the central Arctic Ocean (for more details see Stein et al., 2009a).

References

Bischof, J.F., Darby, D.A., 1997. Mid to Late Pleistocene ice drift in the western Arctic Ocean: evidence for a different circulation in the past. Science 277, 74-78

Clark, D.L., Whitman, R. R., Morgan, K. A., Mackey, S. D., 1980. Stratigraphy and glacialmarine sediments of the Amerasian Basin, central Arctic Ocean. Geol. Soc. Am. Spec. Pap. 181, 57 pp.

Grantz, A., Phillips, R.L., Mullen, M.W., Starratt, S.W., Jones, G.A., Naidu, S.A., Finney, B.P., 1996. Character, paleoenvironment, rate of accumulation, and evidence for seismic triggering of Holocene turbidites, Canada Abyssal Plain, Arctic Ocean. Mar. Geol. 133, 51-73.

Mudie, P.J., Blasko, S.M., 1985. Lithostratigraphy of the CESAR cores, in: Initial Geological report on CESAR: The Canadian Expedition to Study the Alpha Ridge (ed. By H.R. Jackson, P.J. Mudie and S.M. Blasko), Geol. Surv. Can. Pap. 84-22, 59-99.

Nesje, A., Matthews, J.A., Dahl, S.O., Berrisford, M.S., Andersson, C., 2001. Holocene glacier fluctuations of Flatebreen and winter-precipitation changes in the Jostedalsbreen region, western Norvay, based on glaciolacustrine sediment records. The Holocene 11, 267-280.

Phillips, R.L., Grantz, A., 2001. Regional variations in provenance and abundance of ice-rafted clasts in Arctic Ocean sediments: Implications for the configuration of Late Quaternary oceanic and atmospheric circulation in the Arctic. Mar. Geol. 172, 91–115.

Polyak, L.V., Curry, W.B., Darby, D.A., Bischof, J., Cronin, T.M., 2004. Contrasting glacial/interglacial regimes in the western Arctic Ocean as exemplied by a sedimentary record from the Mendeleev Ridge. Palaeogeogr., Palaeoclim., Palaeoecol. 203, 73-93.

Stein, R., Matthiessen, J., Krylov, R., Nam, S., Niessen, F., and the ARK-XXIII/3 Geoscientific Party, 2009a. Re-coring of Ice Island T3 Key Core FL-224 (Nautilus Basin/Amerasian Arctic): Sediment characteristics and stratigraphic framework. Polarforschung, subm.

Stein, R., Matthiessen, J., Niessen, F., Bazhenova, E., Krylov, R., Nam, S., and the ARK-XXIII/3 Geoscientific Party, 2009b. Lithostratigraphy across the Mendeleev Ridge (Arctic Ocean) and its paleoenvironmental significance. Polarforschung, subm.

3.7 Inorganic geochemistry

Sebastian Eckert, Christian März
Institute for Chemistry and Biology, Oldenburg

Scientific background

In basin sediments from the Arctic Ocean, distinct colour cycles (ranging from greyish over yellow to dark brown) are a common phenomenon known for decades. There have been a number of studies on these cycles, which are not limited to certain parts of the Arctic, but occur both in the Eurasian and Amerasian basins and ridges. According to these previous studies, the colour changes in the sediments are strongly associated with sedimentary Mn contents – brown layers are exceptionally rich in Mn (up to several weight-%) compared to other pelagic sediments of the world ocean, while greyish and yellow intervals are comparatively Mn-poor. In the current literature, there are two main explanations concerning the genesis of these pronounced Mn cycles. The first relates Mn cyclicity to primary climatic signals, i.e. glacial-interglacial variability triggered by astronomical forcing. The pathway these climatic signals are translated into the sedimentary record is believed to be variable input of dissolved Mn from the circumarctic rivers during glacial and interglacial conditions, changes in ventilation of the Arctic bottom water masses, or a combination of both. Supportive of this theory are relatively close correlations of Mn cycles to other climate proxies in Arctic Ocean sediments, e.g. magnetic susceptibility, grain size distribution, and $\delta^{18}O$ values of foraminiferal tests. The second hypothesis relates the Mn cycles to early diagenetic processes in the sediments, related to the biogeochemical remineralization of sedimentary organic matter (OM). During OM degradation, in the absence of free oxygen microbes utilize Mn (oxyhyr)oxides as electron acceptors, thereby reducing these Mn(IV) minerals and liberating dissolved Mn(II) to the pore waters. In addition to Mn (oxyhydr)oxide dissolution under suboxic to anoxic conditions, re-precipitation of Mn (oxyhydr)oxide may occur upon diffusion of dissolved Mn(II) at the oxic-suboxic redox boundary (mostly close to the sediment surface). This redistribution of the sedimentary Mn signal can produce multiple solid phase Mn peaks under non-steady state conditions, i.e. if parameters like OM accumulation rates, sedimentation rates, Mn contents of the settling sediment, or bottom waters oxygen contents change over time. It has been shown by numerical models and geochemical studies on short cores from the Arctic Ocean that Arctic deep basinal sediments are susceptible to such varying environmental parameters, and diagenetic redistribution of sedimentary Mn is highly probable.

To help resolving this ongoing controversy, and to evaluate the stratigraphic and paleoceanographic potential of Mn cyclicity in the Arctic environment, a detailed geochemical study of pore waters and sediments from the Arctic Ocean is planned during and after *Polarstern* expedition ARK-XXIII/3. Sampling and preliminary analyses will be conducted on short (up to ~45 cm) and longer (up to ~8 m) sediment cores. In the following, applied sampling strategies, materials and methods will be described in more detail.

Material and methods

Shortly after sediment retrieval from the sea floor with different sampling devices (Multicorer = MUC, Gravity Corer = GC, Giant Box Corer = GKG, Kastenlot = KAL), pore water sampling was performed. During the whole cruise, a total of ~550 pore water samples were retrieved in the Canadian Archipelago, the Canada Basin, the Makarov Basin, and on the Mendeleev Ridge (Tab. 8). All pore water samples were taken with so-called rhizons ("artificial roots"), consisting of a 5 cm polymer filter (0.1 μm pore size) attached to a PVC tube and a luer lock. Pore waters were extracted by sticking the rhizon into the sediment, then applying a vacuum with a 12 ml plastic syringe blocked with a wood or plastic stick. In that way, depending on sediment porosity, permeability and degree of induration, 2 to 12 ml of filtered pore water could be extracted from each sampling interval within at least 2 up to 8 hours. In most sediment cores, pH values were measured parallel to the rhizons with a pre-calibrated WTW push-in pH electrode. Care was taken to measure pH values, and to sample the pore waters, approximately at in situ temperatures (between 0 and 5° C), either on deck, in the cool lab or in the unheated wet lab. After sampling, rhizons were removed, tested for damage, and cleaned with 5 % HCl for later re-use. Pore water samples were transferred from the syringes into Zinser vials or plastic test tubes and stored at 4° C until further analysis or acidification of subsamples. From each MUC run and some of the GC and KAL cores, solid phase samples (10 - 25 ml per sample) were taken in parallel as well, either with plastic spatula or with cut plastic syringes (Tab. 8). On selected GC and KAL cores, a higher resolution sampling of the sediment was conducted (up to 1 cm continuous sampling resolution). Sediment samples were stored in Parafilm-sealed plastic vials or in plastic bags, and were frozen (-20° C) upon sampling.

Tab. 8: List of pore water samples, sediment samples, and geochemical parameters determined onboard during *Polarstern* expedition ARK-XXIII/3. A cross shows that a sample was taken or a parameter was measured, while minus indicates the opposite.

Region	Sampling device	pH	Alkalinity	Ammonium	Phosphate	Acidified pore water	Sediment samples
NW Passage	MUC	X	X	X	X	X	X
NW Passage	GC	X	X	X	X	X	X
Canada Basin	GKG	X	X	_	X	X	X
Mackenzie Slope	GKG	X	_	X	X	X	X
Mackenzie Slope	KAL	X	_	X	X	X	X
Makarov Basin	GKG	X	X	_	_	X	_
Makarov Basin	MUC	X	X	_	_	X	X
Makarov Basin	KAL	X	X	_	_	X	X
Makarov Basin	GC	_	X	_	_	X	X
Makarov Basin	MUC	X	X	_	_	X	X
Canada Basin	GC	_	X	X	_	X	_
Mendeleev Ridge	MUC	X	X	X	_	X	X
Mendeleev Ridge	KAL	X	X	X	_	X	_
Mendeleev Ridge	MUC	X	X	_	_	X	X
Mendeleev Ridge	GC	_	X	_	_	X	_
Mendeleev Ridge	MUC	X	X	_	_	X	X
Mendeleev Ridge	KAL	_	X	_	_	X	_
Mendeleev Ridge	MUC	X	X	_	_	X	X
Mendeleev Ridge	GC	_	X	_	_	X	_
Mendeleev Ridge	MUC	X	X	_	_	X	X
Mendeleev Ridge	KAL	_	X	_	_	X	_

The GKG was sampled on deck shortly after recovery and directly from the cleaned open side wall of the box, after PVC tubes have been pushed into the sediment surface from the top to recover sediment sub-cores (Fig. 40). Sampling resolution generally was 2 cm in the uppermost 15 cm of sediment, and 5 cm with increasing sediment depth, but also depended on optically detectable lithological transitions which were sampled in higher resolution. After collapse of a water-rich GKG surface, all rhizons were destroyed and pore water was lost. Thus, later sampling of GKGs was avoided, and preference was given to sampling of MUC tubes.

Fig. 40: Giant Box Corer on the working deck, sampled with rhizons and plastic syringes. Colour changes probably related to different sedimentary Mn contents are clearly visible.

The MUC was equipped prior to deployment with one PVC tubes prepared for rhizon sampling. Holes of 3.75 mm diameter were drilled in 1 cm intervals into the tubes, and sealed with Tesa tape. After recovery, these tubes were transferred into a cool lab and fixed in a sink, the tape was punctuated, and rhizons were injected through the holes (Fig. 41). Sampling resolution was usually 1 cm from 0 - 5 cm sediment depth, 2 cm from 5 - 15 cm sediment depth, and 5 cm further below. The pH of the sediment was determined on a parallel tube, which was also subjected to solid phase sampling.

Fig. 41: Multicorer tube in the sink, sampled with rhizons and plastic syringes

The GC was cut into 1 m segments after recovery, which were deposited in a cool container at ~2° C. Directly after core recovery, 3.75 mm holes were drilled into the PVC liners, and rhizons were inserted (Fig. 42). Sampling resolution was in regular intervals of 20 cm. As core logging was to be applied to the closed cores after pore water sampling, measurements of pH could not be performed for the sake of least destructive handling of the core segments. Notably, we compared physical properties measured with the Multi Sensor Core Logging tool on parallel cores with and without pore water sampling. Evidently, effects of pore water sampling on physical properties we not detected.

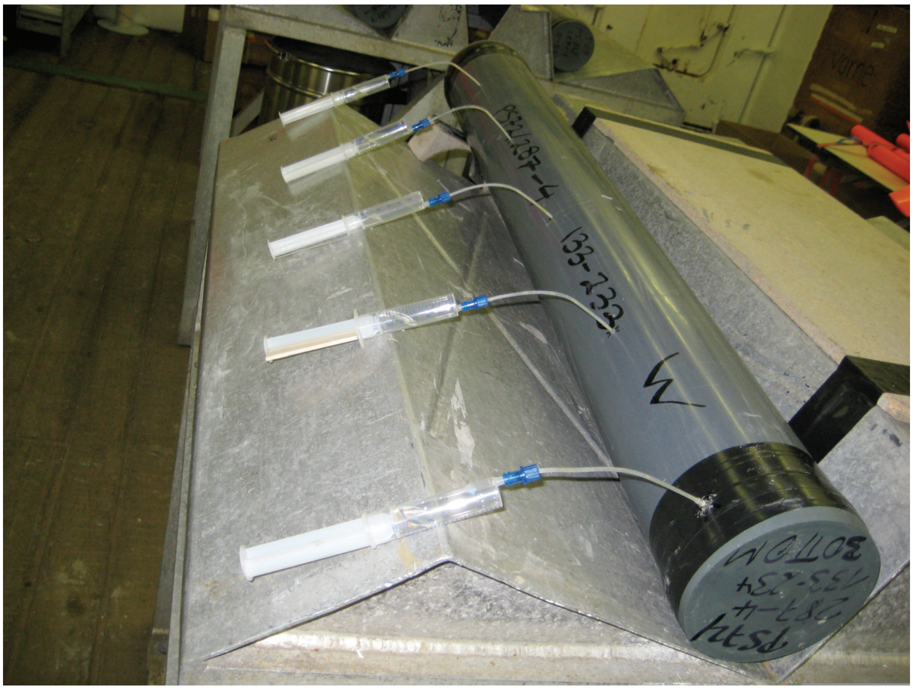

Fig. 42: Segments of Gravity Core sampled with rhizons and plastic syringes

The KAL was sampled on the cleaned open sediment surface, after two layers of sediment had been removed with sampling boxes for later sub-sampling (Fig. 43). In that way, pore waters were recovered from the inner part of the core, where even after core storage over night the sediment was still relatively cold and pristine. Sampling resolution was chosen 10 to 20 cm, depending on lithological or colour contrasts.

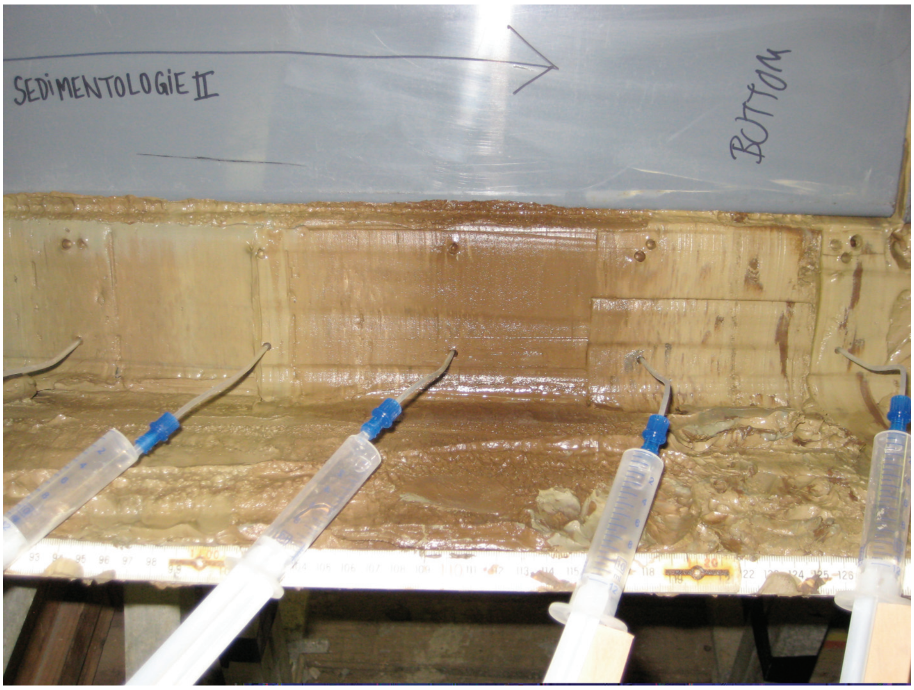

Fig. 43: Kastenlot sampled with rhizons and plastic syringes. Colour changes probably related to different sedimentary Mn contents are clearly visible.

Several geochemical parameters were analysed within few hours after pore water sampling, namely total alkalinity and ammonium. Phosphate analyses were only performed where sufficient pore water was available from the first cores, but was skipped lateron due to methodological problems (non-reproducible results) (Tab. 8). Both alkalinity and ammonium were measured with photometrical methods, consuming less than 1 ml pore water in total. Ammonium analysis was skipped for the last cores, as previous analyses had shown that values were mostly below detection limit. Splits of pore water samples were acidified with concentrated HNO_3 (to 2 vol% HNO_3) for later analysis (e.g. iron, manganese, phosphate, silicate) via ICP-OES and ICP-MS (Tab. 8). In most cases, some of the original pore water sample remained after sub-sampling and was preserved for later anion analysis (sulfate, chloride) via IC. The sediment samples were not further treated onboard, but just frozen and stored away. Back onshore, the sediment will be freeze-dried, ground, and subjected to various analytical procedures. Organic and inorganic carbon will be analysed coulometrically. Sample splits will be used to make melt tablets, which will be analysed for elemental concentrations (mainly major elements) via X-Ray fluorescence. In addition, sample splits will be fully dissolved in an acid mixture, and analysed for major and trace elements via ICP-OES and ICP-MS. In addition to this standard techniques, certain manganese-rich layers will be subjected to a sequential extraction procedure, to identify the main manganese-carrying phases in the sediment. Other potential analytical methods include X-Ray diffraction for mineralogical analyses, and SEM-EDX studies to get an idea about the morphology and composition of single manganese-rich particles.

Preliminary results

Based on the parameters determined onboard, we will try to give some general interpretation of the preliminary onboard analyses (pH, ammonium, alkalinity). In order to keep it short, all cores sampled are combined into two groups, based on their locations and general lithological and geochemical characteristics. The first group comprises 4 stations in the Canadian Archipelago and the Canada Basin (= Canadian stations), while 7 stations on the Mendeleev Ridge and in the Makarov Basin belong to the second group (= East Siberian stations).

Group 1: Canadian Archipelago and Canada Basin

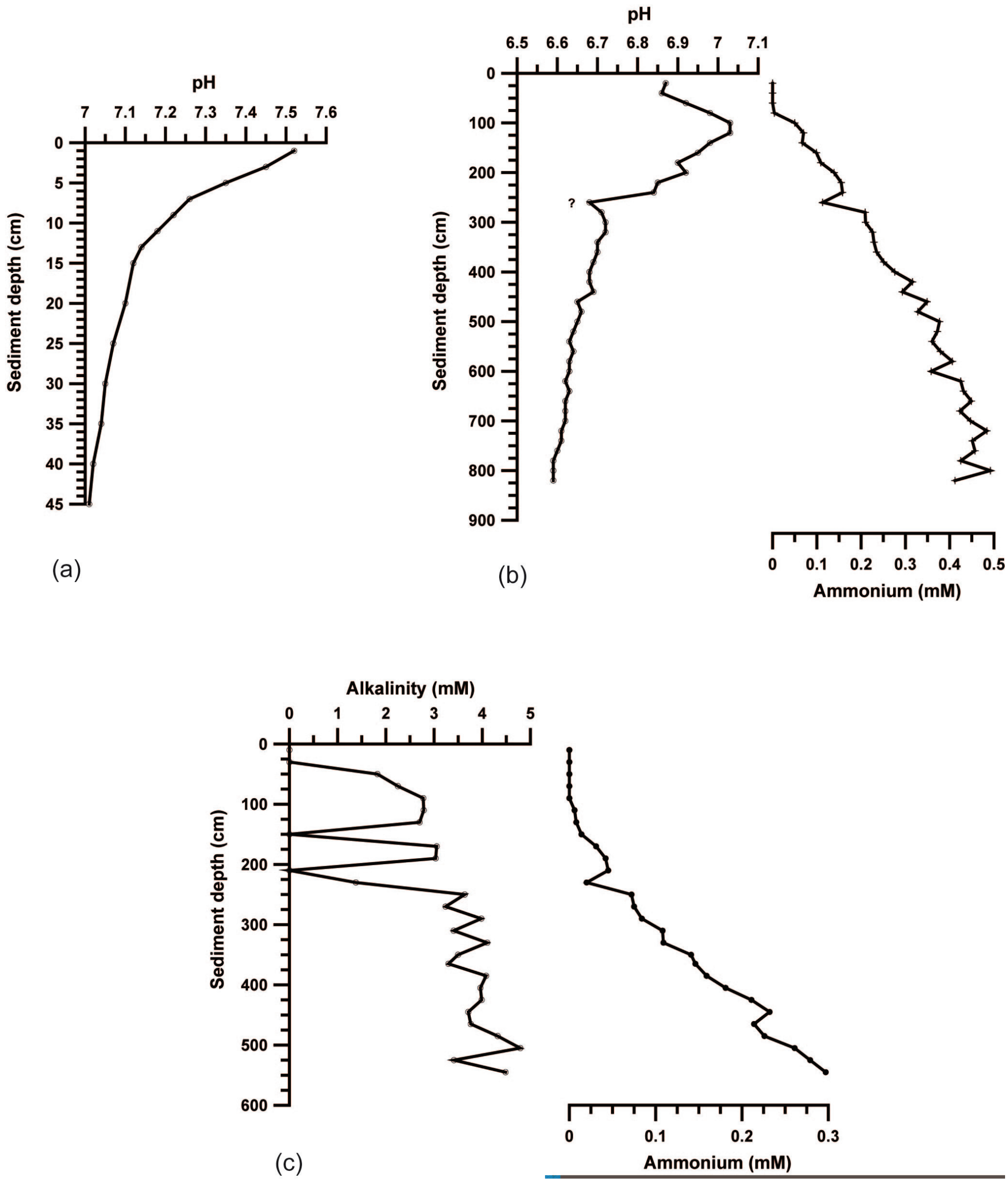

Fig. 44: Pore water profiles of stations PS 72/291 (Canada Basin, off Mackenzie River) and PS 72/393 (Canada Basin, western slope foot of Mendeleev Ridge); (a) pH values of Giant Box Corer PS 72/291-1; (b) pH and Ammonium values of Kastenlot PS 72/291-2; (c) Alkalinity and Ammonium values of Gravity Core PS 72/393-4. Note different depth scales.

pH

Despite limited pH data from these locations, pH is lower than those from sediments recovered from the East Siberian Sea already in the uppermost 30 - 40 cm, with values of 7.0 - 7.2. Comparably low pH values are also documented in deeper sediments, reaching values as low as 6.6 in ~8 m sediment depth (Fig. 44). The fact that pH values are relatively low in sediments from the Canadian stations can be explained by higher rates of OM degradation compared to the East Siberian stations. A certain, maybe even dominant amount of the OM is most probably of terrigenous origin, delivered from the islands of the Canadian Archipelago and, more important, from the Mackenzie River. In simple words, degradation of this OM creates acid, which lowers the pH of pore waters.

Ammonium

The most significant difference between cores from Canadian and East Siberian stations is the concentration of ammonium in the sediments. While being mostly undetectable in the East Siberian sediments, ammonium concentrations in the Canadian stations deposits gradually increase from the sediment surface with depth, reaching values of 0.6 mM in Canadian Archipelago sediments, and 0.3-0.4 mM in Canada Basin deposits, at ~6 m depth (Fig. 44). Higher ammonium and lower pH values both indicate increased degradation of OM in deeper sediments, releasing acid and nutrients to the pore waters. Still, compared with sediments from lower latitude and more productive parts of the world ocean, these ammonium concentrations are more than 1 order of magnitude lower. This fact results from relatively low productivity of the Arctic Ocean in general, as well as from major input of refractory terrigenous OM to the sediments.

Alkalinity

The patterns of alkalinity profiles from the Canadian stations are similar to those from East Siberian stations, with abrupt variations within short depth intervals. However, positive alkalinity excursion reach concentrations of 4-5 mM, compared to 2.5-3 mM in East Siberian sediments. The overall higher alkalinity could be a result of enhanced OM degradation, producing acid that dissolves carbonate particles in the sediment and liberates dissolved bicarbonate to the pore waters.

Group 2: Mendeleev Ridge and Makarov Basin

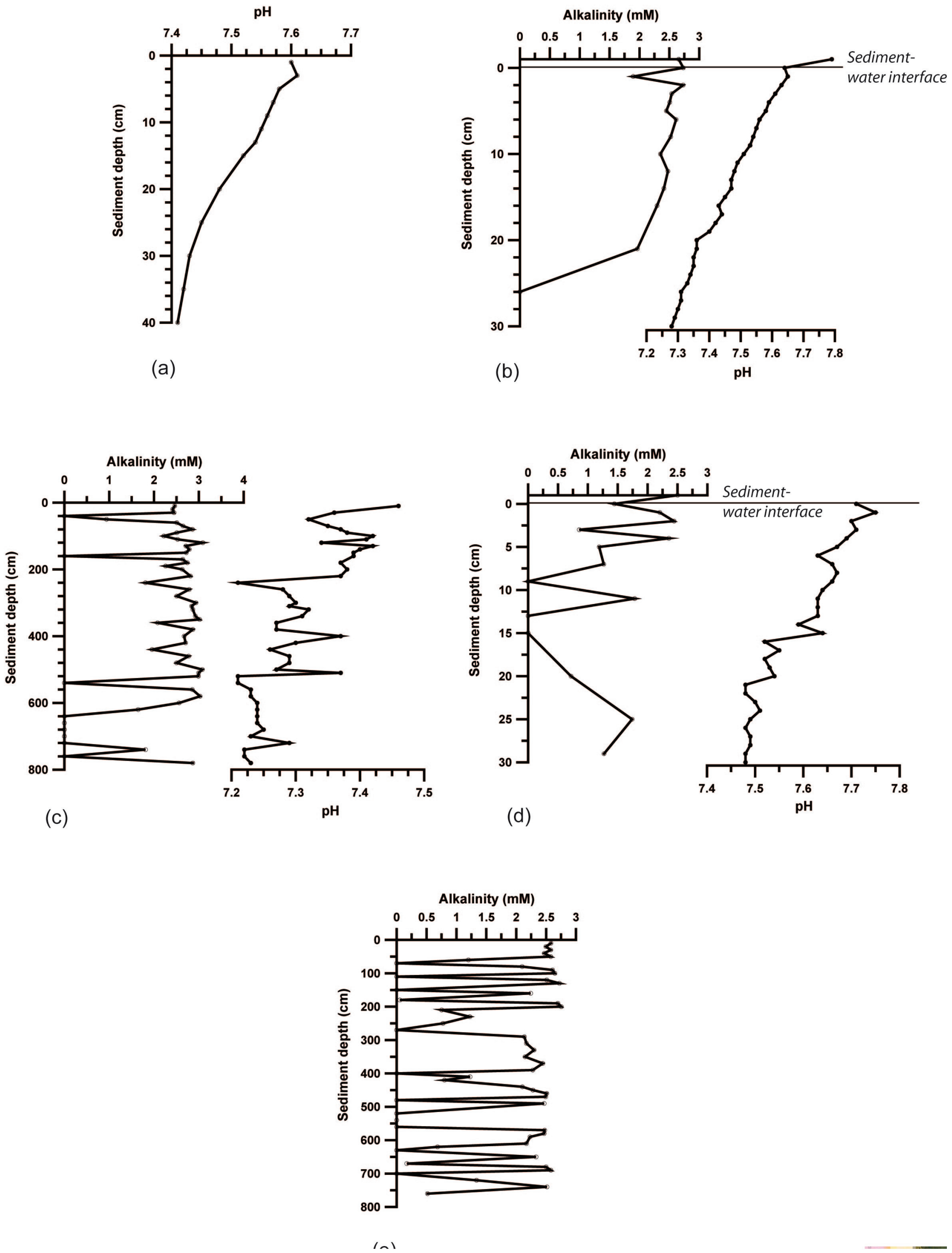

Fig. 45: Pore water profiles of stations PS 72/340 and PS 72/410 (Mendeleev Ridge); (a) pH values of Giant Box Corer PS 72/340-3; (b) Alkalinity and pH values of Multicorer PS 72/340-4; (c) Alkalinity and pH values of Kastenlot PS 72/340-5; (d) Alkalinity and pH values of Multicorer PS 72/410-2; (e) Alkalinity values of Kastenlot PS 72/410-3. Note different depth scales.

pH

In cores from this area, pH values close to the sediment surface are notably higher than from the Canadian stations, i.e. between 7.8 and 7.5. Within the uppermost 30-40 cm of the sediment, the pH drops gradually to values of 7.6-7.3 (Fig. 45). The pH gradients are relatively linear in all near-surface sediments. In deeper sediment layers up to ~8 m depth, the pH further decreases down to values of 7.1-7.2. However, the pH profile shows several positive and negative excursions superimposed on the overall pH decrease (Fig. 45). For further explanation of these patterns, the pH value of pore waters is regarded mainly as a function of acid produced by OM degradation and the total alkalinity which potentially buffers this acid. Consequently, lower pH values represent sediment layers with relatively higher rates of OM degradation, or with lower alkalinity concentrations and therefore lower buffer capacity. As the ammonium concentrations in pore waters from this region are close to detection limit (see below), OM diagenesis in the sediments seems to be weak, at least at the moment of sediment recovery (which is merely a snapshot of diagenetic conditions and not necessarily a representation of yearly averaged organic matter remineralization rates). From our preliminary data, we can conclude that lower pH values document slightly higher rates of OM degradation in a uniformly carbonate-poor sediment column. Alternatively, OM degradation rates could be similar throughout the sediment column, but the carbonate content of the sediment is variable, resulting in intervals with higher and lower acid buffer capacity. Clearly, the pH profiles could also be a combination of both variable carbonate contents and variable OM degradation rates over sediment depth. Further analyses of pore waters and solid sediment are required to answer this question. Notably, from our data we see no clear correlations between pH and alkalinity profiles (Fig. 45).

Ammonium

The ammonium concentrations in the sediments are close to or even below detection limit, and therefore cannot be shown here. This is a clear indication for overall low rates of OM degradation in the sediments, and most probably an effect of low OM export from the sea surface down to the sea floor. Firstly, the Arctic Ocean and especially the East Siberian Sea are known to be regions of very low primary productivity, so little fresh OM is produced on first hand. Secondly, if OM is produced, its remineralization should take place mostly within the fully oxygenated water column, so very little of it shall reach the sediment surface. Finally, as such OM is supposed to arrive at the sea floor in pulses (due to the strong seasonality of Arctic Ocean productivity), a short pulse should be remineralized rapidly and not be documented in the ammonium pore water profile for a prolonged time. This interpretation is consistent with the overall low OM contents of most basinal Arctic Ocean sediments, with TOC values mostly < 0.5 wt%. Additionally, some to most of this OM is probably of terrestrial origin, refractory and not easily degraded by microbes. Conclusively, early diagenesis related to OM degradation is not supposed to have a year-round influence on sediment composition. However, our investigations only represent a snapshot of pore water composition, and seasonal effects of OM export were probably not fully captured.

Alkalinity

The alkalinity values (= dissolved inorganic carbon species) measured in these cores are consistently within a relatively narrow range between 0 and ~3 mM. However, within this range, the variability is very high in nearly all cores from this area (surface and deeper sediments), frequently dropping from ~3 to 0 and back to ~3 mM within few cm sediment depth (Fig. 45). A decrease in alkalinity can either result from a production of acid (H^+ ions) by microbial OM degradation, which dissolves solid phase carbonate to dissolved bicarbonate – or from precipitation of carbonate minerals from pore waters. As both pH values and ammonium concentrations indicate low rates of OM turnover, it can be assumed that carbonate minerals are precipitating from solution in the sediments investigated. As parts of the sediments are known to be rich in manganese, precipitation of $MnCO_3$ (rhodochrosite) or a mixed Mn-Ca carbonate is a probable explanation from the alkalinity drawdown. This thesis is supported by the fact that only certain, relatively isolated layers seem to be prone to carbonate precipitation, similar to the distinct occurrence of manganese in the brown intervals. However, if these drops in alkalinity are really paralleled by drops in the Mn pore water concentration and higher sedimentary Mn contents – and therefore document Mn carbonate formation - will have to be checked by further analyses, as well as by saturation calculations for Mn carbonates, sequential Mn extractions and XRD studies. In any case, the variable alkalinity values indicate that some sort of diagenetic activity is currently taking place even in these supposedly TOC-poor sediments.

3.8 Sea water filtration

Christian März[1)] for
Gesine Mollenhauer[2)] (not on board)

[1)] Institute for Chemistry and Biology, Oldenburg
[2)] Alfred-Wegener-Institut, Bremerhaven

Scientific background

The Arctic Ocean retrieves large amounts of organic material from the surrounding land masses. This organic material can be used to trace the origin of terrestrial input to a certain source area, but also – maybe more important – to date marine sediments via ^{14}C isotopy. However, this dating can result in errors concerning the real age of sediment deposition, as the terrigenous organic material was most probably not formed at the same time as the sediment was deposited, but potentially much earlier. Therefore, sediment dating might result in unrealistically old sediment ages and consequently in sedimentation rates that are much too low. To get an idea about the input of older, "fossil" terrestrial organic material to the Arctic Ocean, compound-specific ^{14}C dating should be applied to specific terrestrial biomarkers that are introduced to the Arctic Ocean mainly via rivers.

Material and methods

In areas where the cruise track runs proximal to potential terrestrial source areas, sea water filtration was performed. In detail, this was the case during crossing the Northwest Passage (Canadian Archipelago), on and close to the East Siberian Shelf, and on the Northeast Passage (Laptev Sea Shelf). *Polarstern* is equipped with an own Teflon pipe system for clean sea water sampling. Sea water is sucked at the base of the ship in ~11 m water depth, and distributed unfiltered via a tube system into most of the ship´s laboratories. Specifically, sea water filtration was performed in the logging room. Via PVC tubes, the sea water system was connected to a filtration setup standing in the sink. The overpressure of the sea water system was high enough to press the water through the filtration device without any further external pumping. The sea water was filtered through pre-weigthed sterilized Wheaton GF/F glass fiber filters, transported in annealed aluminum foil. The UTC time, longitude and latitude were noted at the beginning and end of every single filtration run. In addition, water throughput was measured with a flow-meter. Each filtration run took around 3-6 hours, and ~150-450 liters of sea water were filtered. After filtration, wet filters were removed carefully, dried at 40° C, stored again in aluminum foil and kept frozen until further analysis.

3.9 Sampling of sea ice

Juliane Müller[1)], Christelle Not[2)]

[1)]Alfred-Wegener-Institut, Bremerhaven
[2)]University of Quebec, Montreal

Sea ice samples have been taken on 4 stations (see Tab. 9 for dates and coordinates). Fig. 46 shows the location of the different sites. Only at site 1 a core (cut in two pieces à 30 cm diameter and 30 cm length) has been obtained by the use of stainless steel knifes, ice-picks and an ice-saw. On the snow covered ice floes at sites 2 and 3, which were accessed by helicopter, few sea ice samples bearing dispersed particles of sediment were collected at ice ridges. At site 4, pieces of drift ice covered with algae (at the bottom side) and/or sediment were caught by a lattice box manoeuvred by the ship's crane operator (Fig. 47). All samples were carried in stainless steel barrels (30 l).

Tab. 9: Coordinates of sampling sites, dates and description of sea ice samples taken during ARK-XXIII/3

Site	Date	Latitude	Longitude	Sample description
1	21.09.´08	80° 40' N	166° 39' W	sea ice core
2	29.09.´08	80° 59' N	148° 01' E	sea ice containing sediment
3	30.09.´08	81° 45' N	139° 19' E	sea ice containing sediment
4	01.10.´08	80° 60' N	137° 28' E	sea ice covered with algae and sediment

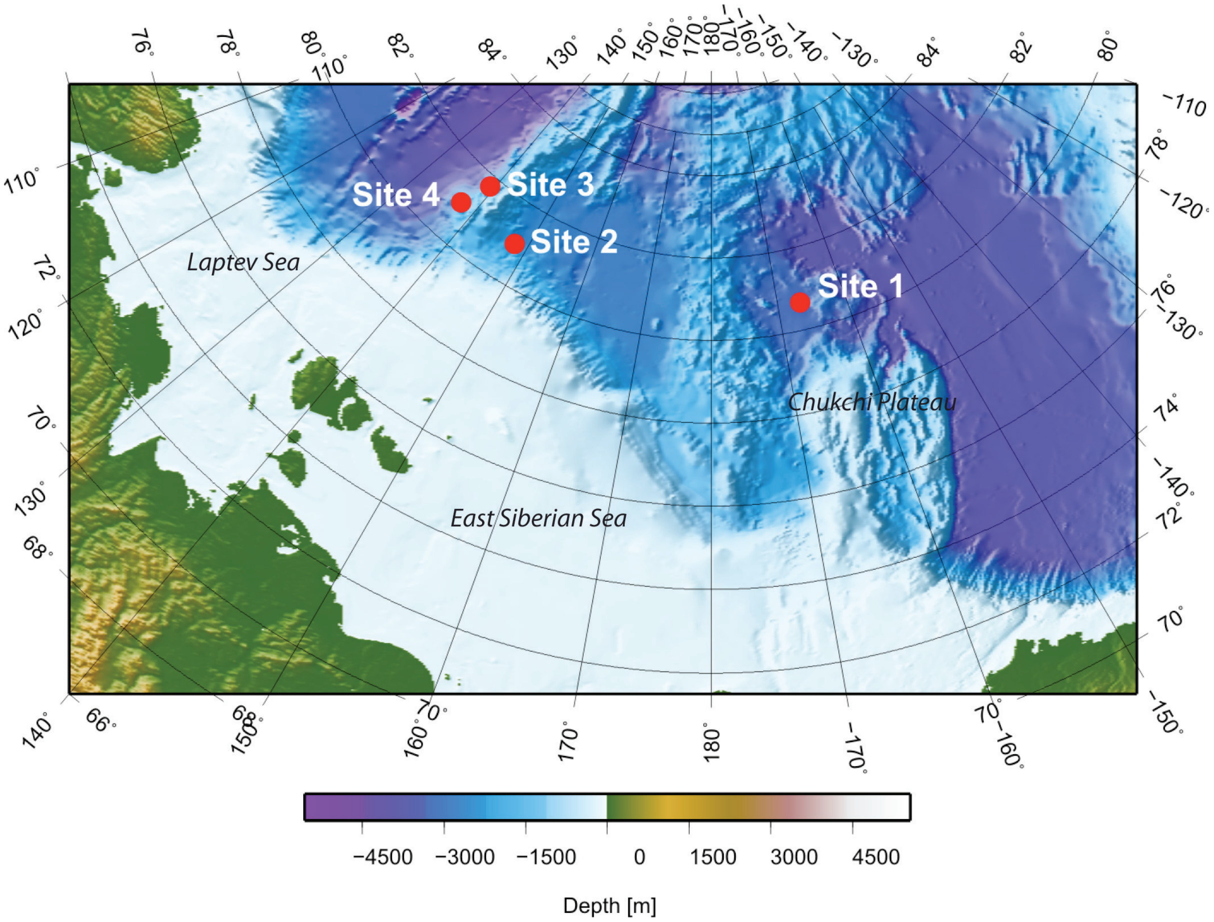

Fig. 46: Map showing locations of sea ice sampling sites during ARK-XXIII/3

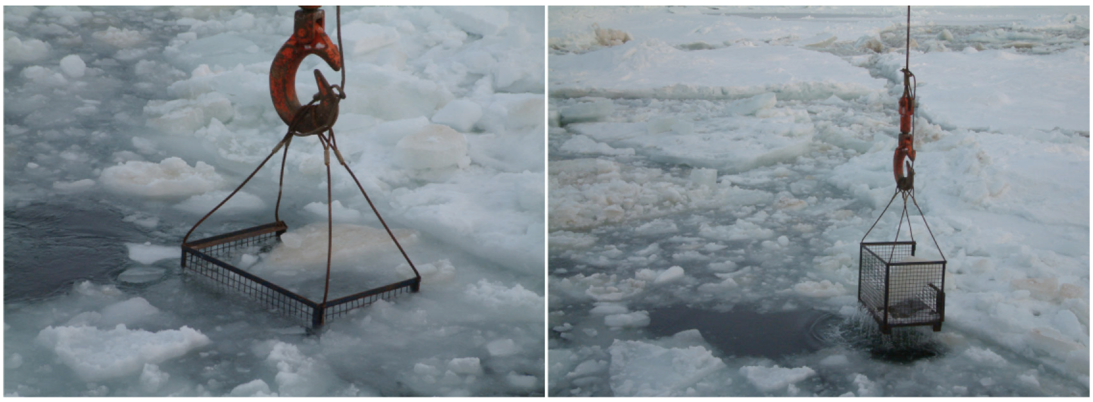

Fig. 47: Collecting pieces of drift ice by using the ship's crane

On board a sub-sample (2 cm^3) from the sea ice that was covered with algae (site 4) was carefully melted at 3°C and examined under the microscope for diatoms (see Fig. 48). Reliable investigations of these algae will be done at home. Likewise, biomarker analyses will be carried out on the ice samples containing algae and the ice core at home laboratories (AWI Bremerhaven). These samples are stored either in steel barrels or in heated glass vials (450 ml) at -30° C until further organic geochemical treatment. The proof of highly branched isoprenoids (HBIs, biomarkers that are supposed to be biosynthesized by sea ice restricted diatoms) within different sections of the ice is of special interest.

Fig. 48: Light micrograph showing diatoms found within the drift ice at site 4

Ice samples containing sediment (ice rafted detritus, IRD) were stored and melted in the stainless steel barrels at 15° C on board. The melt water samples as well as the sediment residue will be investigated on radioactive isotopes (GEOTOP, Canada) to gain information about the role of sediment sea ice in the budget of radioactive isotopes. These budgets will help to determine the intensity of particle scavenging and water mass circulation. Furthermore, mineralogy, strontium and neodynium isotopes will be investigated to identify the IRD provenance.

4. MARINE GEOPHYSICS

Wilfried Jokat, Anne Hegewald, Thomas Kahlberg, Jochen Kollofrath, Stefanie Kessling, Hartmut Martens, Pia Pulm, Morelia Urlaub, FeliciaWinter
Alfred-Wegener-Institut, Bremerhaven

The Mesozoic-Cenozoic tectonic and paleooceanographic history of the Alpha-Mendeleev Ridge Complex, Arctic Ocean

Introduction

Since the discovery of the leaves and fruit of the tropical breadfruit tree in Cenomanian fluvio-deltaic sediments from west Greenland by the Swedish palaeobotanist Alfred Nathorst in 1883, it has been apparent that the Late Cretaceous climate of the northerly high latitudes – at least during certain intervals – was far warmer than it is today. The description of glendonites (pseudomorphs of the low-temperature hydrated form of calcium carbonate, ikaiite) in lower Valanginian and upper Aptian sediments from the Sverdrup Basin in Arctic Canada (70 - 80ºN palaeolatitude), however, implies that Early Cretaceous seawater temperatures were at times close to freezing. Almost certainly these cooler temperatures record global changes because, in the case of the Late Aptian at least, coeval glendonites are also known from the Southern Hemisphere, being found in the Eromanga Basin in Australia at a palaeolatitude of 65°. The implication of these isolated occurrences is that, even in a so-called 'greenhouse' period, the Arctic Cretaceous climate was not uniformly warm and equable but experienced considerable variation. Other palaeontological data support the general contention that the Mid- to Late Cretaceous Arctic climate was generally rather mild: the presence of deciduous trees, and leaves with characteristic morphologies, at 80 - 85ºN, the presence of crocodiles beyond 60°N and, most specifically, the discovery of champosaurs (cold-blooded reptiles) in the Turonian of the Sverdrup Basin at 72°N palaeolatitude. The palaeobotanical data from the Arctic Cretaceous, however, are not in agreement with global climatic trends established from other parts of the world from oxygen-isotope ratios of microfossils and bulk pelagic carbonates. In a study of Arctic floras authors suggest a thermal maximum in the Coniacian. However, oxygen-isotope data from ODP cores in both the southern and northern hemispheres suggest that the global maximum (or maxima) was/were developed between the Cenomanian/Turonian boundary and the Late Turonian. In the northwest circum-Pacific region, oxygen-isotope ratios of aragonitic ammonites and bivalves suggest relative thermal maxima in the early Late Santonian and early Late Campanian: in this area a Campanian surface-water temperature of ~26º C at 40ºN paleo-latitude has been calculated. Only by coring, recovering and analysing the Cretaceous of the Arctic the paleo-temperature evolution of this 'sensitive tip' of the planet can be accurately determined. Did the Cretaceous globe warm and cool relatively uniformly across a range of latitudes, or were local factors dominant in governing temperature at specific locations? And, given the claims for Cretaceous eustatic sea-level changes, is there evidence for high-latitude ice in the northern hemisphere during this interval?

The area to test these hypotheses and observations in the Arctic is the Alpha Mendeleev Ridge complex located in the Amerasia Basin. It is a 450 km wide, irregular transpolar bathymetric feature, which rises over 2,700 m above the adjacent abyssal plain to known water depths of about 1,000 m and is believed to be formed during the Late Cretaceous times. The ridge section north of Canada was named after US ice station Alpha, which made the first crossing in 1957/58. The complementary ridge north of the Siberian margin was named after the Soviet chemist Mendeleev. The complex Horst and Graben Ridge topography of volcanic rocks is covered by 0.5 - 2 km of sediments. The magnetic anomaly pattern over the ridge is partly irregular and generally correlated with ridge topography. A number of hypotheses have been forwarded to explain the origin of the Alpha Mendeleev Ridge:

- a continental fragment
- an extinct axis of seafloor spreading
- a compressional feature representing an incipient island arc or subduction complex
- an inactive transform fault
- a submarine volcanic plateau
- a hot spot trace

Two samples of basalt represent the only fragment of basement of the Alpha Ridge available to date. The CESAR sample consists of tholeiitic basalt, is weathered and documents the volcanic origin of Alpha Ridge. No dating was possible. The ARCTIC-98 sample has a similar composition and was dated to 83 - 100 Ma. Together with seismic data, which indicate that a more or less continuous sediment record, it is obvious that information on the geological and climate history of the Mesozoic Arctic can be achieved by deep drilling.

The geoscientific data base over the Alpha-Mendeleev Ridge Complex

The existing data base from the Alpha- and Mendeleev ridges relevant for scientific drilling is mainly from the pioneering seismic reflection survey and sediment sampling effort from U.S. ice drift station T-3. In several instances, the drift tracks include close parallel as well as crossing lines, which may warrant target definitions. More recently, a two-ship experiment with the Russian nuclear icebreaker *Arktika* and *Polarstern* probed the central part of Alpha Ridge. In total 320 km of multichannel seismic data were acquired along three profiles supplemented by four sonobuoys. The sediment velocities range from 1.6 to 2.7 km/s and the sediment thicknesses vary between 500 m - 1,200 m. The units lie conformably on the basement. Only minor faulting is visible in the area of Lyons Seamount. In general, the sediments can be divided in two units. Their age is quite hypothetical: the upper unit is most likely of Cenozoic, the lower of Cretaceous age. The interpretation of the seismic velocities suggests oceanic basement. The basement velocities range from 4.3 to 6.7 km/s. In combination with a recovered basalt sample there is little doubt of the oceanic origin of Alpha Ridge, at least in its western sector. During the same expedition, undisturbed, up to 7.2 m long sedimentary records were obtained on the Alpha Ridge, probably representing the last about 3 Ma .

In late summer of 2000 geoscientific investigations were carried on Mendeleev Ridge aboard RV *Akademik Fedorov*. Deep seismic soundings accompanied by geological sampling, reflection and gravity observations were performed along a 500-km longitudinal profile crossing the crest of MR at 82°N. In conjunction with the seismic investigations, the total of 41 geological stations were obtained (23 gravity cores, 14 grabs and 4 dredges). In the vicinity of a prominent steepsided bathymetric knob abundant large-sized, semi-angular rock fragments were recovered and appeared composed of uniform lithologies dominated by fossiliferous sedimentary rocks of Middle-Upper Palaeozoic age.

Work at sea

We conducted intensive seismic reflection profiling across the East Siberian Margin and the adjacent deep abyssal plains. The profiling was supplemented by the deployment of a new type of sonobuoys to record more accurate seismic velocity, and gravity measurements with a fixed mounted KSS31 instrument. Magnetic measurements were performed with two vector magnetometers, which are fixed installed on *Polarstern*. The planned magnetic surveys with the *Polarstern* helicopters became a victim on the constantly bad and rapidly changing visibility. In total may be 3 days had sufficient stable weather conditions to conduct long-range flight activities. However, this was not sufficient to gather systematic magnetic data.
The seismic data were acquired with three different setups:

- 1,080 km with a 600 m active streamer (96 chan.) and a 33 l airgun array
- 2,238 km with a 3,000 m active streamer (240 chan.) and a 33 l airgun array
- 1,098 km with a 300 m active streamer (48 chan.) and a 33 l airgun array

The source consisted of 4 G-Guns mounted in a frame 10 m behind the vessel. Whenever, ice and weather allowed sonobuoys were deployed. The seismic line kilometres sum up to 4,416 km with 105.270 shots (Fig. 49). In total 23 sonobuoys were used, which provide high quality information in general up to 30 km or even larger offsets.

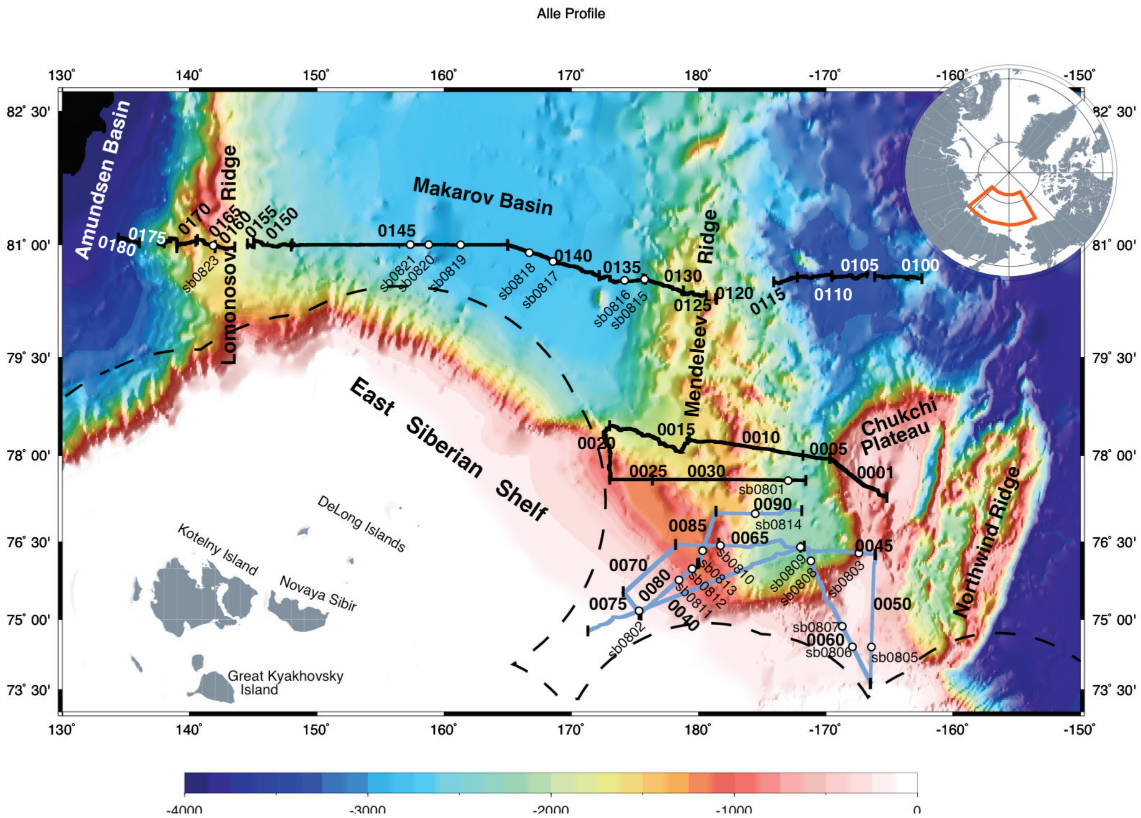

Fig. 49: Location of the seismic reflection profiles. The white dots indicate the position, where sonobuoys were deployed. The black lines were acquired with a 300/600 m long active streamer, the blue lines with a 3000 m long cable. The gaps between some of the lines could not be closed because of difficult ice conditions.

The data will briefly described for each region. The data processing could not be finished for several reasons on the vessel. For the location of the profiles see figure 49.

Chukchi Plateau/Shelf (Lines 20080045-20080060)

In total three seismic profiles were gathered across the plateau and shelf. A long N-S trending line was collected to better understand how the plateau is geologically connected to the southern shelf. The data provided useful signals down to 6s TWT, where weak indications for the presence of the acoustic basement are visible. In the sedimentary column little evidence for strong glacial erosion of the shelf can be found. Moreover, typical seismic units, which indicate Trans-/Regressions are clearly observed. They might provide a possibility to set up a general age model when compared with similar dated/drilled structures in the Beaufort Sea. Glacial sequences are only present in the shallow part of the profile. Non-typical is also the weak energy of the sea floor multiple, which supports the interpretation that this area might not been covered very often by huge ice shields.

East Siberian Shelf (Lines 20080040-20080090)

A more than 400 km long seismic line was acquired from the East Siberian Shelf across the Mendeleev Ridge terminating in the basin between the Chukchi Plateau and the Mendeleev Ridge. Two shorter ones north of line 20080040 were shot to show variations in the sediment structure below the shelf break. The major subject of the three lines across the margin was to understand the general geological evolution of this area in terms of tectonics and glacial erosion.

Similar to the Chukchi Shelf little evidence for a strong glacial erosion can be seen in the sedimentary sequences. Again only the very shallow part of the lines contain evidences for a glacial overprinting or transport. One more evidence for only little glacial erosion is also the shallow water depths of less than 50 m, which is unusual for glacially eroded margins like those off East Greenland and Antarctica. How and if the basement of the Mendeleev Ridge continues underneath the shelf is currently not known, since the data needs processing to unravel this information.

Mendeleev Ridge (Lines 20080001-20080030)

Two seismic lines across the Mendeleev Ridge were acquired with a 600 m streamer to map the transition of the ridge into the basins. Almost along the entire lines the top of the acoustic basement could be imaged. It shows that most of the current ridge's topography is a consequence of current controlled deposition. Several hundred meters below the seafloor there is clear evidence for a massive erosion of older sediments. At the moment a sound dating of this event is not possible, but tentatively it seems that we can relate this event to the separation of the Lomonosov Ridge from the Siberian shelves some 55 Ma ago.

Canada Basin-Amundsen Basin transect (lines 20080100-20080180)

Along this transect the seismic investigations were interrupted to allow at certain location shallow geological sampling of the sediments. The transect is 1,120 km long and was covered mostly by seismic data with a 300 m long streamer. Only at the western flank of the Mendeleev Ridge, the eastern flank of the Lomonosov Ridge, and, finally, in the Amundsen Basin the ice conditions were to heavy for seismic profiling with a single icebreaking vessel. Thus, new seismic data could be acquired along 81°N latitude across the western flank of the Mendeleev Ridge, through the Makarov Basin and finally across the Lomonosov Ridge. The data show that the Makarov Basin is of Mesozoic age. An erosional unconformity generated on the Lomonosov Ridge some 55 Ma ago can be traced across the entire basin, and on the Mendeleev Ridge. All deeper structures must, therefore, be older. A tentative interpretation suggests that the Makarov Basin is at least 100 Myr old. Several sonobuoys were deployed along the lines to provide exact velocity data to calculate the sediment thickness.

The sonobuoys, which were used during the survey, had to be recovered by helicopter. It stores the seismic data on flash memory and keeps contact to the vessel with an Iridium communication system. It sends at specified times its position to the vessel. Only one instrument got lost, because it drifted below an ice floe.

All geophysical instruments were switched off before entering the Exclusive Economic Zone of the Russian Federation. No research permit was granted for the geoscientific projects.

4.1 Heat flow measurements

Wilfried Jokat, Morelia Urlaub
Alfred-Wegener-Institut, Bremerhaven

During the expedition ARK-XXIII/3 heat flow measurements were carried out at a transect across the Mendeleev Ridge, and at isolated spots at the Lomonosov and Gakkel Ridge (Fig. 50). The main target was to obtain information about crustal age and origin.

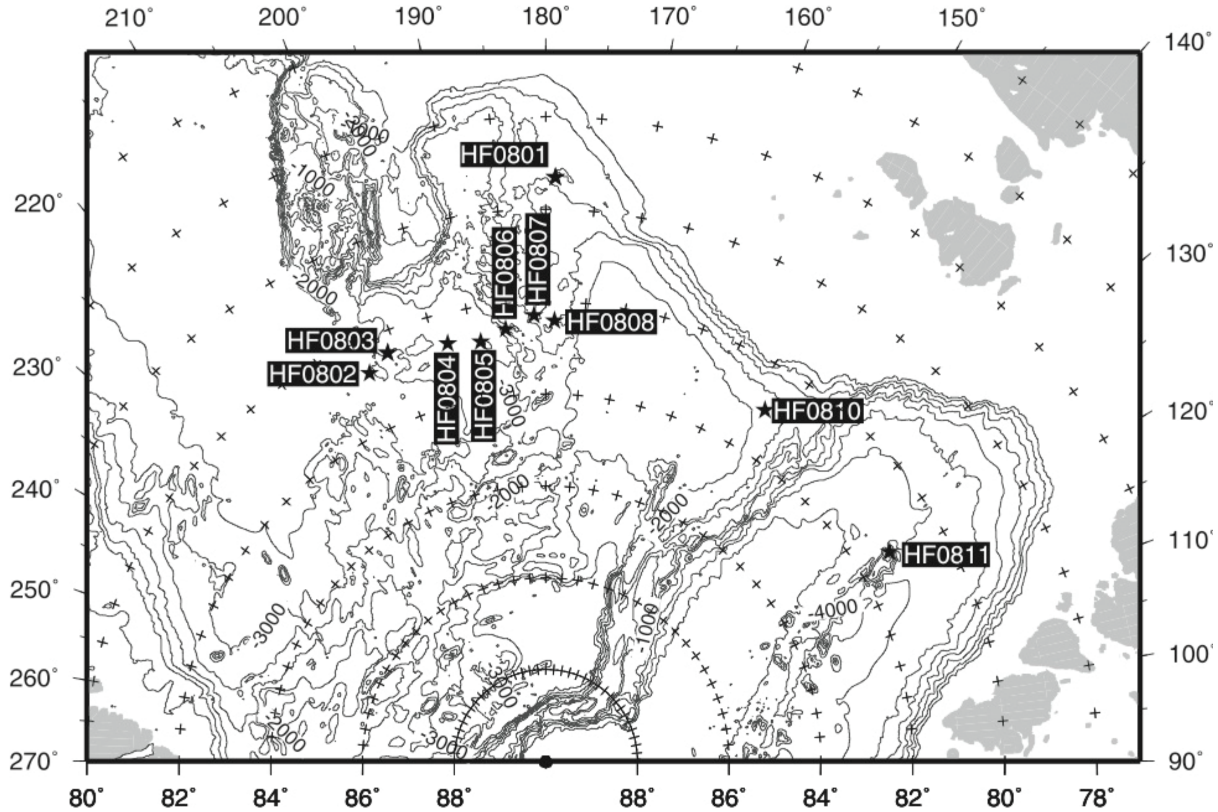

Fig. 50: Bathymetric map of the study area during ARK-XXIII/3 with observed heatflow values [mW/m²]. Contour interval is 500 m.

The heat flow *Q* is defined by

$$Q = k \cdot dT/dz.$$

Through this equation *Q* is related to thermal conductivity *k* with *[k]=W/mK* and the temperature gradient *dT/dz* with temperature *[T]=K* and depth *[z]=m*. To obtain the gradient five temperature sensors were mounted at equal distances of about 0.90 m to each other on a 5 m gravity corer barrel. These Miniaturized Temperature Loggers (MTLs) work autonomously with a sampling rate of 1 s and measure the *in-situ* temperature. After penetration the gravity corer remained 4 - 7 minutes in the sediment. The sites were determined by Parasound surveys. In total 13 measurements were acquired; nine stations of single and two stations of two penetrations. Additionally, bottom water temperature measurements at six stations were taken with a single MTL mounted to the giant box corer. All loggers were calibrated by tying them to a CTD during a CTD station. See Fig. 51 for an example of heatflow measurement data. The heat flow was calculated according to estimates of *k* because thermal conductivity was not measured onboard.

Table 10 lists the calculated heat flow values. E.g., the heat flow across the Mendeleev Ridge varies between 39 mW/m² and 57 mW/m². A maximum of 73 mW/m² occurs at its easternmost part. The values agree very well with the regional trends summarised by Grantz and Johnson (1990). At the southeast flank of Lomonosov Ridge 60 mW/m² were observed. At the flank of the rift valley of the volcanically active Gakkel Ridge a value as high as 118 mW/m² was measured.

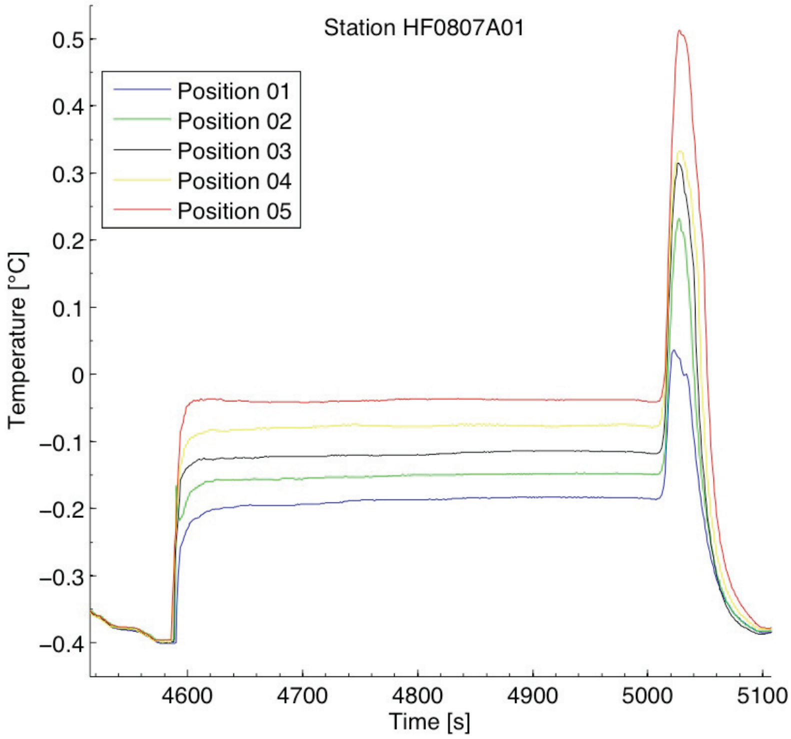

Fig. 51: Extraction from the recorded temperature data at station HF0807A01 (PS72/413). Position numbers indicate the logger's depth below seafloor (01, 5.86 m; 02, 6.69 m; 03, 7.63 m; 04, 8.60 m; 05, 9.54 m). Penetration of the gravity corer into the sediment is followed by an increase in temperature. While pulling the device out of the sediment after five minutes a friction heat pulse occurs.

Tab. 10: List of all heatflow stations during expedition ARK-XXIII/3. k is thermal conductivity, dT/dz is the temperature gradient, Q is the calculated heatflow.

Station	Name	k [W/mK]	dT/dz [K/m]	Q [mW/m²]	T_{bw} [°C]	Depth [m]	Latitude	Longitude
PS72/343	HF0801A01	1.00	0.0496	50		1225	77°18.194'N	179°3.360'E
PS72/343	HF0801A02	1.00	0.0502	50		1226	77°18.331'N	179°2.917'E
PS72/392	HF0802A01	1.00	0.0597	60	-0.287	3599	80°27.862'N	158°49.243'W
PS72/392	HF0802A02	1.00	0.0574	57	-0.287	3607	80°27.825'N	158°49.821'W
PS72/393	HF0803A01	1.00	0.0727	73		3801	80°43.239'N	155°32.759'W
PS72/399	HF0804A01	1.00	0.0557	56	-0.313	3307	80°39.427'N	166°46.465'W
PS72/404	HF0805A01	1.00	0.0425	43		2131	80°45.259'N	171°9.688'W
PS72/408	HF0806A01	1.00	0.0463	46		2534	80°33.179'N	174°42.179'W
PS72/413	HF0807A01	1.00	0.0394	39	-0.39	1237	80°17.31'N	178°29.071'W
PS72/418	HF0808A01	1.00	0.0421	42	-0.409	1991	80°24.052'N	178°51.780'E
PS72/430	HF0809A01	1.00	/	/	/	2813	81°03.984'N	164°43.592'E
PS72/438	HF0810A01	1.00	0.0596	60	-0.384	2420	80°58.951'N	148°01.399'E
PS72/471	HF0811A01	1.00	0.1179	118		3968	81°13.731'N	121°18.307'E

Reference

A. Grantz and L. Johnson (1990). The Arctic Ocean region, Geological Society of America, Boulder Colorado.

5. PHYSICAL OCEANOGRAPHY

Dirk Kalmbach[1),] Takashi Kikuchi [2)], Sebastian Mechler[3)], Alexander Nauels[1)], Benjamin Rabe[1)]

[1)]Alfred-Wegener-Institut, Bremerhaven
[2)]Japan Agency for Marine Earth Science and Technology
[3)]Optimare Sensorsysteme AG

Objectives

Observations from the past decades revealed the Arctic Ocean and its ice cover to be a sensitive indicator of climate change. Arctic sea ice extent was at a minimum in September, 2007, so that in summer 2008, most of the ice cover in the Eurasian Arctic consisted of first-year ice. Furthermore, the Arctic Ocean has been strongly affected by advection from the North Atlantic and Pacific. These imported water masses changed considerably over the past decades. In the Arctic, the ocean waters are subject to transformations through cooling, freezing and melting. Thus, when returning to the North Atlantic, Arctic water masses directly or indirectly influence the Atlantic-wide meridional overturning circulation. Large amounts of fresh water, supplied to the Arctic Ocean by continental runoff (10 % of the global runoff), precipitation and Pacific Water inflow, play a considerable role in these transformations by shielding the ocean from direct atmospheric influence. Furthermore, the fresh water underwent strong variations in supply, storage and circulation pattern during the past decades.

In order to understand the processes behind the changes and to distinguish climate trends from variations that follow the atmospheric oscillation patterns, the changes have to be surveyed with sufficient spatial coverage. For this purpose an international joint effort is undertaken during IPY to conduct a quasi-synoptic Pan-Arctic survey. In 2007, several cruises covered large parts of the Arctic, and the central Eurasian basins were surveyed during ARK-XXII/2. During ARK-XXIII/3, the work of the previous year was extended toward the East-Siberian regions with a final transect in the southern parts of the basins from the Canadian Basin to the Nansen-Gakkel Ridge and onto the Laptev Sea continental slope.

Work at sea

Besides several shallow CTD casts that aided biological observations, we acquired a full-depth transect across the Canadian and Makarov basins to the Amundsen Basin side of the Lomonosov Ridge with one additional station close to the Nansen-Gakkel Ridge (Fig. 52, Tab. 11). In total, 24 CTD profiles were taken and water samples were collected at all stations. Besides our own samples for the calibration of the conductivity and oxygen sensors, the rosette bottles were sampled by other groups on-board.

All casts were carried out with a standard CTD/rosette water sampler from Sea-Bird Electronics Inc. The system components are listed by type and serial number in Tab.

12. The SBE911+ CTD was equipped with duplicate temperature and conductivity sensors and was connected to a SBE32 Carousel Water Sampler with 24 12-liter bottles. Additionally, a Benthos Altimeter, a Wetlabs C-Star Transmissometer and a SBE 43 dissolved oxygen sensor were mounted on the carousel. The SBE 43 contains a membrane polarographic oxygen detector. The algorithm to compute oxygen concentration requires also measurements of temperature, salinity and pressure which are provided by the CTD system. To calibrate the oxygen profiles water samples from CTD casts were collected and measured onboard with Winkler titration. Continuous profiles of the DOM concentration and *Chlorophyll a* fluorescence were obtained by two Dr. Haardt fluorometers, but no water samples for the calibration of the fluoremeters were taken. Salinity of 104 water samples taken at 15 stations was measured using a Guildline salinometer with Standard Water Batch P149 for calibration of the conductivity sensors. From station 396 the CTD deck-unit gave a serial communication error part-way through the cast, either at the bottom or during the upcast. When data acquisition was restarted with a new data file, the rest of each profile was acquired without further problems. After the replacement of the deck-unit with the spare after station 413, no communication errors occurred for the remaining casts.

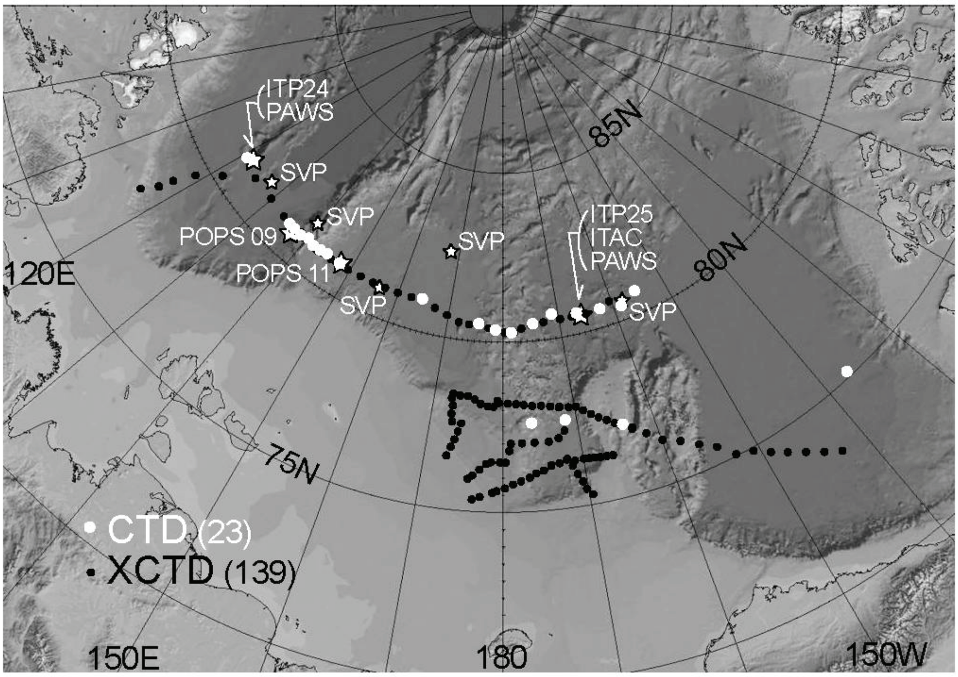

Fig. 52: Seafloor bathymetry with locations of CTD casts (white dots) and XCTD casts (black dots) and buoy deployments (labels)

Tab. 11: List of CTD casts

Station	Cast	Latitude (° ')	Longitude (° ')	Hydrosweep Depth (m)	Altimeter (m above seafloor)	Pressure maximum (dbar)	Profile times (dd/mm/yy hh:mm) during the cast: start, at depth, surface		
290	2	75 6.492 N	137 1.248 W	3482	N/A	254	25/08/08 18:15	25/08/08 18:25	25/08/08 18:42
308	2	77 5.551 N	164 8.741 W	410	N/A	254	30/08/08 01:06	30/08/08 01:14	30/08/08 01:28
340	2	77 34.800 N	171 31.900 W	2291	N/A	254	04/09/08 06:26	04/09/08 06:35	04/09/08 06:50
341	2	77 35.987 N	176 6.592 W	1340	N/A	253	04/09/08 19:41	04/09/08 19:51	04/09/08 20:05
392	2	80 27.772 N	158 40.564 W	3606	9.8	3627	18/09/08 14:12	18/09/08 15:22	18/09/08 16:32
393	2	80 43.097 N	155 29.953 W	3804	N/A	253	19/09/08 06:00	19/09/08 06:10	19/09/08 06:30
396	2	80 35.001 N	162 24.225 W	2677	9.5	2713	19/09/08 23:23	20/09/08 00:17	20/09/08 01:15
399	2	80 38.330 N	166 42.156 W	3307	N/A	254	20/09/08 18:55	21/09/08 10:05	21/09/08 19:25
400	2	80 38.724 N	166 45.540 W	3307	9.1	253	21/09/08 20:41	21/09/08 22:19	21/09/08 23:28
404	2	80 45.417 N	171 9.350 W	2132	N/A	253	22/09/08 14:33	22/09/08 14:47	22/09/08 15:05
408	2	80 32.888 N	174 41.557 W	2523	9.8	2554	23/09/08 14:30	23/09/08 15:21	23/09/08 16:18
413	2	80 18.709 N	178 33.279 W	1275	10	1271	24/09/08 10:44	24/09/08 11:12	24/09/08 11:51
418	2	80 23.325 N	178 42.521 E	2000	99	1014	25/09/08 00:53	25/09/08 01:15	25/09/08 01:44
422	2	80 33.339 N	175 44.549 E	2489	5.8	2531	25/09/08 16:10	25/09/08 17:01	25/09/08 17:56
430	2	81 0.072 N	164 52.042 E	2814	10.2	2847	27/09/08 07:20	27/09/08 08:17	27/09/08 09:10
438	2	80 58.850 N	147 57.520 E	2415	9.2	2436	29/09/08 21:35	29/09/08 22:26	29/09/08 23:16
442	2	81 1.077 N	145 2.186 E	1995	9.5	2006	29/09/08 11:00	29/09/08 11:40	29/09/08 12:25
446	1	80 59.957 N	143 35.558 E	1595	8.9	1605	29/09/08 17:47	29/09/08 18:22	29/09/08 19:02
451	2	80 58.101 N	142 4.710 E	1562	10.5	1586	30/09/08 00:44	30/09/08 01:18	30/09/08 01:54
455	2	81 2.869 N	140 32.170 E	1304	5.6	1313	30/09/08 07:13	30/09/08 07:41	30/09/08 08:15
459	2	80 58.682 N	139 0.756 E	1660	5.6	1668	30/09/08 13:07	30/09/08 13:42	30/09/08 14:21
463	1	80 59.987 N	137 25.239 E	2455	8.1	2485	30/09/08 20:53	30/09/08 21:42	30/09/08 22:38
466	1	81 0.778 N	136 6.327 E	2977	8.8	3012	01/10/08 07:37	01/10/08 08:35	01/10/08 09:38
471	2	81 14.120 N	121 15.980 E	2977	8.8	4261	03/10/08 01:31	03/10/08 02:53	03/10/08 04:13

Tab. 12: CTD rosette components

	Type	SN / remarks
CTD-sonde	SBE 911+	287
CTD-sensors Temperature	SBE3	pri. 1373 / sec. 2929
Conductivity	SBE4	pri. 2470 / sec. 3290
Pressure	Digiquartz 410K-105	51197
altimeter	Benthos PSA916	1228
transmissiometer	Wetlabs C-Star	814
fluorometer chlorophyll a	Dr. Haardt	908
fluorometer yellow substance	Dr. Haardt	SN none / device installed
oxygen	SBE43	743
rosette	SBE 32	55
winch	SE 32/1	

Additional temperature and salinity profiles were obtained by 139 eXpendable CTD (XCTD) casts (Tab. 13). XCTD system manufactured by the Tsurumi-Seiki Co. Ltd. (Yokohama, Japan) can measure ocean temperature and conductivity, i.e., salinity, from sea surface down to 1,100 m depth. It mainly consists of XCTD probe, launcher, digital converter and personal computer for data processing. The XCTD probe is launched from the ship into water, and sinks down with constant velocity measuring temperature and conductivity. These measurements provide a section from the

Canadian to the Makarov Basin, some shorter sections on the Chuckchi Plateau and the continental slope and additional stations in between the CTD stations to increase horizontal resolution in frontal zones.

Underway measurements with a vessel-mounted narrow-band 150 kHz ADCP from RD Instruments and two Sea-Bird SBE45 thermosalinograph were conducted to supply temperature, salinity and current data. The thermosalinographs are installed in 6 m depth in the bow thruster tunnel and in 11 m depth in the keel. The salinity of both instruments was controlled by taking water samples. The ADCP worked well throughout most of the cruise with few data gaps, being hampered only by network access problems. This problem was solved by installing a USB stick as the backup drive on the ADCP acquisition computer, thus not requiring network access during data acquisition. In order to provide year-round measurements of temperature, salinity and velocity, ice-tethered platforms with various instruments were deployed.

Tab. 13: List of XCTD casts

ARK XXIII-3 Arctic Cruise / XCTD station information (1/3)

Sta. No.	XCTD No.	Date/Time (UTC)					Latitude		Longitude			Bottom Depth	Measurement depth
		yyyy	mm	dd	hh	mm	dd	mm.m	dd	mm.m	E/W		
292	1	2008	8	28	6	06	73	17.8	142	34.6	W	3653	1100
293	2	2008	8	28	9	03	73	36.4	144	9.2	W	3712	1100
294	3	2008	8	28	12	06	73	55.2	145	47.3	W	3806	1100
295	4	2008	8	28	15	2	74	13.5	147	24.6	W	3835	1100
296	5	2008	8	28	18	01	74	30.4	148	57.3	W	3884	1100
297	6	2008	8	28	20	58	74	48.3	150	34.5	W	3907	1100
298	7	2008	8	29	0	00	74	57.1	152	25.5	W	3916	1100
299	8	2008	8	29	2	58	75	25.0	154	1.6	W	3919	1100
300	9	2008	8	29	5	56	75	43.2	155	47.6	W	3278	1100
301	10	2008	8	29	9	01	76	2.3	157	41.8	W	534	534
302	11	2008	8	29	12	5	76	15.4	159	42.7	W	2168	1100
303	12	2008	8	29	14	57	76	37.2	161	16.9	W	2119	1100
304	13	2008	8	29	17	58	76	52.3	162	50.7	W	1701	1100
306	14	2008	8	29	20	57	76	54.3	162	50.1	W	1629	1100
307	15	2008	8	29	23	45	77	4.1	164	7.4	W	406	406
309	16	2008	8	30	3	00	77	11.4	164	53.4	W	415	415
311	17	2008	8	30	5	58	77	20.3	165	48.3	W	707	707
312	18	2008	8	30	9	2	77	28.8	166	46.5	W	675	675
313	19	2008	8	30	12	2	77	37.0	167	42.5	W	456	456
314	20	2008	8	30	15	6	77	47.0	168	39.9	W	588	588
315	21	2008	8	30	18	1	77	55.4	169	30.5	W	1450	1100
316	22	2008	8	30	21	0	77	57.3	170	35.5	W	2330	1100
317	23	2008	8	30	23	56	78	0.0	171	48.3	W	2280	1100
318	24	2008	8	31	2	57	78	0.1	171	56.2	W	2291	162
319	25	2008	8	31	5	59	78	2.7	173	9.9	W	2052	1100
320	26	2008	8	31	9	2	78	5.9	174	25.4	W	1886	1100
321	27	2008	8	31	11	57	78	7.3	175	39.0	W	1558	848
323	28	2008	8	31	15	3	78	10.0	176	51.8	W	920	920
324	29	2008	8	31	17	56	78	12.4	177	58.9	W	1580	1100
325	30	2008	8	31	20	59	78	13.5	179	11.4	W	1041	1041
326	31	2008	8	31	23	58	78	14.6	179	33.6	E	1770	1100
327	32	2008	9	1	2	46	78	18.2	179	18.8	E	1802	1100
328	33	2008	9	1	6	8	78	7.0	178	47.2	E	1700	519
329	34	2008	9	1	9	1	78	8.1	177	59.7	E	1767	1100
330	35	2008	9	1	12	4	78	11.9	176	57.4	E	1848	411
331	36	2008	9	1	15	9	78	19.4	176	5.9	E	1946	437
332	37	2008	9	1	18	1	78	24.2	175	2.9	E	1998	1100
333	38	2008	9	1	21	0	78	24.3	173	54.0	E	1965	1100
334	39	2008	9	1	23	56	78	26.3	172	56.0	E	1833	532
335	40	2008	9	2	2	52	78	17.8	172	44.4	E	1517	1100
336	41	2008	9	2	5	56	78	4.8	173	0.6	E	1245	1100
337	42	2008	9	2	8	56	77	49.7	172	58.4	E	1085	1085
338	43	2008	9	2	12	12	77	36.0	173	8.3	E	1109	1100
345	44	2008	9	5	23	33	77	34.0	174	26.4	E	1250	1100
346	45	2008	9	6	1	4	77	19.0	174	6.1	E	1142	1100
347	46	2008	9	6	2	30	77	4.3	173	44.7	E	843	843
348	47	2008	9	6	3	53	76	50.1	173	22.6	E	478	478

ARK XXIII-3 Arctic Cruise / XCTD station information (2/3)

Sta. No.	XCTD No.	Date/Time (UTC)					Latitude		Longitude			Bottom Depth	Measurement depth
		yyyy	mm	dd	hh	mm	dd	mm.m	dd	mm.m	E/W		
349	48	2008	9	6	5	27	76	33.7	172	58.8	E	328	328
352	49	2008	9	7	19	58	75	17.7	176	31.1	E	256	256
353	50	2008	9	7	22	56	75	23.1	177	25.6	E	367	367
354	51	2008	9	8	3	12	75	31.5	178	50.2	E	701	701
355	52	2008	9	8	4	56	75	34.6	179	22.2	E	868	868
356	53	2008	9	8	7	59	75	40.3	179	39.9	W	1029	1029
357	54	2008	9	8	10	57	75	46.7	178	40.7	W	1179	1100
358	55	2008	9	8	14	0	75	51.9	177	40.3	W	1178	1100
359	56	2008	9	8	17	0	75	57.7	176	39.1	W	1760	1100
360	57	2008	9	8	19	58	76	4.4	175	48.2	W	2116	401
361	58	2008	9	8	22	56	76	9.1	174	48.0	W	2253	1100
362-1	59	2008	9	9	1	58	76	16.5	173	53.4	W	2284	314
362-2	60	2008	9	9	2	5	76	16.9	173	51.2	W	2288	473
363	61	2008	9	9	5	2	76	19.2	172	50.2	W	2276	1100
364	62	2008	9	9	7	59	76	23.8	171	51.4	W	2314	1099
365	63	2008	9	9	10	59	76	19.5	170	53.2	W	2257	1100
366	64	2008	9	9	14	5	76	20.9	169	46.1	W	2233	1100
367	65	2008	9	9	16	2	76	20.0	169	4.1	W	2137	1100
368	66	2008	9	9	18	2	76	19.0	168	20.8	W	1805	1100
369	67	2008	9	9	19	57	76	18.0	167	38.9	W	985	985
370	68	2008	9	9	21	55	76	17.0	166	54.0	W	357	357
371	69	2008	9	9	23	56	76	15.9	166	8.8	W	450	450
372	70	2008	9	12	7	57	75	13.5	169	25.4	W	261	261
373	71	2008	9	12	10	58	75	25.5	170	1.7	W	527	527
374	72	2008	9	12	14	2	75	40.6	170	19.5	W	1410	1100
375	73	2008	9	12	16	57	75	54.8	170	48.8	W	1327	448
376	74	2008	9	12	19	59	76	11.3	171	13.0	W	2140	1100
377	75	2008	9	12	22	56	76	25.1	171	47.1	W	2373	1100
378	76	2008	9	13	21	59	76	26.6	179	45.0	E	1197	1100
379	77	2008	9	14	0	57	76	26.9	178	39.9	E	1222	1100
380	78	2008	9	14	4	58	76	23.5	178	3.3	E	1188	1100
381	79	2008	9	14	8	1	76	12.7	177	13.4	E	844	844
382	80	2008	9	14	10	59	76	1.7	176	22.7	E	431	431
383	81	2008	9	14	12	58	75	54.6	175	50.2	E	322	322
384	82	2008	9	16	3	1	76	26.4	179	31.6	W	1133	1100
385	83	2008	9	16	6	56	76	47.7	179	1.3	W	1179	916
386	84	2008	9	16	11	18	77	0.8	178	50.0	W	1505	904
387	85	2008	9	16	15	1	77	0.8	177	21.0	W	1440	1100
388	86	2008	9	16	18	57	77	0.6	175	44.7	W	1812	1100
389	87	2008	9	16	23	1	77	0.2	173	53.9	W	2136	868
390	88	2008	9	17	3	1	77	4.6	172	29.3	W	2207	1099
391	89	2008	9	17	8	0	77	16.4	171	39.5	W	2316	1100
395	90	2008	9	19	18	6	80	43.5	160	5.5	W	3674	583
396	91	2008	9	19	22	16	80	34.5	162	2.5	W	2685	940
398	92	2008	9	20	12	56	80	35.9	164	51.1	W	3089	504
402	93	2008	9	22	4	51	80	35.7	167	23.7	W	3378	631
403	94	2008	9	22	10	23	80	35.9	169	31.7	W	3387	226

ARK XXIII-3 Arctic Cruise / XCTD station information (3/3)

Sta. No.	XCTD No.	Date/Time (UTC)					Latitude		Longitude			Bottom Depth	Measurement depth
		yyyy	mm	dd	hh	mm	dd	mm.m	dd	mm.m	E/W		
407-1	95	2008	9	23	8	13	80	34.8	172	29.4	W	3383	170
407-2	96	2008	9	23	8	19	80	34.8	172	29.4	W	3373	226
409	97	2008	9	23	21	17	80	32.9	174	54.2	W	2484	445
411	98	2008	9	24	5	7	80	27.3	176	33.3	W	2456	266
412	99	2008	9	24	7	24	80	21.4	177	54.3	W	1732	270
416	100	2008	9	24	18	57	80	21.4	179	31.3	W	1761	465
417	101	2008	9	24	22	32	80	23.2	178	53.0	E	2035	332
419	102	2008	9	25	10	41	80	28.6	177	36.5	E	2053	372
421	103	2008	9	25	13	54	80	33.3	175	58.3	E	2418	439
425	105	2008	9	26	2	53	80	33.2	174	6.6	E	2763	1100
426	106	2008	9	26	6	59	80	35.2	172	12.5	E	2808	1100
428	107	2008	9	26	18	53	80	43.8	169	56.5	E	2837	1100
429	108	2008	9	26	23	33	80	52.5	167	30.4	E	2858	576
432	109	2008	9	27	17	30	81	0.0	162	47.2	E	2877	1100
433	110	2008	9	27	22	20	81	0.0	160	4.7	E	2877	1100
434	111	2008	9	28	2	46	81	0.0	157	32.7	E	2837	1100
435	112	2008	9	28	7	16	81	0.0	154	59.8	E	2737	1100
436	113	2008	9	28	11	58	81	0.0	152	25.6	E	2470	1100
437	114	2008	9	28	16	43	81	0.0	149	46.0	E	2553	979
440	115	2008	9	29	5	6	80	59.9	147	10.2	E	2305	211
441	116	2008	9	29	7	24	80	59.7	145	59.4	E	2173	369
443	117	2008	9	29	10	47	81	1.1	144	59.4	E	2035	1100
444	118	2008	9	29	15	4	81	0.3	144	32.7	E	1894	739
445	120	2008	9	29	16	35	80	59.9	144	0.6	E	1729	1100
448	121	2008	9	29	20	26	80	57.5	143	4.0	E	1477	319
449	122	2008	9	29	21	37	80	57.8	142	33.3	E	1496	87
450	123	2008	9	29	22	13	80	58.7	142	14.6	E	1489	436
453	124	2008	9	30	3	52	81	0.0	141	29.9	E	1711	524
454	125	2008	9	30	4	50	81	2.8	141	5.5	E	1694	262
457	126	2008	9	30	9	29	81	1.4	140	3.1	E	1430	245
458	127	2008	9	30	10	31	81	0.5	139	31.3	E	1539	508
461-1	128	2008	9	30	17	6	81	4.6	138	32.2	E	1858	234
461-2	129	2008	9	30	17	12	81	4.6	138	29.6	E	1870	333
462	130	2008	9	30	18	52	81	1.3	138	2.7	E	2291	224
464	131	2008	10	1	4	24	80	58.6	136	52.2	E	2672	1100
465	132	2008	10	1	7	5	81	0.6	136	15.4	E	3010	1100
468	133	2008	10	1	15	31	81	4.2	134	0.8	E	3839	348
469	134	2008	10	1	23	10	81	8.4	129	52.7	E	3959	770
470	135	2008	10	2	10	26	81	7.5	124	57.9	E	3549	933
473	136	2008	10	4	3	27	80	21.6	121	19.0	E	3476	543
474	138	2008	10	4	11	19	79	39.7	118	58.7	E	3286	1082
475	139	2008	10	4	20	57	79	0.2	118	0.3	E	2825	1100
476-1	140	2008	10	5	0	57	78	32.7	117	47.4	E	2347	852
476-2	141	2008	10	5	1	4	78	32.4	117	45.3	E	2333	1100
477	142	2008	10	5	5	51	78	1.7	116	51.8	E	1400	1085

These platforms contribute to an "International Arctic Ocean Observation System" (iAOOS) that aims to maintain a persistent observation network in this harsh climate. The oceanographic work of the cruise was part of the EU-funded Integrated Project "DAMOCLES" (Developing Arctic Modelling and Observing Capabilities for Long-term Environment Studies), the BMBF-funded Project "North-Atlantic" and was also supported by the Japan Agency for Marine Earth Science and Technology (JAMSTEC).

First results from hydrographic observations

Shallow layers to Atlantic Water layer

Potential temperature and salinity data from the central Canada Basin to the area over the Mendeleev Ridge were obtained between August 24th and September 17th 2008 (Figs. 53 and 54). Surface salinity in the central Canada Basin in late August 2008 was less than 23. According to observation results from the spring 2008 mission in the Beaufort Sea, the upper ocean salinity was about 25 psu in April, which was much lower than the climatology. Such a freshening of the surface water could be explained by sea ice melt in summer, and/or the recent spin-up of the Beaufort Gyre collecting more freshwater. Below this surface layer in the Canadian Basin, we found indications of Pacific Summer Water (PSW), which was defined as a temperature maximum layer around the layer of S~31.5, and even further down Pacific Winter Water (PWW), defined as temperature minimum layer around S~33.1 and formed by convection during winter atmospheric cooling and ice formation. Both Pacific-origin water masses were dominant from the Canada Basin to the area over the Chukchi Plateau. Interestingly, no Pacific-origin water signal was observed over the Chukchi Abyssal plain, and at the more western side of the Arctic Ocean. In contrast, we found a temperature minimum around 60 -100 m depth, which was presumably originated from the Siberian Shelf Water (SSW), and a signal of Eurasian basins-origin Lower Halocline Water (LHW) above the warm Atlantic Water (AW) in the western side of this transect. The warm AW on this transect between the Canada Basin and the area over the Mendeleev Ridge is located at several hundred meters depth, and has a characteristic temperature maximum. The maximum temperature of AW core on this transect was about 1.2°C at the Makarov Basin side of the Mendeleev Ridge.

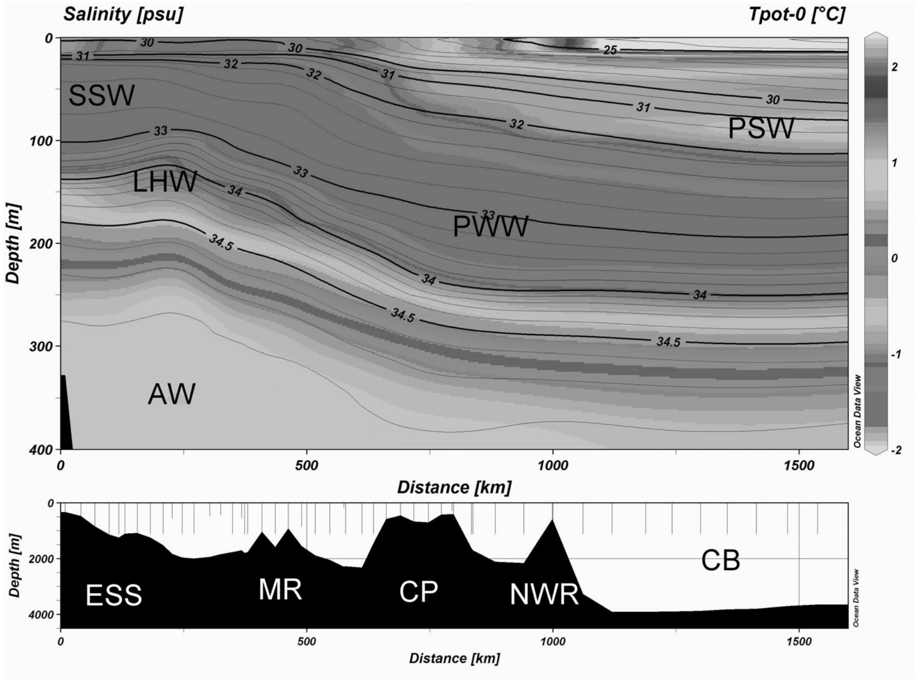

Fig. 53: Potential temperature (referenced to 0 dbar) profiles of the upper 400 m from CTD and XCTD casts. The data are from the sections between the Canadian Basin and the East Siberian Shelf. Abbreviations: Pacific Summer Water (PSW), Siberian Shelf Water (SSW), Pacific Winter Water (PWW), Lower Halocline Water (LHW) and Atlantic Water (AW), East Siberian Shelf (ESS), Mendeleev Ridge (MR), Chukchi Plateau (CP), Northwind Ridge (NWR) and Canadian Basin (CB).

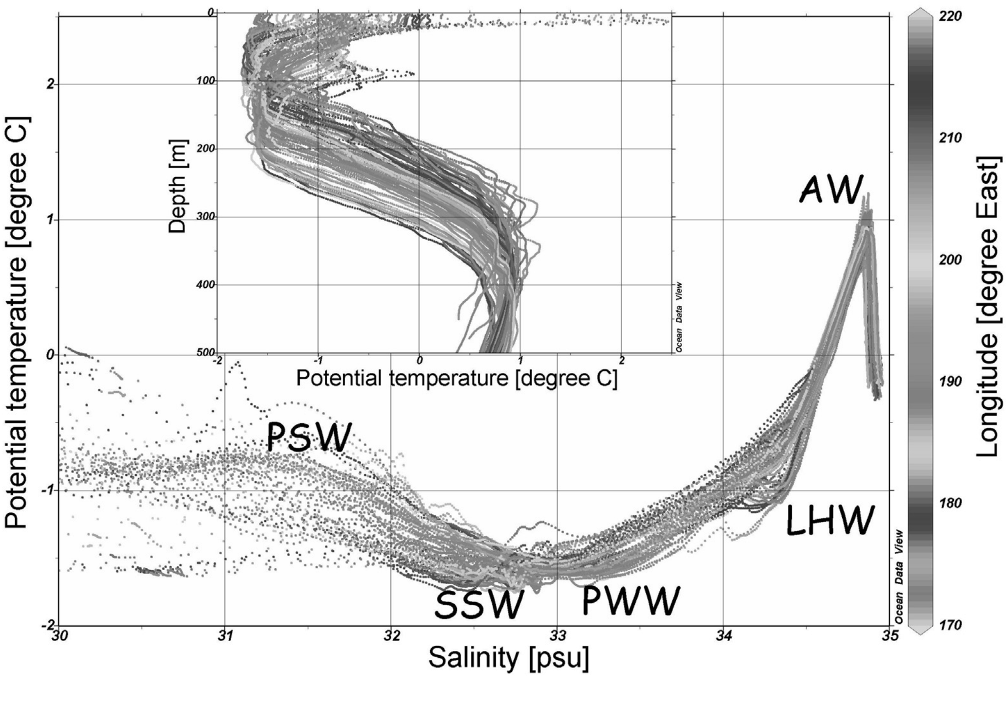

Fig. 54: Potential temperature (referenced to 0 dbar) profiles of the upper 400 m from CTD and XCTD casts shown in fig. 53. Potential temperature and salinity diagram vs. longitude (ºE)

As the ship sailed westward along the 81°North section (see figs. 55 and 56), thermohalines above the AW layer significantly rose up, in particular around the Mendeleev Ridge area. That means there should be a northward geostrophic flow along the Mendeleev Ridge, which is agreeable to the previous studies. Surface salinity of the central Makarov Basin was lower than 27 psu, which was like a freshwater pool. Consistently, below the freshwater pool in the central Makarov Basin, we could find dome-like structure of density elevation above the AW layer. This suggests a counter-clockwise circulation in the central Makarov Basin. However, we do not have any additional evidences to support this suggestion. Further analyses will be needed.

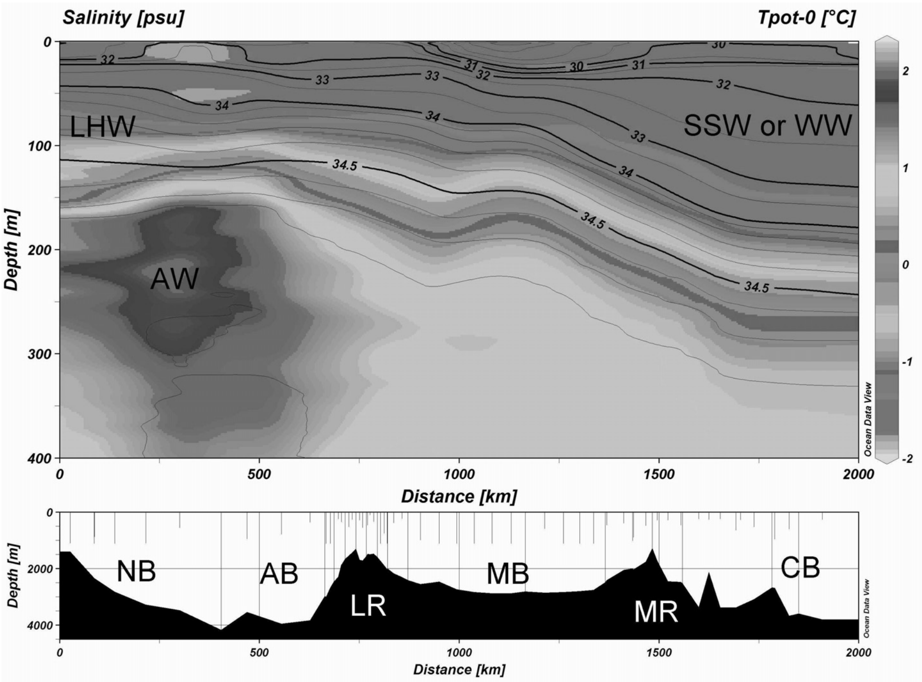

Fig. 55: Abbreviations as in fig. 53, but data is from the cross-basin section. Additional abbreviations: Nansen Basin (NB), Amundsen Basin (AB), Lomonosov Ridge (LR)

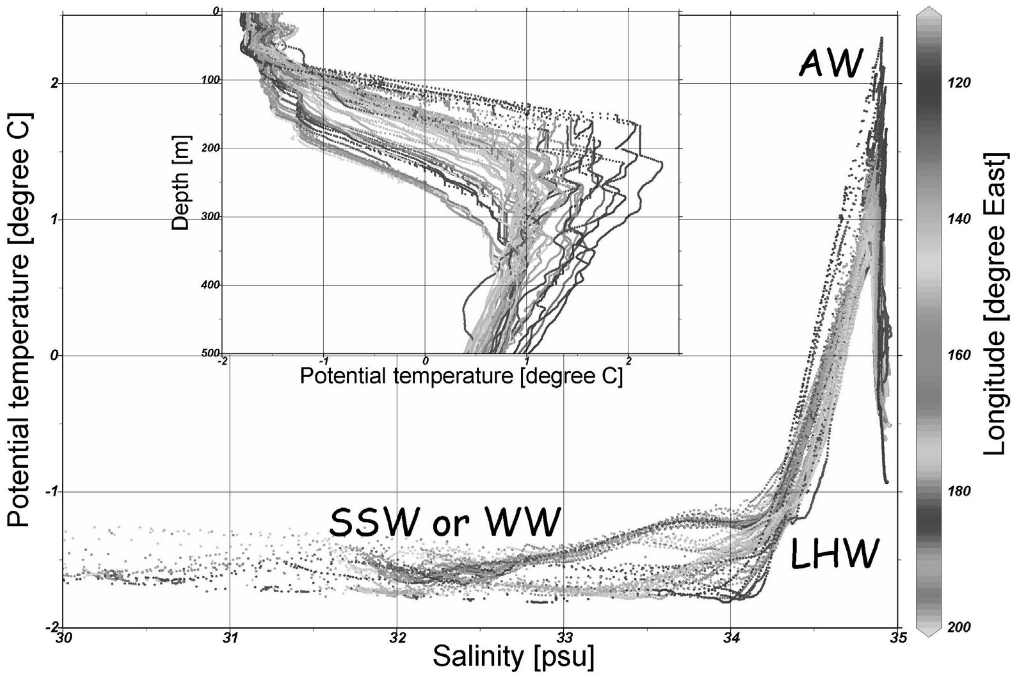

Fig. 56: Abbreviation as in fig. 54, but data is from the cross-basin section. Additional abbreviations: Winter Water (WW)

We could not find a clear frontal structure of surface water masses across the Lomonosov Ridge. However, indications of the convective Lower Halocline Water above the AW layer were found in the Amundsen Basin, but not in the Makarov Basin. Also, the AW temperature significantly increased from the Makarov Basin (1.1~1.2°C) to the Amundsen Basin side (~1.4°C). It is interesting that AW on the Siberian side of the central Amundsen Basin was warmer (>1.5°C) than that of the Amundsen Basin flank of the Lomonosov Ridge. This warmer AW should be a return flow of Fram Strait Branch of AW (FSAW), like a circulation scheme suggested by some of the previous studies. This is further supported by our observational result on the Siberian side of the Nansen Basin, which showed the warmest AW temperature (~2.35°C) during this cruise. Between this warmest AW station and the Laptev Sea slope station (the last XCTD station of this cruise), diapycnal mixing structures were clearly found between the warm and salty Fram Strait branch water masses and the cold and fresh Barents Sea branch water masses, especially in the thermohaline above the AW layer and the AW core layer.

Intermediate and deep layers

The multiple temperature maxima in the Makarov and Amundsen basins suggest interleaving of different branches of Atlantic Water (AW) circulating around the basins, and possibly entering from the shelf (Figs. 57 and 58). The intermediate waters (IW) below 1,000 m show a zig-zag pattern in the temperature-salinity diagram (Fig. 58). This could be due to interleaving water masses from the basin and the shelf or double diffusive processes, which have been reported in the deep and near-surface waters. The salinity around potential temperatures of 0ºC decreased from the Canadian to the Makarov Basin, and decreased again over the Lomonosov Ridge into the Amundsen Basin (Fig. 58). The latter could be due to the increase in the salinity and temperature of the AW temperature maximum that mixes with deep water (DW). The deep water below changes its characteristics around the Lomonosov Ridge, being significantly colder and somewhat fresher in Amundsen Basin than in the Makarov Basin. On top of the ridge, the profile shows salinity and temperature intermediate to that around 1,500 m on either side (potential temperature ~ -0.61ºC, salinity ~39.935; Fig. 58). To what extent the deep waters are influenced by geothermal heating and exchange across the Lomonosov Ridge is yet unclear.

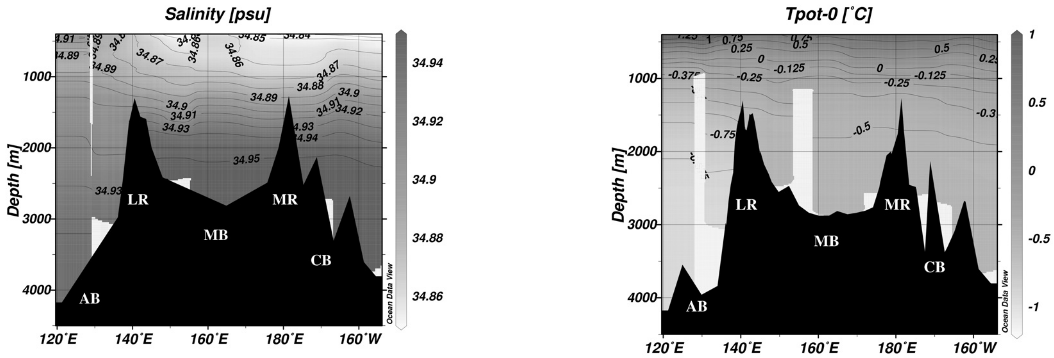

Fig. 57: Potential temperature (referenced to 0 dbar) and salinity of the cross-basin section below 400 m

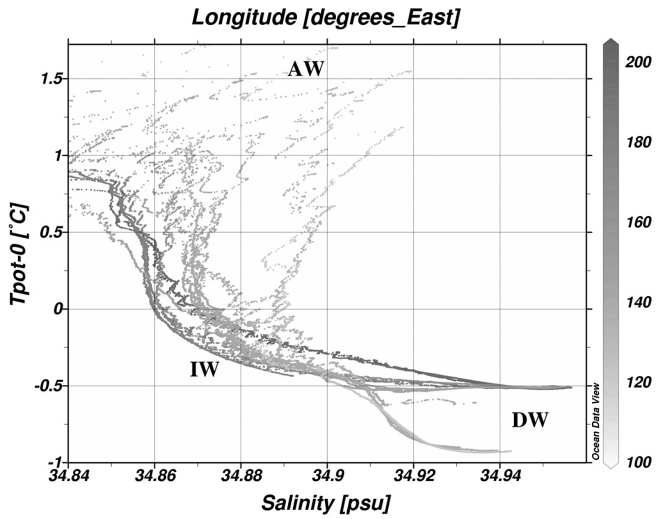

Fig. 58: Potential temperature (referenced to 0 dbar) and salinity below the halocline vs. longitude (ºE). Abbreviations: warm Atlantic Water core (AW), Intermediate Water (IW) and Deep Water (DW)

The results of the CTD casts are still preliminary, as the final calibration using the results of the salt samples from the rosette bottles will be done after the cruise. The ADCP data will be processed after the cruise for further analysis in conjunction with the (X)CTD data.

5.1 Ice-tethered buoys

Dirk Kalmbach[1],Takashi Kikuchi [2], Sebastian Mechler[3], Alexander Nauels[1], Benjamin Rabe[1]

[1]Alfred-Wegener-Institut, Bremerhaven
[2]Japan Agency for Marine Earth Science and Technology
[3]Optimare Sensorsysteme AG

Objectives

In order to obtain year-round measurements of ocean temperature, salinity and velocity as well as air temperature, pressure and wind velocity, ice-tethered platforms with various instruments were deployed. They consist of a sub-ice sensor system that is connected by a cable to a surface unit that transmits the data to shore via satellite. Since they drift with the host ice floe, they have the potential to provide observations over a substantial area of the Arctic Ocean. Five different types of buoys were deployed, all of which record their geographic position at the time of each measurement:

- 2 ITPs (Ice-Tethered Profiler) equipped with Seabird CTDs that will sample temperature and salinity profiles once per day between the surface and 760 m water depth,
- 2 POPS (Polar Ocean Profiling System) equipped with Seabird CTDs that will sample temperature and salinity profiles once per day between the surface and 1,000 m water depth, and meteorological sensors for surface air temperature and barometric pressure,
- 2 PAWS (Polar Atmospheric Weather Station) equipped with sensors for atmospheric pressure, temperature, humidity and an anemometer for wind velocity,
- 1 ITAC (Ice-tethered Acoustic Current profiler) consisting of a RDI ADCP (75 kHz, Long Ranger) that measures the velocity profile of the upper 500 m every two hours,
- 5 SVP (Surface Velocity Profiler) with atmospheric pressure and temperature sensors.

These platforms contribute to the “integrated Arctic Ocean Observation System” (iAOOS) that aims at a persistent observation network.

In total, 12 buoy systems were deployed, 11 on ice floes and one (SVP) into water.

The five Surface Velocity Profilers (SVP) were provided by Meteo-France provide atmospheric pressure, temperature and location. The systems are commonly used to provide surface ocean drifter data, but were modified for use on the ice by cutting off the lower part of the drogue.

Two Ice Tethered Profilers (ITP) by Woods Whole Oceanographic Institution (WHOI) in Woods Hole (Massachusetts, USA) measure twice a day temperature/salinity/depth profiles with 1 m vertical resolution between 8 and 760 m using a profiling CTD unit (Seabird Electronics, Inc. model 41CP) on a wire tether and an inductive modem to communicate the data to a surface unit (SU). The ITP SU records GPS position and transmits all data via an Iridium satellite modem connection to a server at WHOI. The ITPs are manufactured by WHOI with a profiler from McLane Research Laboratories (Falmouth, Massachusetts, USA).

On the same ice floes as the ITPs, two Polar Atmospheric Weather Stations (PAWS) were deployed on behalf of the Meteorological Institute at the University of Hamburg. These systems consist of one surface unit with sensors for atmospheric pressure, temperature, humidity and one anemometer, measuring wind velocity.

Two systems similar to the ITP, Polar Ocean Profiling Systems (POPS) manufactured by MetOcean Data Systems (Dartmouth, Nova Scotia, Canada) and financed by the Japan Agency for Marine-Earth Science and Technology (JAMSTEC, Yokosuka, Japan) were also deployed. The POPS can measure both, 286 levels ocean data of temperature and salinity from 10 to 1,000 m depth, as well as surface atmospheric temperature and barometric pressure. The data sampling intervals for meteorological and ocean profiling data were set to be 1 hour and 1 day, respectively, but these values are re-programmed by sending the commands to the buoy via satellite.

A buoy recently developed by Optimare Sensorsysteme AG (Bremerhaven, Germany) in collaboration with the Alfred-Wegener-Institut in Bremerhaven (Germany) was deployed for the second time: an Ice Tethered Acoustic Current profiler (ITAC), measuring ocean current velocity profiles from 20 m under the ice to a depth of around 500 m, incorporates an ADCP mounted (initially) 50 cm under the ice floe. The ADCP is rigidly connected via a stainless steel pole with a wooden beam on the surface. A cable provides the electrical connection to a SU with a GPS receiver and an Iridium modem. To allow the recording of the ADCP orientation even in regions of low horizontal magnetic field strength, a 2nd GPS is positioned about 98 m away in line with the wooden beam and the ITAC SU. Data are transmitted daily via the Iridium Short Burst Data (SBD) message service to an email address at Optimare. The communication is bi-directional and also allows setting of data sampling parameters via SBD messages, both for the ADCP and the ITAC SU (e.g. GPS sampling rate).

Deployments

Most buoys were deployed along the cruise track, except for two SVP that were deployed by helicopter up to 100 nm away from the ship (Fig. 52 and Tab. 14). In contrast to the previous year, it was generally easier to find a suitable ice flow due to the ice cover in the Eurasian Arctic during September and October (Fig. 59). In total, we had four ocean buoy deployments:

The first was a small 'Super Station' consisting of ITP, PAWS and ITAC. Due to bad weather conditions (fog, icing), the helicopter transport of equipment was limited to few hundred meters distance away from the ship during short periods of clear weather. Hence, the ship docked onto the floe, and instruments were deployed within 300 m from the edge of the ice floe.

The ITP was deployed in about 1.5 m thick ice at 80.6ºN, 166.8ºW on 22 September. The PAWS was located about 30 m away and the ITAC about 100 m away in 2 m thick ice. There were refrozen melt-ponds in several places around the deployment sites.

The two POPS deployments (POPS #11 and #09) were conducted around 81.0ºN, 148.0ºE on 29 September, and at 81.0ºN, 137.6ºE on 1 October, respectively. Both POPS deployments were supported by helicopter operations. The deployment site was some hundred meters away from the ship. The ice thicknesses at both deployment locations for these POPS were about 2.0 m.

Tab. 14: List of SVP deployment positions

ARGOS ID	Latitude	Longitude	Date (yyyy.mm.dd)
76824	80° 30' N	158° 0' W	2008.09.19
76821	82° 21' N	168° 45' E	2008.09.27
76823	81° 0' N	157° 27' E	2008.09.28
76826	81° 39' N	139° 20' E	2008.09.30
76825	81° 16' N	127° 36' E	2008.10.02

The last ocean buoy deployment was at the eastern flank of the Gakkel Ridge at 81.2ºN, 112.3ºE on 3 October. Weather conditions were good for most of the deployments, so that the ITP and the PAWS could be placed in the centre of the ice floe, about 500 m from the open water with ridges starting 20 m on the other side. The ice was about 1.5 m thick around the ITP, becoming gradually thicker toward the ridges.

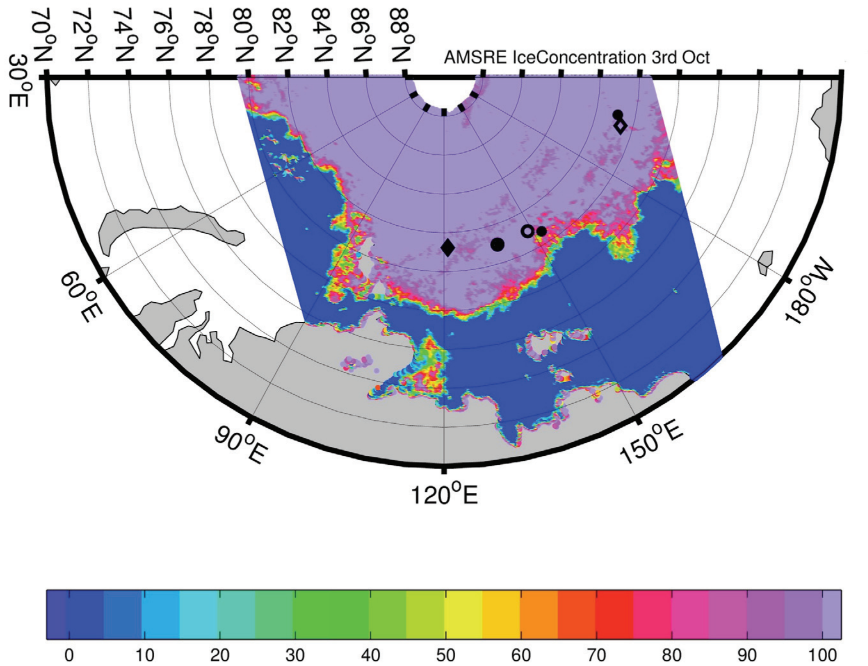

Fig. 59: Ice concentration at 3 October, 2008 (AMSRE; in %) with buoy deployment locations and drift of the ice-ocean buoys (ITP and POPS)

First results

Both ITP systems and POPS #9 worked fine and acquired useful profiles. The ocean profiling data of POPS #11 showed varying gaps in the profiles. This problem might be fixed by sending the commands via satellite to change the parameters for the POPS ocean profiling operation. Meteorological data from both POPS clearly show that air temperature on the ice started decreasing recently, with short-time perturbation of atmospheric circulation pattern (Tab. 15). Both meteorological and ocean profiling data from these POPS will start to be sent to GTS and International Argo Project. The ITP data can be downloaded from the WHOI ITP web site.

Tab. 15: POPS #09 and #11 location, air temperature, and barometric pressure at 0000 and 1200(UTC) between 30 September and 8 October 2008. Note that these POPS are now sending these data every hour.

			POPS #09				POPS #11			
Month	Day	Time	latitude	longitude	AT	BP	latitude	longitude	AT	BP
9	29	12:00UTC					81.00108	148.6290	-4.25	996.4
9	30	00:00UTC					80.94324	149.2352	-5.75	1001.9
9	30	12:00UTC					80.86800	149.8547	-4.75	1007.5
10	1	00:00UTC					80.82948	150.1984	-7.25	1013.1
10	1	12:00UTC	80.97108	137.7538	-14.00	1019.6	80.79972	150.4385	-6.25	1017.3
10	2	00:00UTC	80.98704	137.7559	-6.50	1017.7	80.81436	150.6086	-11.50	1019.1
10	2	12:00UTC	81.06720	137.9211	-2.25	1010.6	80.88372	150.8480	-3.00	1015.1
10	3	00:00UTC	81.08724	138.1416	-5.00	1008.4	80.94600	151.3338	-3.00	1008.7
10	3	12:00UTC	81.09276	138.3166	-4.25	1006.3	80.95032	151.8049	-3.25	1005.3
10	4	00:00UTC	81.08280	138.3628	-9.50	1007.4	80.92752	152.1290	-4.50	1005.0
10	4	12:00UTC	81.06624	138.0954	-12.00	1014.6	80.88420	152.2333	-10.00	1009.5
10	5	00:00UTC	81.05064	138.0534	-10.75	1019.0	80.83116	151.9645	-10.75	1014.5
10	5	12:00UTC	81.02964	138.1031	-11.50	1023.2	80.78904	151.9533	-9.50	1019.9
10	6	00:00UTC	81.01920	138.1325	-11.00	1026.1	80.73624	152.0233	-8.75	1023.6
10	6	12:00UTC	81.01212	138.1899	-12.00	1028.5	80.70276	152.1437	-9.25	1026.5
10	7	00:00UTC	81.00612	138.2557	-18.75	1029.3	80.66832	152.3670	-12.75	1026.7
10	7	12:00UTC	81.00576	138.3516	-19.25	1028.2	80.63760	152.4468	-14.50	1026.7
10	8	00:00UTC	81.01128	138.4860	-15.25	1027.2	80.62080	152.6708	-12.25	1026.5

The autonomous ocean buoys drifted during the cruise, as can be seen in the AMSRE ice concentration map from 3 October (Fig. 59). The drift paths of the since their respective times of the deployments are shown by the solid black dots.

The ITAC ADCP acquired useful profiles up to day 9 after deployment. Unfortunately, the instrument stopped profiling on this day due to a hardware error, causing the transducer to no longer transmit acoustic signals into the water column. However, the surface unit is still able to communicate with the ADCP, which rules out a complete power failure. The cause for the hardware error is currently being investigated by Optimare and RDI.

6. ISOTOPIC TRACERS

Robert Letscher
Rosenstiel School of Marine and Atmospheric Science, Miami

Objectives

Terrigenous dissolved organic carbon (tDOC) enters the global ocean by way of rivers at a rate of ~0.25 Pg C yr^{-1}, representing the largest transfer of reduced carbon from the continents to the open ocean (Cauwet, 2002). This process is of enhanced importance in the Arctic Ocean, owing to the large input (~10 % of global river discharge) of terrestrial freshwater and organic matter from the many rivers emptying into its basins (Anderson, 2002). The fate of tDOC in the global ocean remains uncertain. Salinity-tDOC relationships in coastal margins and estuaries across the globe show conservative behaviour (Cauwet, 2002; Anderson, 2002) suggesting a long-lived material yet low concentrations of tDOC tracers (lignin, stable isotopes) (Opsahl and Benner, 1997; Hedges et al., 1997) in the open ocean indicate active removal processes. The spatiotemporal scales of this tDOC removal remain unknown (Hansell et al., 2004).

As part of the water-sampling programme, seawater samples were collected for analysis of isotopic tracers and other chemical properties along the cruise track of ARKXXIII/3. The application of an isotopic tracer technique will be implored to investigate the rate of exchange between the waters overlying the Arctic shelves with the Arctic Ocean interior. The results of the tracer technique will be applied to the terrigenous dissolved organic carbon (tDOC) system of the surface Arctic Ocean to further the understanding of its spatial distribution and decay rates. This work was carried out previously in the western Arctic with the results published in the journal *Science* (Hansell et al., 2004). The sampling programme as part of ARK-XXIII/3 will continue this work in the eastern Arctic where different time scales of shelf-basin interaction in the Eurasian basins and surface circulation patterns are likely.

The isotopic tracer technique utilizes the measurement of the ratio of two naturally occurring radium isotopes ($^{228}Ra/^{226}Ra$) in the surface waters of the Arctic Ocean. The radium data collected from this cruise will be used to determine the time-since-shelf residence of Arctic surface water; that is, the aging of water with respect to the elapsed time since contact with shelf sediments, the source of radium to the water column. Waters that were recently in contact with shelf sediments will therefore have a higher $^{228}Ra/^{226}Ra$ ratio with a subsequent decrease in this ratio as the waters "age" and move off the shelves into the interior ocean.

Supplementing the radium tracer data, samples were collected for analysis of dissolved organic carbon (DOC). DOC in the global ocean is recognized as one of Earth's largest bioactive reservoirs of carbon, approximately equal in stock (700 Pg

C) to that of CO_2 in the atmosphere (Hansell and Carlson, 2002). Dissolved organic matter plays a significant role in the cycling of carbon through the Earth system, receiving much attention in recent decades (Ducklow, 2002). The transport and removal processes acting on terrestrial derived DOC in the Arctic Ocean is important in light of subsequent export of DOC out of the Arctic via the Transpolar Drift (Hansell et al., 2004). The export of DOC across the Fram Strait via the East Greenland Current brings waters enriched in DOC into the source regions of deep-water formation in the North Atlantic with possible storage of this carbon in the deep ocean with the meridional overturning circulation.

Work at sea

Seawater samples from the polar surface layer (PSL) were obtained using the clean seawater intake pumped on board from below the bow of the ship. The cruise track of ARK-XXIII/3 allowed for extensive sampling in the East Siberian Sea region along with a number of other regions including the Canada Basin, Makarov Basin, Amundsen Basin and Eurasian shelves with station locations shown in Fig. 60. At each station location, samples were collected for DOC (~50 mL aliquots) by filtering through a precombusted GF/F filter (pore size 0.7 mm) into acid-cleaned 60 mL HDPE bottles. The samples were then stored frozen at -20°C for later shipment to the shore-based laboratory.

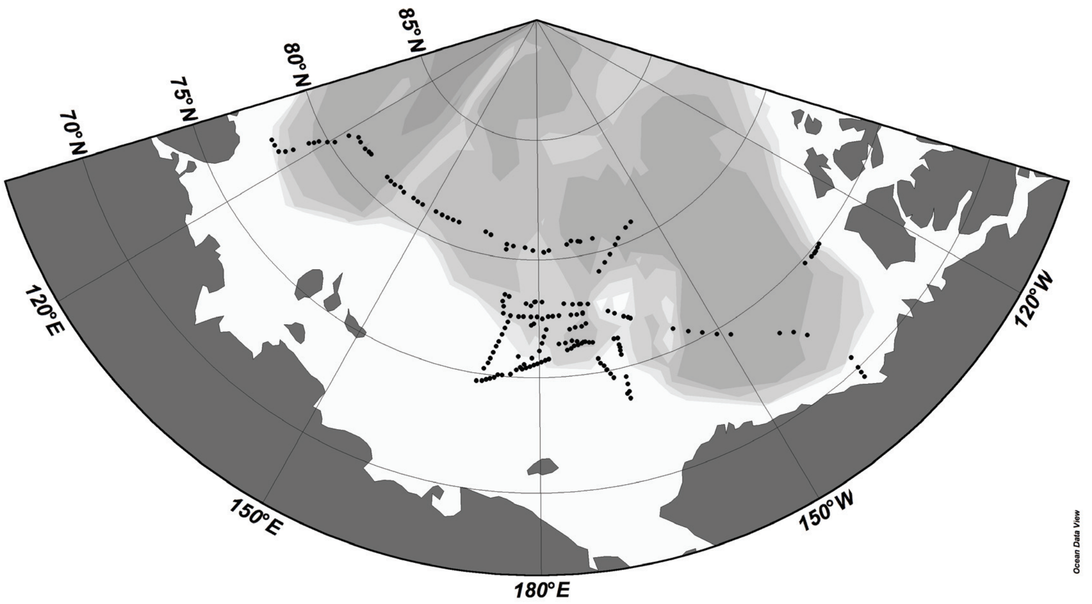

Fig. 60: Station locations for water sampling programme, Polarstern ARK-XXIII/3

At a total of 66 of these stations, additional water samples (200 liters) were collected for the analysis of the dissolved radium isotopes. For each radium sample approximately 200 liters of surface seawater were collected in 300-liter plastic rainwater tanks. The samples were then pumped through a filter cartridge containing manganese coated acrylic filter fibers to collect the radium isotopes with subsequent shipment to the shore-based laboratory for analysis. Samples for the analysis of the stable isotope ^{18}O were also collected unfiltered into 20 mL glass ampoules at the same 66 stations. All analyses of DOC, $^{228}Ra/^{226}Ra$, and $\delta^{18}O$ will be carried out at the shore-based laboratories at the Rosenstiel School of Marine and Atmospheric Science (RSMAS) at the University of Miami in Florida, USA where the methods to be used for the analysis of DOC, $^{228}Ra/^{226}Ra$, and $\delta^{18}O$ are high temperature catalytic oxidation (HTCO), gamma ray spectrometry, and mass spectrometry (MS), respectively.

In conjunction to the main water-sampling programme described above, additional seawater samples were collected from a total of 20 CTD stations carried out along a zonal section nominally across 81°N from 155°W to 120°E (see Fig. 61). Aliquots of 50 mL were collected from each Niskin bottle for DOC analysis along with aliquots of 50 mL for the analysis of the stable isotope ^{18}O composition. To remove the signal of particulate organic matter (POM) from the measurement of DOC, those samples collected from 200 meters or shallower in the water column were filtered using the same procedure detailed above. Below 200 meters, the concentration of POM is expected to be small and is included in the measurement of DOC. No filtration step was taken for the collection of the ^{18}O samples. The DOC samples will be stored frozen and shipped to the shore-based laboratory in Miami, Florida as described previously. The ^{18}O samples collected from the CTD stations will be shipped to a shore-based laboratory at the IFM-GEOMAR at the University of Kiel in Germany for analysis.

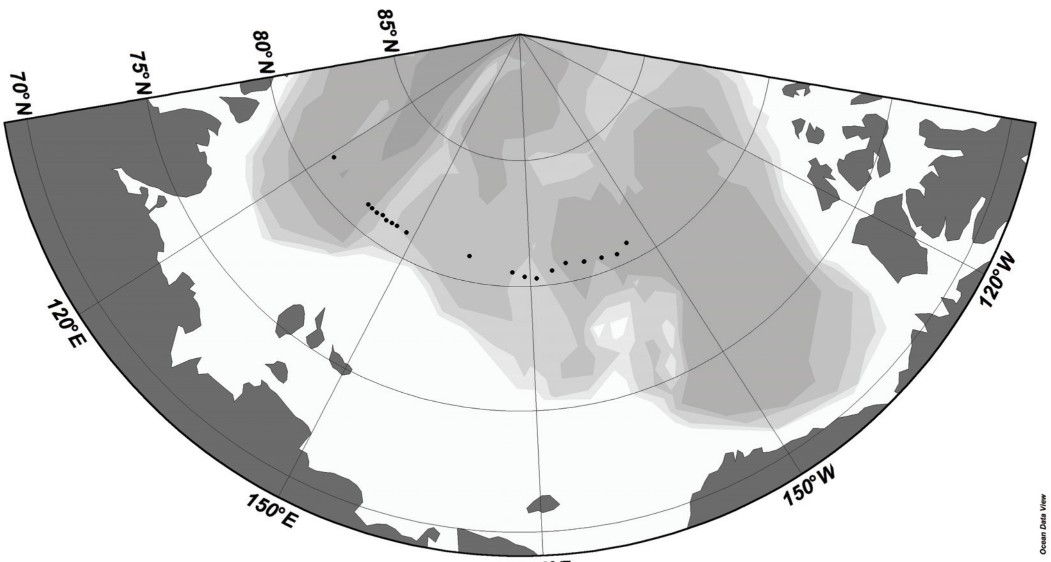

Fig. 61: station locations of CTD casts with water sampling, Polarstern ARK-XXIII/3

Also included in the water-sampling programme was the collection of samples for suspended particulate matter. The rare earth elements (REE) and isotopic Nd content of suspended particulate matter in the water column are useful tracers of water masses and have been collected from the polar surface layer (PSL) on ARK-XXIII/3. Approximately 100 liters of seawater were filtered from the hull-mounted seawater intake through a 0.7 mm pore size cellulose filter for each sample to collect suspended particulate matter on the filters. The filters were then frozen and stored at -20°C for shipment to the shore-based laboratory at the AWI in Bremerhaven, Germany. A total of 24 samples were collected along the cruise track of ARK-XXIII/3 aboard the *Polarstern*.

References

Anderson, L.G., in *Biogeochemistry of Marine Dissolved Organic Matter,* D.A. Hansell, C.A. Carlson, Eds. (Academic Press, San Diego, CA, 2002), pp. 665-683.

Cauwet, G., in *Biogeochemistry of Marine Dissolved Organic Matter,* D.A. Hansell, C.A. Carlson, Eds. (Academic Press, San Diego, CA, 2002), pp. 579-609.

Ducklow, H.W. in *Biogeochemistry of Marine Dissolved Organic Matter,* D.A. Hansell, C.A. Carlson, Eds. (Academic Press, San Diego, CA, 2002), pp. xv-xix.

Hansell, D.A. and C.A. Carlson in *Biogeochemistry of Marine Dissolved Organic Matter,* D.A. Hansell, C.A. Carlson, Eds. (Academic Press, San Diego, CA, 2002), pp. xxi-xxii.

Hansell, D.A., D. Kadko and N.R. Bates, *Science* **304**, 858 (2004).

Hedges, J.I., R.G. Keil and R. Benner, *Org. Geochem.* **27**, 195 (1997).

Opsahl S. and R. Benner, *Nature* **386**, 480 (1997).

7. BIOLOGY OF *OITHONA SIMILIS* (COPEPODA: CYLOPOIDA) IN THE ARCTIC OCEAN

Britta Wend[1)], Natalie Fischer[2)]

[1)]University of Oldenburg, Oldenburg
[2)]Alfred-Wegener Institut, Bremerhaven

Objectives

Oithona similis belongs to the order of cyclopoid copepods. It is highly abundant throughout many parts of the world ocean, and is supposed to be a cosmopolitan species. The work during this cruise was part of a project that challenges whether *O. similis*, a key species in three chosen study areas (Southern Ocean, Arctic Ocean and North Sea), is indeed a cosmopolite or a complex of sibling species. A further goal is a better understanding of its life cycle (or the cycles of the existing cryptic species).

Work at sea

Samples were taken by multinet (meshsize 55 μm) at 21 stations throughout the cruise track. *Oithona similis* is an epipelagic copepod. Therefore, sampling was restricted to the upper 500 m of the water column. Further samples were collected via Niskin bottles mounted on a CTD. The water of each chosen depth was directly concentrated through 20 μm gauze to a final volume of 50 ml per depth. This volume was immediately fixed in formalin for morphological identifications of species, reproduction in the field as well as feeding habits. With this method higher numbers of the first developmental stages are caught than via multinet. For genetical investigations adult individuals of the genus *Oithona* were picked out of all multinet samples and preserved in ethanol. Additional adults were fixed in formalin for closer morphological investigations.

Outlook

The first step at the home laboratory will be morphological investigations of formalin fixed individuals. The aim of these examinations is to classify groups by the means of eventually existing morphological differences. These will then be used for the genetic analysis to figure out whether cryptic species exist within the nominal *O. similis.*

7.1 Phytoplankton ecology in the water column

Natalie Fischer[1)], Britta Wend[2)]
Eva-Maria Nöthig[1)], not on board

[1)]Alfred-Wegener-Institut, Bremerhaven
[2)]University of Oldenburg, Oldenburg

Objectives

Since the nineties phytoplankton investigations on biomass, species composition, productivity, and related biochemical parameters i.e. chlorophyll a have been carried out in arctic waters.

Work at Sea

Water was sampled with the rosette sampling system attached to the CTD at 12 stations during the cruise. Subsamples were taken from the surface layer at 8 different depths (appr. 2,10, 20, 20, 40, 50, 75, 100 m) for species abundances (water samples, ca. 200 ml fixed with buffered formalin), chlorophyll a and phaeopigments (0.5 to 1 litre of water was filtered on Whatman GF/C glass-fibre filters) as well as for particulate organic carbon and silicate. For these parameters samples were taken from the surface down to 2,000 m (1 to 2 litres were filtered in the surface water layers and deeper 2 to 4 litres on Whatman GF/C glass fibre filters or cellulose acetate filters for silicate).

Outlook

The filters were frozen at a temperature of -30°C and will later be analysed in the home laboratory. The investigations aim on a comparison with the old data to understand eventually changes due to a changing environment.

8. BATHYMETRY

Franziska Jurisch, Tanja Dufek, Laura Jensen
Alfred-Wegener-Institut, Bremerhaven

Objectives

The main task of the bathymetric project was the operation of the multibeam sonar system Hydrosweep DS2 (Atlas Hydrographic), and the postprocessing of the Hydrosweep data. In addition several bathymetric charts, derived from this data, were created. This was done to provide the geological and geophysical working groups with precise depth information and bathymetric charts covering the areas of their main research interest.

Furthermore, the data will be a valuable contribution to the bathymetric datasets IBCAO (International Bathymetric Chart of the Arctic Ocean) and GEBCO (General Bathymetric Chart of the Ocean), still containing sparse data within the area of leg ARK-XXIII/3.

Due to the project objectives, no systematic profiling was planned before or during the cruise. Also, no parallel profiles to connect existing tracks were planned, as the cruise led to nearly unsurveyed areas.

Data acquisition

The measurement of multi-beam data was started on 13 August 2008 at 8:00 UTC, the day after leaving the departure harbour of Reykjavik. The data acquisition was stopped on 3 October 2008 at 15:45 UTC before entering the Exclusive Economic Zone (EEZ) of Russia.

Because of a broken electronic board, the multi-beam data of the first three survey days are corrupt and cannot be used for charting. The problem was solved by the ship's electronic engineer, who replaced the broken electronic board with a spare board. After this serious failure the Hydrosweep system was operated without further breakdowns.

The bathymetric survey was performed using the Atlas Hydrosweep DS2, a deep-sea multi-beam echosounding system, which is permanently installed on *Polarstern*. Hydrosweep was operated in the hard-beam mode with a resolution of 59 single depth points (preformed beams) per ping. Most of the time an opening angle of 90° was used, which results in a swath width of twice the water depth. In areas with water depths less than 350 m, the opening angle was switched automatically by the system to 120°. In this mode a swath width of 3.4 times the water depth is recorded.

Depending on water depth, Hydrosweep operates in three different modes: deep-sea mode (~15,000 to 1,000 meter), medium-depth mode (~1,000 to 120 meter) and shallow-water mode (~120 to 11 meter). It is known that the data quality of the shallow-water mode is worse than the quality of the other modes. During this leg, Hydrosweep measured in shallow-water mode near Inuvik, and along the East Siberian Sea for approximately four hours. The data quality was very poor, about 70 % of the data had to be rejected, which may point to a technical problem with this mode (s. fig. 62) and the need for further studies.

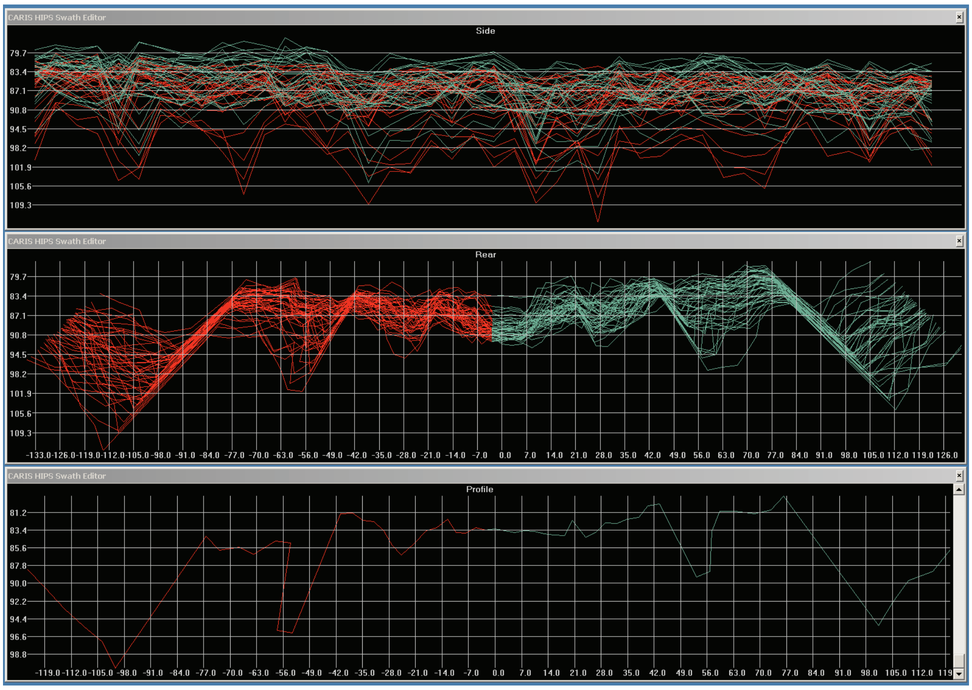

Fig. 62: Wrong depth measurements in shallow water

Sound velocity profiles

The seafloor depth is calculated from the travel time of an acoustic signal sent from the ship to the reflecting seafloor and back. Because of varying water conditions like temperature and salinity, the velocity of sound changes regionally, and has to be determined. The sonar system Hydrosweep DS2 can perform a crossfan-calibration for calculating the mean sound velocity of the water column from sea surface to seafloor.

For high precision depth measurements a more precise sound velocity profile has to be derived by CTD measurements. 14 CTD measurements were carried out to measure temperature, salinity, and pressure within the water column up to a maximum depth of 2,500 m (Fig. 63). The water sound velocity was calculated from these parameters using the formula of Chen and Millerno (1977). In the areas nearby the CTD stations the Hydrosweep system utilized these profiles instead of the mean sound velocity by cross-fan calibration in the other regions.

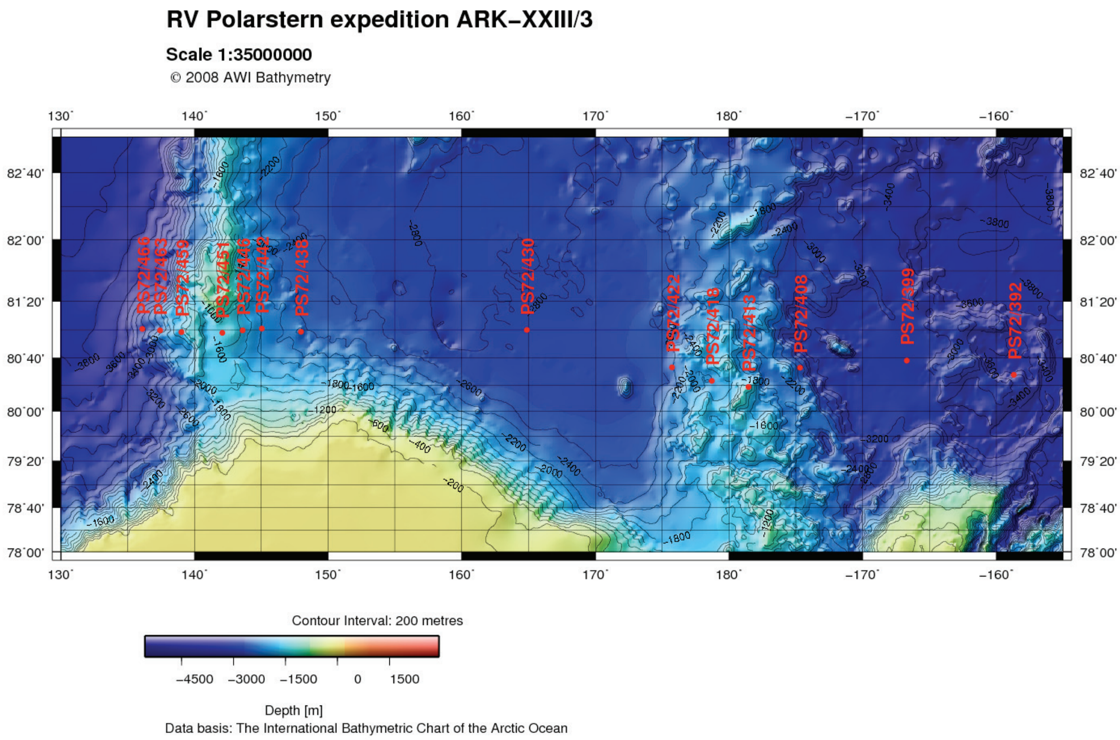

Fig. 63: Overview of applied CTD measurements

The recorded data were exported in eight hour blocks to the internal raw data format SURF. For a first inspection of data quality the navigation editor “Hydromap Offline” was used. It allows to detect gaps in navigation data as well as rough positioning errors. The data were converted into dux-format for preparing data cleaning with the CARIS HIPS & SIPS software. The final processing step was the export of the cleaned data into an ASCII-format x,y,z (longitude, latitude, depth) used for the preparation of bathymetric charts.

As nautical charts are not available for the northern parts of the Arctic Ocean, the bathymetric group created maps for the area between 120°E – 120°W and 72°N - 85°N.

Results

Until the end of the cruise it was possible to process all collected bathymetric data by means of navigation control, manually depth editing using Caris HIPS and all necessary format conversions.

Bathymetric maps with contour lines as well as colour shaded charts have been created with GMT (Generic Mapping Tool) for other working groups covering their research areas. Global datasets like GEBCO or ETOPO2 have been used as backdrop. Further charts have been produced to support the navigation of the ship in these sparsely surveyed areas of the Arctic Ocean.

The insufficient quality of existing data had to be attested at a coring station: It was planned to take sediment cores from the top of a seamount (800 m above seabed) located 80°19'N 172°15'W, but the swath data did not show any seamount at this location (see fig. 64). It must be stated that the seamount is an error in the IBCAO dataset, which results from the prediction of bathymetry from satellite altimetry.

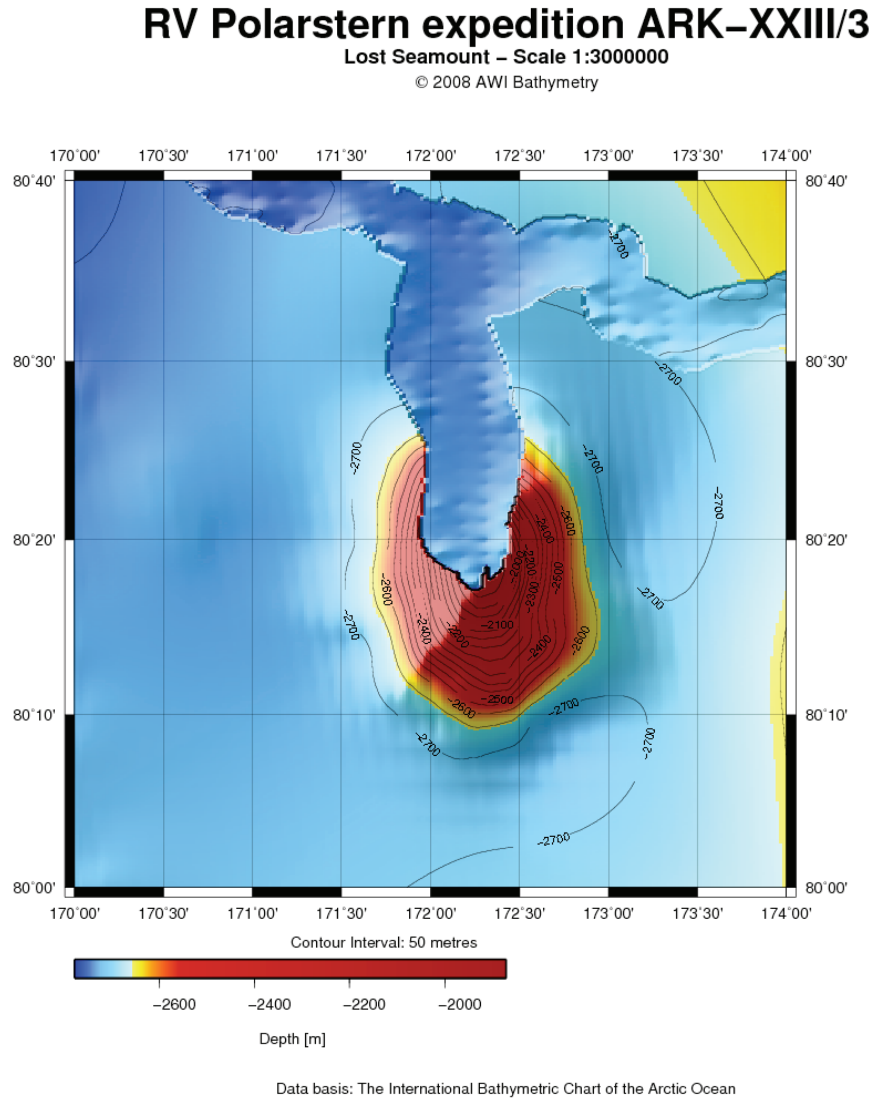

Fig. 64: Different depth values from IBCAO and ARK-XXIII/3 multi-beam data

Statistics

During 52 days a track length of 7,248 NM (13,424 km) and an area of ~53,800 km² was surveyed with the number of 561,195 pings and 33,017,483 beams (before editing). The depths could be measured with accuracy of ~ 0.5 to 1 % of water depth, between minimum depth of 59 meter and maximum depth of 4,259 meter.

The raw data have been converted into files of ATLAS exchange format SURF, containing a time period of 8 hours each. The 174 files amounts to 3.98 GB. The bathymetry and the CTD measurements will be published in the "Publishing Network for Geoscientific & Environmental data".

9. AT-SEA DISTRIBUTION OF SEABIRDS AND MARINE MAMMALS

Claude R. Joiris
Laboratory for Polar Ecology, Ramillies, Belgium

Objectives

This research copes with the quantitative distribution of the higher trophic levels – seabirds, cetaceans and pinnipeds - at sea. The main aim is to identify the factors determining their presence: different water masses, as recognised by their salinity and water temperature and ice coverage, and especially fronts and ice edge. In poor environments such as the Arctic seas, the higher trophic levels indeed tend to accumulate in the few areas with high food availability (zooplankton and krill, and small fish for the baleen whales, larger fish and sometimes squid for toothed cetaceans and seals) and, thus, present a very patchy distribution.

Work at sea

This Arctic circumpolar expedition represents a big première. On the one hand, very little is known about the distribution of seabirds and marine mammals in the high Arctic, with the exception of the Greenland Sea: in text books, many distribution maps still show question marks "?" for the high Arctic. On the other hand, it is important to collect data by the same team and from the same platform (moving *Polarstern*, with confirmations from helicopter flights) and the same methodology, in order to make sure that the results can be directly compared with the previous ones (this is part of a long term study of the Arctic seas started 30 years ago – actually since 1988 on board *Polarstern*, i.e. including pack ice).

Transect counts were realised on a (almost) continuous basis, i.e. light conditions allowing: interruptions were due to dark nights, as well as heavy fog. This resulted in more than 800 half-an-hour counts devoted to seabirds and marine mammals.

Preliminary results

The most striking conclusions are that:

- biodiversity (i.e. the numbers of species and of individuals) is extremely low, clearly lower than e.g. the Greenland and Barents seas: the numbers of empty counts, without any bird nor mammal, was very high. This also reflects a very low biological production as a whole;
- moreover, their distribution is very patchy, and presents local high concentrations, generally bound to local small scale hydrological events such as fronts between water masses and ice edge. This was the case for a frontal zone off W Greenland, with a high concentration of kittiwakes (8,000 on 3 icebergs) and little auks accompanied by recently fledged juveniles (2,000) – out a total of

12,000 birds in 75 half-an-hour transect counts - and cetaceans (pilot, fin and minke whales: 70 in total in the same zone);

- the seabirds going the farthest north in the Outer Marginal Ice Zone (OMIZ) are: kittiwake in relatively large numbers, regularly accompanied by some pomarine jaegers; ivory, Ross's, Sabine's and glaucous gulls;
- some Atlantic birds were unexpectedly encountered in the Beaufort Sea and the Beaufort Gyre: fulmar, Iceland gull, gannet (less than 10 exemplars each), 1 greater shearwater. If confirmed, such data might be the sign of a redistribution of some seabirds species, probably as a consequence of the opening of the NE and NW passages due to strongly decreasing ice coverage;
- cetaceans were almost absent: out of W Greenland (see higher) and the NW Passage (4 bowheads and 1 fin whale) and the coast off the McKenzie (5 bowheads and 20 belugas), only 2 unexpected belugas were encountered in the centre of the Beaufort Gyre;
- numbers of seals were very low as well; the species going the farthest in the pack ice being the ringed seal, including a few breathing holes detected by helicopter in the pack ice. Other species were harp and bearded in lower numbers;
- finally, numbers of polar bears seem very low, but they were actually met in their biotope: at or close to the ice edge and OMIZ: about 12 in total, including 2 mothers with one pup each. They are basically absent both in open water far from pack ice, and in closed pack ice (CPI). One exemplar was possibly in difficult conditions: isolated on a medium-sized floe in the middle of open water, it was meagre, showed abnormal panic reactions when the helicopter approached, and was standing on the same floe for very long, as shown by the huge amount of tracks on the snow.

Ice conditions during this expedition were very special, consisting of 1st year mainly, after the year 2007 presenting the lowest ice coverage ever recorded: this zone was then basically ice-free. At the end of the expedition, much newly formed ice was encountered as well. If this trend was to be continued, the effect of older second ice year on seabirds and marine mammals clearly deserve attention in following years. Figures from animals observed during this cruise can be found in Appendix A.5

A general question remains at a much larger scale: why is CPI so poor in the Arctic, and orders of magnitude higher in the Antarctic (Weddell Sea), with huge concentrations of krill-eating penguins (mainly Adélie and chinstrap) and seals (mainly crabeater, and leopard).

10. POLLEN AND SPORE FLOW IN THE AIR OF THE ARCTIC SEA

Mark Herrmann
Senckenberg Research Institute, Frankfurt

Objectives

The major interest of this project was to determine the extent of pollen and spore transport across the Arctic Ocean. Additionally, the transport of other palynomorphs like Fungal Spores or Algae was also investigated. In other words, which species/genera of palynomorphs are transported in between the Arctic air masses, and how far have they been transported. Where are the source areas from which those palynomorphs have been emitted? Which factors do have an influence on this transport? Which conclusions can be made about the colonization of the Arctic islands after the last Ice Age by long distance transport of pteridophytes and mosses? Additional these results will help to better interpret palynological data from Cenozoic Arctic sediments.

Work at Sea

At the Peildeck of *Polarstern* a Burkard Pollen Trap (Fig. 65) was installed by Dorte Janussen (Senckenberg Research Institute, Frankfurt) during *Polarstern* cruise ARK-XXIII/2. The pollen trap is sucking a constant air volume of 10 litres/minute throughout a small orifice into its case. In between the case there is a 24 hours assembly (Fig. 66) where a slide (coated with Glyceringelatine) can be fixed. Hereby the slide moves with a constant speed of 2 mm/hour along the orifice. Pollen, spores and other particles like fungal spores, algae or dust embedded in the sucked air now get stick by the Glyceringelatine.

Fig. 65: Burkard Pollen Trap at Peildeck

Fig. 66: 24 Hours Assembly with coated Sampling Slide

Daily work at sea was:

1. to coat a slide with Glyceringelatine, which is coloured by Safranin. The Safranin is necessary to colour the pollen and spores for a better recognition of those palynomorphs during investigation with the microscope. Thereby, the Glyceringelatine has to be melted and the liquid is then put on the slide using a pipette. After waiting until the liquid got solid the slide was ready for use.
2. Now every day at the same time the 24 hour assembly in the Pollen trap was filled by a new slide and the old slide was taken out for investigation at the microscope.

3. Preparing the slide for investigation by heating the slide with a heating plate until the Glyceringelatine is melting. Then a cover glass was put on the Glyceringelatine. After waiting until the Glyceringelatine was solid the border of the cover glass was fixed and sealed by nail polish.
4. Next step of investigation was the work at the microscope. Hereby every slide was searched for palynomorphs. They got counted and documented. This work was carried out with an Olympus BX 41 microscope (using a magnification of 200 x, 400 x and 600 x) together with an Altra 20 camera.

As result each single palynomorph is counted and its position on slide is known by its coordinates on slide. Now every particular palynomorph can be assigned to a special time and hence to the ships position at the moment of embedding on slide.

Additional a determination of the palynomorphs was carried out by using the pollen atlas of Beug (2006) and other literature (Lacey & West, 2006 und Winkler et al., 2001).

Preliminary Results

All in all 92 slides have been counted and their palynomorph content was documented. It was possible to determine about 4 different types of gymnosperm pollen, 5 types of pteridophyte/bryophyte spores, 28 types of angiosperm pollen (Tab. 16) and 30 different types of fungal spores. Additional about 6 types of algae and several types of dust particles like soot and charcoal also have been detected. About 0 to 36 pollen and spores (Fig. 68) but also up to more than 1,000 fungal spores have been counted in single slides.

Tab. 16: Identified Types of Palynomorphs (see also Fig. 67)

Gymnosperms:

Pinaceae
cf. *Abies* sp.
Pinus sp.
Picea sp.
Larix sp.

Pteridophytes/Bryophytes

Monolete Typs:
Polypodiaceae – 2 Typs

Trilete Typs:
cf. Sphagnaceae (1 Type)
and 3 other yet unknown forms

Angiosperms

cf. Apiaceae

Betulaceae
Betula sp.
Carpinus sp.
Alnus sp.

Chenopodiaceae/Amaranthaceae

Compositae
Taraxacum sp.
and 3 other yet unknown forms

Plantaginaceae
cf. *Plantago* sp.

Poaceae
Secale sp.
and several other yet unknown forms

Polygonaceae

cf. Rosaceae

Salicaceae
Salix sp. (2 types)

Saxifragaceae
cf. Ribes sp.
and one other yet unknown form

Tiliaceae
Tilia sp.

Ulmaceae
cf. *Ulmus* sp.

As well as 8 other yet unknown forms

Fungi

Except the spores of *Alternaria* sp., *Cladosporium* sp.and *Epicoccum* sp no other fungal spores have been identified so far.

Algae

Except the diatoms no other algae have been identified so far.

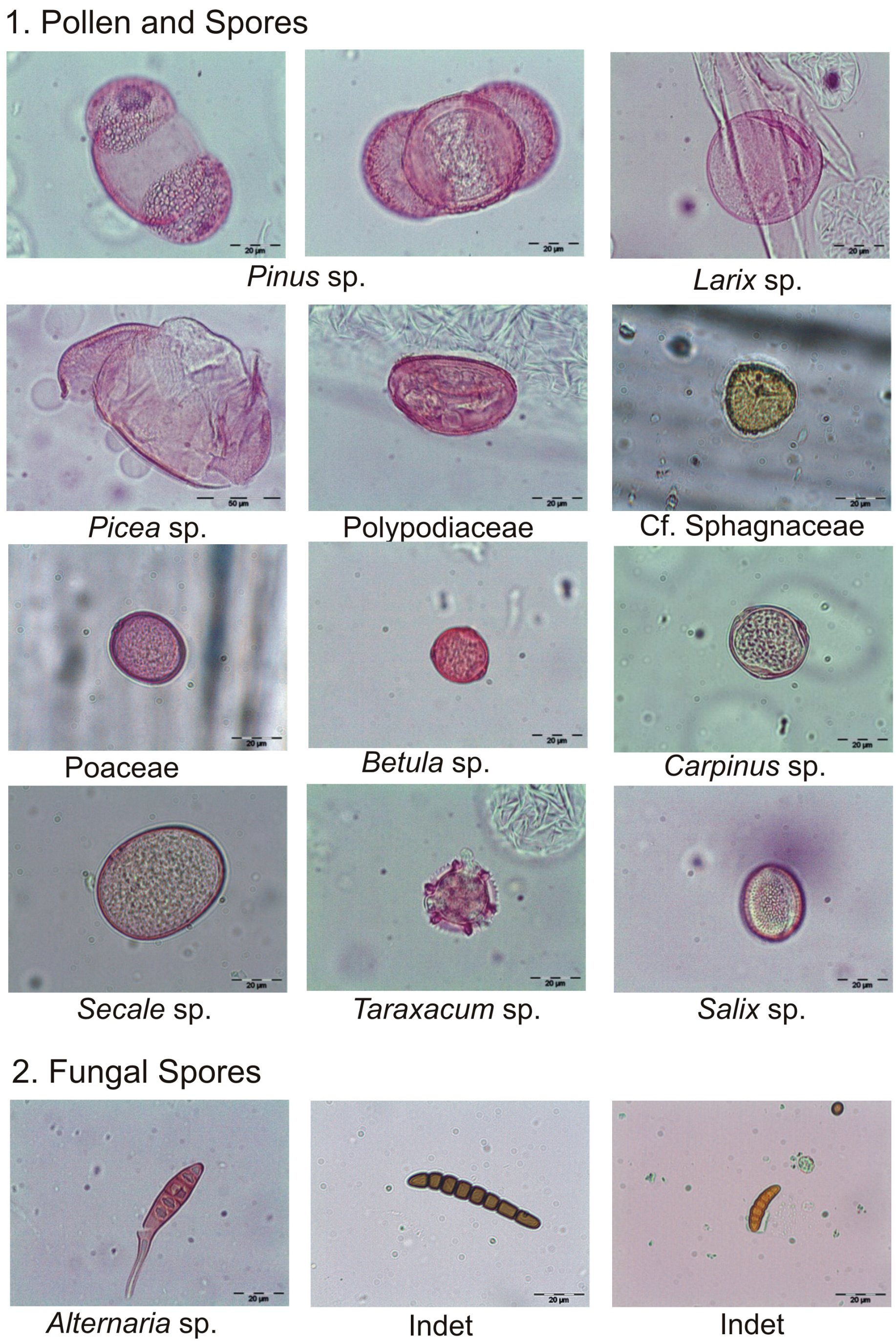

Fig. 67: Selected Palynomorphs

Preliminary Counting Results

Best results have been achieved during cruise ARK-XXIII/2 between Longyearbyen and Reykjavik and between Iceland and entrance into the Arctic Ocean after passing the Northwest Passage respectively. Here, the amount of collected palynomorphs as well as the diversity was highest. When reaching the Arctic Ocean the amount of palynomorphs strongly decreased (Fig. 67, day 41). Explanations for these observations have to be investigated by comparing with the results with the available weather data. Possibly the wet weather above the Arctic Ocean was responsible for the sharp drop.

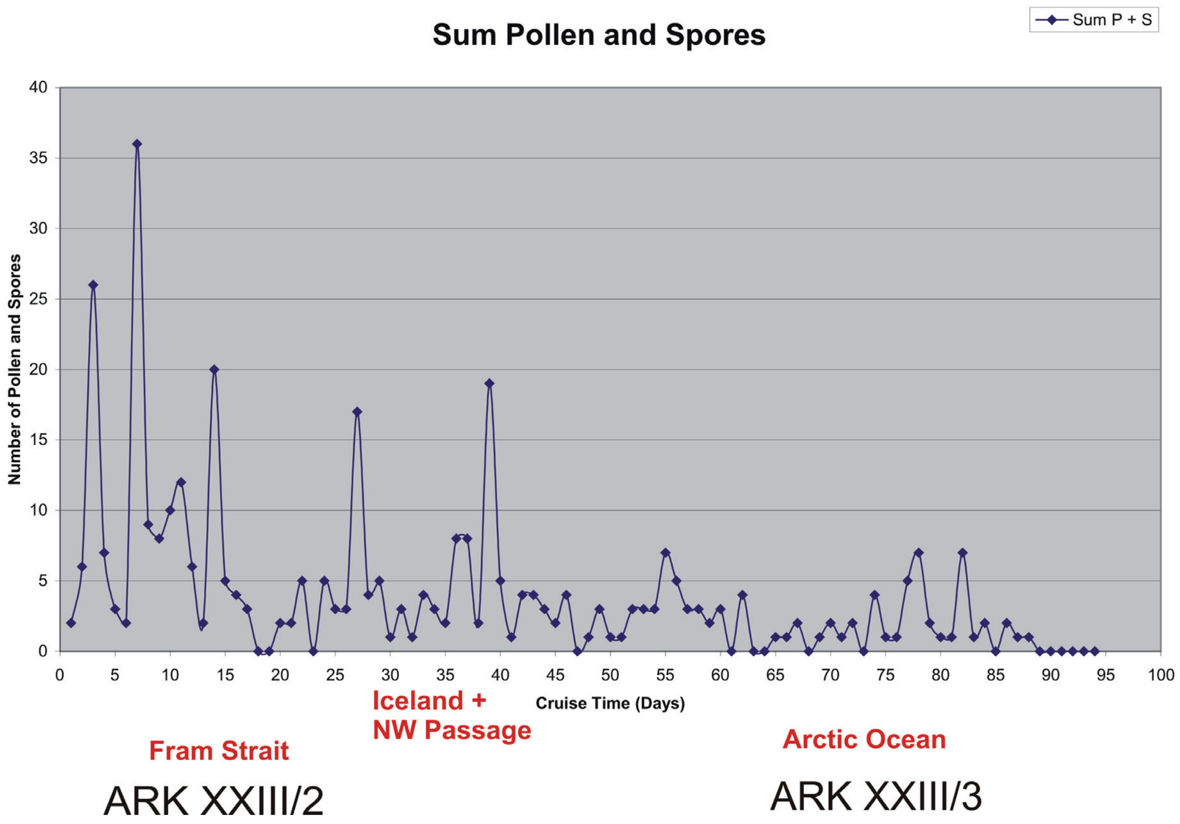

Fig. 68: Number of pollen and spores during cruise ARK-XXIII/2 and /3

But also the flowering season might have been ended. Much more common in slides have been carbonized particles like soot or charcoal. There is no single sample, which has not a lot or even some of those particles included. Here, the comparison to the weather data will clarify to what extent the *Polarstern* itself is responsible for those soot particles in the slides.

All in all pollen of Gymnosperms (mainly *Pinus* sp.) are the most common pollen types in sample slides. *Pinus*-pollen can be found in nearly all slides even in slides very late in season. This might be due to the high pollen production rate of *Pinus,* and due to its very good flying characteristic and, hence, its long lasting stay in the air masses. Its end of flowering season could have been the end of July or the beginning of August.

Pollen of angiosperms however only occurs sporadically since the end of August and with less different species (Poaceae, *Betula* sp.). The end of flowering season around the Arctic Ocean therefore might have been in the middle to the end of August.

In the palynomorph report spores of pteridophytes as well as spores of the bryophytes are rare. A spreading of those plants by air transport therefore is possible but probably is not very frequent. But this has to be analysed in detail.

A strong spreading of fungi by air transport however is confirmed. Also a lot of different forms of fungi/lichens are involved.

Ongoing work

First work at the Senckenberg Research Institute will be a better determination of detected palynomorphs. Then, a comparison from collected weather data and position data with the exact time of embedding of the single palynomorphs shall be carried out. Then using Hysplit_Method (Draxler und Hess, 1997), the so called backward trajectories shall be reconstructed. With this method it is possible to reconstruct the transport pathways of air masses the single palynomorphs have been embedded in. As result the possible source region of embedded palynomorphs and also the length of transportation can be identified.

References

Beug, H.-J. (2006): Leitfaden der Pollenbestimmung für Mitteleuropa und angrenzende Gebiete. – Verlag Dr. Friedrich Pfeil; München.

Draxler, R.R. & Hess, G.D. (1997): Description of the Hysplit_4 modelling system, NOAA Tech Memo ERL ARL-224, Dec, 24 p. http://www.arl.noaa.gov/HYSPLIT_pubs.php

Lacey, M., E.; West, J., S. (2006): The Air Spora – A manual for catching and identifying airborne biological particles. – Springer Verlag; Dordrecht, Netherlands.

Winkler, H.; Ostrowski, R.; Wilhelm, M. (2001): Pollenbestimmungsbuch der Stiftung Deutscher Polleninformationsdienst. – TAKT-Verlag; Paderborn.

APPENDIX

A.1 PARTICIPATING INSTITUTIONS

A.2 CRUISE PARTICIPANTS

A.3 SHIP'S CREW

A.4.1 GRAPHICAL CORE DESCRIPTION OF GKG AND SEDIMENT CORES (B. BAZHENOVA, R. STEIN)

A.4.2 DATA OF SMEAR-SLIDE ANALYSIS

A.4.3 OCCURRENCE OF LARGE-SIZED DROPSTONES

A.4.4 SUMMARY PLOTS OF LOGGING DATA

A.5 SEABIRDS AND MARINE MAMMALS

A.6 STATION LIST

A.1 TEILNEHMENDE INSTITUTE/ PARTICIPATING INSTITUTIONS

	Adresse Address
AWI	Alfred-Wegener-Institut für Polar- und Meeresforschung in der Helmholtz-Gemeinschaft Postfach 120161 27515 Bremerhaven / Germany
DWD	Deutscher Wetterdienst Abteilung Seeschiffahrt Bernhard-Nocht-Straße 76 20359 Hamburg /Germany
GEOTOP	Centre GEOTOP, Universite du Quebec a Montreal C.P. 8888, succursale Centre-Ville Montreal, Quebec Canada, H3C 3P8
Heli Service	Heli Service International GmbH Im Geisbaum 2 63329 Egelsbach/ Germany
ICBM	Institute for Chemistry and Biology of the Marine Environment Microbiogeochemistry, Oldenburg University, POB 2503, 26111 Oldenburg Germany
IFM-GEOMAR	Leibniz Institute for Marine Sciences, University of Kiel Wischhofstrasse 1-3, 24148 Kiel Germany
IORAS	P.P. Shirshov Institute of Oceanology The Russian Academy of Sciences 36, Nakhimovsky Prospekt Moscow 117997 Russia

	Adresse Address
JAMSTEC	Institute of Observational Research for Global Change, Japan Agency for Marine-Earth Science and Technology (JAMSTEC) 2-15, Natsushima-cho, Yokosuka Kanagawa, 237-0061 / Japan
KIGAM	Korean Institute of Geoscience and Mineral Resources 30 Gajeong-dong, Yuseong-gu 305-350 Daejeon Korea
OPTIMARE	Optimare Sensorsyteme AG Am Luneort 15A 27572 Bremerhaven Germany
PolE	Laboratory for Polar Ecology Rue du Fodia 18 B-1367 Ramillies Belgium
RSMAS	Rosenstiel School of Marine and Atmospheric Science (RSMAS) University of Miami 4600, Rickenbacker Cswy. Miami, Florida 33149 USA
Senkenb.	Forschungsinstitut und Naturmuseum Senckenberg Marine Evertebraten I Senckenberganlage 25 D-60325 Frankfurt a.M. Germany
SERCEL	SERCEL 16, Rue de Bel Air F - 44474 CARQUEFOU France
SPU	State University of St. Petersburg, POMOR, 33, 10th Line V.O., St. Petersburg, 199178 Russia

	Adresse Address
taglicht media	Film- und Fernsehproduktion GmbH Cäsarstr. 58 50968 Köln Germany
University of Oldenburg	Universität Oldenburg POB 2503 26111 Oldenburg Germany
VNIIO	All-Russian Research Institute for Geology and Mineral Resources VNIIOkeangeologia 1, Maklina pr., St. Petersburg, 190121 Russia

A.2 FAHRTTEILNEHMER / CRUISE PARTICIPANTS

Name/ Last name	Vorname/ First name	Institut/ Institute	Beruf/ Profession
Bazhenova	Evgenia	AWI/SPU	Student, geology
Büchner	Jürgen	Heli Service	Pilot
Dufek	Tanja	AWI	Student, bathymetry
Eckert	Sebastian	ICBM	Chemist
Feldt	Oliver	Heli Service	Mechanic
Fischer	Natalie	AWI	Student, geology
Gall	Fabian	Heli Service	Mechanic
Gebauer	Manfred	DWD	Meteorologist
Hammrich	Klaus	Heli Service	Pilot
Hegewald	Anne	AWI	Student, geophysics
Herrmann	Mark	Senkenberg	Geologist
Isbert	Rainer	FWS	Teacher
Jensen	Laura	AWI	Student, bathymetry
Joiris	Claude	PolE	Biologist
Jokat	Wilfried	AWI	Geophysist
Jurisch	Franziska	AWI	Student, bathymetry
Kahlberg	Thomas	AWI	Student, geophysics
Kalmbach	Dirk	AWI	Technician
Kessling	Stefanie	AWI	Student, geophysics
Kikuchi	Takashi	Jamstec	Oceanographer
Kollofrath	Jochen	AWI	Student, geophysics
Krylov	Alexey	VNIIO	Geologist
Lacambra	Julien	SERCEL	Engineer
Letscher	Robert	RSMAS	Student, geology
Martens	Hartmut	AWI	Engineer
März	Christian	ICBM	Geologist
Maschke	Stephan	taglicht media	Journalist
Matthiessen	Jens	AWI	Geologist
Mechler	Sebastian	Optimare	Engineer
Müller	Juliane	AWI	Student, geology
Naafs	Bernhard D.	AWI	Student, geology
Nam	Seung-Il	KIGAM	Geologist
Nauels	Alexander	AWI	Student, oceanography
Niessen	Frank	AWI	Geologist
Not	Christelle	GEOTOP	Student, geology
Poggemann	David	IFM GEOMAR	Geologist
Pulm	Pia Valerie	AWI	Student, geophysics

Name/ Last name	**Vorname/ First name**	**Institut/ Institute**	**Beruf/ Profession**
Rabe	Benjamin	AWI	Scientist
Schreck	Michael	AWI	Geographer
Schulte-Loh	Isabell	AWI	Student, geology
Shevchenko	Vladimir	IORAS	Geologist
Sonnabend	Hartmut	DWD	Technician
Stein	Rüdiger	AWI	Geologist
Urlaub	Morelia	AWI	Student, geophysics
Wend	Britta	University of Oldenburg	Biologist
Winter	Felicia	AWI	Student, geophysics

A.3 SCHIFFSBESATZUNG / SHIP'S CREW

No.	Name	Rank
01.	Schwarze, Stefan	Master
02.	Spielke, Steffen	1.Offc.
03.	Farysch, Bernd	Ch. Eng.
04.	Ettlin, Margrith	2.Offc./L.
05.	Fallei, Holger	2.Offc.
06.	Peine, Lutz	2.Offc.
07.	Leichtle, Marion	Doctor
08.	Hecht, Andreas	R.Offc.
09.	Minzlaff, Hans-Ulrich	2.Eng.
10.	Sümnicht, Stefan	2.Eng.
11.	Schaefer, Marc	3.Eng.
12.	Scholz, Manfred	Elec Eng.
13.	Nasis, Ilias	Electron.
14.	Verhoeven, Roger	Electron.
15.	Muhle, Helmut	Elec.Tech
16.	Himmel, Frank	Electron.
17.	Loidl, Reiner	Boatsw.
18.	Reise, Lutz	Carpenter
19.	Guse, Hartmut	A.B.
20.	Rhau, Lars-Peter	A.B.
21.	Winkler, Michael	A.B.
22.	Vehlow, Ringo	A.B.
23.	Hagemann, Manfred	A.B.
24.	Schmidt, Uwe	A.B.
25.	Bäcker, Andreas	A.B.
26.	Wende, Uwe	A.B.
27.	Preußner, Jörg	Storek.
28.	Ipsen, Michael	Mot-man
29.	Voy, Bernd	Mot-man
30.	Elsner, Klaus	Mot-man
31.	Hartmann, Ernst-Uwe	Mot-man
32.	Pinske, Lutz	Mot-man
33.	Müller-Homburg, Ralf-Dieter	Cook
34.	Silinski, Frank	Cooksmate
35.	Martens, Michael	Cooksmate
36.	Jürgens, Monika	1.Stewardess
37.	Wöckener, Martina	Stwdss/Kr
38.	Czyborra, Bärbel	2.Stewardess

No.	Name	Rank
39.	Silinski, Carmen	2.Steward
40.	Gaude, Hans-Jürgen	2.Stewardess
41.	Möller, Wolfgang	2.Steward
42.	Huang, Wu-Mei	2.Stewardess
43.	Yu, Kwok Yuen	Laundrym.
44.	Henning, Marcus	Apprent.
45.	Keller, Maik	Apprent.

A.4.1 GRAPHICAL CORE DESCRIPTION OF GKG AND SEDIMENT CORES (B. BAZHENOVA, R. STEIN)

PS72/287-3 (SL) Barrow Strait **ARK-XXIII/3**

Recovery: 4.63 m 74° 15.95´ N, 90° 59.09´ W Water depth: 337 m

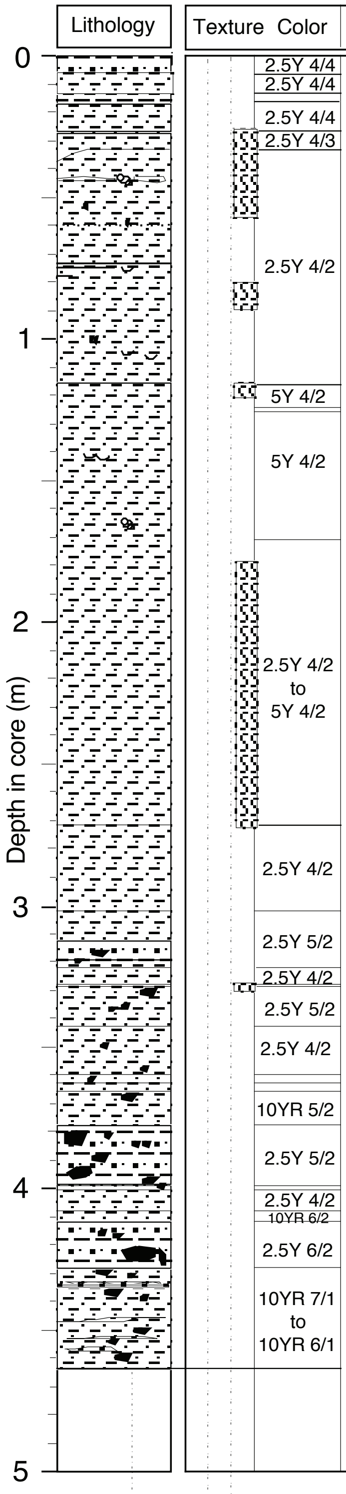

Description | Age

0 - 6 cm: olive brown (2.5Y 4/4) sandy silty clay
6 - 13 cm: olive brown (2.5Y 4/4) silty clay
13 - 17 cm: olive brown (2.5Y 4/3) sandy silty clay
17 - 27 cm: olive brown (2.5Y 4/4) silty clay
27 - 33 cm: olive brown (2.5Y 4/3) silty clay; mottled/bioturbated
33 - 116 cm: dark grayish brown (2.5Y 4/2) silty clay with some sand, partly bioturbated/mottled (2.5Y 4/1); more sandy layer at 60 cm; dark gray layers at 73, 74, and 77 cm; small dropstones (0.5 cm in diameter) at 53, 59, and 100 cm; well-preserved large gastropode (3 cm in length) at 43-45 cm, shell debris at 74, 103, and 105 cm
116 - 171 cm: olive gray (5Y 5/2) silty clay with some sand; mottled/ bioturbated between 116 and 121 cm; dark grayish brown (2.5Y 4/2) interval at 124-126 cm; abundant shell debris at 141-142 cm, well-preserved large gastropode at 165-166 cm
171 - 272 cm: olive gray (5Y 4/2) to dark grayish brown (2.5Y 4/2) silty clay with some sand, slightly bioturbated
272 - 302 cm: dark grayish brown (2.5 4/2) silty clay with some sand
302 - 322 cm: grayish brown (2.5Y 5/2) silty clay with some sand, more sandy in the lower part (sandy silty clay); dropstones at 317-319 cm (3 cm in diameter) and 320 cm (0.5 cm in diameter)
322 - 328 cm: dark grayish brown (2.5 4/2) silty clay with some sand
328 - 329 cm: light brownish gray (10YR 6/2) silty clay with some sand; some bioturbation
329 - 343 cm: grayish brown (2.5Y 5/2) silty clay with some sand; dropstones at 331-332 cm (1 cm in diameter), 336 cm (0.5 cm in diameter), and 337 cm (0.5 cm in diameter)
343 - 360 cm: dark grayish brown (2.5 4/2) silty clay with some sand; dropstones (0.5 cm in diameter) at 350 and 358 cm
360 - 363 cm: grayish brown (10YR 5/2) silty clay with some sand; dropstone (0.5 cm in diameter) at 362 cm
363 - 366 cm: grayish brown (2.5Y 5/2) silty clay with some sand
366 - 378 cm: grayish brown (10YR 5/2) silty clay with some sand
378 - 399 cm: grayish brown (2.5Y 5/2) (sandy) silty clay (diamicton); dropstones at 380-384 cm (4cm in diameter), 382-383 (1 cm in diameter), 390-391 cm (1 cm in diameter), 393-396 cm (3 cm in diameter), and 398-399 cm (1 cm in diameter); abundant very small dropstones (<0.3 cm) at 387-389 cm
399 - 400 cm: light brownish gray (10YR 6/2) silty clay
400 - 408 cm: dark grayish brown (2.5Y 4/2) silty clay
408 - 412 cm: light brownish gray (10YR 6/2) silty clay; small light gray lenses/spots (10YR 7/2)
412 - 428 cm: light brownish gray (2.5Y 6/2) sandy silty clay (diamicton); dropstones at 415-416 cm (1 cm in diameter), 417 (0.5 cm in diameter), 421-422 (1 cm in diameter), 423-424 cm (1 cm in diameter), 423-427 (7 cm in diameter), and 425-426 cm (2 cm in diameter)
428 - 463 cm: light gray (10YR 7/1) to gray (10YR 6/1) silty clay with some sand (diamicton); sandy layers at 433, 434, 438, 453, and 457-458 cm; weak red (7.5R 5/3) sandy layer at 448 cm; dropstones at 429-432 (3 cm in diameter), 432-433 (1 cm in diameter), 437-438 (2 cm in diameter), 439-440 (1 cm in diameter), 442-444 (3 cm in diameter), 449-452 (3 cm in diameter), and 458-460 cm (3 cm in diameter)

PS 72/ 291-1 (GKG) Mackenzie Slope **ARK- XXIII/3 (Arctic 08)**

Recovery: 42 cm **71°16,17’ N 137°10,80’ W** **Water depth: 1502 m**

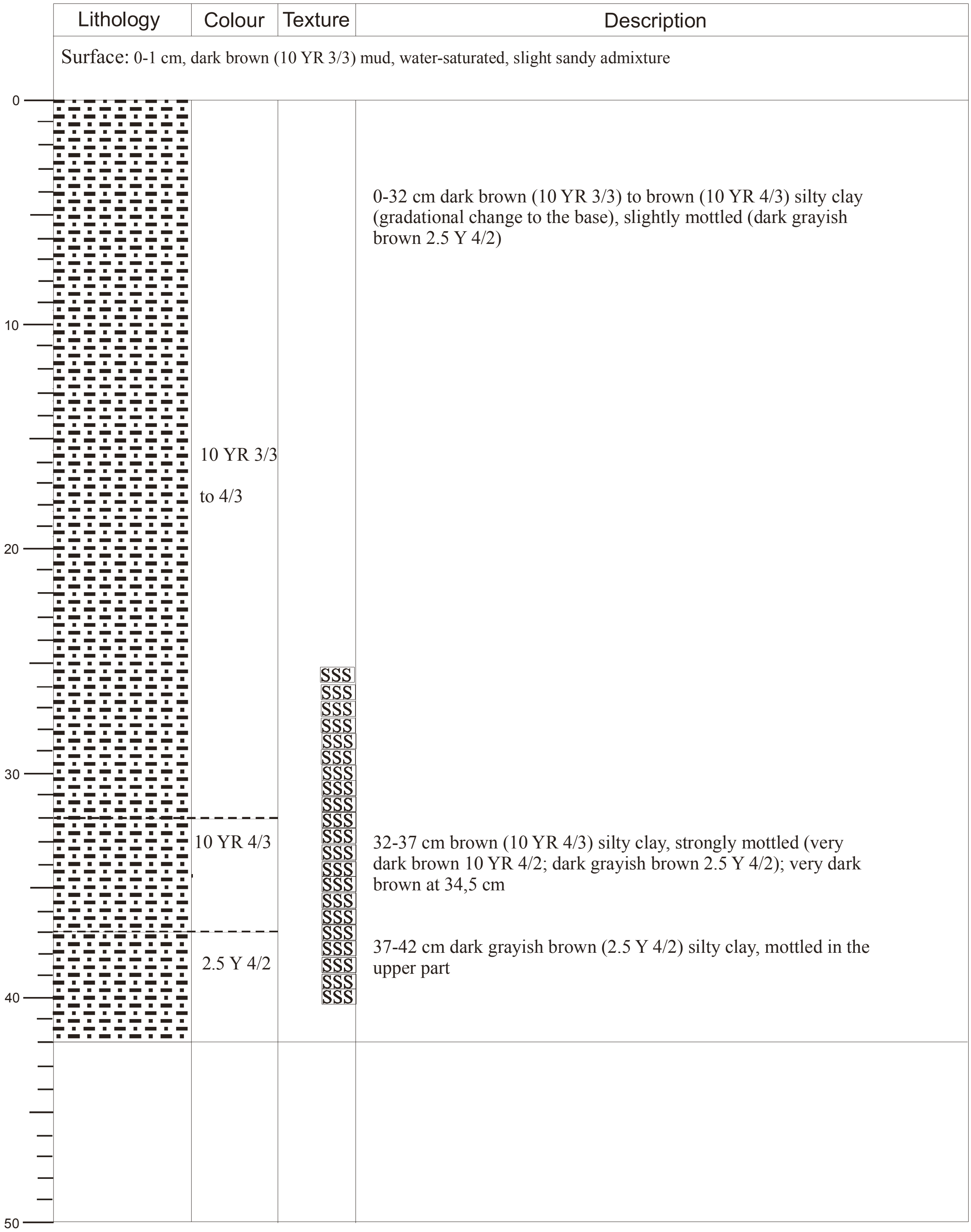

PS72/291-2 KAL Mackenzie Slope **ARK-XXIII/3**

Recovery: 8.51 m 71° 16.18´ N, 137° 10.82´ W Water depth: 1502 m

Lithology	Texture Color	Description	Age

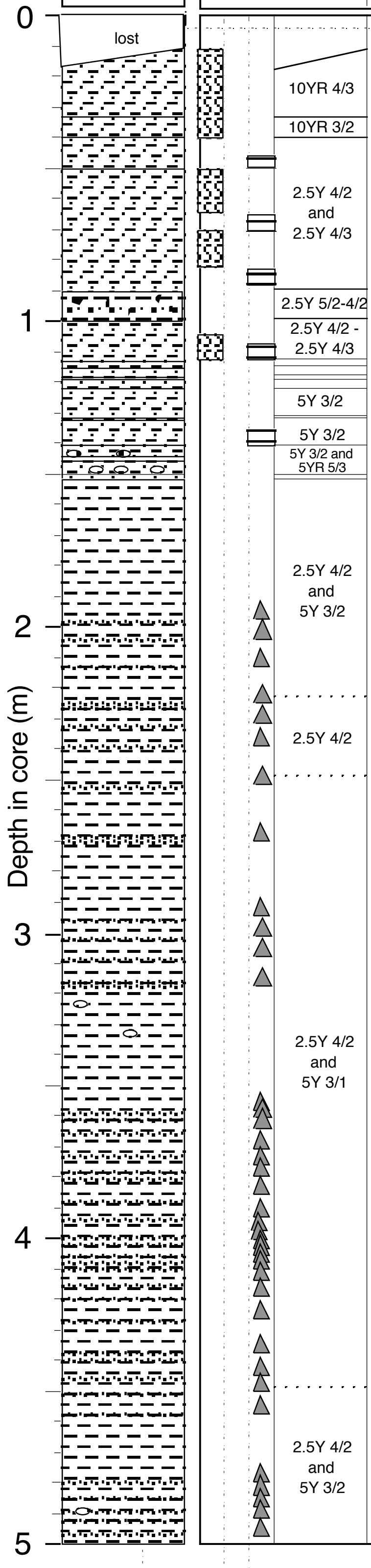

0 - 11 cm: coring lost (see GKG)
11 - 33 cm: brown (10YR 4/3) silty clay; mottled (grayish brown, 10YR 5/2) /bioturbated
33 - 40 cm: very dark grayish brown (10YR 3/2) to dark brown (10YR 3/3) silty clay, mottled (10YR 3/2)/bioturbated
40 - 90 cm: dark grayish brown (2.5Y 4/2) and olive brown (2.5Y 4/3) silty clay; partly bioturbated; some lamination at 46 to 49 cm (very dark gray thin layers), 65 - 70 cm, and 82 - 88 cm; very dark grayish brown (2.5Y 3/2) sandy-silty layer
90 - 99 cm: grayish brown (2.5Y 5/2) to dark grayish brown (2.5Y 4/2) sandy silty clay with pinkish gray (5YR 7/2) more sandy lenses and small dropstones (0.2 to 0.5 cm in diameter); one larger dropstone (1 cm in diameter, probably dolomite) at 92 cm
99 - 113 cm: dark grayish brown (2.5Y 4/2) and olive brown (2.5Y 4/3) silty clay; some lamination; bioturbated in lower part; gray (2.5Y 5/1) horizon at 101 cm
113 - 115 cm: olive brown (2.5Y 4/3) silty clay; thin brownish lamina at 115 cm
115 - 118 cm: dark gray (2.5Y 4/1) silty clay
118 - 119 cm: gray (2.5Y 5/1) silty clay
119 - 122 cm: olive brown (2.5Y 4/3) silty clay
122 - 141 cm: dark olive gray (5Y 3/2) silty clay; gray layer at 132 cm
141 - 150 cm: dark olive gray (5Y 3/2) and dark grayish brown (2.5Y 4/2) silty clay with abundant reddish brown (5YR 5/3) (dolomitic?) lenses; thin more sandy layer at 143 cm
150 - 152 cm: olive brown (2.5Y 4/3) silty clay
152 - 831 cm: dark grayish brown (2.5Y 4/2), very dark gray (2.5Y 3/1) to dark olive gray (5Y 3/2) clay; silty layers most abundant between about 360 and 500 cm: thin coarser-grained (silty) layers/laminae at 199, 204, 205, 225, 226, 227, 232, 240, 243, 253, 269, 270, 296, 302, 308, 316, 317, 359, 361, 366, 367, 373, 379, 381, 388, 394, 400, 402, 405, 407, 409, 410, 411, 415, 419, 420, 427, 428, 437-438, 445, 451, 458, 480, 481, 485, 489, 492, 497, 498, 507, 519, 526, 528, 535, 550 (gray), 561, 568, 584, 586, 597, 599, 681, 712, 723, 763, 785, 805, and 810 cm (fining-upward cycles?); small pinkish gray (5YR 7/2) lenses at 323 - 325, 333, 489 (also reddish brown), 612, 622, 660, 705, and 818 cm

831 - 851 cm: Core catcher (tubes not opened yet)

PS72/291-2 KAL Mackenzie Slope **ARK-XXIII/3**

Recovery: 8.51 m 71° 16.18´ N, 137° 10.82´ W Water depth: 1502 m

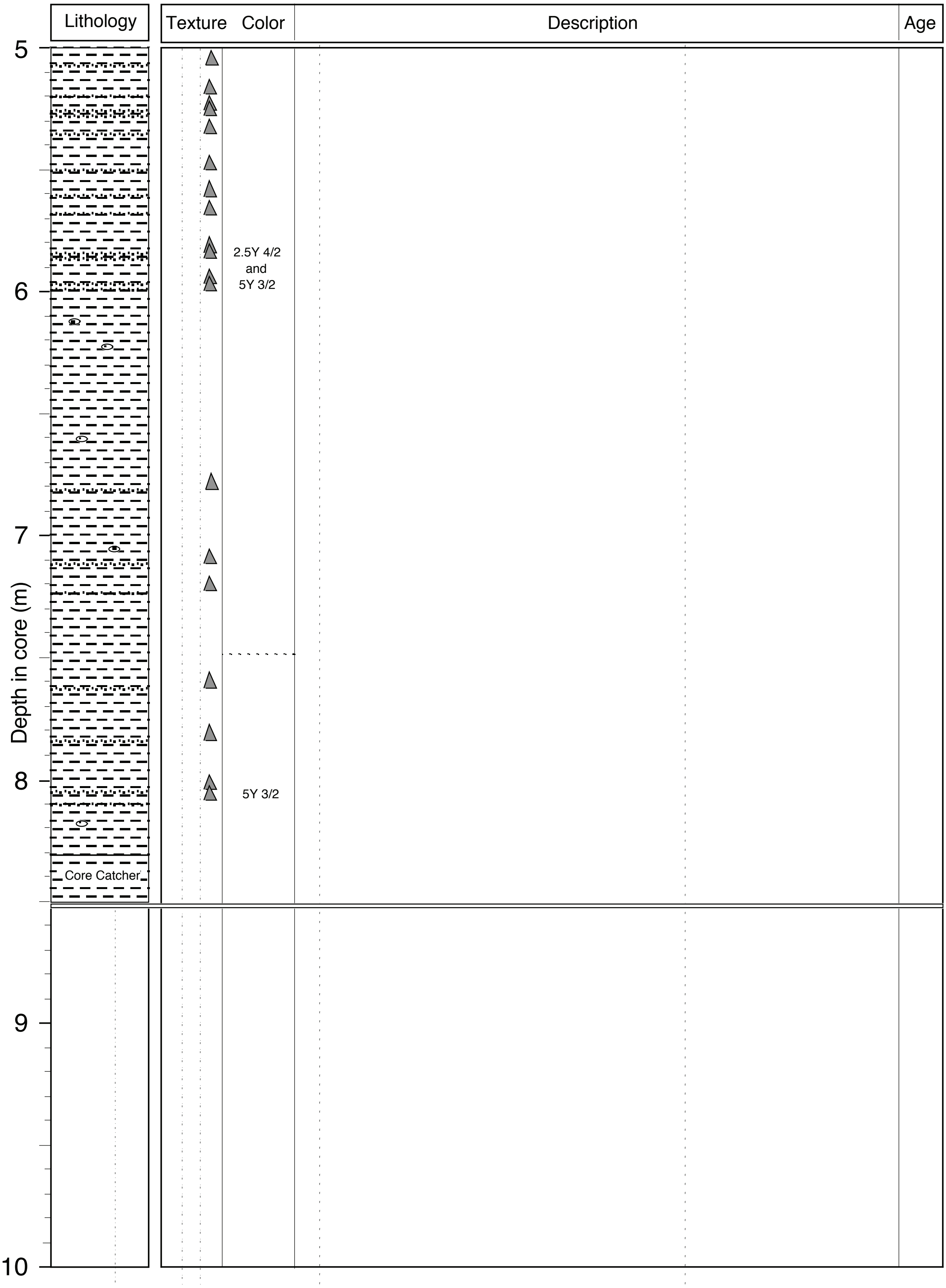

PS 72/ 340-3 (GKG) Southern Mendeleev Ridge **ARK- XXIII/3 (Arctic 08)**

Recovery: 39 (41) cm **77°35,42' N 171°32,56' W** **Water depth: 2298 m**

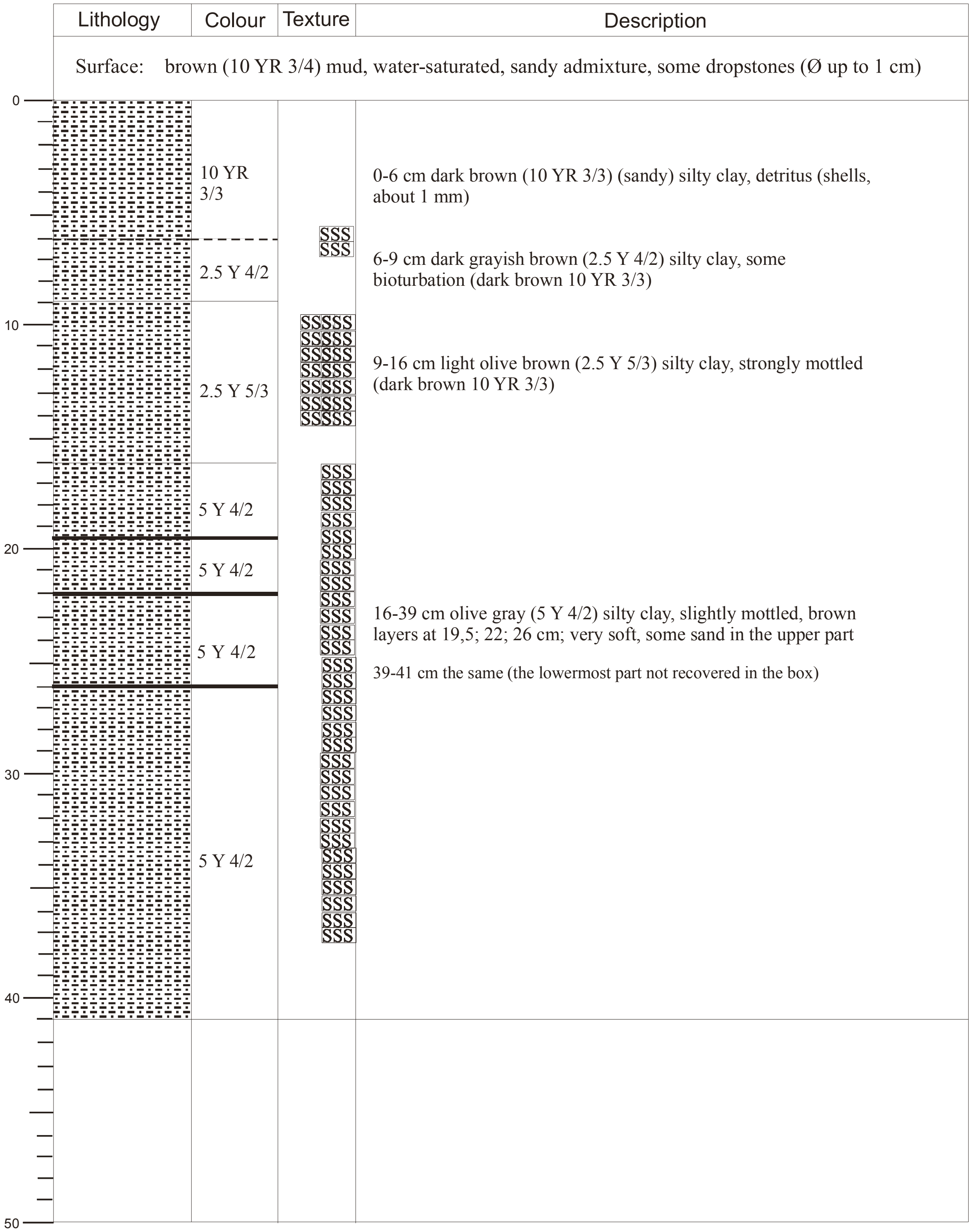

PS72/340-5 KAL Southern Mendeleev Ridge **ARK-XXIII/3**

Recovery: 8.3 m 77° 36.23´ N, 171° 29.65´ W Water depth: 2298 m

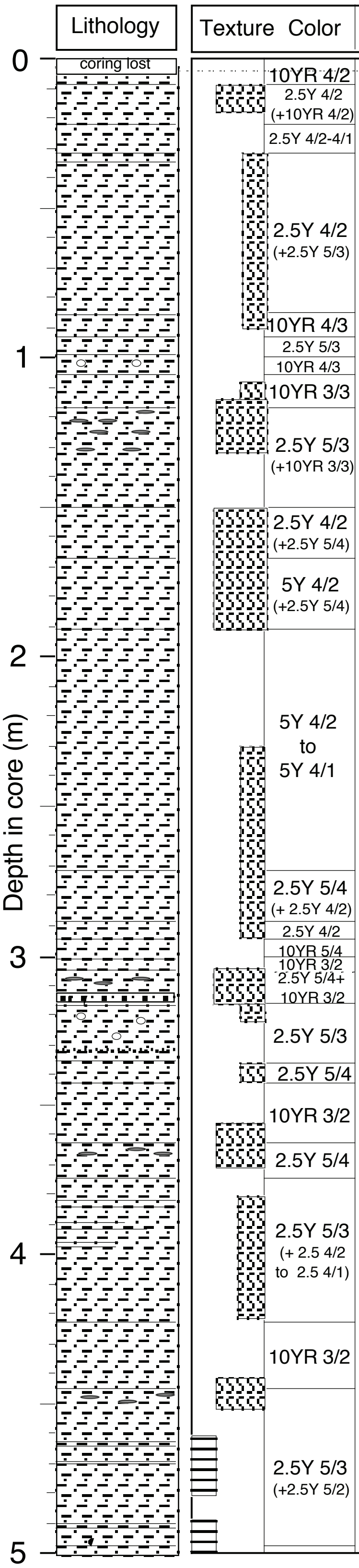

Description

0 - 4 cm: coring lost
4 - 9 cm: dark grayish brown (10YR 4/2) silty clay, some sand
9 - 22 cm: dark grayish brown (2.5Y 4/2) silty clay, dark grayish brown mottling
22 - 32 cm: dark grayish brown (2.5Y 4/2) to dark gray (2.5Y 4/1), between 22-25 cm some more silty layers
32 - 85 cm: dark grayish brown (2.5Y 4/2) silty clay, light olive brown mottling (2.5Y 5/3) bioturbation, dark brown layer at 34 cm; coarser-grained near base
85 - 93 cm: brown (10YR 4/3) to yellowish brown (10YR 5/4) silty clay, some bioturbation at 89-91 cm
93 - 100 cm: light olive brown (2.5Y 5/3) silty clay, small brown spots, sharp contact at the base
100 - 106 cm: brown (10YR 4/3) to yellowish brown (10YR 5/4) silty clay, small pinkish lenses at 102-103 cm (more coarse-grained)
106 - 117 cm: dark brown (10YR 3/3) silty clay, brownish mottling at 106 -110 cm
117 - 150 cm: light olive brown (2.5Y 5/3 to 5/4) silty clay, strongly mottled (dark brown 10YR 3/3) at 117-120 cm, very dark brown to brown lenses between 126 and 133 cm (mottling/bioturbation) (Planolites?)
150 - 167 cm: dark grayish brown (2.5Y 4/2) silty clay, strongly mottled (2.5Y 5/4)
167 - 191 cm: olive gray (5Y 4/2) silty clay, strongly mottled (2.5Y 5/4)
191 - 272 cm: olive gray (5Y 4/2) to dark gray (5Y 4/1) silty clay, some mottling (2.5Y 5/3) below 231 cm
272 - 289 cm: light olive brown (2.5Y 5/4) silty clay, dark grayish brown mottling
289 - 295 cm: dark grayish brown (2.5Y 4/2) to light olive brown (2.5Y 5/4) (mottling) silty clay, 289-292 cm more coarse-grained
295 - 301 cm: yellowish brown (10YR 5/4) silty clay
301 - 317 cm: very dark grayish brown (10YR 3/2) silty clay, strongly mottled below 305 cm (light olive brown 2.5Y 5/4); 314-316 cm very pale brown (10 YR 7/3), more coarse-grained, small dropstones (Ø 0.5 cm) (diamict)
317 - 336 cm: light olive brown (2.5Y 5/3) to grayish brown (2.5Y 5/2) silty clay; dark brown mottling at 317-323 cm; small "pinkish" lenses at 321-326 cm; at 332 cm more coarse-grained layer
336 - 343 cm: light olive brown (2.5Y 5/4) silty clay, slightly bioturbated, sharp contact at the base
343 - 363 cm: very dark grayish brown (10YR 3/2) silty clay; at the top very pale brown lense (10YR 7/3), at 343-346 cm brown (10YR 4/3), strongly mottled at 350-353 and 359-363 cm (2.5Y 5/4)
363 - 375 cm: light olive brown (2.5Y 5/4) silty clay, very dark grayish brown lenses at 363-366 cm
375 - 423 cm: light olive brown (2.5Y 5/3) silty clay; at 382-383, 390-392, 396-398, and 409-418 cm dark grayish brown (2.5Y 4/2) to dark gray (2.5Y 4/1) mottling, sharp contact at the base
423 - 445 cm: very dark grayish brown (10YR 3/2) silty clay, strongly mottled 2.5Y5/3
445 - 498 cm: light olive brown (2.5Y 5/3) silty clay, at 445-449 cm strongly mottled (very dark grayish brown 10 YR 3/2 lenses; Planolites); at 463-463,469-470, and 491-492 cm grayish brown (2.5Y 5/2); at 473-481 thin laminae (grayish brown 2.5Y 5/2, brown 10YR 4/3); at 495-498 cm more yellowish brown (10YR 5/4); few small black spots throughout the interval; one dropstone (Ø 1 cm) at 497 cm
498 - 507 cm: brown (10YR 4/3) silty clay, mottled (light reddish brown 5YR 6/4, coarse-grained); dropstones at 500 and 505 cm (Ø 0.5-1 cm) (diamict)
507 - 513 cm: light reddish brown (5YR 6/4) ("pinkish") sandy silty clay, several large dropstones (up to 10 cm in Ø) (diamict)
513 - 524 cm: brown (10YR 4/3) to grayish brown (2.5Y 5/2) silty clay, strongly mottled, few small light reddish brown spots
524 - 528 cm: grayish brown (2.5Y 5/2) silty clay
528 - 533 cm: light olive brown (2.5Y 5/3) silty clay
533 - 550 cm: very dark grayish brown (10YR 3/2) to dark brown (10YR 3/3) silty clay, at 541-550 cm strongly mottled (2.5Y 5/3); dropstone (Ø 0.5 cm) at 533 cm
550 - 553 cm: light olive brown (2.5Y 5/3) silty clay, strongly mottled (dark brown)

PS72/340-5 KAL Southern Mendeleev Ridge **ARK-XXIII/3**

Recovery: 8.3 m 77° 36.23´ N, 171° 29.65´ W Water depth: 2298 m

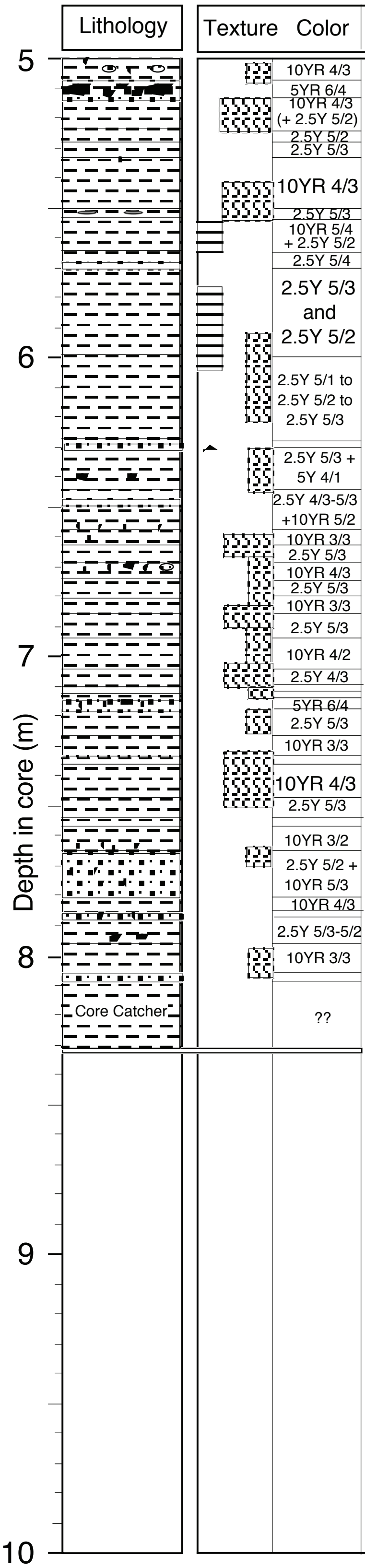

Description

553 - 564 cm: alternations of yellowish brown (10YR 5/4) and grayish brown (2.5Y 5/2) silty clay, partly more coarse-grained (sand)

564 - 570 cm: light olive brown (2.5Y 5/3) silty clay, more coarse-grained in lower part

570 - 600 cm: light olive brown (2.5Y 5/3) and grayish brown (2.5Y 5/2) silty clay, very dark brown spots throughout the interval

600 - 627 cm: gray (2.5Y 5/1), grayish brown (2.5Y 5/2) to light olive brown (2.5Y 5/3) silty clay; at 601-617 cm very dark brown to black spots

627 - 628 cm: light olive brown (2.5Y 5/3) silty clay; sharp contact at the base

628 - 630 cm: olive brown (2.5Y 4/3) (sandy) silty clay to silty clay (fining upwards), sharp contact at the base

630 - 644 cm: light olive brown (2.5Y 5/3) and dark gray (5Y 4/1) silty clay, strongly mottled/bioturbated, at 637-639 cm “pinkish red” lenses; some dropstones

644 - 658 cm: olive brown (2.5Y 4/3), light olive brown (2.5Y 5/3), grayish brown (10YR 5/2) silty clay; more coarse-grained at 647-649 cm; small black spots throughout; at the base small dropstones (Ø 0.5 cm)

658 - 663 cm: dark brown (10YR 3/3) silty clay, light olive brown (2.5Y 5/3) mottling, small dropstone at 660 cm

663 - 669 cm: light olive brown (2.5Y 5/3) silty clay, dark brown mottling (10 YR 3/3)

669 - 674 cm: brown (10YR 4/3) silty clay (some sand), at 670-671 cm some small dropstones (Ø 0.3-1cm), several small “pinkish red” lenses, light olive brown mottling

674 - 680 cm: light olive brown (2.5Y 5/3 to 5/4) silty clay, slightly mottled (dark brown 10YR3/3); small black spots, sharp contact at the base

680 - 686 cm: dark brown (10YR 3/3) silty clay, slightly mottled; more silty layers at 683 and 684 cm; few “pinkish red” lenses, light yellowish brown (2.5Y 6/4) lenses on top

686 - 694 cm: light olive brown (2.5Y 5/3) silty clay, dark brown (10YR 3/3) mottling

694 - 704 cm: dark grayish brown (10YR 4/2) silty clay, slightly bioturbated; some black spots

704 - 710 cm: olive brown (2.5Y 4/3) and dark grayish brown (10 YR 4/2), strongly mottled/bioturbated

710 - 712 cm: light olive brown (2.5Y 4/4) (silty) clay, dark brown and black spots

712 - 714 cm: olive brown silty clay, dark brown lenses

714 - 718 cm: light reddish brown (5 YR 6/4; “pinkish”) (sandy) silty clay, several dropstones (Ø 0.5 to 1 cm) (diamict)

718 - 726 cm: light olive brown (2.5Y 5/3) silty clay, small black spots throughout

726 - 727 cm: light olive brown (2.5Y 5/3) silty clay

727 - 733 cm: dark brown (10YR 3/3) silty clay, mottled (2.5Y 5/3)

733 - 736 cm: light olive brown (2.5Y 5/4) silty clay, dark brown (10YR 3/3) mottling

736 - 747 cm: brown (10YR 4/3) silty clay, light olive brown mottling, dark brown spots

747-754 light olive brown (2.5Y 5/3) silty clay, abundant brown spots/bioturbation

754 - 757 cm: pale olive (5Y 6/3) silty clay, sharp base

757 - 765 cm: very dark grayish brown (10YR 3/2) silty clay, light yellowish brown (10YR 3/2) mottling, few very small dropstones at 764 cm

765 - 781 cm: light olive brown (2.5Y 5/2) to brown (10YR 5/3) (sandy) silty clay; at 771-772 and 775-776 cm light reddish brown (5 YR 6/4; “pinkish”), several dropstones (Ø 0.3 to 0.5cm) at 770-777 cm

781 - 785 cm: brown (10YR 4/3) silty clay

785 - 787 cm: light reddish brown (5 YR 6/4; “pinkish”) (sandy) silty clay, some dark brown spots; dropstone (Ø 1.5 cm) (diamict)

787 - 796 cm: light olive brown (2.5Y 5/3) to grayish brown (2.5Y 5/2) silty clay; dark brownish spots throughout; some dropstones

796 - 806 cm: dark brown (10YR 3/3) silty clay, light yellowish brown mottling

806 - 809 cm: light olive brown (2.5Y 5/3) to grayish brown (10YR 5/2) (sandy) silty clay; mottling; 807-809 coring disturbance

809 - 829 cm: Core catcher (tubes not opened yet)

PS 72/ 341-3 (GKG)

Southern Mendeleev Ridge

ARK- XXIII/3 (Arctic 08)

Recovery: 41 (48) cm

77°36,46’ N 176°7,37’ W

Water depth: 1339 m

Lithology	Colour	Texture	Description
Surface: dark yellowish brown (10 YR 3/4) sandy mud, water-saturated, some dropstones (Ø up to 1,5 cm); living organisms: Hydrozoa, polychets, shell detritus			

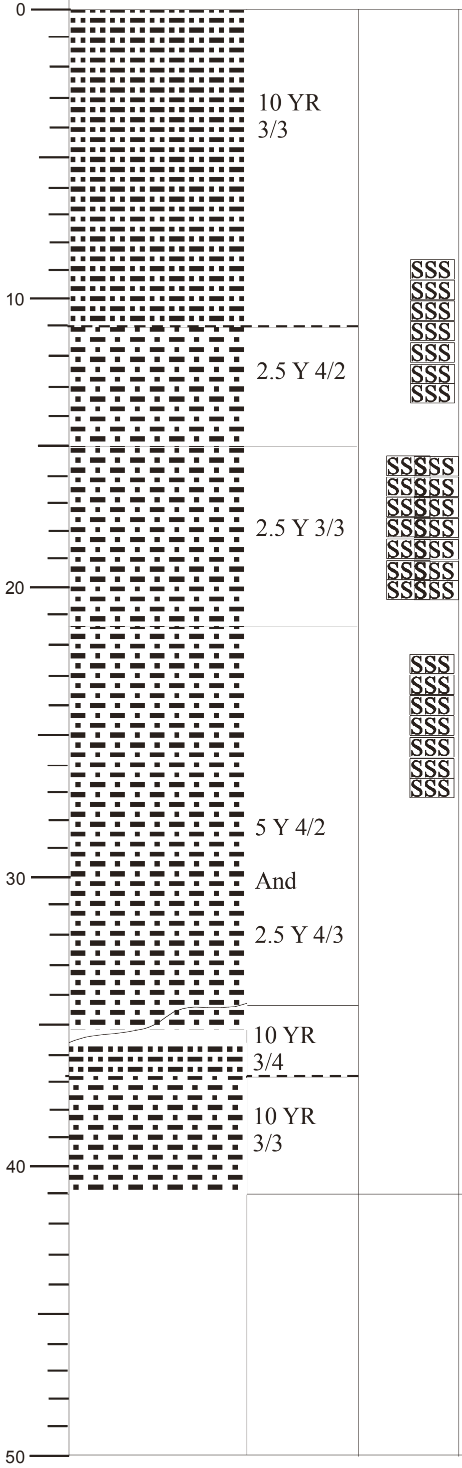

0-11 dark brown (10 YR 3/3) (sandy) silty clay, fining to the base

11-15 cm dark grayish brown (2.5 Y 4/2) silty clay

15-21,5 cm light olive brown (2.5 Y 5/3) silty clay, mottled (dark brown 10 YR 3/3)

21,5-35,5 cm grayish brown (5 Y 4/2) to olive brown (2.5 Y 4/3) silty clay, very soft, slightly mottled in the upper part (dark brown 10 YR 3/3), sharp contact at the base

35,5-37 cm dark brown (10 YR 3/3) (sandy) silty clay, fining to the base

37-41 cm dark yellowish brown (10 YR 3/4) silty clay

! at 9-19 cm some lenses of coarse-grained material (coarse-grained sand and gravel, dark-green (with glauconite?), Some shells (Bivalvia)

41-48 cm lowermost part (same as 37-41 cm) not recovered in the box

PS72/341-5 KAL Recovery: 3.03 m

Southern Mendeleev Ridge 77° 35.85' N, 176° 06.28´ W

ARK-XXIII/3 Water depth: 1339 m

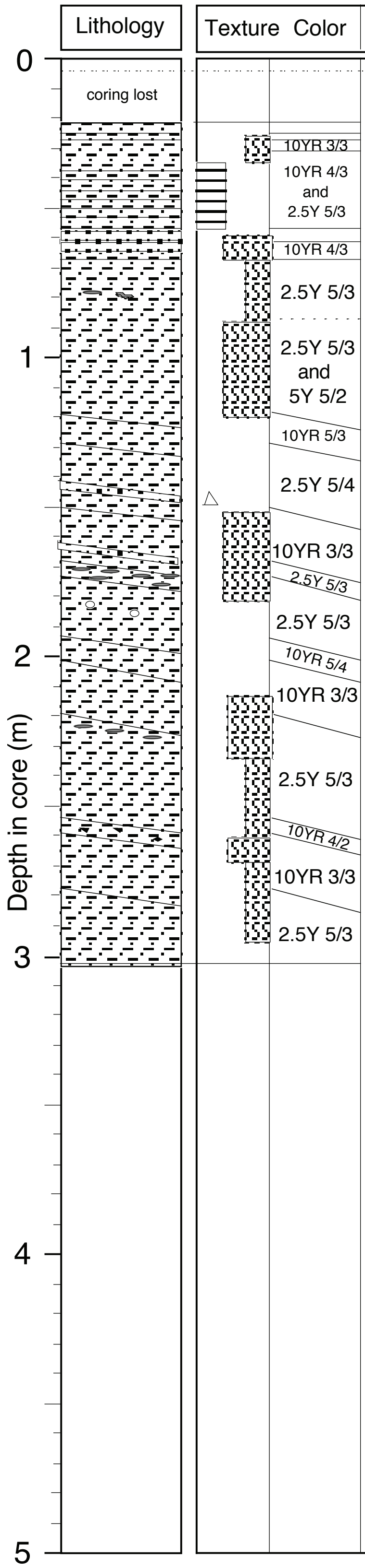

Description

0 - 22 cm: coring lost
22 - 25 cm: dark brown (10YR 3/3) silty clay
25 - 27 cm: light olive brown (2.5Y 5/3) silty clay
27 - 31 cm: dark brown (10YR 3/3) silty clay
31 - 57 cm: alternation of brown (10YR 4/3) and light olive brown (2.5Y 5/3) silty clay; gray (2.5Y 5/1) layer at 41 cm
57 - 61 cm brown (10YR 4/3) sandy silty clay; sharp contact at base
61 - 67 cm: brown (10YR 4/3) to yellowish brown (10YR 5/4) silty clay, upper part more sandy; some mottling/bioturbation
61 - 122 cm: light olive brown (2.5Y 5/3) silty clay, strongly motled (olive gray 5Y 5/2) /bioturbated below 88 cm; large dark brown (10YR 3/3) burrows at 77 - 78 cm
122 - 130 cm: yellowish brown (10YR 5/4) silty clay
130 - 152 cm: light olive brown (2.5Y 5/4) silty clay; more sandy interval at 143 - 147 cm (sharp base, fining-upward)
152 - 169 cm: brown (10YR 4/3) silty clay, strongly mottled/bioturbated; beige ("pinkish") layers/lenses (more coarse-grained) at 164 - 166 cm
169 - 175 cm: light olive brown (2.5Y 5/3) silty clay; large brown (10YR 4/3) burrows (Planolites); beige lense at 173 cm
175 - 195 cm: light olive brown (2.5Y 5/3) silty clay; dark gray layer at 188 cm; small beige ("pink") lenses at 182 cm
195 - 202 cm: yellowish brown (10YR 5/4) and brown (10YR 4/3) silty clay
202 - 221 cm: dark brown (10YR 3/3) silty clay, light olive brown mottling in lower part
221 - 256 cm: light olive brown (2.5Y 5/3) silty clay; upper part strongly mottled (dark brown lenses), below also bioturbated
256 - 260 cm: dark grayish brown (10YR 4/2) and light olive brown (2.5Y 5/4) silty clay, mottled/bioturbated); small dropstones (0.5 to 1 cm in diameter)
260 - 279 cm: dark brown (10YR 3/3) silty clay, light olive brown mottling (more strongly in upper part
279 - 303 cm: light olive brown (2.5Y 5/3) and grayish brown (2.5Y 5/2) silty clay, mottled/bioturbated

<u>Note:</u>
Most of the sediment layers/intervals strongly tilted due to coring disturbance

PS72/341-5 KAL Southern Mendeleev Ridge **ARK-XXIII/3**

Recovery: 3.03 m 77° 35.85' N, 176° 06.28´ W Water depth: 1339 m

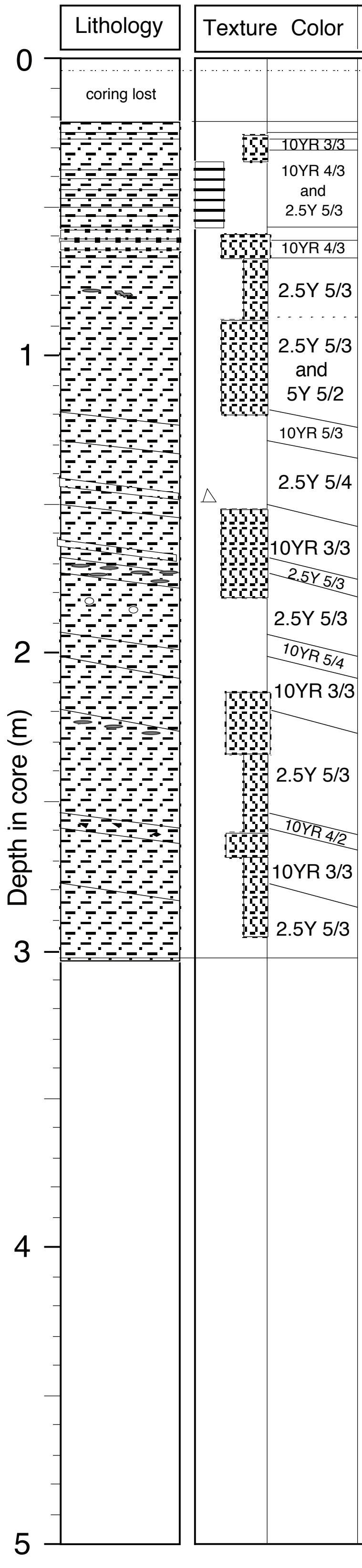

Description

0 - 22 cm: coring lost
22 - 25 cm: dark brown (10YR 3/3) silty clay
25 - 27 cm: light olive brown (2.5Y 5/3) silty clay
27 - 31 cm: dark brown (10YR 3/3) silty clay
31 - 57 cm: alternation of brown (10YR 4/3) and light olive brown (2.5Y 5/3) silty clay; gray (2.5Y 5/1) layer at 41 cm
57 - 61 cm brown (10YR 4/3) sandy silty clay; sharp contact at base
61 - 67 cm: brown (10YR 4/3) to yellowish brown (10YR 5/4) silty clay, upper part more sandy; some mottling/bioturbation
61 - 122 cm: light olive brown (2.5Y 5/3) silty clay, strongly motled (olive gray 5Y 5/2) /bioturbated below 88 cm; large dark brown (10YR 3/3) burrows at 77 - 78 cm
122 - 130 cm: yellowish brown (10YR 5/4) silty clay
130 - 152 cm: light olive brown (2.5Y 5/4) silty clay; more sandy interval at 143 - 147 cm (sharp base, fining-upward)
152 - 169 cm: brown (10YR 4/3) silty clay, strongly mottled/bioturbated; beige ("pinkish") layers/lenses (more coarse-grained) at 164 - 166 cm
169 - 175 cm: light olive brown (2.5Y 5/3) silty clay; large brown (10YR 4/3) burrows (Planolites); beige lense at 173 cm
175 - 195 cm: light olive brown (2.5Y 5/3) silty clay; dark gray layer at 188 cm; small beige ("pink") lenses at 182 cm
195 - 202 cm: yellowish brown (10YR 5/4) and brown (10YR 4/3) silty clay
202 - 221 cm: dark brown (10YR 3/3) silty clay, light olive brown mottling in lower part
221 - 256 cm: light olive brown (2.5Y 5/3) silty clay; upper part strongly mottled (dark brown lenses), below also bioturbated
256 - 260 cm: dark grayish brown (10YR 4/2) and light olive brown (2.5Y 5/4) silty clay, mottled/bioturbated); small dropstones (0.5 to 1 cm in diameter)
260 - 279 cm: dark brown (10YR 3/3) silty clay, light olive brown mottling (more strongly in upper part
279 - 303 cm: light olive brown (2.5Y 5/3) and grayish brown (2.5Y 5/2) silty clay, mottled/bioturbated

<u>Note:</u>
Most of the sediment layers/intervals strongly tilted due to coring disturbance

PS72/343-2 SL Southern Mendeleev Ridge **ARK-XXIII/3**

Recovery: 7.49 m 77° 18.33´ N, 179° 02.70´ E Water depth: 1193 m

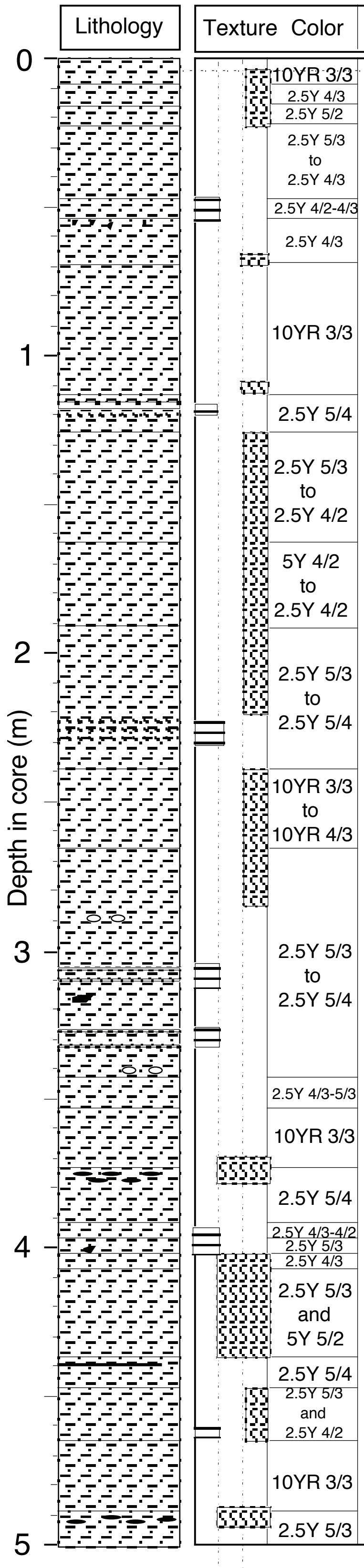

Description

0 - 9 cm: dark brown (10 YR 3/3) silty clay; between 6 and 9 cm olive brown (2.5 Y 4/3) mottling
9 - 16 cm: olive brown (2.5 Y 4/3) silty clay, slightly bioturbated
16 - 22 cm: grayish brown (2.5 Y 5/2) silty clay, olive brown mottling
22 - 47 cm: light olive brown (2.5 Y 5/3) to olive brown (2.5 Y 4/3) silty clay
47 - 54 cm: alternation of dark grayish brown (2.5 Y 4/2) and olive brown (2.5 Y 4/3) silty clay
54 - 69 cm: olive brown (2.5 Y 4/3) silty clay, several small dropstones at 55 - 59 cm; light olive brown (2.5 Y 5/4) horizon at 65 - 66 cm, between 66 - 69 cm slightly mottled
69 - 113 cm: dark brown (10 YR 3/3) silty clay, between 110 and 113 cm slightly mottled
113 - 126 cm: light olive brown (2.5 Y 5/4) silty clay; sandy horizon at 116 - 117 cm , thin sandy layers at 120 and 121 cm
126 - 163 cm: light olive brown (2.5 Y 5/3) and dark grayish brown (2.5 Y 4/2) silty clay, mottled/bioturbated
163 - 191 cm: olive gray (5 Y 4/2) to dark grayish brown (2.5 Y 4/2) silty clay, light olive brown mottling
191 - 239 cm: light olive brown (2.5 Y 5/3 to 5/4), mottling at 191-223 cm, at 223-231 cm thin sandy layers
239 - 266 cm: dark brown (10 YR 3/3) to brown (10YR 4/3) silty clay, some light olive brown to light olive gray mottling (bioturbation); at the base some light reddish brown (5 YR 6/4) small spots
266 - 343 cm: light olive brown (2.5 Y 5/3 to 5/4) silty clay; dark gray horizons at 307-308, 310-311, 326-327, and 332-333 cm; large dropstone (Ø 3 cm) at 315-317 cm, small light reddish brown (5 YR6/4) lenses at 287 and 340 cm; slightly bioturbated at 266-285 cm
343 - 353 cm: olive brown (2.5 Y 4/3) to light olive brown (2.5 Y 5/3) silty clay
353 - 373 cm: dark brown (10 YR 3/3) silty clay, strongly mottled at 369-373 cm
373 - 392 cm: light olive brown (2.5 Y 5/4) silty clay, 373-378 cm strongly mottled (dark brown)
392 - 397 cm: olive brown (2.5 Y 4/3) and dark grayish brown (2.5 Y 4/2) silty clay
397 - 402 cm: light olive brown (2.5 Y 5/3) silty clay; thin silty laminae at 401 and 402 cm, very small dropstone (Ø 0.2 cm) at 400.5 cm
402 - 407 cm: olive brown (2.5 Y 4/3) and dark grayish brown (2.5 Y 4/2) silty clay, strongly mottled
407 - 437 cm: light olive brown (2.5 Y 5/3) and olive gray (5 Y 5/2) silty clay, strongly mottled; sharp contact at the base
437 - 447 cm: light olive brown (2.5 Y 5/4) silty clay, dark grayish brown horizon at 439-440 cm
447 - 465 cm: light olive brown (2.5 Y 5/3) and dark grayish brown (2.5 Y 4/2) silty clay, mottled/bioturbated; some more silty laminae at 461-463 cm; sharp contact at the base
465 - 489 cm: dark brown (10 YR 3/3) silty clay, strongly mottled at 489-490 cm
489 - 505 cm: light olive brown (2.5 Y 5/3) silty clay, at 489-495 cm dark brown mottling
505 - 512 cm: light olive brown (2.5 Y 5/3) (sandy) silty clay
512 - 544 cm: light olive brown (2.5 Y 5/3) to dark grayish brown (2.5 Y 4/2) silty clay, dark gray interval at 533-534 cm
544 - 569 cm: dark gray (5 Y 4/1) silty clay, strongly mottled; at 553-555 cm olive brown (2.5 Y 4/3) interval; gradational contact at the base
569 - 580 cm: olive brown (2.5 Y 4/3) silty clay; at 575-580 cm light olive brown mottling; very small dropstone (Ø 0.3 cm) at 577 cm
580 - 585 cm: light olive brown (2.5 Y 5/3) silty clay; some mottling and black spots throughout
585-589 cm: light reddish brown (5 YR 6/4), several dropstones (Ø <0.5 to 2 cm)
589 - 600 cm: light olive brown (2.5 Y 5/3) silty clay; some mottling

PS72/343-2 SL Southern Mendeleev Ridge **ARK-XXIII/3**

Recovery: 7.49 m 77° 18.33´ N, 179° 02.70´ E Water depth: 1193 m

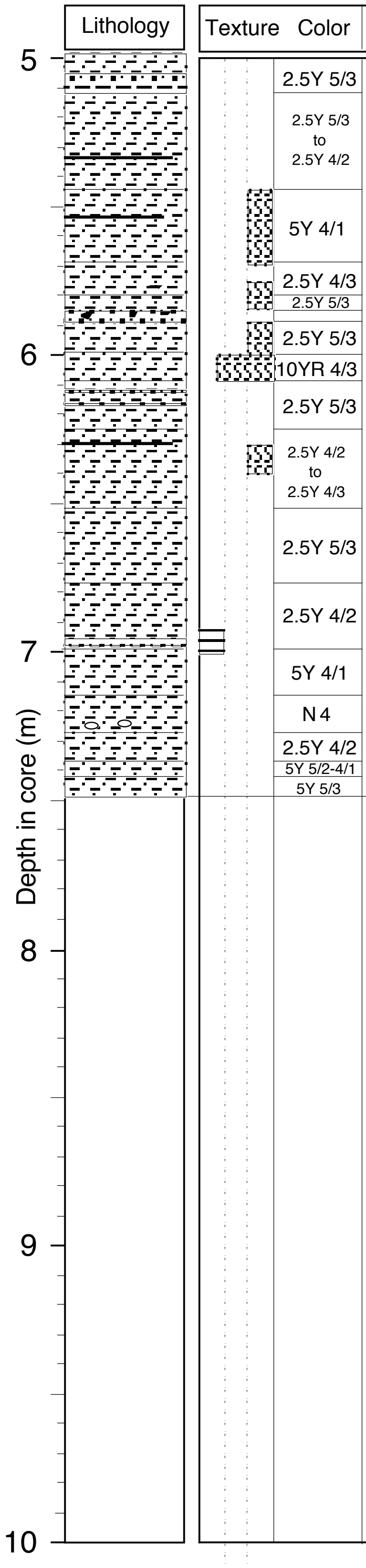

Description

600 - 609 cm: brown (10 YR 4/3) silty clay, strongly mottled (2.5 Y 5/3)
609 - 625 cm: light olive brown (2.5 Y 5/3) silty clay; sandy layers at 612 and 616 cm
625 - 652 cm: dark grayish brown (2.5 Y 4/2) to olive brown (2.5 Y 4/3) silty clay; at 629 cm dark grayish brown (10 YR 4/2), some bioturbation at 630-640 cm
652 - 677 cm: light olive brown (2.5 Y 5/3) silty clay, some black spots throughout
677 - 699 cm: olive gray (5 Y 4/2) silty clay, more sandy horizons at 695-696 and 697-698 cm
699 - 715 cm: dark gray (5 Y 4/1) silty clay
715 - 727 cm: dark gray (N 4) silty clay, small light reddish brown (5 YR 6/4) spots at 723 and 724 cm
727 - 737 cm: dark grayish brown (2.5 Y 4/2) silty clay
737 - 742 cm: olive gray (5 Y 5/2) and dark gray (5 Y 4/1) silty clay
742 - 749 cm: olive (5 Y 5/3) silty clay

PS 72/ 343-3 (GKG) Southern Mendeleev Ridge **ARK- XXIII/3 (Arctic 08)**

Recovery: 39 (40) cm **77°18,34' N 179°2,92' E** **Water depth: 1193 m**

Lithology	Colour	Texture	Description
Surface: dark yellowish brown (10 YR 3/4) sandy mud, water-saturated; valves of Brachiopoda, polychets			

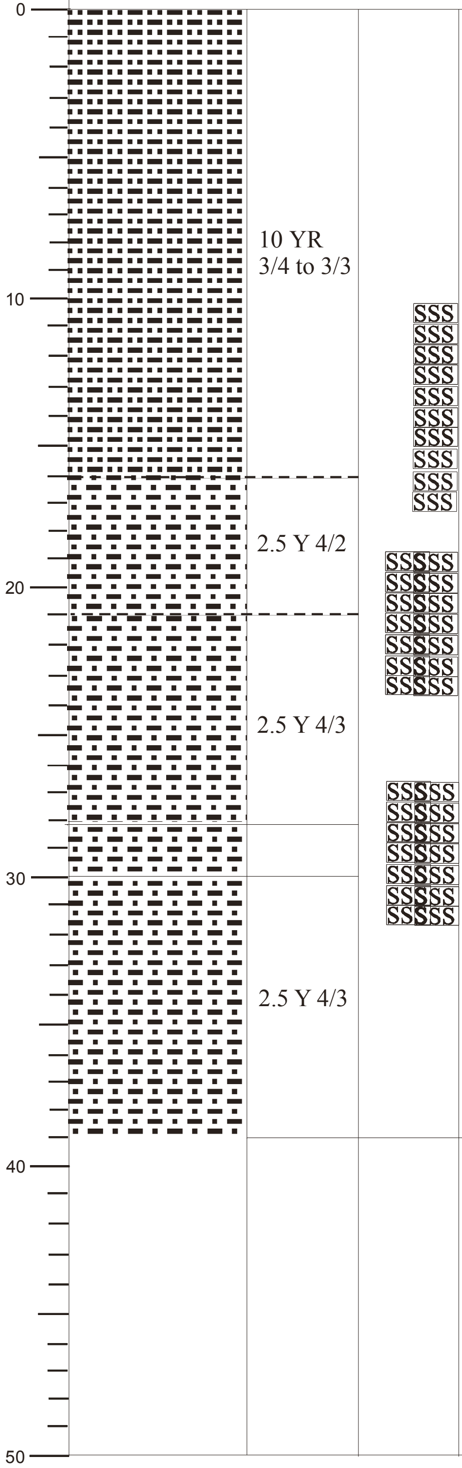

Colour	Description
10 YR 3/4 to 3/3	0-16 cm dark yellowish brown (10 YR 3/4) to dark brown (10 YR 3/3) (sandy) silty clay, fining to the base, slightly bioturbated in the lower part
2.5 Y 4/2	16-21 cm dark grayish brown (2.5 Y 4/2) silty clay, slightly mottled (dark brown 10 YR 3/3)
2.5 Y 4/3	21-28 cm olive brown (2.5 Y 4/3) silty clay, strongly mottled in the upper part (dark brown 10 YR 3/3)
	28-30 cm gray (5 Y 5/1) to grayish brown (2.5 Y 5/2) silty clay, strongly mottled
2.5 Y 4/3	30-39 cm olive brown (2.5 Y 4/3) silty clay, dark grayish brown (2.5 Y 4/2) layer at 33-34 cm 39-40 cm the same (lowermost part not recovered in the box)

PS72/344-3 KAL Southern Mendeleev Ridge **ARK-XXIII/3**

Recovery: 8.2 m 77° 36.49´ N, 174° 32.46´ E Water depth: 1224 m

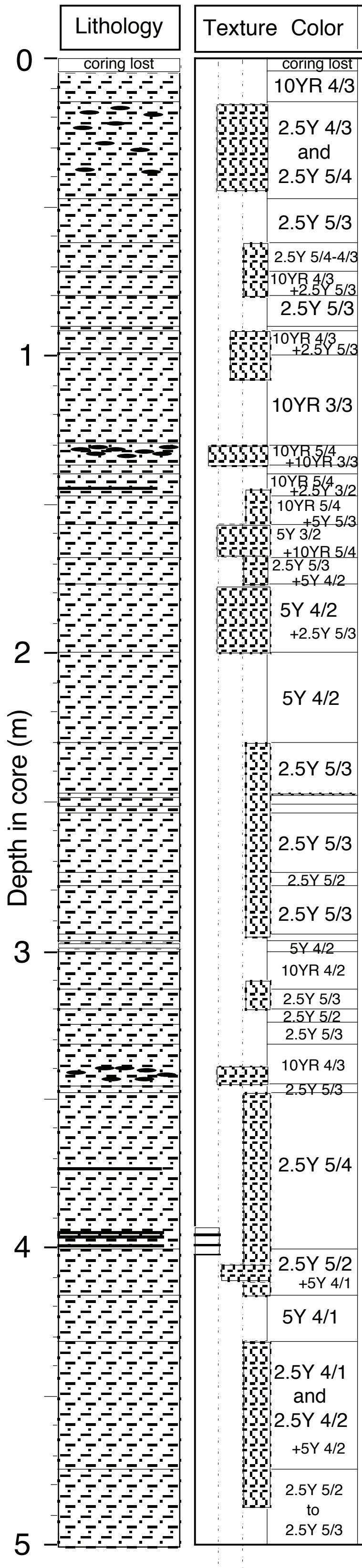

Description

0 - 4 cm: coring lost

4 - 15 cm: brown (10YR 4/3) silty clay (coring disturbance)

15 - 47 cm: olive brown (2.5Y 4/3) and light olive brown (2.5Y 5/4) silty clay, strongly mottled/bioturbated (10YR4/3) (Planolites)

47 - 62 cm: light olive brown (2.5Y 5/3) silty clay

62 - 72 cm: light olive brown (2.5Y 5/4) and olive brown (2.5Y 4/3) silty clay, mottled/bioturbated

72 - 80 cm: brown (10 YR 4/3) and light olive brown (2.5Y 5/3) silty clay, slightly bioturbated

80 - 90 cm: light olive brown (2.5Y 5/3) silty clay

90 - 92 cm: light olive brown (2.5Y 5/4) silty clay

92 - 100 cm: brown (10YR 4/3) and light olive brown (2.5Y 5/3) silty clay, mottled (Chondrites)

100 - 130 cm: dark brown (10YR 3/3) silty clay, 100-108 cm mottled (2.5Y 5/3)/ bioturbated (Planolites and Chondrites)

130 - 137 cm: yellowish brown (10YR 5/4) silty clay, some sand, strongly mottled (10YR3/3)/ bioturbated (Planolites)

137 - 140 cm: yellowish brown (10YR 5/4) silty clay

140 - 147 cm: yellowish brown (10YR 5/4) and very dark grayish brown (2.5Y 3/2); dark layer at 145 cm

147 - 157 cm: yellowish brown (10YR 5/4) silty clay, olive (5Y 5/3) mottling/ bioturbation

157 - 168 cm: olive (5Y 3/2) silty clay, strongly mottled (10YR 5/4)

168 - 177 cm: light olive brown (2.5Y 5/3) silty clay, olive gray (5Y 4/2) mottling

177 - 200 cm: olive gray (5Y 4/2) silty clay, strongly mottled (2.5Y 5/3)/ bioturbated

200 - 230 cm: olive gray (5Y 4/2) silty clay

230 - 295 cm: light olive brown (2.5Y 5/3) silty clay, mottled /bioturbated; grayish brown (2.5Y 5/2) silty clay intervals at 247-248, 251-254, and 274-278 cm

295 - 297 cm: light yellowish brown (2.5Y 6/3) silty clay

297 - 301 cm: olive gray (5Y 4/2) silty clay, some sand; sharp contact at the base

301 - 313 cm: dark grayish brown (10YR 4/2) silty clay, near base mottled /bioturbated

313 - 320 cm: light olive brown (2.5Y 5/3) silty clay; dark grayish brown (10YR 4/2) mottling; some black spots

320 - 324 cm: grayish brown (2.5Y 5/2) silty clay

324 - 332 cm: light olive brown (2.5Y 5/3) and dark grayish brown (2.5Y 4/2) silty clay; some coarser (more silty) layers

332 - 345 cm: brown (10YR 4/3) silty clay, lower part strongly mottled (2.5Y 5/3)/ bioturbated

345 - 348 cm: light olive brown (2.5Y 5/3) silty clay

348 - 401 cm: light olive brown (2.5Y 5/4) silty clay; very dark gray horizon (2.5Y 3/1) at 374-375 cm, directly below some very dark gray mottling/ bioturbation; dark gray horizons at 395, 397, 399 and 400 cm, partly mottled /bioturbated

401 - 416 cm: grayish brown (2.5Y 5/2) silty clay, dark gray (5Y 4/1) mottling/ bioturbation; more silty layer at 411 cm

416 - 432 cm: dark gray (5Y 4/1) silty clay

432 - 475 cm: dark gray (5Y 4/1) and dark grayish brown (2.5Y 4/2) silty clay; olive gray (5Y 4/2) mottling/bioturbation; black spots/lenses at 432 and 464 cm, black horizon at 462-463 cm

475 - 500 cm: grayish brown (2.5Y 5/2) to light olive brown (2.5Y 5/3) (in the lower part) silty clay; upper part mottled/bioturbated

PS72/344-3 KAL Southern Mendeleev Ridge **ARK-XXIII/3**

Recovery: 8.2 m 77° 36.49´ N, 174° 32.46´ E Water depth: 1224 m

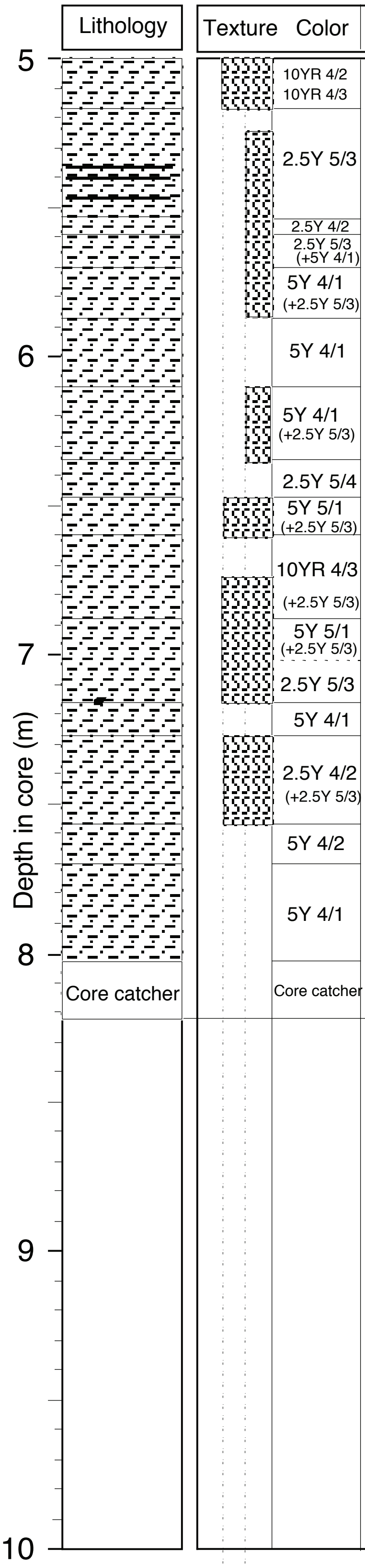

Description

500 - 517 cm: dark grayish brown (10YR 4/2) to brown (10YR 4/3) silty clay, light olive brown mottling (strongly bioturbated)

517 - 554 cm: light olive brown (2.5Y 5/3) silty clay; at 537-540 and 546-548 cm very dark gray/black horizons; some bioturbation

554 - 559 cm: dark grayish brown (2.5Y 4/2) silty clay, mottled bioturbated (2.5Y 5/3)

559 - 570 cm: light olive brown (2.5Y 5/3) silty clay, mottled (5Y 4/1)/ bioturbated, very dark gray layer at 563 cm

570 - 587 cm: dark gray (5Y 4/1) silty clay, light olive brown (2.5Y 5/3) mottling /bioturbation (Chondrites)

587 - 610 cm: dark gray (5Y 4/1) silty clay

610 - 635 cm: dark gray (5Y 4/1) silty clay, light olive brown (2.5Y 5/3) mottling/ bioturbation

635 - 647 cm: light olive brown (2.5Y 5/4) silty clay

647 - 660 cm: gray (5Y 5/1) silty clay, strongly mottled (2.5Y 5/3)/bioturbated, sharp contact at base

660 - 688 cm: brown (10YR 4/3) silty clay, below 674 strongly mottled (light olive brown 2.5Y 5/3)/bioturbated

688 - 716 cm: gray (5Y 5/1) and light olive brown (2.5Y 5/3) silty clay, strongly mottled/bioturbated (below 702 cm light olive brown colours becoming dominant)

716 - 727 cm: dark gray (5Y 4/1) silty clay, single small dropstone (Ø 0.5 cm) at 716 cm

727 - 757 cm: dark grayish brown (2.5Y 4/2) silty clay, strongly mottled (2.5Y 5/3)

757 - 770 cm: olive gray (5Y 4/2) silty clay

770 - 803 cm: dark gray (5Y 4/1) silty clay

803 - 820 Core catcher (not opened yet)

PS72/350-2 (SL) East Siberian Shelf **ARK-XXIII/3**

Recovery: 2.16 m 74° 40.19´ N, 169° 50.30´ E Water depth: 61 m

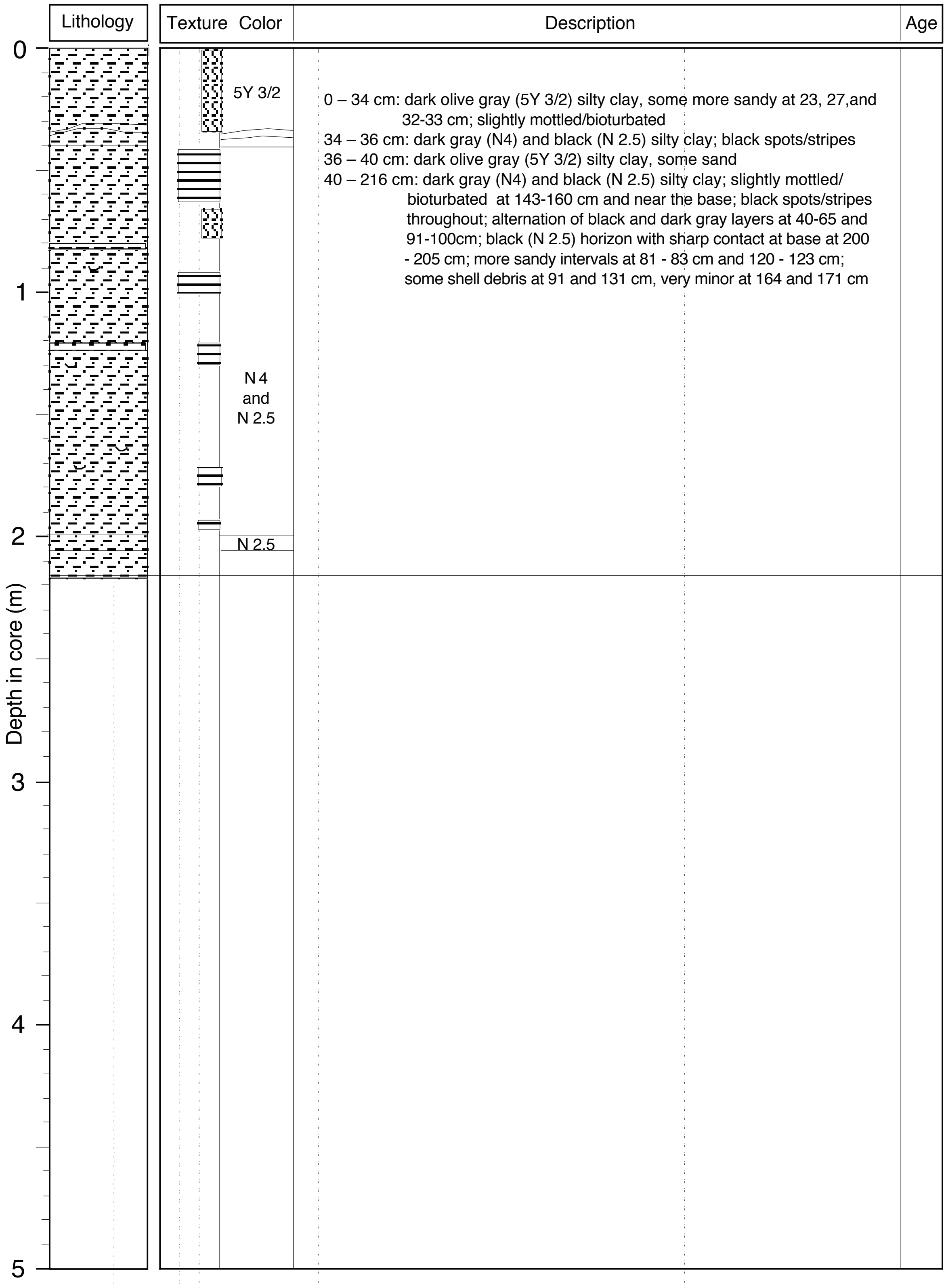

0 – 34 cm: dark olive gray (5Y 3/2) silty clay, some more sandy at 23, 27,and 32-33 cm; slightly mottled/bioturbated

34 – 36 cm: dark gray (N4) and black (N 2.5) silty clay; black spots/stripes

36 – 40 cm: dark olive gray (5Y 3/2) silty clay, some sand

40 – 216 cm: dark gray (N4) and black (N 2.5) silty clay; slightly mottled/ bioturbated at 143-160 cm and near the base; black spots/stripes throughout; alternation of black and dark gray layers at 40-65 and 91-100cm; black (N 2.5) horizon with sharp contact at base at 200 - 205 cm; more sandy intervals at 81 - 83 cm and 120 - 123 cm; some shell debris at 91 and 131 cm, very minor at 164 and 171 cm

PS72/392-5 SL Mendeleev Ridge **ARK-XXIII/3**

Recovery: 6.15 m 80° 27.98´ N, 158° 50.46´ W Water depth: 3582 m

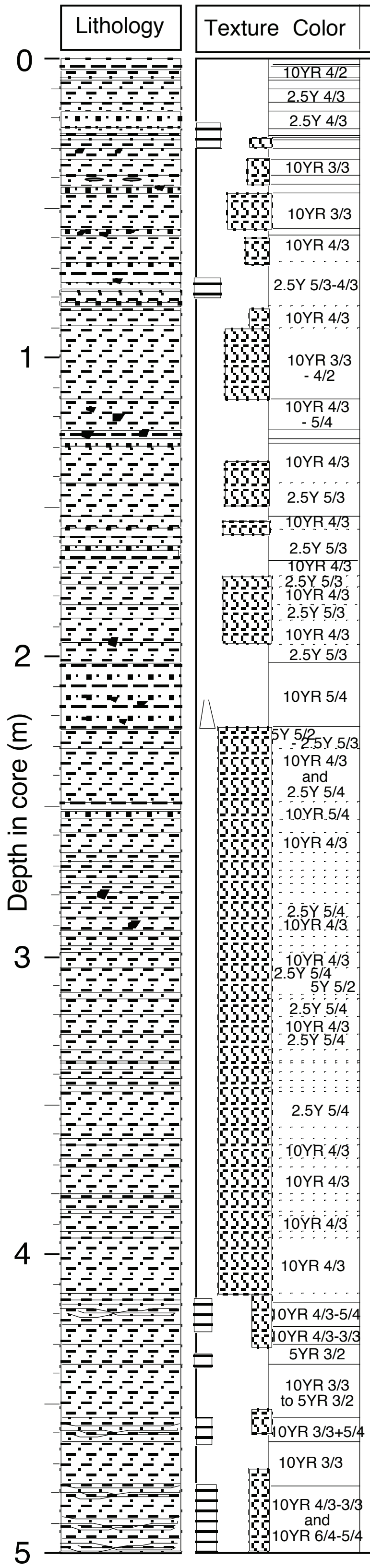

Description

0 – 2 cm: brown (10YR 4/3) (sandy) silty clay

2 – 3 cm: grayish brown (2.5Y 5/2) (sandy) silty clay; some gray mud clasts

3 – 6.5 cm: dark grayish brown (10YR 4/2) silty clay

6.5 – 7.5 cm: very pale brown (10YR 7/ 3) (sandy) silty clay; dropstone (0.5 cm in diameter) at 7.5 cm („white layer")

7.5 – 10 cm: dark brown (10YR 3/3) silty clay; at 9-10 cm yellowish brown mottling

10 – 15 cm: olive brown (2.5Y 4/3) (sandy) silty clay; some lamination; 14.5-15 cm more fine-grained and lighter (2.5Y 5/3)

15 – 18 cm: yellowish brown (10YR 5/4) silty clay; very dark gray lamina at 16 cm

18 – 23.5 cm: olive brown (2.5Y 4/3) sandy silty clay

23.5 – 25.5 cm: olive gray (5Y 472) silty clay, some sand; some yellowish brown mottling

25,5 – 26.5 cm: dark gray (2.5Y 4/1) silty clay; sharp contact at base

26.5 – 27 cm: yellowish brown (10YR 5/6) silty clay; sharp contact at base

27 – 30 cm: dark brown (10YR 3/3) silty clay; gradational contact at base

30 – 34 cm: yellowish brown (10YR 5/4) and dark brown (10YR 3/3) (sandy) silty clay; some lamination; small very pale brown (10YR 7/3) and pinkish clasts; two dropstones (0.5 and 1 cm in diameter) at 31 cm

34 – 39 cm: dark brown (10YR 3/3) silty clay

39 – 42 cm: yellowish brown (10YR 5/4) and dark brown (10YR 3/3) silty clay; strongly motted (Planolites)

42 – 45 cm: light yellowish brown (2.5Y 6/3) (sandy) silty clay; some mud clasts; „white" lense on top, small dropstone (0.5 cm in diameter) at the base; very sharp contact at base

45 – 57 cm: dark brown (10YR 3/3) silty clay; yellowish brown to brown mottling decreasing upward

57 – 59 cm: light yellowish brown (10YR 6/3) and light reddish brown (2.5YR 6/3) („pinkish") sandy silty clay; several dropstones of 0.5 to 1.5 cm in diameter

59 – 68 cm: brown (10YR 4/3) (sandy) silty clay, fining upward; gradational contact at base

68 – 83 cm: light olive brown (2.5Y 5/3) to olive brown (2.5Y 4/3) sandy silty clay, abundant olive and (some) pinkish – especially at 81-82 cm, dark gray clasts; silty clay intervals at 75-76, 78.5-81, and 82-83 cm

83 – 114 cm: brown (10YR 4/3) to dark brown (10YR 3/3) silty clay; bioturbated, light olive brown mottling, especially at 91-92 and 99-102 cm (i.e., more brown/dark brown at 83-91, 92-99, 102-114 cm)

114 – 124 cm: brown (10YR 4/3) and yellowish brown (10YR 5/4) silty clay (some sand in uppermost part); dropstones (0.5-1 cm in diameter) at 117 and 121 cm; some pinkish lenses/clasts at 117 cm; some small Fe-Mn micronodules

124 – 127 cm: light yellowish brown (10YR 6/4) and brown (10YR 4/3) sandy silty clay; small light yellowish brown clasts; dropstones at 125 cm (0.5 cm in diameter) and 126 cm (1 cm in diameter)

127 – 129 cm: light reddish brown (2.5YR 6/3) (sandy) silty clay („pink layer"); sharpcontact at base

129 – 142 cm: brown (10YR 4/3) silty clay; dark brown and light olive brown mottling; Fe-Mn micronodules in upper part

142 – 153 cm: light olive brown (2.5Y 5/3) and olive gray (5Y 5/2) sandy silty clay; fining upward; sharp contact at base

153 – 157 cm: brown (10YR 4/3) silty clay; lower half strongly mottled (light olive brown 2.5Y 5/3); Fe-Mn micronodules in upper brown part

157 – 168 cm: light olive brown (2.5Y 5/4) and yellowish brown (10YR 5/4) sandy silty clay (157-160, 162-164, and 165-168 cm) to silty clay (160-162 and 164-165 cm); olivegray spots/lenses at 164-168 cm, pinkish lenses at 159 cm; sharp contact at base

168 – 196 cm: alternation of brown (10YR 4/3) (168-173, 177-184, and 188-196 cm) and light olive brown (2.5Y 5/3) (173-177 and 184-188 cm) silty clay; strong dark brown andyellowish brown mottling (strongly bioturbated; Chondrites-type); abundant small Fe-Mnmicronodules at 169-181 and 188-193 cm

PS72/392-5 SL Mendeleev Ridge **ARK-XXIII/3**

Recovery: 6.15 m 80° 27.98´ N, 158° 50.46´ W Water depth: 3582 m

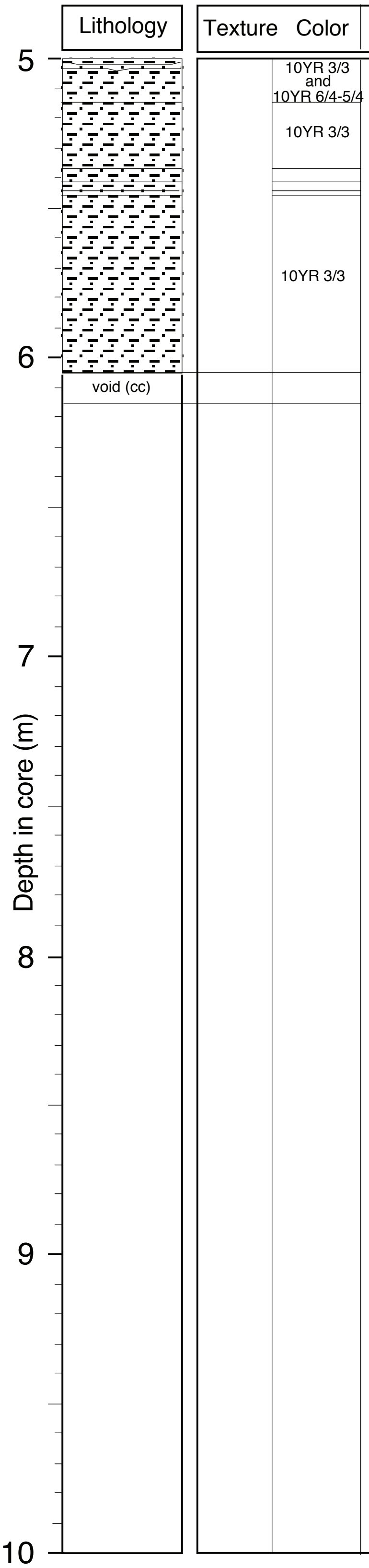

Description

196 – 202 cm: light olive brown (2.5Y 5/3) (sandy) silty clay, abundant dark gray/dark olive gray lenses/clasts; dropstone (2 cm in diameter) at top

202 – 224 cm: yellowish brown (10YR 5/4) sandy silty clay, more sandy in lower part (fining upward); some dark graay, dark olive gray, and pinkish lenses/clasts; several small dropstones (< 0.4 cm) at 208, 209, 213, 215, 216, 221, and 222 cm; Fe-Mn micronodules; sharp contact at base

224 – 231 cm: light olive brown (2.5Y 5/3) and olive gray (5Y 5/2) silty clay; some mottling/bioturbation; gradational contact at base

231 – 249 cm: dark brown (10YR 4/3) and light olive brown (2.5Y 5/4) silty clay; dominantly dark brown at 231-235 and 240-243 cm; strongly bioturbated (Chondrites-type)

249 – 255 cm: yellowish brown (10YR 5/4) and light olive brown (2.5Y 5/4) sandy silty clay (249-251 and 252-255 cm) and silty clay (251-252 cm); Fe-Mn micronodules

255 – 259 cm: light olive brown (2.5Y 5/3) silty clay; some dark brown mottling; Fe-Mn micronodules

259 – 305 cm: alternation of dominantly brown (10YR 4/3) and more light olive brown (2.5Y 5/4) silty clay (brown intervals at 259-266, 269-272, 274-277, 279-283, 287-292, 294-297, and 300-304 cm); strongly mottled/bioturbated (Chondrites-type); Fe-Mn-coated dropstones (1-2 cm in diameter) at 281 and 289 cm; Fe-Mn micronodules; gradational contact at base

305 – 313 cm: light olive brown (2.5Y 5/4) and olive gray (5Y 5/2) silty clay, some sand; strongly mottled; Fe-Mn micronodules

313 – 414 cm: alternation of brown (10YR 4/3) (to dark brown 10YR 3/3) and light olive brown (2.5Y 5/4) silty clay (brown at 313-315, 321-327, 332-335, 336-337, 339-342, 344-346, 358-362, 364-368, 371-380, 382-386, 387-393, 399-414 cm; dark brown at 287-390, 396-399, and 405-408 cm; light olive brown in between); dark brown mottling/strongly bioturbated; Fe-Mn micronodules (more abundant above 367 cm)

414 – 416 cm: brown (10YR 5/3) silty clay

416 – 423 cm: brown (10YR 4/3) and yellowish brown (10YR 5/4) silty clay; at 421-423 cm also pale yellow (2.5Y 7/4) colors; some lamination (check X-Ray) and mottling/bioturbation; some Fe-Mn micronodules

423 – 429 cm: brown (10YR 4/3 to 5/3) silty clay; some mottling/bioturbation; some Fe-Mn micronodules

429 – 435 cm: dark reddish brown (5YR 3/2) silty clay

435 – 455 cm: dark brown (10YR 3/3) to dark reddish brown (5YR 3/2) silty clay; some thin brown (lighter) laminae at 435-438 cm

455 – 462 cm: yellowish brown (10YR 5/4) and dark brown (10YR 3/3) silty clay; moderately mottled/bioturbated; dark brown at 457-459 cm

462 – 474 cm: dark brown (10YR 3/3) silty clay; slightly mottled/bioturbated

474 – 515 cm: dark brown (10YR 3/3) to brown (10YR 4/3) silty clay with intervals of light yellowish brown (10YR 6/4) and yellowish brown (10YR 5/4) laminae/spots (most prominent at 474-476, 478-480, 491-493, 500-501, and 504-505 cm); some bioturbation/mottling; Fe-Mn micronodules throughout

575 – 615 cm: dark brown (10YR 3/3) silty clay, slightly mottled (brown); at 512 cm thin light yellowish brown (10YR 6/4) lamina; at 537-541 and 544-546 cm light yellowishbrown laminae/spots; Fe-Mn micronodules at 515-522 cm

PS 72/ 399-3 (GKG)

Mendeleev Ridge

ARK- XXIII/3 (Arctic 08)

Recovery: 43 cm

80° 38,48’ N 166° 42,99’ W

Water depth: 3375 m

Lithology	Colour	Texture	Description
Surface:			dark brown (10 YR 3/3) sandy mud, very water-saturated; polychets, surface bioturbated
	10 YR 3/3	SSS	0-4,5 cm dark brown (10 YR 3/3) sandy silty clay, gradational contact at the base
	5 Y 4/2	SSS	4,5-7 cm olive gray (5 Y 4/2) silty clay, slightly mottled (dark brown)
	10 YR 6/2		7-8,5 cm light brownish gray (10 YR 6/2) silty clay
			8,5-8,8 cm dark gray (2.5 Y 4/1) sandy silty clay
	5 Y 4/3	SSS	8,8-10 cm olive (5 Y 4/3) silty clay, slightly mottled (gray)
	2.5 Y 4/3		10-12 cm olive brown (2.5 Y 4/3) silty clay, gradational contact at the base
	10 YR 4/3 and 2.5 Y 4/4	SSS	12-15,5 cm brown (10 YR 4/3) to olive brown (2.5 Y 4/4) (sandy) silty clay
	10 YR 4/3	SSS	15,5-17,5 cm brown (10 YR 4/3) (sandy) silty clay, 'white' spots and lenses at the base
		SSS	17,5-18,5 cm 'white' horizon (grayish brown 2.5 Y 5/2 and light yellowish brown 10 YR 6/4 sandy silty clay)
	10 YR 3/3 and 2/2	SSS	19-25 cm dark brown (10 YR 3/3) silty clay to very dark brown (10 YR 2/2) (sandy) silty clay, gradational contact at the base
	2.5 Y 5/4	SSSSS	25-26 cm light olive brown (2.5 Y 5/4) silty clay, strongly mottled (dark brown)
	10 YR 5/3 2.5 Y 4/1	SSS	26-29 cm brown (10 YR 5/3) and dark gray (2.5 Y 4/1) silty clay, slight lumpiness
	2.5 Y 5/2 to 5/4	SSS	29-33 cm grayish brown (2.5 Y 5/2) to light olive brown (2.5 Y 5/4) silty clay, dark brown mottling, very soft, lumpiness
	10 YR 4/4		33-35 cm dark yellowish brown (10 YR 4/4) silty clay, insignificant sandy admixture
	2.5 Y 5/4 and 5 Y 4/1	SSS	35-40 cm light olive brown (2.5 Y 5/4) and dark gray (5 Y 4/1) (mottling) silty clay
	10 YR 4/4		40-41 cm dark yellowish brown (10 YR 4/4) silty clay
	10 YR 3/3 to 3/4		41-43 cm dark brown (10 YR 3/3) to dark yellowish brown (10 YR 3/4) (sandy) silty clay

PS72/393-4 SL Mendeleev Ridge **ARK-XXIII/3**

Recovery: 5.56 m 80° 43.27´ N, 155° 32.81´ W Water depth: 3801 m

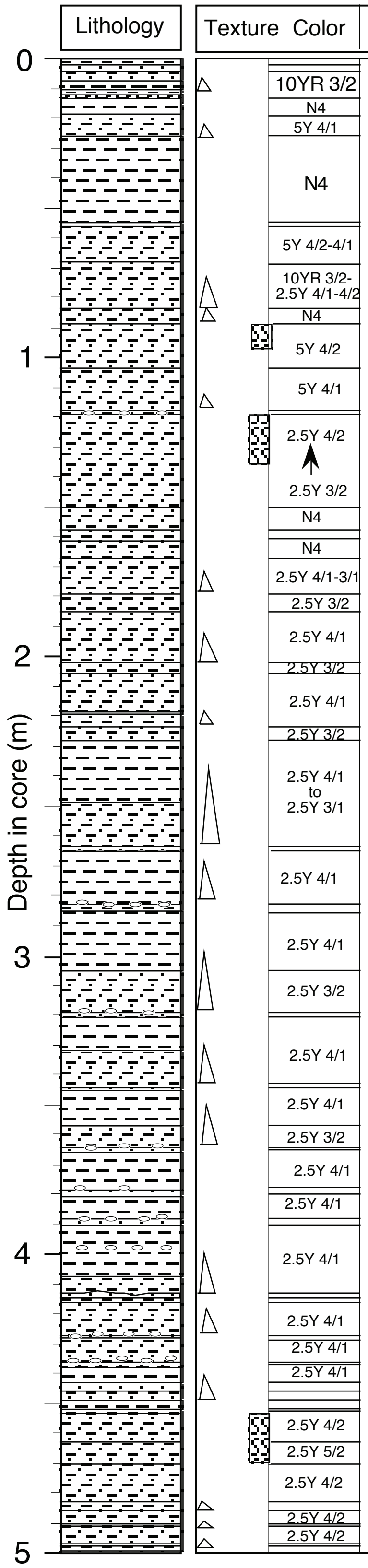

Description

0 – 2 cm: very dark grayish brown (10YR 3/2) (silty) clay
2 – 4 cm: dark gray (N4) clay
4 – 13.5 cm: very dark grayish brown (10YR 3/2) silty clay; more coarsed-grained at 7-10cm (fining upward) and at 12.5-13.5 cm
13.5 – 19 cm: dark gray (N4) clay
19 – 26 cm: dark gray (5Y 4/1) silty clay; sharp contact at base
26 – 55 cm: dark gray (N4) clay
55 – 55.5 cm: gray (N5) silty clay; sharp contact at base
55.5 – 68 cm: olive gray (5Y 4/2) to dark gray (5Y 4/1) silty clay
68 – 83.5 cm: very dark grayish brown (10YR 3/2) to olive brown (2.5Y 4/2) to dark gray (2.5Y 4/1) silty clay; fining upward, sharp contact at base
83.5 – 88.5 cm: dark gray (N4) silty clay; fining upward; gray horizon at base; sharp contact at base
88.5 – 103.5 cm: olive gray (5Y 4/2) clay (97-103.5 cm) to silty clay (88.5-97 cm); slightly mottled in the silty clay interval; small light (very pale brown?) lenses at 97 cm; sharp contact at base
103.5 – 118 cm: dark gray (5Y 4/1) silty clay to clay; fining upward (check by X-ray); sharp contact at base
118 – 119 cm: light olive brown (2.5Y 5/3) silty clay; very small very pale brown (10YR7/3) and pinkish lenses; sharp contact at base
119 – 150 cm: very dark grayish brown (2.5Y 3/2) to dark grayish brown (2.5Y 4/2) (silty) clay; upper part slightly mottled
150 – 167 cm: dark gray (N4) (silty) clay; very dark grayish brown (2.5Y 3/2) interval at 158 – 161 cm
167 – 179 cm: dark gray (2.5Y 4/1) to very dark gray (2.5Y 3/1) silty clay to clay; fining upward; sharp contact at base
179 – 185 cm: very dark grayish brown (2.5Y 3/2) clay
185 – 202 cm: dark gray (2.5Y 4/1) silty clay to clay; fining upward; sharp contact at base
202 – 206 cm: very dark grayish brown (2.5Y 3/2) clay
206 – 223.5 cm: dark gray (2.5Y 4/1) silty clay to clay; fining upward; sharp contact at base; coarser-grained (more silty) layer at 219 cm
223.5 – 228 cm: very dark grayish brown (2.5Y 3/2) clay
228 – 263.5 cm: very dark gray (2.5Y 3/1) to dark gray (2.5Y 4/1) silty clay (below 249 cm) to clay (above 249 cm); sharp contact at base
263.5 – 265 cm: very dark grayish brown (2.5Y 3/2) clay
265 – 443 cm: dark gray (2.5Y 4/1) to very dark grayish brown (2.5Y 3/2) silty clay to clay (fining-upward cycles), intercalated with dark olive brown (2.5Y 3/3) silty clay at 282.5-285, 319-321, 343-344, 364-365, 378-380, 388-389.5, 415-416, 427-428, and 436-437 cm; on top of the dark olive brown horizons (except at 343 cm) at 282.5, 319, 364,380, 388, 413-415, 427, and 435-436 cm as well as at 399 cm light gray (10YR 7/2) to very pale brown (10YR 7/3) sandy silty clay, partly as clasts/lenses
443 – 446 cm: olive gray (5Y 4/2) silty clay
446 – 449 cm: very dark grayish brown (2.5Y 3/2) silty clay
449 – 452.5 cm: dark gray (2.5Y 4/1) clay
452.5 – 453 cm: thin layer of light olive gray (2.5Y 5/3) silty
453 – 463 cm: dark grayish brown (2.5Y 472) silty clay; some mottling
463 – 470 cm: grayish brown (2.5Y 5/2) silty clay; some mottling
470 –556 cm: alternation of dark grayish brown (2.5Y 4/2) silty clay and dark gray (2.5Y 4/1)silty clay to clay (fining upward cycles); dark gray intervals at 483-486, 490-491, 497-498,501-503, 504-505, 508-512, 517-519, 525-528, 532-534, 538-539, 541-547, and 552-554 cm; very pale brown (10YR 7/3) lenses at 545 cm

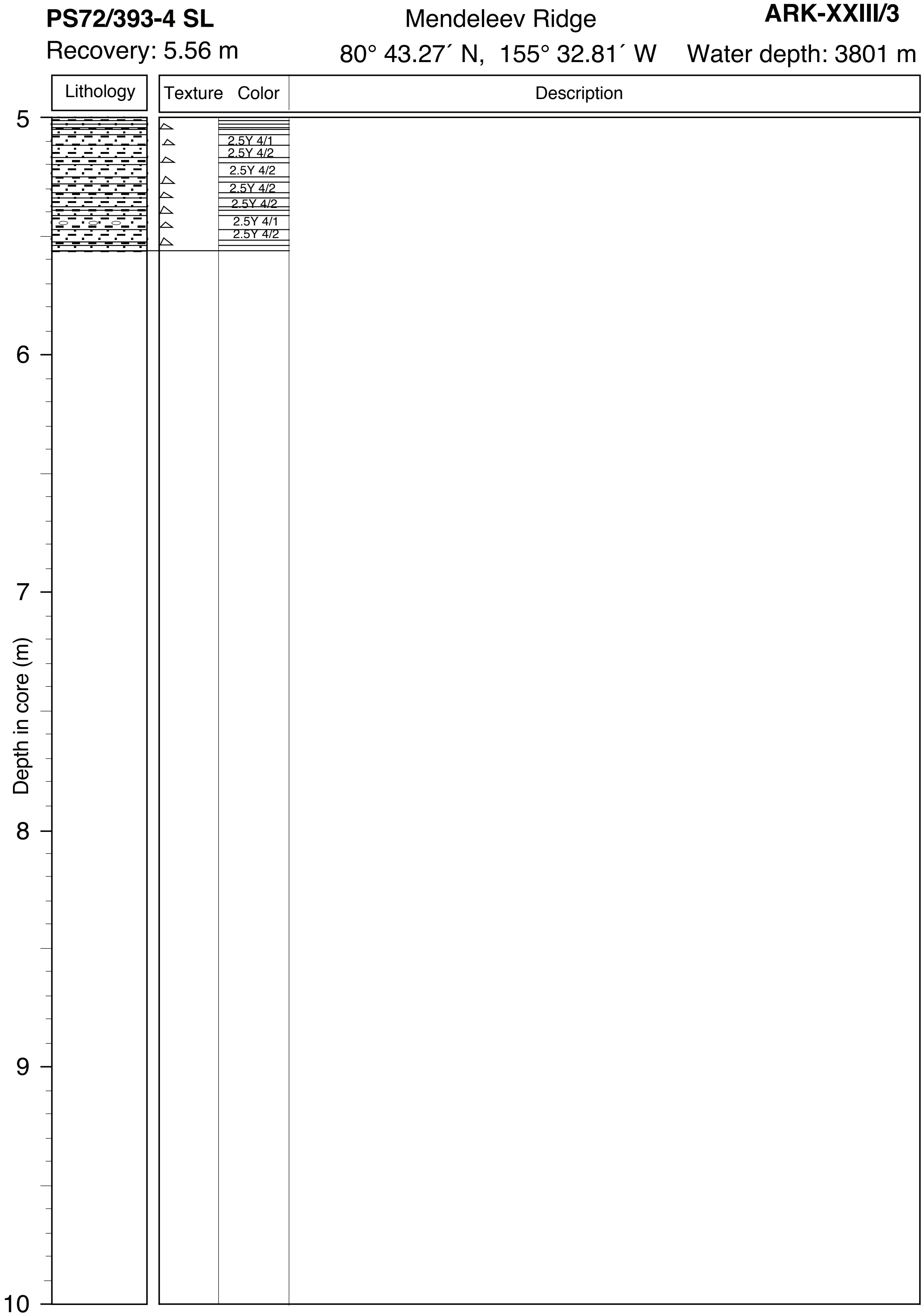
PS72/393-4 SL
Recovery: 5.56 m
Mendeleev Ridge
80° 43.27´ N, 155° 32.81´ W
ARK-XXIII/3
Water depth: 3801 m
Lithology
Texture
Color
Description
2.5Y 4/1
2.5Y 4/2
2.5Y 4/2
2.5Y 4/2
2.5Y 4/2
2.5Y 4/1
2.5Y 4/2
Depth in core (m)
5
6
7
8
9
10

PS72/396-5 KAL Mendeleev Ridge **ARK-XXIII/3**

Recovery: 8.06 m 80° 34.67´ N, 162° 19.15´ W Water depth: 2663 m

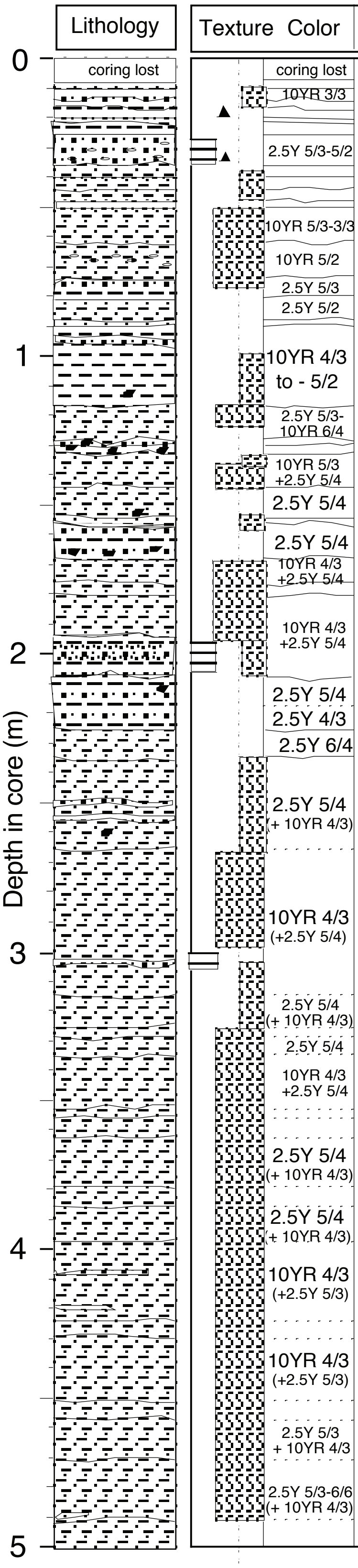

Description

0 – 8 cm: coring lost
8 - 10 cm: brown (10YR 4/3) to grayish brown (10YR 4/2) silty clay; very pale brown (10YR 7/3) horizon at 9 cm ("white layer"?) (Note: 8-10 cm described from logging sub-core)
10 – 14 cm: dark brown (10YR 3/3) (sandy) silty clay
14 – 16 cm: dark brown (10YR 3/3) and light olive brown (2.5Y 5/3) (sandy) silty clay
16 – 20 cm: light olive brown (2.5Y 5/3) to grayish brown (2.5Y 5/2) sandy silty clay; sharp contact at base
20 - 21.5 cm: grayish brown (2.5Y 5/2) (silty) clay
21.5 – 26 cm: light olive brown (2.5Y 5/3) (sandy) silty clay
26 – 36 cm: olive brown (2.5Y 4/3) and light olive brown (2.5Y 5/3) sandy silty clay (++sand); abundant clasts and sand lenses
36 – 40 cm: dark brown (10YR 3/3) to dark grayish brown (10YR 4/2) silty clay; pale yellow (2.5Y 8/3) lense at base
40 – 44 cm: brown (10YR 5/3) to grayish brown (10YR 5/2) silty clay, lower half mottled
44 – 48 cm: dark brown (10YR 3/3) silty clay, mottled
48 – 50 cm: light olive brown (2.5Y 5/3) and dark brown (10YR 3/3) (sandy) silty clay, mottled; abundant small pale yellow (2,5Y 8/3) lenses/clasts
50 – 62 cm: brown (10YR 5/3-5/2) and dark brown (10YR 3/3) silty clay (at 50-55 and 59-61 cm more dark brown), strongly mottled
62 – 74 cm: grayish brown (10YR 5/2) (sandy) silty clay, mottled (2.5Y 5/3); at 63-66 cm pale yellow (2.5Y 8/3) and pink (7.5YR 7/4) lenses; clasts
74 – 81 cm: light olive brown (2.5Y 5/3) sandy silty clay; dark brown mottling (74-79 cm); mud clasts; sharp contact at base
81 – 88 cm: grayish brown (2.5Y 5/2) (sandy) silty clay, some mud clasts
88 – 90 cm: light olive brown (2.5Y 5/3) silty clay
90 – 117 cm: brown (10YR 4/3) to grayish brown (10YR 5/2) silty clay, some sand; light olive brown mottling; more coarse-grained (sandy) at 93-97 cm; dropstone (1 cm in diameter) at 113-114 cm
117 – 128 cm: light olive brown (2.5Y 5/3-5/4) and light yellowish brown (10YR 6/4) siltyclay; small mud clasts
128 – 130 cm: very pale brown (10YR 7/3) sandy silty clay (“white layer”); large drostone (2cm in diameter) at 129 – 130 cm
130 – 133 cm: light reddish brown (2.5YR 6/3) sandy silty clay (“pink layer”); several dropstones of 1-2 cm in diameter (diamict); sharp boundary at base
133 – 144 cm: brown (10YR 5/3) and light olive brown (2.5Y 5/4) silty clay, strongly mottled in lower half; very small dark spots/lenses (Fe-Mn micronodules?); gradational contact at base
144 – 154 cm: light olive brown (2.5Y 5/4) silty clay; dropstone (1 cm in diameter) at base
154 – 156 cm: brown (10YR 4/3) silty clay, strongly mottled
156 – 168 cm: light olive brown (2.5Y 5/4) sandy silty clay; dropstones (0.5, 1, and 3 cm, respectively, in diameter) at 165-167 cm; sharp contact at base
168 – 176 cm: brown (10YR 4/3) and light olive brown (2.5Y 5/4) silty clay, strongly mottled
176 – 180 cm: light olive brown (2.5Y 5/4) silty clay, brown mottling
180 – 194 cm: brown (10YR 4/3) and light olive brown (2.5Y 5/4) silty clay, strongly mottled
194 – 208 cm: brown (10YR 4/3) and light olive brown (2.5Y 5/4) sandy silty clay; more sandy at 194-195, 197-198, and 200-204 cm; abundant mud clasts; layer of very dark gray clasts (Fe-Mn micronodules?) at 207 cm
208 - 225 cm: olive brown (2.5Y 4/3) to light olive brown (2.5Y 5/3) sandy silty clay; dropstone (1 cm in diameter) at 212 cm; sharp contact at base
225 – 236 cm: light yellowish brown (2.5Y 6/4) (silty) clay; at 225-226 some brown (10YR 4/3)
236– 266 cm: light olive brown (2.5Y 5/4) (sandy) silty clay, some brown (10YR 4/3) mottling (at 245-246 cm more brown colour); more sandy at 254-255 cm; small dark lenses/clasts throughout (more abundant at 248-261 cm); Fe-Mn micronodules; dropstone (0.5 cm in diamter) at 260 cm
266 – 308 cm: brown (10YR 5/3) (sandy) silty clay, strongly mottled (light olive brown (2.5Y5/4)); some lamination at 301-308 cm; very small dark clasts/spots (Fe-Mn micronodules); sandy layer at 303-304 cm; dropstone (1 cm in diameter) at 301 cm
308 – 316 cm: brown (10YR 4/3) silty clay with light olive brown (2.5Y 5/3-5/4) mottling, strongly bioturbated
316 – 326 cm: light olive brown (2.5Y 5/3-5/4) silty clay with brown (10YR 4/3) mottling, strongly bioturbated
326 – 329 cm: brown (10YR 4/3) silty clay with light olive brown (2.5Y 5/3-5/4) mottling, strongly bioturbated
329 - 335 cm: light olive brown (2.5Y 5/3-5/4) silty clay with brown (10YR 4/3) mottling, strongly bioturbated
335 - 353 cm: brown (10YR 4/3) silty clay with light olive brown (2.5Y 5/3-5/4) mottling, strongly bioturbated; large dark brown (10YR 4/3) burrows (Planolites) at 336-340 cm
353 - 356 cm: light olive brown (2.5Y 5/3-5/4) silty clay with brown (10YR 4/3) mottling, strongly bioturbated
356 - 363 cm: brown (10YR 4/3) silty clay with light olive brown (2.5Y 5/3-5/4) mottling, strongly bioturbated
363 - 379 cm: light olive brown (2.5Y 5/3-5/4) silty clay with brown (10YR 4/3) mottling, strongly bioturbated; large dark brown (10YR 4/3) burrows (Planolites) at 376 - 380 cm
379 - 386 cm: brown (10YR 4/3) silty clay with light olive brown (2.5Y 5/3-5/4) mottling,strongly bioturbated
386 - 398 cm: light olive brown (2.5Y 5/3-5/4) silty clay with brown (10YR 4/3) mottling,strongly bioturbated
398 - 424 cm: brown (10YR 4/3) silty clay with light olive brown (2.5Y 5/3-5/4) mottling,strongly bioturbated; large dark brown (10YR 4/3) burrows (Planolites) at 398 – 404 cm; small sand lenses at 407-409 and 418-420 cm; very small dark clasts/lenses (Fe-Mn micronodules)
424 – 430 cm: light olive brown (2.5Y 5/3-5/4) silty clay with brown (10YR 4/3) mottling,strongly bioturbated; very small dark clasts/lenses (Fe-Mn micronodules)

PS 72/ 396-3 (GKG)

Mendeleev Ridge

ARK- XXIII/3 (Arctic 08)

Recovery: 39 cm

80° 35,17' N 162° 22,57' W

Water depth: 2663 m

Lithology	Colour	Texture	Description
Surface: dark yellowish brown (10 YR 4/4) sandy mud, very water-saturated; dropstones (Ø up to 15 cm); living organisms: Hydrozoa (?), Worms			
	10 YR 3/3		0-3 cm dark grayish brown (10 YR 3/3 to 3/2) (sandy) silty clay, some light yellowish brown (2.5 Y 6/3) spots
	10 YR 4/2		3-4,5 cm dark grayish brown (10 YR 4/2) silty clay, some light yellowish brown (2.5 Y 6/3) spots
	2.5 Y 5/2		4,5-7 cm grayish brown (2.5 Y 5/2) sandy silty clay, abundant light yellowish brown mud clasts, coarse/fine lamination; sharp base
	10 YR 4/2 to 2.5 Y 4/3		7-12,5 cm grayish brown (10 YR 3/2) to olive brown (2.5 Y 4/3) sandy silty clay to silty clay (fining upwards)
	10 YR 7/3		12,5-14 cm pale yellow (10 YR 7/3) and light olive brown (2.5 Y 5/3) sandy silty clay, abundant pale yellow clasts ('white layer')
	10 YR 3/3		14-21,5 cm dark brown (10 YR 3/3) silty clay, light olive brown (2.5 Y 5/3) mottling in the lower half
	2.5 Y 5/4 to 5/3		21,5-24,5 cm light olive brown (2.5 Y 5/4- 5/3) sandy silty clay, dark brown mottling
	2.5 Y 5/2		24,5-25,5 cm grayish brown (2.5 Y 5/2) (silty) clay, brown mottling
	2.5 Y 5/3		25,5-29 cm light olive brown (2.5 Y 5/3) (sandy) silty clay
	2.5 Y 4/3 to 5/3		29-37 cm olive brown (2.5 Y 4/3) and light olive brown (2.5 Y 5/3) sandy silty clay (a lot of sand), finer/coarser alternations, abundant clasts and sand lenses
	10 YR 3/3		37-39 cm dark brown (10 YR 3/3) to dark grayish brown (10 YR 4/2) silty clay

0 10 20 30 40 50

PS72/396-5 KAL Mendeleev Ridge **ARK-XXIII/3**

Recovery: 8.06 m 80° 34.67´ N, 162° 19.15´ W Water depth: 2663 m

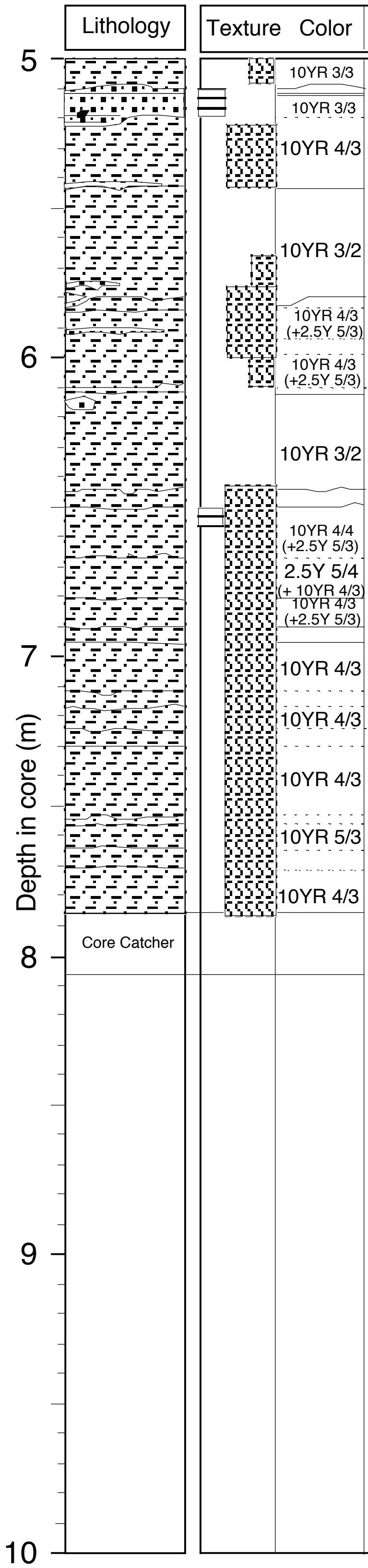

Description

430 - 438 cm: brown (10YR 4/3) silty clay with light olive brown (2.5Y 5/3-5/4) mottling,strongly bioturbated; very small dark clasts/lenses (Fe-Mn micronodules)
438 - 451 cm: light olive brown (2.5Y 5/3-5/4) silty clay with brown (10YR 4/3) mottling,strongly bioturbated; very small dark clasts/lenses (Fe-Mn micronodules)
451 - 457 cm: brown (10YR 4/3) silty clay with light olive brown (2.5Y 5/3-5/4) mottling,strongly bioturbated; very small dark clasts/lenses (Fe-Mn micronodules)
457 - 471 cm: light olive brown (2.5Y 5/3-5/4) silty clay with brown (10YR 4/3) mottling,strongly bioturbated; very small dark clasts/lenses (Fe-Mn micronodules)
471 – 491 cm: olive yellow (2.5Y 6/6) silty clay with dark brown (10YR 3/3) to brown (10YR4/3) mottling, strongly bioturbated; very small dark clasts/lenses (Fe-Mn micronodules)
491 - 511 cm: brown (10YR 4/3) silty clay with light olive brown (2.5Y 5/3-5/4) mottling,strongly bioturbated; sand lenses at 498 and 499 cm; very small dark clasts/lenses (Fe-Mn micronodules)
511 – 513 cm: brown (10YR 5/3) silty clay
513 – 513.5 cm: pale yellow (10YR 7/4) sandy silty clay layer
513.5 – 521 cm: brown (10YR 4/3) sandy silty clay; sandy layers at 520 and 521 cm; light olive brown layers at 518, 519, and 523 cm; dropstone (1 cm in diamter) at 519 cm
521 – 544 cm: brown (10YR 4/3) silty clay, mottled; some sand; light olive brown (2.5Y 5/3) lenses/layers between 535 and 537; sandy layer at 543 cm
544 – 580 cm: very dark grayish borwn (10YR 3/2) silty clay, below 671 cm mottled (10YR 4/3); more sandy between 575 and 582 cm; yellowish brown (10YR 5/4) layer at 575 cm
580 - 585 cm: light olive brown (2.5Y 5/3) silty clay with brown (10YR 4/3) mottling,strongly bioturbated; more sandy between 582 and 584 cm; occasionally Fe-Mn micronodules
585 – 594 cm: brown (10YR 4/3) silty clay with light olive brown (2.5Y 5/3) mottling; sandy layer at at 591-592 cm; occasionally Fe-Mn micronodules
594 - 599 cm: light olive brown (2.5Y 5/3) silty clay with brown (10YR 4/3) mottling,strongly bioturbated; occasionally Fe-Mn micronodules
599 - 610 cm: brown (10YR 4/3) silty clay with light olive brown (2.5Y 5/3) mottling;occasionally Fe-Mn micronodules
610 – 612 cm: brown (10YR 4/3) silty clay
612 – 645 cm: very dark grayish brown (10YR 3/2) silty clay; sand lense at 614-616 cm
645 –651 cm: yellowish brown (10YR 5/6) and light yellowish brown (2.5Y 6/4) silty clay; brown mottling
651 – 668 cm: dark yellowish brown (10YR 4/4) and light olive brown (2.5Y 5/4) silty clay; some lamination at 651-658 cm, below strongly mottled
668 - 680 cm: light olive brown (2.5Y 5/4) to yellowish brown (10YR 5/4) silty clay with brown (10YR 4/3) mottling; occasionally small Fe-Mn micronodules
680 - 691 cm: brown (10YR 4/3) silty clay with light olive brown (2.5Y 5/4) to yellowish brown (10YR 5/4) mottling; occasionally small Fe-Mn micronodules
691 - 696 cm: light olive brown (2.5Y 5/4) to yellowish brown (10YR 5/4) silty clay with brown (10YR 4/3) mottling; occasionally small Fe-Mn micronodules
696 - 712 cm: brown (10YR 4/3) silty clay with light olive brown (2.5Y 5/4) to yellowish brown (10YR 5/4) mottling; occasionally small Fe-Mn micronodules
712 - 717 cm: light olive brown (2.5Y 5/4) to yellowish brown (10YR 5/4) silty clay with brown (10YR 4/3) mottling; occasionally small Fe-Mn micronodules
717 - 725 cm: brown (10YR 4/3) silty clay with light olive brown (2.5Y 5/4) to yellowish brown (10YR 5/4) mottling; occasionally small Fe-Mn micronodules
725 - 730 cm: light olive brown (2.5Y 5/4) to yellowish brown (10YR 5/4) silty clay with brown (10YR 4/3) mottling; occasionally small Fe-Mn micronodules
730 - 754 cm: brown (10YR 4/3) silty clay with light olive brown (2.5Y 5/4) to yellowish brown (10YR 5/4) mottling
754 - 757 cm: light olive brown (2.5Y 5/4) to yellowish brown (10YR 5/4) silty clay with brown (10YR 4/3) mottling
757 - 765 cm: brown (10YR 4/3) silty clay with light olive brown (2.5Y 5/4) to yellowish brown (10YR 5/4) mottling
765 - 772 cm: light olive brown (2.5Y 5/4) to yellowish brown (10YR 5/4) silty clay with brown (10YR 4/3) mottling; occasionally small Fe-Mn nodules
772 - 786 cm: brown (10YR 4/3) silty clay with light olive brown (2.5Y 5/4) to yellowish brown (10YR 5/4) mottling

786 – 806 cm: Core Catcher (tube not opened yet)

PS72/399-4 SL Mendeleev Ridge **ARK-XXIII/3**

Recovery: 5.69 m 80° 39.49´ N, 166° 46.54´ W Water depth: 3305 m

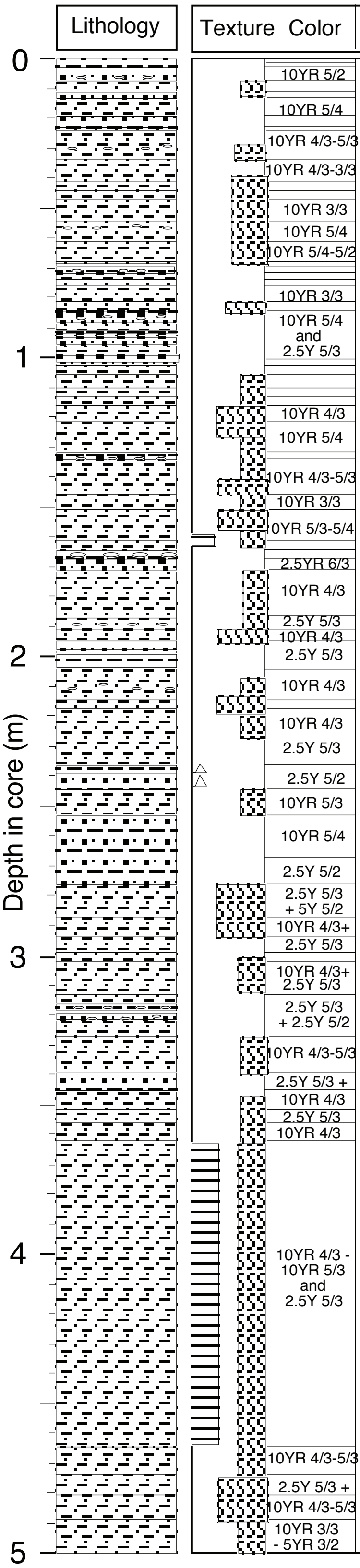

Description

0 – 1 cm: dark brown (10YR 3/3) (sandy) silty clay
1 – 3 cm: olive brown (2.5Y 4/3) (sandy) silty clay
3 – 7.5 cm: grayish brown (10YR 5/2) sandy silty clay; near base more coarse-grained and small very pale brown (10YR 7/3) lenses/spots
7.5 – 11 cm: dark brown (10YR 3/3) silty clay; some mottling near base
11 – 13.5 cm: light olive brown (2.5Y 5/3) sandy silty clay
13.5 – 19 cm: yellowish brown (10YR 5/4) silty clay
19 – 23 cm: light olive brown (2.5Y 5/3) sandy silty clay
23 – 24 cm: yellowish brown (10YR 5/6) silty clay
24 – 31.5 cm: brown (10YR 4/3-5/3) silty clay, some sand; abundant very small very pale brown (10YR 7/3) and light reddish brown (2.5YR 6/3) (“pinkish”) lenses
31.5 – 34 cm: yellowish brown (10YR 5/4) silty clay; mottled (dark brown)
34 – 41 cm: brown (10YR 4/3) to dark brown (10YR 3/3) silty clay; lower part mottled
41 – 44 cm: light olive brown (2.5Y 5/4) silty clay; brown mottling; sharp contact at base
44 – 47 cm: dark grayish brown (10YR 4/2) silty clay; dark brown mottling
47 – 55 cm: dark brown (10YR 3/3) silty clay; yellowish brown mottling
55 – 61 cm: yellowish brown (10YR 5/4) silty clay; large dark brown burrows/ mottling; small light (very pale brown) lenses/clasts
61 – 68 cm: brown (10YR 5/4) to grayish brown (10YR 5/2) silty clay; yellowish brown mottling
68 – 69 cm: dark brown (10YR 3/3) silty clay
69 – 71 cm: very pale brown (10YR 7/3) (top 0.5 cm) and light reddish brown (2.5YR 6/3) (“pinkish”) sandy silty clay; (pinkish) mud clasts (“pink-white layer”)
71 – 74 cm: brown (10YR 4/3) (sandy) silty clay
74 – 77 cm: brown (10YR 5/3) silty clay
77 – 81 cm: dark brown (10YR 3/3) silty clay
81 – 84 cm: yellowish brown (10YR 5/4) and dark brown (10YR 3/3) silty clay; strongly mottled
84 – 101 cm: yellowish brown (10YR 5/4) and light olive brown (2.5Y 5/3) silty clay and sandy silty clay; coarser intervals at 84-88.5 cm (abundant dark gray mud clasts), 90.5, 92-92.5, 93-95, and 99.5-101 cm; sharp contact at base
101 – 103 cm: brown (10YR 5/3) silty clay; mottled
103 – 106 cm: brown (10YR 4/3) silty clay; mottled
106 – 110 cm: brown (10YR 5/3) silty clay; mottled
110 – 113 cm: brown (10YR 4/3) silty clay; mottled
113 – 116 cm: light olive brown (2.5Y 5/3) (sandy) silty clay
116 – 121 cm: brown (10YR 4/3) silty clay
121 – 132 cm: yellowish brown (10YR 5/4) silty clay; above 125 cm strongly mottled (brown)
132 – 134 cm: light olive brown (2.5Y 5/3) (sandy) silty clay; some very pale brown (10YR7/3) lenses/clasts; abundant Fe-Mn micronodules
134 – 146 cm: brown (10YR 4/3-5/3) silty clay; yellowish brown mottling
146 – 151 cm: dark brown (10YR 4/3) silty clay
151 – 161 cm: brown (10YR 5/3) to yellowish brown (10YR 5/4) silty clay; mottled; some lamination
161 – 164 cm: brown (10YR 4/3) silty clay
164 – 167 cm: very pale brown (10YR 7/3) sandy silty clay; large-sized lenses in upper part
167 – 171 cm: light reddiswh brown (2.5YR 6/3) sandy silty clay (“pink layer”); mud clasts; small dropstones at 167-168 cm, large dropstone (3 cm in diameter) at 171 cm; Fe-Mn micronodules; sharp contact at base
171 – 187 cm: brown (10YR 4/3) silty clay; mottled
187 – 191 cm: light olive brown (2.5Y 5/3) silty clay, some sand; gray and pinkish mudclasts; Fe-Mn micronodules; sharp contact at base
191 – 195 cm: brown (10YR 4/3) silty clay; lower part strongly mottled

PS72/399-4 SL Mendeleev Ridge **ARK-XXIII/3**

Recovery: 5.69 m 80° 39.49´ N, 166° 46.54´ W Water depth: 3305 m

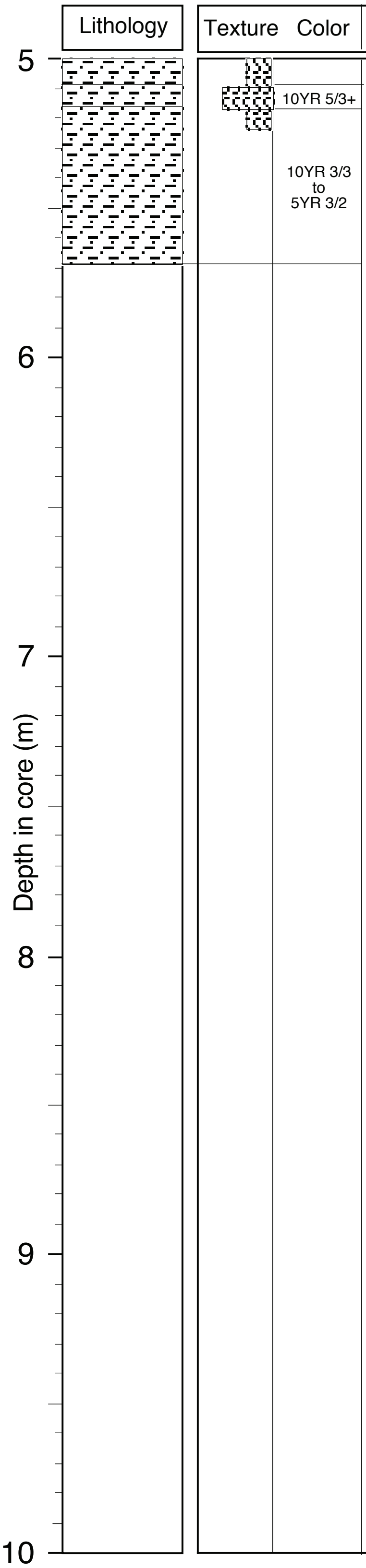

Description

195 – 204 cm: light olive brown (2.5Y 5/3) sandy silty clay; at 198-200 cm silty clay horizon;sharp contact at base

204 – 215 cm: brown (10YR 4/3) silty clay; mottled (below 217 cm strongly mottled); Fe-Mn micronodules

215 – 218 cm: light olive brown (2.5Y 5/3) silty clay; sharp contact at base

218 – 225 cm: brown (10YR 4/3) silty clay; mottled

225 – 236 cm: light olive brown (2.5Y 5/3) silty clay; mottled

236 – 244 cm: two intervals of grayish brown (2.5Y 5/2) sandy silty clay (236-239 and 239-244 cm); fining upward within the intervals; sharp (wavy/erosional?) contact at base

244 – 253 cm: brown (10YR 5/3) sandy silty clay (lower part) to silty clay; yellowish brown silty clay horizon at 248 cm

253 – 276 cm: yellowish brown (10YR 5/4) (253-270.5 cm) and grayish brown (2.5Y 5/2) (270.5-276 cm) sandy silty clay; Fe-Mn micronodules (abundant below 270 cm)

276 – 287 cm: light olive brown (2.5Y 5/3) and olive gray (5Y 5/2) silty clay; strongly mottled

287 – 294 cm: brown (10YR 4/3) and light olive brown (2.5Y 5/3) silty clay; strongly mottled; layer of brown clasts at 291 cm

294 – 299 cm: light olive brown (2.5Y 5/3) sandy silty clay; sharp contact at base

299 – 302 cm: brown (10YR 4/3) silty clay

302 – 313 cm: brown (10YR 4/3) and light olive brown (2.5Y 5/3) silty clay; strongly mottled

313 – 327 cm: light olive brown (2.5Y 5/3) and grayish brown (2.5Y 5/2) sandy silty clay and silty clay; more coarse-grained intervals with abundant mud clasts at 315.5-318 and 319-320.5 cm; sharp contact at base

327 – 339 cm: brown (10YR 4/3-5/3) silty clay; mottled

339 – 345 cm: brown (10YR 4/3) and light olive brown (2.5Y 5/3) (sandy) silty clay; abundant Fe-Mn micronodules

345 – 352 cm: brown (10YR 4/3) silty clay; mottled

352 – 356 cm: light olive brown (2.5Y 5/3) silty clay; abundant Fe-Mn micronodules

356 – 362 cm: brown (10YR 4/3) silty clay; some light olive brown mottling

362 – 368 cm: light olive brown (2.5Y 5/3) and brown (10YR 4/3) silty clay; mottled

368 – 464 cm: alternation of brown (10YR 4/3-5/3) and light olive brown (2.5Y 5/3) silty clay; mottled; more sandy at 396-400 and 425-437 cm; Fe-Mn micronodules throughout,especially enriched at about 367-390, 404-408, 415-425, and 455-468 cm

464 – 474 cm: brown (10YR 4/3-5/3) silty clay; mottled

474 – 481 cm: light olive brown (2.5Y 5/3) to yellowish brown (10YR 5/4) silty clay; strongly mottled; sharp contact at base

481 – 489 cm: brown (10YR 4/3-5/3) silty clay; strongly mottled (yellowish brown); Fe-Mn micronodules; sharp contact at base

489 – 509 cm: dark brown (10YR 3/3) to dark reddish brown (5YR 3/2) silty clay; mottled; Fe-Mn micronodules

509 – 517 cm: dark brown (10YR 3/3) and brown (10YR 5/3) silty clay; strongly mottled; Fe-Mn micronodules

517 – 569 cm: dark brown (10YR 3/3) to dark reddish brown (5YR 3/2) silty clay; at 560-568cm mottled (brown 10YR 5/3)

PS 72/ 404-3 (GKG)

Mendeleev Ridge

ARK- XXIII/3 (Arctic 08)

Recovery: 37 cm

80° 45,39' N 171° 9,69' W

Water depth: 2182 m

Lithology	Colour	Texture	Description
Surface: brown sandy mud, water-saturated, dropstones (Ø up to 2 cm); living orgamisms: Brachiopoda (valves), Foraminifera; polychets			
	10 YR 3/3		0-1,5 cm dark brown (10 YR 3/3) sandy silty clay
	10 YR 4/4		1,5-4 cm dark yellowish brown (10 YR 4/4) and very dark grayish brown (10 YR 3/2) (mottling) (sandy) silty clay
	10 YR 3/2		4-5 cm very dark grayish brown (10 YR 3/2) and dark grayish brown (2.5 Y 4/2) (mottling) (sandy) silty clay
	2.5 Y 4/3		5-6,5 cm olive brown (2.5 Y 4/3) silty clay, very dark grayish brown (10 YR 3/2) and dark grayish brown (2.5 Y 4/2) mottling
	10 YR 4/2		6,5-13 cm dark grayish brown (2.5 Y 4/2) silty clay, fining upwards, olive brown (2.5 Y 4/4) mottling at 8,5-10 cm; some 'white' spots at 11-13 cm
	10 YR 2/2 and 3/2		13-16,5 cm very dark brown (10 YR 2/2) and very dark grayish brown (10 YR 3/2) sandy silty clay, dark gray (5 Y 4/1) and dark grayish brown mottling
	5 Y 5/2 and 5 Y 5/4		16,5-30,5 cm olive gray (5 Y 5/2) and olive (5 Y 5/4) silty clay, fining upwards, dark brown (10 YR 3/3) and very dark brown (10 YR 2/2) mottling (strongly up to 25 cm); some lumpiness
	10 YR 3/3		30,5-33,5 cm dark brown (10 YR 3/3) sandy silty clay, strongly mottled (very dark brown 10 YR 2/2)
	10 YR 3/3 and 2.5 Y 4/4		33,5-37,5 cm dark brown (10 YR 3/3) and olive brown (2.5 Y 4/4) sandy silty clay, some light olive brown (2.5 Y 5/3) and 'white' spots up to 35 cm, 1 'pinkish' spot at 35 cm

PS72/404-4 SL Mendeleev Ridge **ARK-XXIII/3**

Recovery: 5.62 m 80° 45.24´ N, 171° 09.69´ W Water depth: 2131 m

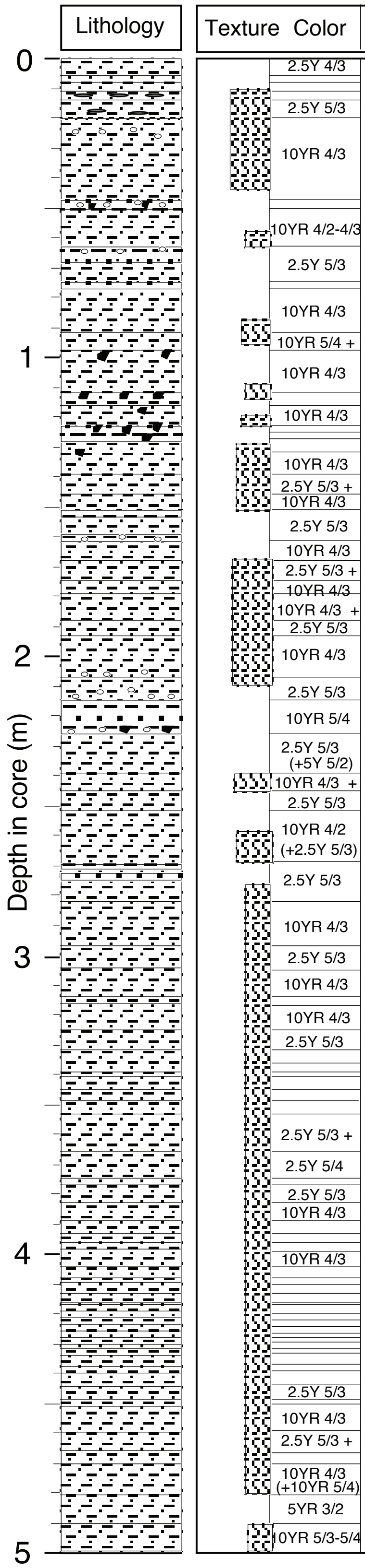

Description

0 – 6 cm: olive brown (2.5Y 4/3) silty clay; dropstone (1.5 cm in diameter) at 6 cm; sharp contact at base
6 - 8 cm: dark brown (10YR 3/3) silty clay
8 – 11 cm: light olive brown (2.5Y 5/3) silty clay; dropstone (1 cm in diameter) at 10 cm
11 – 14 cm: light olive brown (2.5Y 5/3) and dark brown (10YR 3/3) silty clay; strongly mottled
14 – 20 cm: light olive brown (2.5Y 5/3) (sandy) silty clay; large dark brown burrow at 18 cm
20 – 47 cm: dominantly brown (10YR 4/3) to dark brown (10YR 3/3) silty clay (dark brown below 42 cm); strongly mottled (2.5Y 5/3); very pale brown (10YR 7/3) and pinkish lenses/clasts at 24-26 cm; sharp contact at base
47 – 50 cm: very pale brown (10YR 7/3) (sandy) silty clay; light clasts; some small dropstones; few pinkish speckles at base („pink-white layer")
50 – 63 cm: dark grayish brown (10YR 4/2) to brown (10YR 4/3) silty clay; light olive brown (2.5Y 5/3) mottling, more intensive at 55-61 cm
63 – 75 cm: light olive brown (2.5Y 5/3) sandy silty clay (63-65 and 66.5-68 cm) and silty clay (65-66.5 and 68-75 cm); dark gray mud clasts in upper sandy interval
75 – 77 cm: (light) olive brown (2.5Y 4/3) silty clay, some sand; sharp contact at base
77 – 92 cm: brown (10YR 4/3) silty clay; lower half mottled
92 – 98 cm: yellowish brown (10YR 5/4) and brown (10YR 4/3) silty clay; mottled; dark gray and pinkish clasts at 92-93 cm; Fe-Mn micronodules; sharp contact at base
98 – 112 cm: brown (10YR 4/3) silty clay; lower part mottled; large dropstone (2.5 cm in diameter) at 98-100 cm, small dropstone at 100 cm; Fe-Mn micronodules
112 – 116 cm: yellowish brown (10YR 5/4) silty clay; several dropstones (0.5-1 cm in diameter) at 112-113 cm
116 – 123 cm: brown (10YR 4/3) and yellowish brown (10YR 5/4) silty clay; small dropstone at 118 cm
123 – 125 cm: very pale brown (10YR 7/3) (sandy) silty clay; several dropstones (0.5-1.5cm in diameter); some brown mottling („white layer")
125 – 128 cm: light reddish brown (2.5YR 6/3) (sandy) silty clay; dropstone (1 cm in diameter) at 127 cm; sharp contact at base („pink layer")
128 – 139 cm: brown (10YR 5/3-4/3) silty clay, below 132 more 10YR 4/3; light olive brown (2.5Y 5/3) mottling; dropstone at 132 cm; Fe-Mn micronodules
139 – 146 cm: light olive brown (2.5Y 5/3) silty clay; brown mottling; Fe-Mn micronodules; sharp contact at base
146 – 151 cm: brown (10YR 4/3) silty clay; light olive brown mottling increasing downwards
151 – 161 cm: light olive brown (2.5Y 5/3) sandy silty clay (151.5-153, 157, and 159-161cm) and silty clay; dark gray mud clasts in lower part; Fe-Mn micronodules; sharp contactat base
161 – 168 cm: brown (10YR 4/3) silty clay
168 – 175 cm: light olive brown (2.5Y 5/3) and brown (10YR 4/3) silty clay; strongly mottled
175 – 179 cm: brown (10YR 4/3) silty clay
179 – 188 cm: brown (10YR 4/3) and light olive brown (2.5Y 5/3) silty clay; mottled
188 – 193 cm: light olive brown (2.5Y 5/3) silty clay
193 – 207 cm: light olive brown (2.5Y 5/3) and brown (10YR 4/3) silty clay; strongly mottled; dark mud clasts at 206-207 cm; Fe-Mn micronodules
207 – 215 cm: light olive bhrown (2.5Y 5/3) silty clay; common dark gray mud clasts; Fe-Mn micronodules
215 – 226 cm: yellowish brown (10YR 5/4) sandy silty clay; some dark gray mud clasts and dropstones at 224-226 cm; Fe-Mn micronodules
226 – 239 cm: light olive brown (2.5Y 5/3) silty clay; some olive gray (5Y 5/2) and brown(10YR 4/3) mottling; Fe-Mn micronodules

PS72/404-4 SL Mendeleev Ridge **ARK-XXIII/3**

Recovery: 5.62 m 80° 45.24´ N, 171° 09.69´ W Water depth: 2131 m

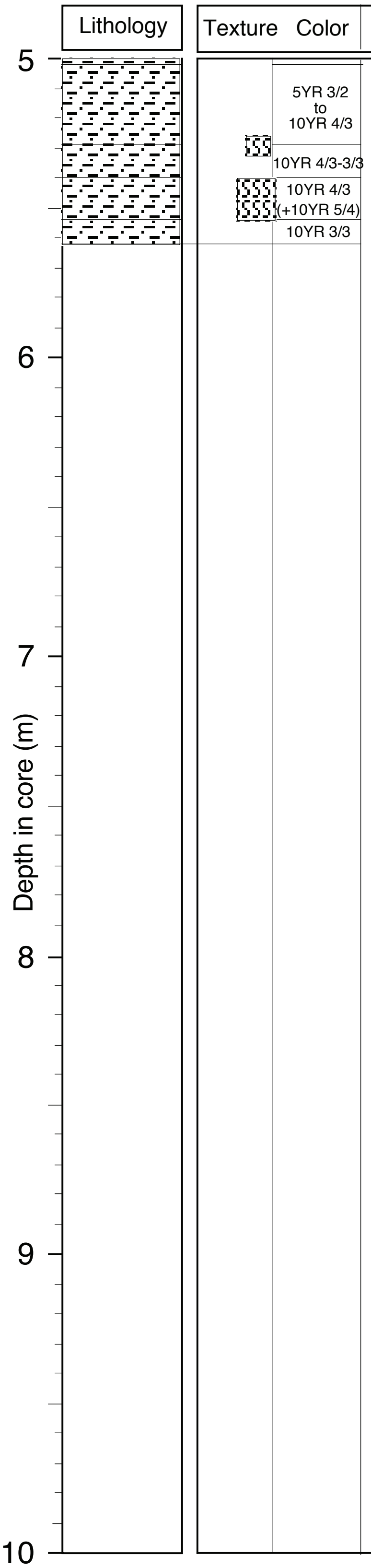

Description

239 – 245 cm: brown (10YR 4/3) and light olive brown (2.5Y 5/3) silty clay; strongly mottled; Fe-Mn micronodules
245 – 252 cm: light olive brown (2.5Y 5/3) silty clay
252 – 269 cm: dark grayish brown (10YR 4/2) to brown (10YR 5/3) and light olive brown (2.5Y 5/3) silty clay; strongly mottled; Fe-Mn micronodules
269 – 282 cm: light olive brown 82.5Y 5/3) silty clay; sandy silty clay at 269-270 and 272.5-274 cm; common mud clasts at 272.5-274 cm
282 – 366 cm: alternation of brown (10YR 4/3) silty clay with light olive brown (2.5Y5/3) mottling and light olive brown (2.5Y 5/3) silty clay with brown mottling; dominantly brown intervals at 282-297, 305-314, 317-325, 332-336, 339-340.5, 341-343, 345-348,and 349-353 cm; Fe-Mn micronodules throughout
366 – 375 cm: light olive brown (2.5Y 5/4) silty clay
375 – 466 cm: alternation of brown (10YR 4/3) silty clay with olive brown mottling and light olive brown (2.5Y 5/3) silty clay with brown mottling; dominantly brown intervals at 375-377, 383-389, 393-396, 399-404, (408-410), 413-416, 417-420, 422-424, 426-428,430-432, 434-437, 440-444, 449-451 (10YR 3/3), and 451-460 cm; Fe-Mn micronodules between 370 and 426 cm
466 – 470 cm: light olive brown (2.5Y 5/3) silty clay
470 – 481 cm: brown (10YR 4/3) and yellowish brown (10YR 5/4) silty clay; mottled; Fe-Mn micronodules
481 – 490 cm: dark reddish brown (5YR 3/2) silty clay
490 – 502 cm: dark brown (10YR 3/3), brown (10YR 5/3) and yellowish brown (10YR5/4) silty clay; mottled; Fe-Mn micronodules
502 – 529 cm: dark reddish brown (5YR 3/2) to dark brown (10YR 3/3) silty clay; Fe-Mn micronodules between 515-525 cm
529 – 540 cm: dark brown (10YR 3/3) to brown (10YR 4/3) silty clay; near top some bioturbation (10YR 5/4)
540 – 554 cm: brown (10YR 4/3) and yellowish brown (10YR 5/4) silty clay; strong mottling, increasing downward (below 547 cm yellowish brown colour dominant); Fe-Mnmicronodules
554 – 562 cm: dark brown (10YR 3/3) silty clay

PS 72/ 408-3 (GKG)

Mendeleev Ridge

ARK- XXIII/3 (Arctic 08)

Recovery: 42 cm

80° 32,92' N   174° 40,17' W

Water depth: 2576 m

Lithology	Colour	Texture	Description
Surface:			brown mud, water-saturated, insignificant sandy admixture; rather soft; some dropstones (Ø up to 4 cm); valves of Brachiopoda, Bivalvia; polychets, surface bioturbated, traces of worms
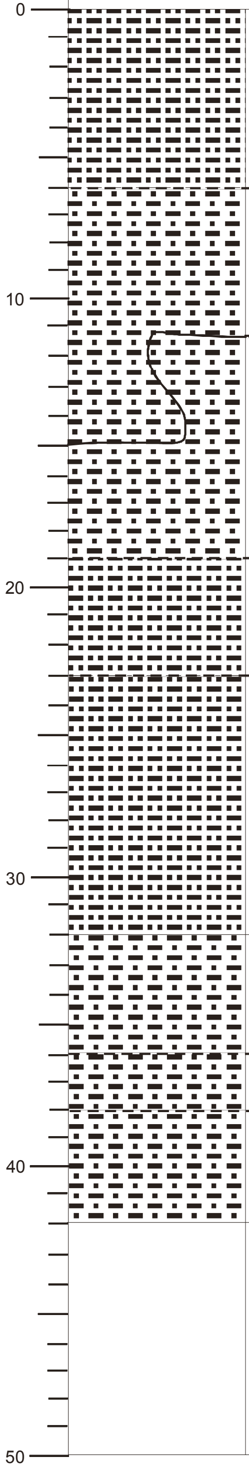	10 YR 3/3		0-6 cm dark brown (10 YR 3/3) sandy silty clay
	5 Y 4/2 and 4/3		6-15 cm olive gray (5 Y 5/2) and olive (5 Y 4/3) silty clay, dark brown mottling, some light olive gray (5 Y 6/2) spots at 8-9 cm (and 'pinkish' spots)
	2.5 Y 4/3		15-19 cm olive brown (2.5 Y 4/3) silty clay, slightly mottled (olive 5 Y 5/4)
	2.5 Y 4/3 and 10 YR 3/3		19-23 cm olive brown (2.5 Y 4/3) to dark brown (10 YR 3/3) (mottling) sandy silty clay, a lot of small 'white' and 'pinkish' spots
	10 YR 3/4		23-32 cm dark yellowish brown (10 YR 3/4) (sandy) silty clay; dark brown (10 YR 3/3) mottling at 23-25 cm, 29-32 cm
	2.5 Y 4/4 and 5 Y 3/2		32-36 cm olive brown (2.5 Y 4/4) and dark olive gray (5 Y 3/2) (lumpiness) silty clay, dark brown mottling at 32-34 cm, very soft
	2.5 Y 4/3 to 5/3		36-38 cm olive brown (2.5 Y 4/3) to light olive brown (2.5 Y 5/3) silty clay, dark brown mottling, very soft
	2.5 Y 4/4 to 5/3		38-42 cm olive brown (2.5 Y 4/4) to light olive brown (2.5 Y

PS72/408-5 SL Mendeleev Ridge **ARK-XXIII/3**

Recovery: 6.33 m 80° 33.20´ N, 174° 42.31´ W Water depth: 2535 m

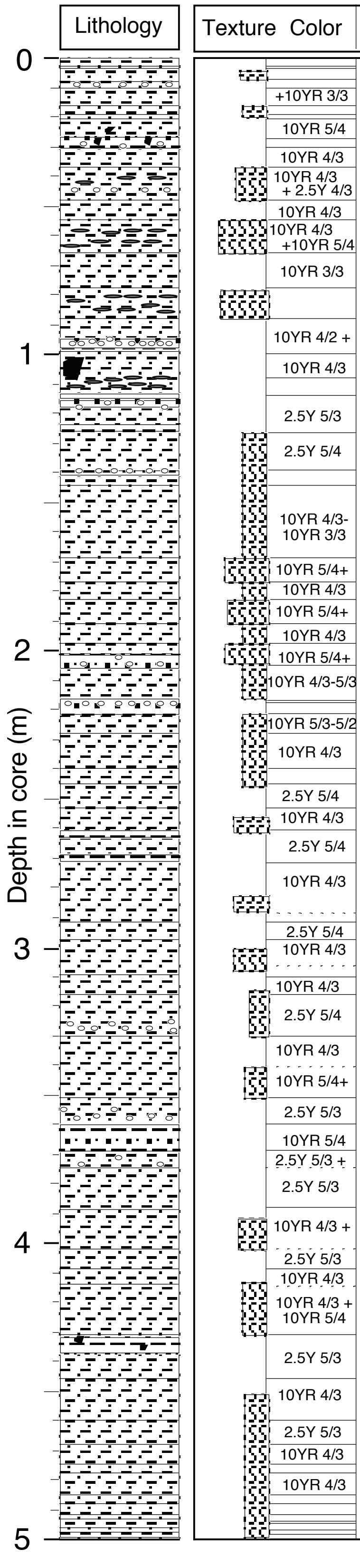

Description

0 – 2.5 cm: dark brown (10YR 3/3) (sandy) silty clay
2.5 - 3 cm: grayish brown (2.5Y 5/2) silty clay
3 – 7.5 cm: olive brown (2.5Y 4/3) silty clay
7.5 - 10 cm: brown (10YR 4/3-5/3) silty clay; sharp contact at base; horizon of very pale brown (10YR 7/3) lenses („white layer“)
10 - 16 cm: dark brown (10YR 3/3) silty clay
16 - 19 cm: dark brown (10YR 3/3) and light olive brown (2.5Y 5/3) silty clay; strongly mottled
19 – 20.5 cm: light olive brown (2.5Y 5/3) sandy silty clay
20.5 – 27 cm: yellowish brown (10YR 5/4) silty clay; some mottling; dropstone (1 cm in diameter) at 24 cm
27 – 30 cm: light olive brown (2.5Y 5/3) sandy silty clay; common mud clasts; dropstone (0.5 cm in diameter) at 28 cm
30 – 37 cm: brown (10YR 4/3) silty clay
37 – 48 cm: brown (10YR 4/3) and olive brown (2.5Y 4/3) to olive brown (2.5Y 4/3) silty clay; strongly mottled at 37-42 cm; very pale brown (10YR 7/3) and light reddish brown(2.5YR 6/3) („pinkish“) lenses/clasts
48 – 55 cm: brown (10YR 4/3) silty clay
55 – 66 cm: brown (10YR 4/3) and yellowish brown (10YR 5/4) silty clay; strongly mottled
66 – 78 cm: dark brown (10YR 3/3) silty clay; yellowish brown mottling at 66-69 cm
78 – 88 cm: dark brown (10YR 3/3) and yellowish brown (10YR 5/4) silty clay; strongly mottled (dark brown Planolites-type burrows)
88 – 100 cm: dark grayish brown (10YR 4/2) silty clay; abundant light reddish brown (2.5YR 6/3) lenses/clasts („pink layer“)
100 – 108 cm: brown (10YR 4/3) silty clay; large dropstone (6 cm in diameter) at 101-107cm
108 – 114 cm: brown (10YR 4/3) and light olive bhrown (2.5Y 5/3) silty clay; strongly mottled
114 – 126.5 cm: light olive brown (2.5Y 5/3) and brown (10YR 4/3) to light olive brown (2.5Y 5/3) sandy silty clay and silty clay; mottled at 114-118 cm; more sandy intervals at 114-115, 116-118, 119.5, 123, and 124.5-126 cm; common occurrence of dark gray mudclasts (more abundant between 114 and 118 cm); sharp contact at base
126.5 – 139 cm: light olive brown (2.5Y 5/3) (silty) clay; abundant dark gray mud clasts at138-139 cm; sharp contact at base
139 – 141 cm: olive brown (2.5Y 4/3) sandy silty clay
141 – 144 cm: olive brown (2.5Y 4/3) silty clay
144 – 169 cm: brown (10YR 4/3) to dark brown (10YR 3/3) silty clay; mottled; very small very pale brown (10YR 7/3) lenses at 155-156 cm; Fe-Mn micronodules
169 – 177 cm: brown (10YR 5/3) to yellowish brown (10YR 5/4) silty clay; some sand; mottled; Fe-Mn micronodules; sharp contact at base
177 – 183 cm: brown (10YR 4/3) silty clay; some yellowish brown mottling
183 – 191 cm: brown (10YR 5/3) to yellowish brown (10YR 5/4) silty clay; strongly mottled; some more sandy at 190 cm
191 – 198 cm: brown (10YR 4/3) to dark brown (10YR 3/3) silty clay; some mottling
198 – 205 cm: brown (10YR 5/3) to yellowish brown (10YR 5/4) silty clay to sandy silty clay (upper part more sandy and light, pinkish, and dark gray mud clasts)
205 – 217 cm: brown (10YR 4/3-5/3) silty clay; some mottling
217 – 218 cm: very pale brown (10YR 7/3) and light yellowish brown (10YR 6/4) silty clay; light clasts („white layer“)
218 – 221 cm: light reddish brown (2.5YR 6/3) (sandy) silty clay („pink layer“)
221 – 228 cm: brown (10YR 5/3) to grayish brown (10YR 5/2) silty clay; mottled
228 – 245 cm: brown (10YR 4/3) silty clay; strongly mottled (2.,5Y 5/4) at 240-245 cm; Fe-Mn micronodules
245 – 253 cm: light olive brown (2.5Y 5/4) silty clay; some more sandy below 250 cm; sharp contact at base
253 – 262 cm: brown (10YR 4/3) silty clay; strongly mottled (2.5Y 5/4) at 258-262 cm

PS72/408-5 SL Mendeleev Ridge **ARK-XXIII/3**

Recovery: 6.33 m 80° 33.20´ N, 174° 42.31´ W Water depth: 2535 m

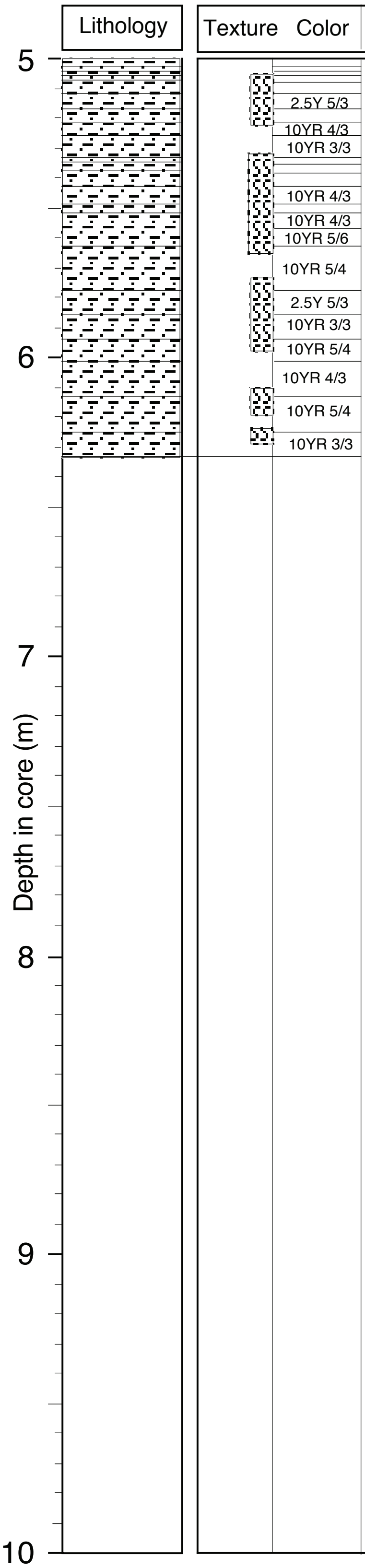

Description

262 – 272 cm: light olive brown (2.5Y 5/4) sandy silty clay (262-263.5, 265, and 270-272cm) and silty clay; some olive gray (5Y 5/2) mottling; sharp contact at base

272 – 292 cm: brown (10YR 4/3) silty clay; yellowish brown mottling at 274-281 cm; strongly mottled (light olive brown 2.5Y 5/3) at 289-292 cm

292 – 295 cm: light olive brown (2.5Y 5/4) silty clay

295 – 298 cm: brown (10YR 4/3) and light olive brown (2.5Y 5/4) silty clay; mottled

298 – 307 cm: brown (10YR 4/3) silty clay; below 302 cm strongly mottled

307 – 310 cm: light olive brown (2.5Y 5/3) silty clay; brown mottling

310 –316 cm: brown (10YR 4/3-5/3) silty clay; some mottling

316 – 330 cm: light olive brown (2.5Y 5/4) silty clay; dark gray mud clasts below 326 cm

330 – 351 cm: brown (10YR 4/3-5/3) (especially above 343 cm) and yellowish brown (10YR 5/4) silty clay; mottled; Fe-mn micronodules

351 – 360 cm: light olive brown (2.5Y 5/3) (sandy) silty clay; abundant dark gray mudclasts

360 – 369 cm: yellowish brown (10YR 5/4) sandy silty clay

369 – 374.5 cm: light olive brown (2.5Y 5/3) to olive gray (5Y 5/2) silty clay; some mudclasts and Fe-Mn micronodules

374.5 – 388 cm: light olive brown (2.5Y 5/3) silty clay; Fe-Mn micronodules

388 – 402 cm: brown (10YR 5/3-4/3) and yellowish brown (10YR 5/4) silty clay; strongly mottled; abundant Fe-Mn micronodules

402 – 409 cm: light olive brown (2.5Y 5/3) silty clay

409 – 431 cm: brown (10YR 4/3) and yellowish brown (10YR 5/4) silty clay, dominantly brown at 409-414 cm; mottled; some more sandy at 419-420 cm; Fe-Mn micronodules below 420 cm

431 – 446 cm: light olive brown (2.5Y 5/3) silty clay; sandy silty clay intervals at 432.5-433.5 and 435-437 cm; small dropstones (0.5-1 cm in diameter); Fe-Mn micronodules

446 – 460 cm: brown (10YR 4/3) silty clay; yellowish brown mottling

460 – 468 cm: light olive brown (2.5Y 5/3); brown mottling; Fe-Mn micronodules

468 – 475 cm: brown (10YR 4/3) silty clay; yellowish brown mottling; Fe-Mn micronodules

475 – 478 cm: light olive brown (2.5Y 5/3) silty clay; sharp contact at base

478 – 485 cm: brown (10YR 4/3) silty clay

485 – 488 cm: light olive brown (2.5Y 5/3) silty clay; sharp contact at base

488 – 512 cm: alternation of brown (10YR 4/3) and light olive brown (2.5Y 5/3) silty clay; mottled; more brown intervals at 488-492, 494-495, 497-499, 500-503, (504-506), and 508-512 cm

512 – 517 cm: light olive brown (2.5Y 5/3) silty clay; Fe-Mn micronodules

517 – 521 cm: brown (10YR 4/3) silty clay; light olive brown mottling

521 – 526 cm: light olive brown (521-522 and 524-526 cm) and brown (522-524 cm) silty clay

526 – 533 cm: dark brown (10YR 3/3) to dark grayish brown (10YR 3/2) silty clay

533 – 535 cm: light olive brown (2.5Y 5/3) silty clay; brown mottling

535 – 538 cm: brown (10YR 4/3) silty clay; mottled

538 – 543 cm: light olive brown (2.5Y 5/3) silty clay; brown mottling

543 – 549 cm: brown (10YR 4/3) silty clay; mottled; Fe-Mn micronodules

549 – 552 cm: light olive brown (2.5Y 5/3) silty clay; mottled; Fe-Mn micronodules

552 – 563 cm: brown (10YR 4/3) to yellowish brown (10YR 5/4) silty clay; Fe-Mn micronodules in upper (brown) part

563 – 578 cm: yellowish brown (10YR 5/4) silty clay

578 – 586 cm: light olive brown (2.5Y 5/3) silty clay; Fe-Mn micronodules

586 – 594 cm: dark brown (10YR 3/3) silty clay; upper part mottled

594 – 601 cm: yellowish brown (10YR 5/4) silty clay, mottled

601 – 613 cm: brown (10YR 4/3) silty clay

613 – 625 cm: yellowish brown (10YR 5/4) silty clay; upper part brown mottling; some more sand

625 – 633 cm: dark brown (10YR 3/3) to very dark grayish brown (10YR 3/2) silty clay; upper part mottled

PS 72/ 410-1 (GKG)

Mendeleev Ridge

ARK- XXIII/3 (Arctic 08)

Recovery: 38 cm

80° 30,37' N 175° 44,38' W

Water depth: 1808 m

Surface: dark brown (10 YR 3/3) sandy mud, many dropstones (Ø up to 2 cm); some valves

Lithology	Colour	Texture	Description
	10 YR 3/3		0-4 cm dark brown (10 YR 3/3) sandy silty clay
	5 Y 4/3		4-5,5 cm olive (5 Y 4/3) silty clay, dark brown mottling
	10 YR 4/2		5,5-7 cm dark grayish brown (10 YR 4/2) sandy silty clay
	10 YR 3/2 and 4/2		7-10 cm very dark grayish brown (10 YR 3/2) and dark grayish brown (10 YR 4/2) (mottling) sandy silty clay
	5 Y 4/3		10-11 cm olive (5 Y 4/3) silty clay, very dark brown (10 YR 2/2) mottling
	10 YR 4/3		11-14 cm brown (10 YR 4/3) (sandy) silty clay, very dark brown mottling, some 'white' spots
	10 YR 3/3 and 3/4		14-16 cm dark brown (10 YR 3/3) and dark yellowish brown (10 YR 3/4) silty clay, strongly mottled, 'white' lenses throughout the interval
	10 YR 3/4		16-19 cm dark yellowish brown (10 YR 3/4) silty clay, dark brown mottling, some 'white' spots at 17-17,5 cm
	2.5 Y 4/2 and 2.5 Y 4/3		19-22 cm dark grayish brown (2.5 Y 4/2) and olive brown (2.5 Y 4/3) (sandy) silty clay, brown (10 YR 4/3) mottling
	2.5 Y 4/4 and 2.5 Y 4/2		22-31 cm olive brown (2.5 Y 4/4) and dark grayish brown (2.5 Y 4/2) silty clay, strongly mottled (dark yellowish brown 10 YR 3/4)
	10 YR 4/3		31-32 cm brown (10 YR 4/3) sandy silty clay, dark yellowish brown (10 YR 3/4) mottling
	10 YR 4/3 and 3/3		32-36 cm brown (10 YR 4/3) and dark brown (10 YR 3/3) (mottling) sandy silty clay; some 'pinkish' spots (very small)
	10 YR 3/3		36-38 cm dark brown (10 YR 3/3) silty clay; some 'pinkish' spots

PS72/410-3 KAL | Mendeleev Ridge | **ARK-XXIII/3**

Recovery: 7.8 m | 80° 31.38´ N, 175° 43.26´ W | Water depth: 1808 m

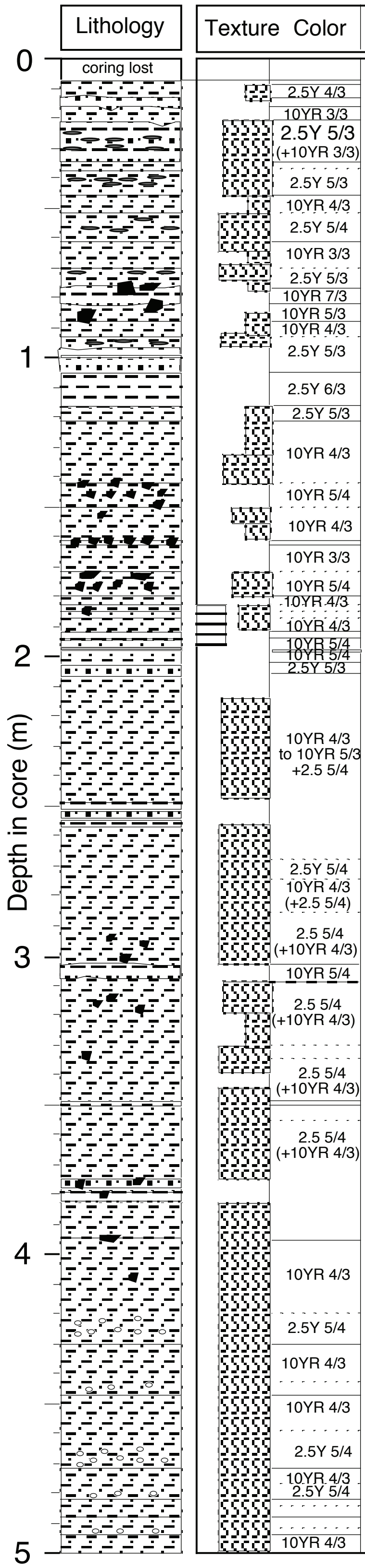

Description

0 - 7 cm: coring lost

7 – 9 cm: dark grayish brown (2.5Y 4/2) silty clay

9 – 13 cm: olive brown (2.5Y 4/3) silty clay; lower part mottled/bioturbated

13 - 17 cm: brown (10YR 5/3) sandy silty clay; very pale brown (10YR 7/3) lenses

17 – 21 cm: dark brown (10YR 3/3) silty clay

21 – 35 cm: light olive brown (2.5Y 5/3) sandy silty clay (21-24 cm, 32-34 cm) to silty clay; strongly mottled (10 YR 3/3) between 24 and 32 cm (large Planolites-type burrows)

35 – 46 cm: brown (10YR 4/3) (35-37 cm) and light olive brown (2.5Y 5/3) (more brown at 35-40 cm) silty clay; strongly mottled (10YR 4/3) between 37 and 43 cm, large burrows (Planolites); occasionally white spots/lenses

46 – 61 cm: brown (10YR 4/3) (46-52 cm) and light olive brown (2.5Y 5/3) (52-61 cm) silty clay; strongly mottled below 52 cm (large borrows; 10YR 3/3); dropstone (2 cm in diameter) at 60 cm

61 – 70 cm: dark brown (10YR 3/3) silty clay; olive brown (2.5 4/3) mottling, increasing downward

70 – 77 cm: brown (10YR 5/3) to olive brown (2.5Y 4/3) silty clay (some sand); two large dropstones (3 and 6 cm in diameter) at 74-77 cm

77 – 82 cm: very pale brown (10YR 7/3) and brown (10YR 5/3) sandy silty clay; abundant light and pinkish clasts/lenses; dropstone at 81-82 cm

82 – 88 cm: brown (10YR 5/3) silty clay; light olive brown mottling; some small light lenses; at 86 cm light olive brown layer (large burrow?); dropstones at 81-85 cm and 85-88 cm, both about 5 cm in diameter and encrusted by Fe-Mn

88 – 93 cm: brown (10YR 4/3) silty clay; lower part strongly mottled

93 – 99 cm: light olive brown (2.5Y 5/3) silty clay; dark brown mottling (Planolites-type)

99 – 105 cm: light olive brown (2.5Y 5/3) sandy silty clay; small mud clasts; silty clay horizon at 99-100 cm; sharp contact at base

105 – 116 cm: light yellowish brown (2.5Y 6/3) clay; sharp contact at base

116 – 121 cm: light olive brown (2.5Y 5/3) silty clay; slightly mottled; dark gray mud clast (0.5 cm in diameter) and small dropstone (0.5 cm in diameter) at the base

121 – 142 cm: brown (10YR 4/3) silty clay; light yellowish brown mottling, increasing toward the base; Fe-Mn micronodules

142 – 150 cm: light olive brown (2.5Y 5/4) silty clay, brown mottling; several dropstones (0.5 – 2 cm in diameter) at 142-143 and 145-146 cm, single dropstone (1 cm in diameter) at 149 cm; Fe-Mn micronodules

150 – 161 cm: brown (10YR 4/3) silty clay; strongly mottled (10YR 5/4); dropstone (0.5cm in diameter) at 153 cm; Fe-Mn micronodules

161 – 163 cm: light yellowish brown (10YR 5/4) silty clay; abundant dropstones (0.5 – 2cm in diameter); mud clasts

163 – 172 cm: dark brown (10YR 3/3) silty clay; mottled (increasing toward the base); dropstone at 169 cm; Fe-Mn micronodules

172 – 180 cm: light yellowish brown (10YR 5/4) silty clay; numerous dropstones (0.5 – 6 cm in diameter), especially at 176 – 178 cm

180 – 183 cm: brown (10YR 4/3) silty clay; mottled

183 – 185 cm: light olive brown (2.5Y 5/4) silty clay, brown mottling; some lamination(?); Fe-Mn micronodules

185 – 192 cm: brown (10YR 4/3) silty clay; mottled; some light (very pale brown, 10YR7/3) lenses; dropstone (15 cm in diameter) at top; Fe-Mn micronodules

192 – 194 cm: very pale brown (10YR 7/3) and yellowish brown (10YR 5/4) sandy siltyclay („white layer“); abundant light lenses/clasts; small dropstone (0.5 cm in diameter)

194 – 202 cm: brown (10YR 4/3) and yellowish brown (10YR 5/4) silty clay; at 197 cm thin (0.5 cm thick) light reddish brown (2.5 YR 6/4) silty clay („pink layer“); pinkish clasts; Fe-Mn micronodules below pink layer

202 – 205 cm: light olive brown (2.5Y 5/3) sandy silty clay

PS72/410-3 KAL **ARK-XXIII/3**

Recovery: 7.8 m 80° 31.38´ N, 175° 43.26´ W Water depth: 1808 m

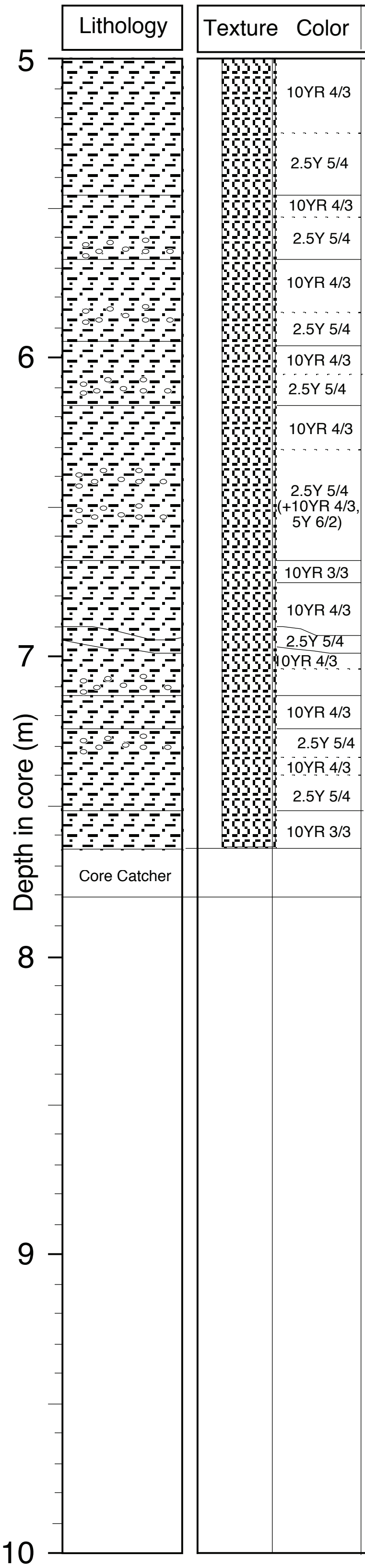

Description

205 – 248 cm: brown (10YR 4/3) and light olive brown (2.5Y 5/4) silty clay; strongly mottled/bioturbated; below 235 cm Fe-Mn micronodules

248 – 255 cm: light olive brown (2.5Y 5/4) and brown (10YR 4/3) sandy silty clay (248-249.5 , 252-253, and 254-255 cm) and silty clay

255 – 286 cm: brown (10YR 4/3) and light olive brown (2.5Y 5/4) silty clay; strongly mottled/bioturbated; Fe-Mn micronodules throughout

286 – 303 cm: light olive brown (2.5Y 5/4) sandy silty clay; brown (10YR 4/3) mottled (strongly bioturbated); abundant gray mud clasts throughout; dropstones at 294 cm (1 cm in diameter), 298 cm (3 cm in diameter), and 300 cm (1 cm in diameter)

303 – 308.5 cm: yellowish brown (10YR 4/3) sandy silty clay; several very small dropstones and mud clasts

308.5 – 375 cm: light olive brown (2.5Y 5/4) silty clay, at 330-340 and 350-357 cm some more brownish; brown (10YR 4/3) mottling (strongly bioturbated); light yellowish brown (10YR 6/4) layer at 349-350 cm; dropstones (0.5 – 1cm in diameter) at 314, 316, 320, 334, and 374 cm

375 - 382 cm: light olive brown (2.5Y 5/4) sandy silty clay, between 377 and 380 cm more fine-grained = silty clay; common gray mud clasts; dropstones (about 1 cm indiameter) at 376-377 and 381 cm

382 – 752 cm: light olive brown (2.5Y 5/4) and brown (10YR 4/3-5/3) silty clay; strongly mottled/bioturbated; brown intervals with light olive brown mottling at 395-420, 430-443, 447-459, 472-477, 482-484, 489-492, 494-525, 546-553, 567-585, 596-606, 616-132, 668- 690 (668-680 cm dark brown), 697-704, 713-724, and 734-740 cm, alternating with dominantly light olive brown intervals with brown to dark brown mottling (below about 580 cm additionally light olive gray (5Y 6/2) mottling in the light intervals); below 400cm abundant dark brown speckles nodules (Fe-Mn nodules, 0.1 to 0.5 cm in diameter),especially in the light olive brown intervals; dropstones at 395-396 cm (3 cm in diameter) and 408 cm (1 cm in diameter)

752 – 764 cm: dark brown (10YR 3/3) silty clay; light olive brown (2.5Y 5/4) mottling, increasing toward the base

764 – 780 cm: Core catcher (tube not opened yet)

PS 72/ 413-3 (GKG) Mendeleev Ridge **ARK- XXIII/3 (Arctic 08)**

Recovery: 37 cm **80° 16,49’ N 178° 31,29’ W** **Water depth: 1264 m**

Surface: dark yellowish brown (10 YR 3/4) sandy mud, water-saturated, many dropstones (Ø up to 3 cm); valves of Brachiopoda, Bivalvia; shell detritus

Lithology	Colour	Texture	Description
	10 YR 3/3		0-4 cm dark brown (10 YR 3/3) sandy silty clay
	2.5 Y 5/3	SSSSSSS	4-8 cm light olive brown (2.5 Y 5/3) silty clay, strongly mottled (dark brown 10 YR 3/3)
	10 YR 3/2	SSSSS	8-10 cm very dark grayish brown (10 YR 3/2) and dark gray (5 Y 4/1) (mottling) silty clay
	2.5 Y 5/3	SSSSS	10-12,5 cm light olive brown (2.5 Y 5/3) (sandy) silty clay, strongly mottled (dark gray 5 Y 4/1)
	10 YR 3/3 and 2/2		12,5-15 cm dark brown (10 YR 3/3) and very dark brown (10 YR 2/2) silty clay, some small 'pinkish' spots
	2.5 Y 5/4 to 4/4		15-23 cm light olive brown (2.5 Y 5/4) to olive brown (2.5 Y 4/4) silty clay, very dark brown and dark gray (5 Y 4/1) mottling
	10 YR 3/3		23-25 cm dark brown (10 YR 3/3) silty clay, olive brown (2.5 Y 4/4) mottling
	2.5 Y 4/3	SSSSSSS / SSSSS	25-37 cm olive brown (2.5 Y 4/3) (sandy) silty clay up to 31 cm, then silty clay (very soft), light yellowish brown spots (10 YR 6/4) up to 34 cm, strongly mottled (dark brown 10 YR 3/3 and very dark brown 10 YR 2/2)

Depth scale (cm): 0, 10, 20, 30, 40, 50

PS72/413-5 SL Mendeleev Ridge **ARK-XXIII/3**

Recovery: 6.44 m 80° 17.33´ N, 178° 29.07´ W Water depth: 1237 m

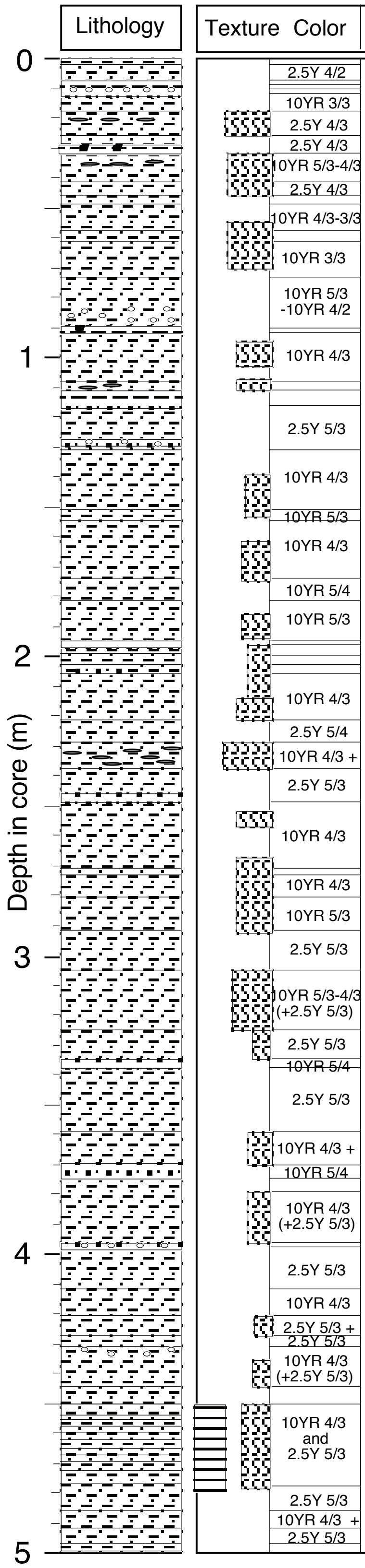

Description

0 - 2 cm: very dark grayish brown (10YR 3/2) (sandy) silty clay
2 - 7 cm: dark grayish brown (2.5Y 4/2) silty clay
7 - 9 cm: brown (10YR 5/3) to dark grayish brown (10YR 4/2) (sandy) silty clay
9 – 10 cm: very pale brown (10YR 7/3) sandy silty clay layer („semi-lithified“); abundant light clasts; several dropstones („white layer“)
10 – 12 cm: brown (10YR 5/3) sandy silty clay; abundant light clasts; sharp contact at base
12 - 18 cm: dark brown (10YR 3/3) silty clay
18 - 26 cm: olive brown (2.5Y 4/3) and dark brown (10YR 3/3) silty clay; strongly mottled (10 YR 3/3) (large Planolites-type burrows)
26 – 32 cm: olive brown (2.5Y 4/3) silty clay (26-29 cm) and sandy silty clay (29-32 cm); few small dropstones (0.2-0.5 cm in diameter) in lower part
32 – 41 cm: brown (10YR 5/3-4/3) to olive brown (2.5Y 4/3) silty clay; mottled; small light (very pale brown) lenses at 37-38 cm
41 – 46 cm: olive brown (2.5Y 4/3) to light olive brown (2.5Y 5/3) silty clay; strongly mottled (10YR 3/3), Planolites-type burrows
46 – 49 cm: light olive brown (2.5Y 5/3) silty clay; sharp contact at base
49 – 58 cm: dark brown (10YR 3/3) to brown (10YR 4/3) silty clay; mottled in lower part
58 – 61 cm: light olive brown (2.5Y 5/3) and brown (10YR 4/3) silty clay; strongly mottled
61 – 73 cm: dark brown (10YR 3/3) to very dark grayish brown (10YR 3/2) silty clay; light olive brown mottling throughout; sharp „wavy“ contact at base
73 – 90 cm: brown (10YR 5/3) to dark grayish brown (10YR 4/2) silty clay; abundant very pale brown (10YR 7/3) lenses/clasts at 83-90 cm
90 – 92 cm: light reddish brown (2.5YR 6/3) sandy silty clay; small dropstone (0.5 cm in diameter) at 91 cm; sharp contact at base („pink layer“)
92 – 108 cm: brown (10YR 4/3) silty clay; light olive brown mottling (92-102 cm)
108 – 111 cm: light olive brown (2.5Y 5/3) silty clay
111 – 116 cm: grayish brown (10YR 5/2) sandy silty clay
116 – 131 cm: light olive brown (2.5 5/3) silty clay; 116-124 cm brown mottling; brown layer at 124 cm; sandy silty clay with abundant olive brown and dark gray mud clasts at127-129 cm
131 – 151 cm: brown (10YR 4/3) silty clay; light olive brown mottling in lower part; Fe-Mn micronodules at 131-132 cm; light clast at 142 cm
151 – 155 cm: brown (10YR 5/3) silty clay
155 – 174 cm: brown (10YR 4/3) silty clay; yellowish brown (10YR 5/4) mottling; small very pale brown lenses at 169-174 cm; sharp contact at base
174 – 181 cm: yellowish brown (10YR 5/4) (sandy) silty clay; sharp contact at base
181 – 195 cm: brown (10YR 5/3) and yellowish brown (10YR 5/4) silty clay; mottled; very pale brown lenses at 189-192 cm
195 – 196 cm: light reddish brown (2.5YR 6/3) sandy silty clay („pink layer“)
196 – 200 cm: yellowish brown (10YR 5/4) silty clay
200 – 203 cm: light olive brown (2.5Y 5/3) (sandy) silty clay; brown mottling
203 – 206 cm: yellowish brown (10YR 5/4) silty clay
206 – 221 cm: brown (10YR 4/3) silty clay; mottled below 229 cm, mottling (2.5Y 5/4) increasing toward the base
221- 229 cm: light olive brown (2.5Y 5/4) silty clay
229 – 238 cm: light olive brown (2.5Y 5/4) and brown (10YR 4/3) silty clay; strongly mottled; Fe-Mn micronodules
238 – 249 cm: light olive brown (2.5Y 5/3) silty clay; sandy silty clay at 238-239 and 247.5-249 cm; dark brown horizon at 244-245 cm
249 – 271 cm: brown (10YR 4/3) silty clay; mottled; at 266-268 cm more light olive brown
271 – 273 cm: light olive brown (2.5Y 5/3) silty clay
273 – 281 cm: brown (10YR 4/3) silty clay; strongly mottled (2.5Y 5/3)
281 – 292 cm: brown (10YR 5/3) silty clay; strongly mottled (2.5Y 5/3)
292 – 305 cm: light olive brown (2.5Y 5/3) silty clay
305 – 325 cm: brown (10YR 4/3-5/3) silty clay; strongly mottled (2.5Y 5/3)

PS72/413-5 SL Mendeleev Ridge **ARK-XXIII/3**

Recovery: 6.44 m 80° 17.33´ N, 178° 29.07´ W Water depth: 1237 m

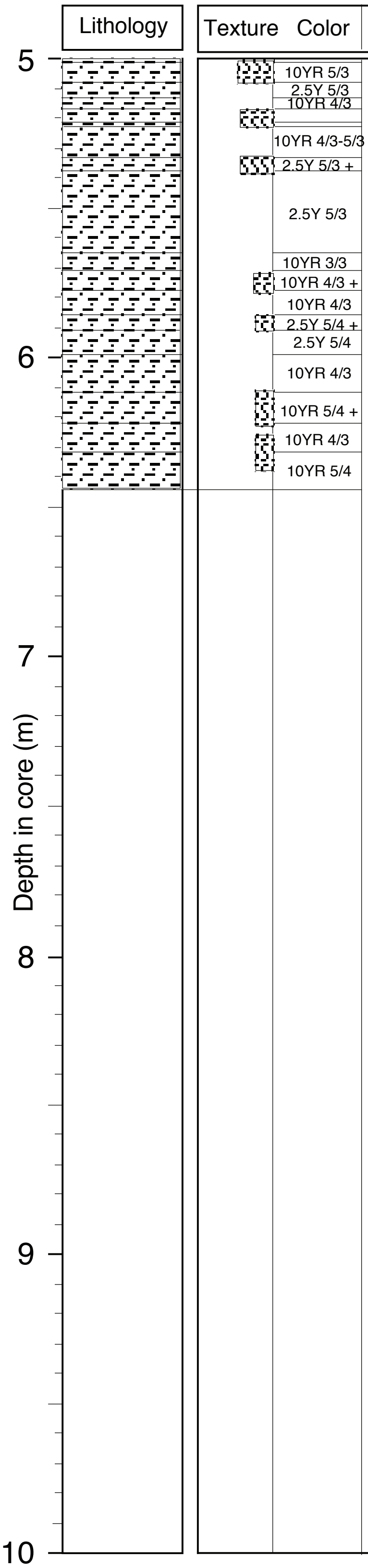

Description

325 – 335 cm: light olive brown (2.5Y 5/3) (sandy) silty clay; common occurrence of (dark gray) mud clasts; Fe-Mn micronodules; sharp contact at base
335 – 338 cm: yellowish brown (10YR 5/4) sandy silty clay; sharp contact at base
338 – 359 cm: light olive brown (2.5Y 5/3) silty clay; Fe-Mn micronodules
359 – 370 cm: brown (10YR 4/3) and light olive brown (2.5Y 5/3) silty clay; mottled; Fe-Mn micronodules
370 – 375 cm: yellowish brown (10YR 5/4) (sandy) silty clay
375 – 379 cm: yellowish brown (10YR 5/4) and light olive brown (2.5Y 5/3) silty clay
379 –396 cm: brown (10YR 4/3) and light olive brown (2.5Y 5/3) silty clay, some sand; mottled; Fe-Mn micronodules
396 – 398 cm: yellowish brown (10YR 5/4) (sandy) silty clay; some mud clasts; Fe-Mn micronodules
398 – 412 cm: light olive brown (2.5Y 5/3) silty clay; some mud clasts; Fe-Mn micronodules; sharp contact at base
412 – 421 cm: brown (10YR 4/3) silty clay
421 – 427 cm: light olive brown (2.5Y 5/3) and brown (10YR 4/3) silty clay; mottled
427 –431 cm: light olive brown (2.5Y 5/3) silty clay; mud clasts at base
431 – 444.5 cm: brown (10YR 4/3) and light olive brown (2.5Y 5/3) silty clay, some sand; mottled in lower part; mud clasts near top; Fe-Mn micronodules
444.5 – 450 cm: light olive brown (2.5Y 5/3) silty clay; Fe-Mn micronodules
450 – 478 cm: alternation of brown (10YR 4/3) and light olive brown (2.5Y 5/3) silty clay (6 cycles); mottled; Fe-Mn micronodules
478 – 486 cm: light olive brown (2.5Y 5/3) silty clay; some sand
486 – 492 cm: brown (10YR 4/3) and light olive brown (2.5Y 5/3) silty clay; Fe-Mn micronodules
492 – 497 cm: light olive brown (2.5Y 5/3) silty clay; some sand
497 – 501 cm: brown (10YR 4/3) silty clay
501 – 508 cm: brown (10YR 5/3) and light olive brown (2.5Y 5/3) silty clay; mottled
508 – 513 cm: light olive brown (2.5Y 5/3) silty clay; Fe-Mn micronodules
513 – 517 cm: brown (10YR 4/3) silty clay; Fe-Mn micronodules
517 – 521 cm: brown (10YR 4/3) and light olive brown (2.5Y 5/3) silty clay; mottled
521 – 523 cm: light olive brown (2.5Y 5/3) silty clay; Fe-Mn micronodules
523 – 533 cm: brown (10YR 4/3-5/3) silty clay
533 – 538 cm: brown (10YR 4/3) and light olive brown (2.5Y 5/3) silty clay; mottled
538 – 565 cm: light olive brown (2.5Y 5/3) silty clay, some sand; lenses of Fe-Mn micronodules at 545 and 551 cm; sharp contact at base
565 – 571 cm: dark brown (10YR 3/3) silty clay, some sand; yellowish brown mottling at 565-568 cm
571 – 578 cm: brown (10YR 4/3) and yellowish brown (10YR 5/4) silty clay, some sand; mottled
578 – 586 cm: brown (10YR 4/3) silty clay
586 – 591 cm: brown (10YR 4/3) and light olive brown (2.5Y 5/4) silty clay, some sand; mottled; Fe-Mn micronodules
591 – 599 cm: light olive brown (2.5Y 5/4) silty clay, some sand
599 – 612 cm: brown (10YR 4/3) silty clay; below 609 cm mottled
612 – 622 cm: yellowish brown (10YR 5/4) and brown (10YR 5/3) silty clay, some sand; mottled; Fe-Mn micronodules
622 – 632 cm: brown (10YR 4/3) silty clay
632 – 644 cm: yellowish brown (10YR 5/4) silty clay, some sand; mottled; abundant Fe-Mn micronodules

PS 72/ 418-5 (GKG) Mendeleev Ridge **ARK- XXIII/3 (Arctic 08)**

Recovery: 50 cm

80° 23,54' N 178° 49,00' E

Water depth: 2046 m

Lithology	Colour	Texture	Description
Surface: brown mud, very water-saturated, soft, slight sandy admixture; bioturbated, some valves, Cephalopoda (?)			
0–19 cm	10 YR 3/3		0-19 cm dark brown (10 YR 3/3) silty clay, water-saturated, slight sandy admixture
19–23 cm	2.5 Y 4/3	SSS	19-23 cm olive brown (2.5 Y 4/3) (sandy) silty clay, dark grayish brown (10 YR 4/2) and dark brown mottling, some small 'white' spots at 19,5-20 cm
23–27 cm	2.5 Y 5/3	SSS	23-27 cm light olive brown (2.5 Y 5/3) silty clay, very soft, dark grayish brown (10 YR 4/2) and dark brown mottling
27–30 cm	2.5 Y 4/3	SSS	27-30 cm olive brown (2.5 Y 4/3) silty clay, dark grayish brown mottling, some 'white' spots at 29-30 cm
30–37,5 cm	10 YR 3/3	SSS	30-37,5 cm brown (10 YR 4/3) silty clay, dark grayish brown mottling, very small 'pinkish' spots throughout
37,5–39,5 cm	10 YR 5/4	SSS	37,5-39,5 cm yellowish brown (10 YR 5/4) silty clay, brown mottling, small 'white' spots at 38,5 cm
39,5–44 cm	10 YR 4/3	SSS	39,5-44 cm brown (10 YR 4/3) silty clay, many 'pinkish' spots throughout
44–50 cm	10 YR 3/3		44-50 cm dark brown (10 YR 3/3) silty clay, very soft

Depth scale (cm): 0, 10, 20, 30, 40, 50

PS72/418-7 SL Mendeleev Ridge **ARK-XXIII/3**

Recovery: 6.88 m 80° 24.03´ N, 178° 51.69´ E Water depth: 1990 m

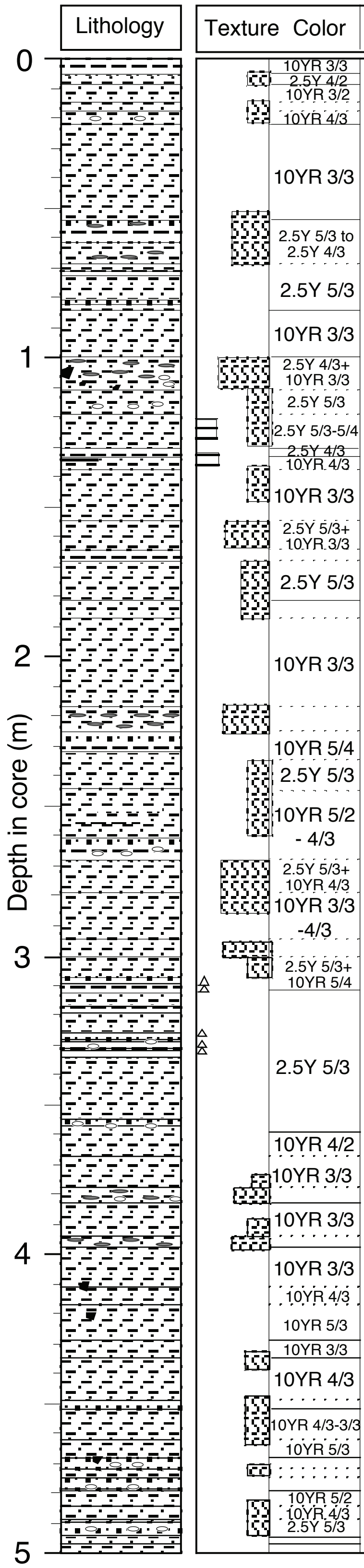

Description

0 - 5 cm: dark brown (10YR 3/3) (sandy) silty clay

5 – 9 cm: dark grayish brown (2.5Y 4/2) to olive brown (2.5Y 4/3) siltyclay; dark brown lenses/spots (bioturbation)

9 – 15 cm: very dark grayish brown (10YR 3/2) silty clay

15 – 18 cm: light olive brown (2.5Y 5/3) and dark grayish brown (2.5Y 4/2) silty clay; mottled; few small very pale brown (10YR 7/3) lenses at 17cm

18 – 22 cm: brown (10YR 4/3) silty clay; some mottling; some small very pale brown (10YR 7/3) and „pinkish“ lenses throughout

22 – 54 cm: dark brown (10YR 3/3) to dark reddish brown (2.5YR 3/3) silty clay, homogeneous

54 – 69 cm: light olive brown (2.5Y 5/3) to olive brown (2.5Y 4/3) silty clay (61-69 cm) to sandy silty clay (54-61 cm); dark brown mottling; distinct more sandy layers at 59 and 60 cm

69 – 84 cm: light olive brown (2.5Y 5/3) silty clay; more sandy layers at 71-72 and 81-82 cm; sharp contact at base

84 – 100 cm: dark brown (10YR 3/3) silty clay; some small very pale brown and pinkish lenses at 100 cm

100 – 111 cm: olive brown (2.5Y 4/3) and dark brown (10YR 3/3) silty clay; strongly mottled; small very pale brown lenses at 107 and 109cm; dropstone (3 cm in diameter) at 102-105 cm, few small (<0.5 cm) dropstones at 108 and 111 cm

111 – 119 cm: light olive brown (2.5Y 5/3) to olive gray (5Y 5/2) silty clay; slightly mottled; some dark gray mud clasts; some small very pale brown and pinkish lenses

119 – 130 cm: light olive brown (2.5Y 5/3-5/4) silty clay; some mottling and lamination; pinkish lense at 121 cm

130 – 133 cm: olive brown (2.5Y 4/3) sandy silty clay

133 – 138 cm: brown (10YR 4/3) silty clay; thin very dark gray (10YR3/1) laminae between 133 and 134 cm

138 – 155 cm: dark brown (10YR 3/3) silty clay; 138-143 cm brown mottling

155 – 164 cm: dark brown (10YR 3/3) and light olive brown (2.5Y 5/3) silty clay; strongly mottled

164 – 168 cm: dark brown (10YR 3/3) and light olive brown (2.5Y 5/3) sandy silty clay; some mottling; small Fe-Mn micronodules; at top layer of dark brown sand (Fe-Mn nodules)

168 – 181 cm: light olive brown (2.5Y 5/3) silty clay; olive gray (5Y5/2) mottling, some dark brown lenses/burrows

181 – 187 cm: dark brown (10YR 3/3) and light olive brown (2.5Y 5/3) silty clay; mottled

187 – 217 cm: dark brown (10YR 3/3) silty clay

217 – 225 cm: dark brown (10YR 3/3) and light olive brown (2.5Y 5/3) silty clay; strongly mottled

225 – 235 cm: yellowish brown (10YR 5/4) sandy silty clay; below 232cm silty clay

235 – 245 cm: light olive brown (2.5Y 5/3) silty clay; some mottling; Fe-Mn micronodules in lower half

245 – 268 cm: grayish brown (10YR 5/2) and brown (10YR 4/3) (sandy) silty clay; at 260-266 cm abundant light reddish brown (2.5YR 6/3) („pinkish“) clasts, more sandy; dropstone (1 cm in diameter) at 261 cm

268 – 279 cm: brown (10YR 4/3) and light olive brown (2.5Y 5/3) silty clay; strongly mottled; some Fe-Mn micronodules

279 – 295 cm: dark brown (10YR 3/3) and brown (10YR 4/3) silty clay; mottled

295 - 301 cm: brown (10YR 4/3) and yellowish brown (10YR 5/4) silty clay; strongly mottled

301 – 312 cm: light olive brown (2.5Y 5/3) to yellowish brown (10YR5/4) silty clay; some mottling in upper part; at 307-308.5 and 309-312 cm sandy silty clay, sharp base, fining upward (turbidites); lower turbidite has „pinkish“ colour at base

PS72/418-7 SL Mendeleev Ridge **ARK-XXIII/3**

Recovery: 6.88 m 80° 24.03´ N, 178° 51.69´ E Water depth: 1990 m

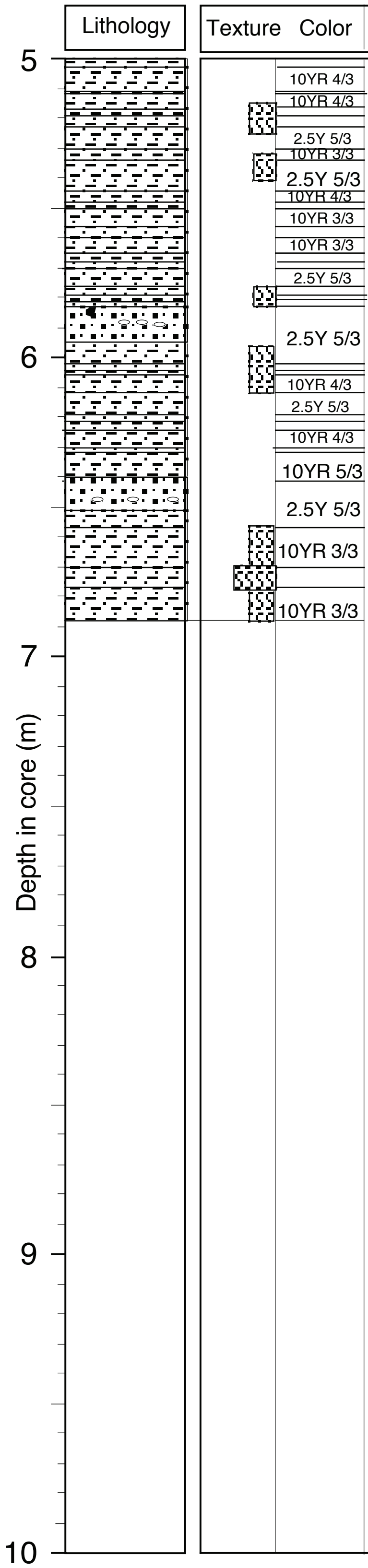

Description

312 – 359 cm: light olive brown (2.5Y 5/3) silty clay; thin lamina of lenses/clasts (Fe-Mn?) at 318.5 cm; thin very dark gray lamina at 319 cm; sandy silty clay with small „pinkish“ clasts, sharp base, and fining upward at 325-326 cm; sandy silty clay with sharp base and fining upward at 329.5-331.5 cm and 332-333.5 cm; sandy silty clay with abundant olive gray and very pale brown clasts at 354.5 and 356.5 cm

359 – 367 cm: dark grayish brown (10YR 4/2) silty clay; light olive brown mottling

367 – 378 cm: dark brown (10YR 3/3) silty clay; between 370 and 374 cm some light olive brown mottling

378 – 383 cm: dark brown (10YR 3/3) and light olive brown (2.5Y 5/3) silty clay; strongly mottled; some small very pale brown lenses

383 – 394 cm: dark brown (10YR 3/3) silty clay

394 – 398 cm: light olive brown (2.5Y 5/3) and dark brown (10YR 3/3) silty clay; mottled

398 – 411 cm: dark brown (10YR 3/3) silty clay

411 – 417 cm: brown (10YR 4/3) silty clay; dropstone (1 cm in diameter) at top

417 – 429 cm: brown (10YR 5/3) silty clay; dropstone (1 cm in diameter) at 422 cm

429 – 435 cm: dark brown (10YR 3/3) silty clay; at base mottled

435 – 449 cm: brown (10YR 4/3) silty clay

449 – 452 cm: light olive brown (2.5Y 5/3) (sandy) silty clay; some brownish mottling

452 – 462 cm: dark brown to brown silty clay; some mottling (yellowishbrown)

462 – 468 cm: brown (10YR 5/3) silty clay

468 – 472 cm: yellowish brown (10YR 5/4) (sandy) silty clay; small pinksih lenses; drop stone (1 cm in diameter) at 369 cm; dark brown layer at 369 cm

472 – 475 cm: brown (10YR 4/3) silty clay

475 – 479 cm: light olive brown (2.5Y 5/3) to olive brown (2.5Y 4/3) sandy silty clay; pinkish lenses and clasts

479 – 484 cm: grayish brown (10YR 5/2) silty clay; thin very dark gray layer on top

484 – 489 cm: dark brown (10YR 3/3) silty clay; some mottling

489 – 494 cm: light olive brown (2.5Y 5/3) to olive brown (2.5Y 4/3) (sandy) silty clay; some very pale brown and pink lenses/clasts

494 – 583 cm: alternation of brown (10YR 4/3) to dark brown (10YR3/3) and light olive brown (2.5Y 5/3) silty clay; partly mottled/bioturbated; brown/dark brown intervals at 494-497, 503-511, 512-517, 519-523, 530-534, 544-548, 550-556, 560-565, 568-570, 576-579, and 580-583 cm; in between light olive brownintervals; more sandy intervals at 525-530, 538-541, 557-560, and 565-568 cm

583 – 595 cm: light olive brown (2.5Y 5/3) to olive brown (2.5Y 4/3) sandy silty clay; abundant dark gray mud clasts; dropstone (1 cm in diameter) at 585 cm

595 – 657 cm: alternation of brown to dark brown and light olive brown silty clay; brown/dark brown intervals at 602-604, 606-612, 619-621, 624-630, and 632-641 cm; in between dominantly lightolive brown intervals; sandy silty clay interval with small mud clasts and Fe-Mn nodules at 639-651 cm

657 – 688 cm: dark brown (10YR 3/3) silty clay; mottled throughout with strong mottling (brown to yellowish brown) at 670-677 cm

PS 72/ 422-3 (GKG) Mendeleev Ridge **ARK- XXIII/3 (Arctic 08)**

Recovery: 40 cm **80° 33,08’ N 175° 44,75’ E** **Water depth: 2546 m**

Lithology	Colour	Texture	Description
			Surface: 0-1 cm, dark brown sandy mud, very water-saturated, soft; ; bioturbated, some valves of Bivalvia
	10 YR 3/3		1-8 cm dark brown (10 YR 3/3) sandy silty clay
	2.5 Y 4/3 and 4/2		8-12 cm olive brown (2.5 Y 4/3) and dark grayish brown (10 YR 4/2) sandy silty clay, slightly mottled (dark brown)
	2.5 Y 5/3		12-17,5 cm light olive brown (2.5 Y 5/3) silty clay, very soft, dark brown mottling, a few very small 'pinkish' spots
	2.5 Y 5/3 and 4/2		17,5-20 cm light olive brown (2.5 Y 5/3) and dark grayish brown (2.5 Y 4/2) sandy silty clay, some gravel, some small 'pinkish' spots
	10 YR 4/3		20-26 cm brown (10 YR 4/3) (sandy) silty clay, slightly mottled (dark grayish brown), some 'pinkish' spots (the largest at 23-24 cm)
	2.5 Y 5/4		26-28 cm light olive brown (2.5 Y 5/4) silty clay, brown (10 YR 4/3) mottling, some very small 'pinkish' spots throughout
	10 YR 4/3		28-31,5 cm brown (10 YR 4/3) silty clay, dark grayish brown mottling
	2.5 Y 5/4		31,5-35,5 cm light olive brown (2.5 Y 5/4) silty clay, very soft, slightly mottled (dark brown 10 YR 3/3), sharp contact at the base
	10 YR 3/4		35,5-40 cm dark yellowish brown (10 YR 3/4) (sandy) silty clay

Depth scale (cm): 0, 10, 20, 30, 40, 50

PS72/422-5 KAL Mendeleev Ridge **ARK-XXIII/3**

Recovery: 7.96 m 80° 32.58´ N, 175° 44.75´ E Water depth: 2463 m

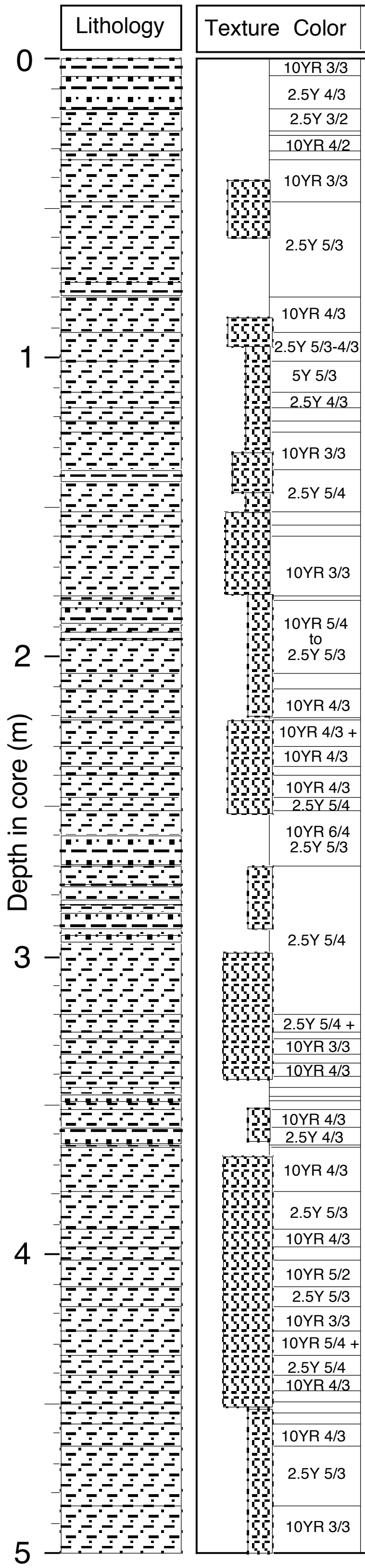

Description

Note : upper part (0-20 cm) coring disturbance (see GKG for more detailed lithology)

0 – 6 cm: dark brown (10YR 3/3) (sandy) silty clay
6 - 17 cm: olive brown (2.5Y 4/3) (sandy) silty clay
17 - 24 cm: very dark grayish brown (2.5Y 3/2) silty clay; few light (very pale brown 10YR 7/3) lenses in lower part
24 – 26 cm: olive brown (2.5Y 4/3) silty clay
26 – 31 cm: dark grayish brown (10YR 4/2) silty clay
31 – 34 cm: olive brown (2.5Y 4/3) silty clay; sharp contact at base
34 – 48 cm: dark brown (10YR 3/3) silty clay; lower part slightly mottled
48 – 80 cm: light olive brown (2.5Y 5/3) silty clay to (sandy) silty clay (more sandy intervals at 48-56, 63-64, and >74 cm); strongly mottled between 48 and 56 cm; more olive (sandy) silty clay horizon at 74-75 cm; sharp contact at base
80 – 92 cm: brown (10YR 4/3) silty clay; slight mottling, increasing toward the base; layer of very pale brown (10YR 7/3) and pinkish clasts/lenses at 91-92 cm
92 – 101 cm: (light) olive brown (2.5Y 5/3-4/3) silty clay; strongly mottled (dark brown); several light reddish brown (2.5YR 6/3) (“pinkish”) lenses at 98-99 cm
101 – 112 cm: olive (5Y 5/3) silty clay; few very pale brown (10YR 7/3) lenses/clasts at 110-111cm
112 - 117 cm: olive brown (2.5Y 4/3) silty clay; slightly mottled; horizon of dark gray and pinkish clasts at 114 cm
117 – 121 cm: light olive brown (2.5Y 5/3) silty clay; sharp contact at base
121 – 125 cm: brown (10YR 4/3) silty clay
125 – 138 cm: dark brown (10YR 3/3) silty clay; strongly bioturbated in lower half; Fe-Mn micronodules
138 – 152 cm: light olive brown (2.5Y 5/4) silty clay; strongly mottled in upper half (dark brown 10YR 3/3 and olive gray 5Y 5/2); at 139 and 140-141.5 cm more sandy (sandy silty clay)
152 – 156 cm: light olive brown (2.5Y 5/3) silty clay; slightly bioturbated
156 – 160 cm: brown (10YR 4/3) silty clay; mottled
160 – 180 cm: dark brown (10YR 3/3) silty clay; lower half strongly mottled (2.5Y 5/4 and 5Y 5/2)
180 – 180.5 cm: thin olive gray (5Y 5/2) horizon of sandy silty clay
180.5 – 206 cm: yellowish brown (10YR 5/4) to light olive brown (2.5Y 5/3) silty clay; some dark brown mottling at 183-185 cm, less mottling/bioturbation in lower part; more sand (sandy silty clay) at 183-184 cm and, especially, at 185-186 and 191-192.5 cm; sand lense at 202 cm
206 – 211 cm: grayish brown (10YR 5/2) silty clay
211 – 220.5 cm: brown (10YR 4/3) silty clay; some light olive brown mottling
220.5 – 221 cm: light reddish brown (2.5YR 6/3) and brown (10YR 4/3) (sandy) silty clay (“pink layer”?)
221 – 230 cm: brown (10YR 4/3), olive brown (2.5Y 4/3), and light olive brown (2.5Y 5/3) silty clay; strongly mottled; few light (very pale brown) and pinkish lenses
230 – 237 cm: brown (10YR 4/3) silty clay; strongly mottled (light olive brown)
237 – 240 cm: light olive brown (2.5Y 5/4) and brown (10YR 4/3) silty clay; strongly mottled (Planolites-type burrows); sharp contact at base
240 – 247 cm: brown (10YR 4/3) silty clay; mottled
247 – 252 cm: light olive brown (2.5Y 5/4) and brown (10YR 4/3) silty clay; strongly mottled
252 – 270 cm: light yellowish brown (10YR 6/4), light olive brown (2.5Y 5/3), and olive gray (5Y 5/2) silty clay (252-260 cm) and sandy silty clay (260-270 cm); in the lower part some reddish colour; fining upward; some mottling
270 – 320 cm: light olive brown (2.5Y 5/4) silty clay; strongly mottled; Fe-Mn micronodules; thin sandy layer at 277 cm; light reddish brown (2.5YR 6/3) layer at 282-283 cm; at 286-292 and 293-296 cm light olive brown (2.5Y 5/3) to olive brown (2.5Y 4/3) sandy silty clay intervals with fining upward and sharp contact at base (turbidites?); at 295-296 cm light reddish brown (2.5YR 6/3) colour (“pink layer”)
320 – 326 cm: light olive brown (2.5Y 5/4) and dark grayish brown (10YR 4/2) silty clay; mottled; thin sandy laminae at 321-322 cm
326 – 328 cm: dark grayish brown (10YR 4/2) silty clay
328 – 333 cm: dark brown (10YR 3/3) silty clay; mottled
333 – 336 cm: light olive brown (2.5Y 5/4) and dark brown (10YR 3/3) silty clay; strongly mottled
336 – 341 cm: brown (10YR 4/3) silty clay; mottled
341 – 344 cm: yellowish brown (10YR 5/4) silty clay; strongly mottled (brown); sharp contact at base
344 – 347 cm: brown (10YR 4/3) silty clay; mottled
347 – 349 cm: olive brown (2.5Y 4/3) to olive gray (5Y 5/2) sandy silty; fining upward; sharp contact at base (turbidite)
349 – 352 cm: grayish brown (10YR 5/2) silty clay; yellowish brown mottling
352 – 358 cm: brown (10YR 4/3) silty clay; below 356 cm strongly mottled (yellowish brown)
358 – 363.5 cm: olive brown (2.5 4/3), light olive brown (2.5Y 5/4), and olive gray (5Y 5/2) sandy silty clay; near top brown (10YR 4/3) mottling; fining upward; sharp contact at base (turbidite?)
363.5 – 364 cm: light olive brown (2.5Y 5/4) clay
364 – 379 cm: brown (10YR 4/3-5/3) silty clay; strongly mottling (upper part dark brown, lower part light olive brown)
379 – 392 cm: light olive brown (2.5Y 5/3) silty clay; olive brown (2.5Y 4/3) and brown (10YR 5/3) mottling
392 – 398 cm: brown (10YR 4/3) to dark brown (10YR 3/3) silty clay; mottled
398 – 402 cm: light olive brown (2.5Y 5/3) silty clay; sand lense at 401 cm
402 – 411 cm: grayish brown (10YR 5/2) silty clay; mottled
411 – 418 cm: light olive brown (2.5Y 5/3) silty clay; strongly mottled
418 – 426 cm: dark brown (10YR 3/3) silty clay; mottled
426 – 434 cm: yellowish brown (10YR 5/4) and brown (10YR 4/3); strongly mottled; dropstone (0.5 cm in diameter) at base

PS72/422-5 KAL Mendeleev Ridge **ARK-XXIII/3**

Recovery: 7.96 m 80° 32.58´ N, 175° 44.75´ E Water depth: 2463 m

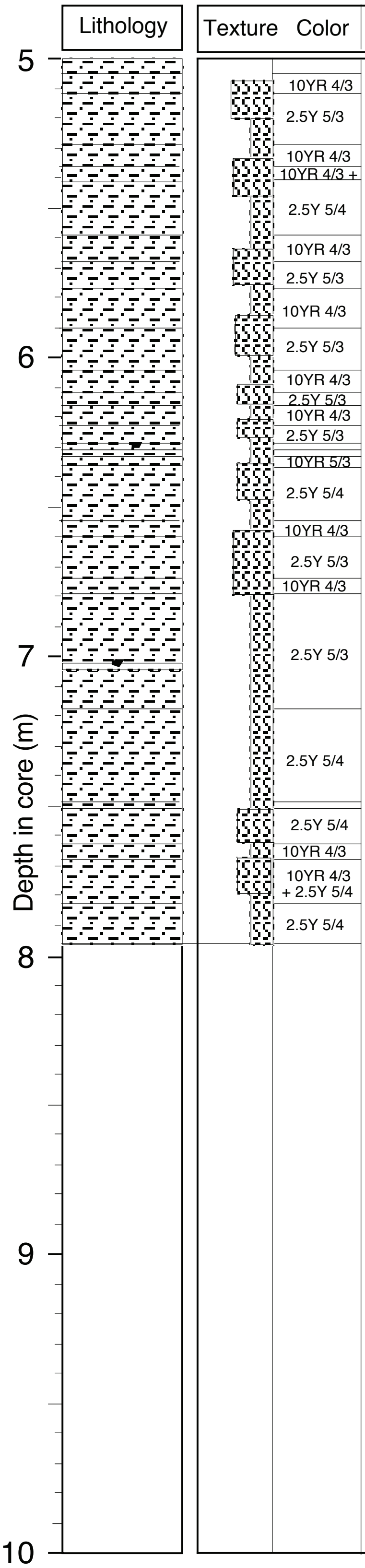

Description

434 – 441 cm: light olive brown (2.5Y 5/3) silty clay; mottled (olive gray spots/clouds); sharp contact at base
441 – 446 cm: brown (10YR 4/3) silty clay; 444-446 cm strongly mottled (light olive brown)
446 – 450 cm: light olive brown (2.5Y 5/3) silty clay; mottled; dropstone (1.5 cm in diameter) at 447 cm
450 – 453 cm: brown (10YR 5/3) silty clay; mottled
453 – 457 cm: light olive brown (2.5Y 5/3) silty clay; brown mottling; silty-sandy lamina at 456.5 cm; sharp contact at base
457 – 464 cm: brown (10YR4/3) silty clay ; mottled in lower part
464 – 484 cm: light olive brown (2.5Y 5/3) silty clay; slightly mottled; at 475-479 cm more brown (10YR 5/3); sharp contact at base
484 – 500 cm: dark brown (10YR 3/3) silty clay; 494-497 cm strongly mottled
500 – 505 cm: yellowish brown (10YR 5/6) and brown (10YR 4/3) silty clay; mottled
505 – 512 cm: brown (10YR 4/3) silty clay; lower part mottled
512 – 529 cm: light olive brown (2.5Y 5/3) silty clay; brown mottling; Fe-Mn nodules
529 – 536 cm: brown (10YR 4/3) silty clay
536 – 541 cm: brown (10YR 4/3) and light olive brown (2.5Y 5/4) silty clay; strongly mottled
541 – 559 cm: light olive brown (2.5Y 5/4) silty clay; some Fe-Mn nodules (541-545 cm); sharp contact at base
559 – 568 cm: brown (10YR 4/3-5/3) silty clay
568 – 577 cm: brown (10YR 4/3) and light olive brown (2.5Y 5/3) silty clay; strongly mottled
577 – 578 cm: light olive brown (2.5Y 5/3) silty clay; sharp contact at base
578 – 590 cm: brown (10YR 4/3) silty clay
590 – 604 cm: light olive brown (2.5Y 5/3) silty clay (592-595 cm more brownish); 590-596 and 602-604 cm strongly mottled
604 – 612 cm: brown (10YR 4/3) silty clay
612 – 616 cm: light olive brown (2.5Y 5/3) and brown (10YR 4/3) silty clay; strongly mottled
616 – 623 cm: brown (10YR 4/3-5/3) silty clay
623 – 629 cm: light olive brown (2.5Y 5/3) silty clay; sharp contact at base
629 – 631 cm: dark grayish brown (10YR 4/2) silty clay; dropstone (1 cm in diameter) at top
631 – 633 cm: light olive brown (2.5Y 5/3) and brown (10YR 5/3) silty clay; strongly mottled
633 – 637 cm: brown (10YR 5/3) silty clay; mottled
637 – 655 cm: light olive brown (2.5Y 5/4) and brown (10YR 5/3) silty clay; strongly mottled; 653-655 light olive brown
655 – 660 cm: brown (10YR 4/3) silty clay
660 – 674 cm: yellowish brown (10YR 5/4) and brown (10YR 5/3) silty clay; strongly mottled; Fe-Mn nodules in upper part
674 –679 cm: brown (10YR 4/3) silty clay; lower part strongly mottled
679 – 704 cm: light olive brown (2.5Y 5/3) silty clay; dark brown mottling; some more sandy in lower half; sandy-silty lamina at 702 cm;dropstone (1 cm in diameter) at 701 cm
704 – 718 cm: light olive brown (2.5Y 5/3) (and some brownish) (sandy) silty clay; mottled; mud clasts at 702-704 cm; below 710 cm Fe-Mnnodules
718 – 749 cm: light olive brown (2.5Y 5/4) silty clay; some mottling
749 – 751 cm: dark brown (10YR 3/3) silty clay; some Fe-Mn micronodules
751 –763 cm: light olive brown (2.5Y 5/4) silty clay; brown mottling; some more brownish interval at 759-761 cm; Fe-Mn micronodules; sharp contact at base
763 – 768 cm: brown (10YR 4/3) silty clay
768 – 783 cm: brown (10YR 4/3) and light olive brown (2.5Y 5/4) silty clay; some mottling
783 – 796 cm: light olive brown (2.5Y 5/4) silty clay; some mottling

796 – 813 cm: Core Catcher (subcore not opened yet)

PS 72/ 430-3 (GKG)

Makarov Basin

ARK- XXIII/3 (Arctic 08)

Recovery: 36 cm

81° 2,29' N 164° 45,59' E

Water depth: 2875 m

Surface: brown sandy mud, very water-saturated; bioturbated, some valves

Colour	Texture	Description
10 YR 3/3		0-6 cm dark brown (10 YR 3/3) sandy silty clay
10 YR 5/4 / 5 Y 4/2	SSSSS SSSSS SSSSS	6-8 cm yellowish brown (10 YR 5/4) and olive gray (5 Y 4/2) (sandy) silty clay, very dark brown (10 YR 2/2) mottling
5 Y 4/2	SSS SSS SSS	8-11,5 cm olive gray (5 Y 4/2) silty clay, very dark brown (10 YR 2/2) mottling
10 YR 5/4	SSSSS SSSSS SSSSS	11,5-15 cm yellowish brown (10 YR 5/4) silty clay, olive gray and very dark brown mottling
10 YR 4/4 and 5/4		15-22,5 cm dark yellowish brown (10 YR 4/4) and yellowish brown (10 YR 5/4) silty clay, dark gray (5 Y 4/1) mottling, 'pinkish' spots at 20-22 cm
2.5 Y 5/4		22,5-23,5 cm light olive brown (2.5 Y 5/4) silty clay
10 YR 4/4		23,5-25 cm dark yellowish brown (10 YR 4/4) silty clay, very soft
5 Y 5/2		25-26 cm olive gray (5 Y 5/2) silty clay, some 'pinkish' spots
10 YR 4/4 and 5/4	SSS SSS SSS SSS	26-29,5 cm dark yellowish brown (10 YR 4/4 and 3/4) silty clay, some 'pinkish' spots at 26 cm
10 YR 3/4	SSS SSS SSS SSS SSS SSS	29,5-36 cm dark yellowish brown (10 YR 3/4) (sandy) silty clay, slightly mottled (dark yellowish brown 10 YR 4/4)

A. 4.2 DATA OF SMEAR-SLIDE ANALYSIS (A. KRYLOV)

App. 4.2 Tab. 1: Grain-size and composition of Core PS72/287-3, based on smear-slide estimates

Depth cmbsf	a	b	c	d	e	f	g	h	i	j	k	l	m	n	o	p	q	r	Sediment
4	8	30	62	10	2	1	1	62	15	0	0	3	0	1	0	0	3	2	silty clay
65	5	30	65	10	2	2	1	65	12	2	0	2	0	0	0	0	3	1	silty clay
130	2	35	63	15	3	1	1	60	15	2	0	2	0	0	0	0	1	0	silty clay
230	5	35	60	17	2	1	1	60	13	1	1	2	0	0	0	0	1	1	silty clay
280	5	35	60	16	3	1	2	60	13	1	0	3	0	0	0	0	0	1	silty clay
290	5	30	65	10	2	2	1	50	30	1	0	3	0	0	1	0	0	0	silty clay
318	5	25	70	10	3	2	1	49	30	1	0	3	0	0	1	0	0	0	silty clay
328	4	30	66	10	2	0	1	64	18	1	0	2	0	0	1	0	0	1	silty clay
356	2	28	70	10	3	1	1	69	10	1	0	2	0	0	1	0	1	1	silty clay
370	2	30	68	15	3	0	1	58	20	1	0	2	0	0	0	0	0	0	silty clay
390	2	23	75	10	2	1	1	33	50	1	0	2	0	0	0	0	0	0	silty clay
407	3	30	67	15	3	0	1	32	45	1	0	3	0	0	0	0	0	0	silty clay
414	2	35	63	16	2	0	1	63	15	0	0	3	0	0	0	0	0	0	silty clay
427	2	35	63	15	2	0	2	63	15	1	0	2	0	0	0	0	0	0	silty clay
457	1	30	69	12	2	0	1	63	20	0	0	2	0	0	0	0	0	0	silty clay

App. 4.2 Tab. 2: Grain-size and composition of Core PS72/291-2, based on smear-slide estimates

Depth cmbsf	a	b	c	d	e	f	g	h	i	j	k	l	m	n	o	Sediment
20	1	25	74	10	2	1	2	74	1	1	3	0	5	1	0	silty clay
52	1	20	79	10	2	1	1	79	2	0	3	0	1	0	1	(silty) clay
94	3	30	67	10	2	0	2	62	20	0	3	1	0	0	0	silty clay
114	1	29	70	12	2	2	2	70	8	0	4	0	0	0	0	silty clay
117	2	35	63	15	2	2	2	63	10	0	5	1	0	0	0	silty clay
132	2	35	63	18	2	1	1	63	8	0	4	1	0	2	0	silty clay
145	5	35	60	18	1	2	1	60	16	0	2	0	0	0	0	silty clay
147	2	35	63	12	0	1	1	63	19	1	2	0	0	1	0	silty clay

App. 4.2 Tab. 3: Grain-size and composition of Core PS72/340-5, based on smear-slide estimates

Depth cmbsf	a	b	c	d	e	f	g	h	i	j	k	l	m	n	o	p	Sediment
7	15	30	55	10	4	3	1	55	5	0	2	0	8	3	7	2	sand-bearing silty clay
25	3	25	72	12	2	1	2	72	2	1	3	0	2	2	1	0	silty clay
49	3	20	77	10	1	2	2	77	1	0	3	1	0	2	1	t.	silty clay
88	10	30	60	14	3	2	2	60	7	1	2	0	5	3	1	t.	silty clay
103	15	30	55	7	3	5	2	55	22	0	2	0	0	2	2	0	sand-bearing silty clay
110	10	30	60	6	3	1	1	60	7	0	2	0	7	3	7	3	silty clay
112	7	28	65	5	2	1	1	65	5	0	2	0	10	0	8	1	silty clay
140	3	25	72	12	3	0	3	72	1	1	1	0	2	5	0	0	silty clay
200	2	20	78	10	2	0	3	78	t.	1	2	0	0	4	0	0	silty clay
280	2	20	78	11	2	0	3	78	t.	0	2	1	0	3	0	0	silty clay
304	6	30	64	8	3	2	3	64	5	0	3	1	5	2	2	2	silty clay
308	6	30	64	14	2	1	3	64	4	0	3	1	3	1	2	2	silty clay
315	6	30	64	4	1	1	1	38	50	0	2	0	0	2	1	t.	silty clay
316	10	40	50	5	1	2	1	48	40	0	2	0	0	0	1	0	silty clay
355	7	28	65	11	3	2	2	65	4	0	3	1	5	0	2	2	silty clay
400	3	25	72	13	2	0	3	72	1	0	2	1	0	6	t.	t.	silty clay
427	3	25	72	11	2	3	2	72	2	0	3	0	5	0	0	0	silty clay
460	4	26	70	14	2	1	3	70	1	0	3	1	0	5	0	0	silty clay
502	10	30	60	12	3	3	1	60	12	0	3	1	5	0	0	0	silty clay
510	15	35	50	5	1	1	1	50	40	0	2	0	0	0	0	0	sand-bearing silty clay
512	10	25	65	4	1	2	1	40	50	0	2	0	0	0	0	0	silty clay
520	10	30	60	10	2	1	2	50	25	0	2	1	3	0	3	1	silty clay
540	5	25	70	6	2	1	1	70	7	0	2	1	5	0	3	2	silty clay
580	4	25	71	11	3	1	3	71	1	0	3	1	2	4	0	0	silty clay
660	10	30	60	10	2	1	1	60	15	0	2	1	5	0	2	1	silty clay
665	5	25	70	7	2	1	1	70	10	0	2	1	3	0	2	1	silty clay
671	8	35	57	10	3	1	2	57	15	0	3	1	5	0	2	1	silty clay
676	5	25	70	5	2	1	2	70	12	0	2	1	3	0	2	t.	silty clay
682	5	30	65	11	3	1	3	65	4	0	3	1	5	0	2	2	silty clay
690	4	30	66	13	3	2	3	66	3	0	2	1	4	0	1	2	silty clay
700	5	30	65	14	3	1	2	65	3	0	3	1	5	0	2	1	silty clay
710	4	25	71	10	3	2	3	71	5	0	2	2	1	0	t.	1	silty clay
716	10	20	70	2	0	0	0	37	60	0	1	0	0	0	0	0	silty clay
730	7	25	68	13	3	1	1	68	3	1	2	1	5	0	1	1	silty clay
740	5	25	70	12	3	1	1	70	3	0	2	1	5	0	1	1	silty clay
750	5	20	75	12	2	1	2	75	3	0	2	1	2	0	0	0	silty clay
760	5	25	70	12	2	0	2	70	4	0	2	1	5	0	1	1	silty clay
770	20	25	55	5	2	1	0	52	35	0	2	1	2	0	0	0	sand-bearing silty clay
783	20	30	50	14	5	1	1	50	20	0	3	1	4	0	1	0	silty clay
786	25	30	45	3	0	1	0	27	65	0	2	1	1	0	0	0	
800	10	25	65	13	4	1	1	65	8	0	2	1	5	0	t.	0	silty clay
807	20	30	50	3	0	0	1	43	50	0	2	1	0	0	0	0	sand-bearing silty clay

App. 4.2 Tab. 4: Grain-size and composition of Core PS72/342-1, based on smear-slide estimates

Depth a b c d e f g h i j k l m n o p q r Sediment
cmbsf
1 10 30 60 10 2 2 2 60 10 0 0 2 0 6 0 4 2 silty clay
10 4 20 76 9 2 1 2 76 3 0 0 3 0 2 0 1 1 silty clay
25 3 25 72 5 2 3 2 72 4 0 0 1 0 8 0 2 1 silty clay
30 10 30 60 12 3 1 2 60 15 0 0 1 0 2 0 3 1 silty clay
43 10 40 50 10 2 2 2 40 30 0 0 1 0 4 3 5 1 silty clay
50 10 25 65 8 2 2 1 65 10 0 0 2 1 5 0 3 1 silty clay
100 3 25 72 14 3 2 3 72 0 0 0 3 1 0 2 0 0 silty clay
120 15 25 60 15 3 3 3 60 10 0 0 2 1 0 2 1 0 sand-bearing silty clay
132.5 8 27 65 7 3 3 1 65 10 0 0 1 1 3 0 5 1 silty clay
138 10 30 60 10 3 2 1 60 12 0 0 1 1 3 0 5 2 silty clay
141 5 30 65 6 2 2 1 65 12 0 1 2 1 2 0 4 2 silty clay
160 5 20 75 10 2 2 3 75 2 0 0 2 0 0 2 1 1 silty clay
173 5 25 70 8 2 1 1 70 4 0 0 2 0 4 2 4 2 silty clay
175 6 25 69 8 3 3 2 69 5 0 0 1 1 2 0 5 1 silty clay
180 6 25 69 9 3 4 2 69 5 0 0 2 1 0 0 4 1 silty clay
200 2 20 78 10 3 2 3 78 1 0 0 2 0 1 0 0 0 silty clay
260 8 30 62 13 4 4 3 62 6 1 0 2 1 3 0 1 t. silty clay
320 10 30 60 17 5 5 3 60 4 0 0 2 1 3 0 0 0 silty clay

App. 4.2 Tab. 5: Grain-size and composition of Core PS72/344-3, based on smear-slide estimates

Depth a b c d e f g h i j k l m n o p q r Sediment
cmbsf
27 5 25 70 12 3 2 4 70 4 0 0 3 0 2 0 0 silty clay
58 1 25 74 12 2 1 3 74 1 0 0 2 1 4 0 0 silty clay
112 3 25 72 11 2 2 3 72 1 0 0 2 1 6 0 0 silty clay
215 3 25 72 15 2 2 3 72 1 0 0 4 1 0 0 0 silty clay
290 1 20 79 9 2 1 3 66 15 0 0 3 1 0 0 0 silty clay
298 5 25 70 16 3 1 3 70 2 0 0 3 1 0 1 0 silty clay

App. 4.2 Tab. 6: Grain-size and composition of Core PS72/392-5, based on smear-slide estimates

Depth a b c d e f g h i j k l m n o p q r Sediment
Cmbsf
3 7 30 63 6 1 2 1 63 25 0 0 2 0 0 0 0 silty clay
7 10 30 60 5 1 2 0 54 35 0 0 2 0 0 1 t. silty clay
8,5 10 25 65 10 2 3 1 65 5 0 0 1 0 8 3 2 silty clay
22,5 15 35 50 32 7 4 3 50 1 0 0 3 0 0 0 0 sand-bearing silty clay

25,5	10	30	60	25	2	2	1	60	5	0	0	2	0	3	0	t.	silty clay
44	5	35	60	5	1	3	1	60	28	0	0	2	0	0	0	0	silty clay
47	5	20	75	5	1	2	2	75	7	0	0	1	0	5	1	1	silty clay
57,5	10	35	55	5	2	3	1	51	35	0	0	2	0	0	1	0	silty clay
59	15	35	50	5	2	2	0	44	45	0	0	2	0	0	0	0	sand-bearing silty clay
73,5	15	30	55	27	6	3	3	55	1	0	1	3	1	0	0	0	sand-bearing silty clay
95	7	25	68	14	2	2	2	68	3	0	0	3	1	3	1	1	silty clay
128,5	10	30	60	10	2	4	0	52	30	0	0	2	0	0	0	0	silty clay
134	5	20	75	9	1	3	2	75	3	0	0	2	0	3	1	1	silty clay
150	15	30	55	10	1	4	0	53	30	0	0	1	1	0	0	0	sand-bearing silty clay
165	10	30	60	9	2	3	3	60	20	0	0	3	0	0	0	0	silty clay
179	5	20	75	6	1	1	1	75	5	1	0	2	0	6	1	1	silty clay
205	15	35	50	23	5	6	3	50	7	0	0	3	1	2	0	0	sand-bearing silty clay
222	10	30	60	18	3	3	1	60	12	0	0	2	1	0	0	0	silty clay
229	3	20	77	12	2	1	1	77	4	1	0	2	0	0	0	0	silty clay
244	4	20	76	1	2	1	1	76	1	1	0	2	1	3	0	0	silty clay
264	10	25	65	19	4	2	2	65	1	0	0	2	1	4	0	0	silty clay
310	5	30	65	23	3	3	3	65	0,1	1	0	2	0	0	0	0	silty clay
434	5	20	75	11	3	1	2	75	0,1	0	0	2	1	5	0	0	silty clay
478	7	25	68	19	2	3	2	68	0,1	0	0	2	1	3	0	0	silty clay
550	7	25	68	16	2	2	2	68	0	0	0	2	1	7	0	0	silty clay
603	5	25	70	17	2	2	2	70	0	0	0	1	1	5	0	0	silty clay

App. 4.2 Tab. 7: Grain-size and composition of Core PS72/396-5, based on smear-slide estimates

Depth cmbsf	a	b	c	d	e	f	g	h	i j k l m n o p q r							Sediment
11	7	25	68	11	2	1	2	68	5	0	2	0	4	4	1	silty clay
19,5	15	30	55	28	4	4	3	55	1	1	3	1	0	0	0	sand-bearing silty clay
34	20	35	45	40	5	3	3	45	1	0	3	0	0	0	0	sand-bearing silty clay
65	10	35	55	10	1	2	1	42	40	0	3	0	0	1	0	silty clay
87	7	30	63	20	3	3	4	63	4	1	2	0	0	0	t.	silty clay
106	8	30	62	16	2	2	2	62	9	0	2	0	3	1	1	silty clay
107	10	30	60	14	2	4	2	60	10	0	2	2	4	0	t.	silty clay
129,5	7	30	63	7	1	2	0	39	50	0	1	0	0	t.	0	silty clay
134	6	30	64	8	2	2	1	64	20	0	3	0	0	0	0	silty clay
166	10	30	60	14	2	2	1	60	18	0	2	1	0	0	0	silty clay
193	20	30	50	30	5	2	1	50	7	0	3	0	0	1	1	sand-bearing silty clay
230	4	25	71	10	2	4	2	71	8	0	2	1	0	0	0	silty clay
269	7	30	63	21	3	3	2	63	1	0	3	1	3	0	0	silty clay
305	5	25	70	14	3	3	3	70	1	0	2	1	3	0	0	silty clay
420	30	30	40	44	8	3	2	40	t.	0	3	0	0	0	0	mixed sediment
487	8	25	67	18	2	3	3	67	1	0	3	1	2	0	0	silty clay
500	10	30	60	20	3	3	2	60	1	0	3	1	7	0	0	silty clay
513	10	25	65	20	4	3	3	65	1	0	3	1	0	0	0	silty clay
550	6	25	69	19	2	1	1	69	1	0	1	1	5	0	t.	silty clay

612,5	5 25 70 15 3 1 2 70 1 0 2 1 5 0 t.	silty clay
649	10 25 65 18 3 4 3 65 t. 0 2 1 4 0 0	silty clay
651	10 30 60 25 5 3 3 60 t. 0 3 1 0 0 0	silty clay

App. 4.2 Tab. 8: Grain-size and composition of Core PS72/422-5, based on smear-slide estimates

Depth cmbsf	a b c d e f g h i j k l m n o p q r	Sediment
37	4 25 71 13 2 0 2 71 2 0 1 0 5 2 1 1	silty clay
66	2 25 73 14 2 1 2 73 2 0 1 0 2 3 t. 0	silty clay
75	20 40 40 34 7 3 4 40 2 1 6 1 2 0 0 0	mixed sediment
93	5 35 60 5 0 0 0 50 45 0 0 0 0 0 0 0	silty clay
113	3 20 77 12 1 0 0 77 2 0 2 0 3 3 0 0	silty clay
141	15 25 60 22 2 2 3 60 3 0 3 2 3 0 0 0	sand-bearing silty clay
167	5 25 70 12 3 1 2 70 2 0 3 1 4 2 t. 0	silty clay
192	7 25 68 21 2 1 1 68 1 0 2 1 0 3 0 0	silty clay
220	10 35 55 5 0 0 0 42 50 0 2 0 0 0 1 0	silty clay
269	15 25 60 19 6 3 2 60 1 0 3 1 2 3 0 0	sand-bearing silty clay
295	10 25 65 22 4 3 3 65 1 0 2 0 0 0 0 0	silty clay
348	7 38 55 25 5 3 5 55 1 0 5 1 0 0 0 0	silty clay
362	10 30 60 25 2 2 2 60 5 0 3 1 0 0 0 0	silty clay

t.: traces

a Sand (%)
b. Silt (%)
c. Clay (%)
d. Quartz
e. Feldspar
f. Rock Fragments
g. Mica
h. Clay
i. Terrigenous Carbonates
j. Pyrite
k. Glaukonite
l. Heavy Minerals
m. Micronodules
n. Fe-hydro-oxides
o. Foramininfers
p. Coccoliths
q. Diatoms
r. Spicules

A.4.3 OCCURRENCE OF LARGE-SIZED DROPSTONES (A. KRYLOV)

No	Size, cm	Rock	Comments
PS72/287-1 (40 stones)			
BC-1	7 x 6 x 5	Carbonate	
BC-2	7 x 5 x 2	Carbonate	
BC-3	5 x 3 x 1	Carbonate	
BC-4	6 x 4 x 1,5	Carbonate	laminated
BC-5	4 x 3,5 x 3,5	Carbonate	
BC-6	4,5 x 4 x 1,5	Carbonate	
BC-7	5 x 3,5 x 1,5	Carbonate	
BC-8	4,5 x 3 x 1,5	Carbonate	
BC-9	3,5 x 2 x 1,5	Carbonate	black
BC-10	4 x 2 x 1,5	Carbonate	
BC-11	3 x 1,5 x 1,5	Carbonate	
BC-12	3 x 2 x 1,5	Carbonate	
BC-13	2,5 x 2 x 1	Carbonate	
BC-14	2,5 x 2 x 1	Carbonate	
BC-15	2 x 2 x 1	Carbonate	
BC-16	2,5 x 2 x 1	Carbonate	
BC-17	2 x 2 x 0,7	Carbonate	
BC-18	3,5 x 1,3 x 1	Carbonate	
BC-19	2,5 x 1,8 x 1	Carbonate	
BC-20	2,5 x 1,5 x 1	Carbonate	
BC-21	2,5 x 1,5 x 1	Carbonate	
BC-22	3 x 1,5 x 0,8	Carbonate	
BC-23	2,5 x 1,5 x 0,7	Carbonate	
BC-24	2 x 1,7 x 0,5	Carbonate	
BC-25	1,8 x 1,7 x 0,8	Carbonate	
BC-26	2 x 1,5 x 1	Carbonate	
BC-27	2 x 1,3 x 0,9	Carbonate	
BC-28	2 x 1,5 x 0,8	Carbonate	
BC-29	2 x 1,2 x 1	Carbonate	
BC-30	2 x 1,5 x 0,8	Carbonate	
BC-31	2 x 1,5 x 0,5	Carbonate	
BC-32	1,8 x 1,3 x 1,2	Carbonate	
BC-33	2 x 1,2 x 1	Carbonate	
BC-34	1,7 x 1,7 x 0,7	Carbonate	
BC-35	2,5 x 1 x 0,9	Carbonate	
BC-36	2 x 1,2 x 0,9	Carbonate	
BC-37	3 x 2 x 0,7	non-carbonate	
BC-38	2 x 1,6 x 0,5	Sandstone	
BC-39	1,8 x 1,1 x 0,8	Carbonate	
BC-40	1,5 x 1,4 x 0,8	Carbonate	
PS72/289-1			
no stones			
PS72/291-1			

no stones			
PS72/340-3 (11 stones)			
BC-41	2 x 1,4 x 0,7	Dolomite	from surface
BC-42	2,5 x 1,3 x 1	Granite	
BC-43	2 x 1,5 x 1,2	Dolomite	
BC-44	1,5 x 1 x 1	Dolomite	
BC-45	1,5 x 1,3 x 1	Sandstone	
BC-46	1,8 x 1,1 x 0,8	Dolomite	
BC-47	1,7 x 1,3 x 1	Dolomite	
BC-48	2 x 1,6 x 0,5	Sandstone	
BC-49	2 x 1 x 0,5	non-carbonate	
BC-50	1,7 x 1,1 x 0,5	Dolomite	
BC-51	1,7 x 1 x 0,5	non-carbonate	
PS72/341-3 (20 stones)			
BC-52	2,7 x 2 x 2	Dolomite	
BC-53	2,2 x 2,2 x 1,2	Dolomite	
BC-54	3,1 x 2 x 1,9	Dolomite	
BC-55	2,3 x 2 x 1,1	Dolomite	
BC-56	2,2 x 1,5 x 1,5	Dolomite	
BC-57	2,3 x 1,3 x 1	Dolomite	
BC-58	1,8 x 1,6 x 1	Dolomite	
BC-59	2 x 1,6 x 1	Dolomite	
BC-60	2,5 x 1,7 x 0,8	Dolomite	
BC-61	2 x 1,4 x 0,9	Dolomite	
BC-62	1,9 x 1,3 x 0,8	Dolomite	
BC-63	1,7 x 1 x 0,8	Sandstone	
BC-64	2,2 x 1 x 0,8	Dolomite	
BC-65	1,5 x 1 x 0,8	Dolomite	
BC-66	1,7 x 1,2 x 1	Dolomite	
BC-67	1,1 x 1 x 0,6	Dolomite	
BC-68	1,7 x 1,1 x 0,6	Dolomite	
BC-69	1,8 x 1,2 x 0,8	Dolomite	
BC-70	1,8 x 1,3 x 0,8	Sandstone	
BC-71	1,7 x 1,2 x 0,2	Schist	
PS72/343-3 (3 stones)			
BC-72	1,7 x 1,3 x 1,3	Limestone	
BC-73	1,5 x 1,2 x 0,8	Sandstone(?)	
BC-74	1,3 x 1,1 x 0,8	Quartzite	
PS72/344-1 (4 stones)			
BC-75	1,9 x 1,9 x 1,4	Dolomite	
BC-76	2 x 1,4 x 1	non-carbonate	black
BC-77	2 x 1,5 x 1	Dolomite	5-7 cmbsf
BC-78	2 x 2 x 0,6	Dolomite	7-9 cmbsf
PS72/392-6 (41 stones)			
BC-79	7,5 x 6,5 x 3	Limestone	10-12 cmbsf
BC-80	5,5 x 3,5 x 2,5	Dolomite	10-12 cmbsf
BC-81	4,3 x 3 x 1	Dolomite	
BC-82	3 x 3 x 1,5	Dolomite	

BC-83	4,5 x 3 x 0,9	Limestone	
BC-84	2,5 x 2,2 x 1,7	Dolomite	
BC-85	2,5 x 2 x 1,2	Limeston	
BC-86	2,2 x 2 x 0,7	Dolomite	
BC-87	2,3 x 2 x 1,8	Dolomite	
BC-88	2,3 x 1,3 x 0,8	Dolomite	
BC-89	2 x 1,5 x 0,8	Dolomite	
BC-90	2,7 x 1,1 x 1,1	Sandstone	
BC-91	2,2 x 1,2 x 1	Dolomite	
BC-92	1,6 x 1,5 x 0,7	Quartzite	
BC-93	1,7 x 1,5 x 1,2	Quartzite	
BC-94	1,4 x 1,1 x 1,1	Quartzite	
BC-95	1,5 x 1 x 0,7	Quartzite	
BC-96	1,5 x 1,3 x 0,7	Quartzite	
BC-97	1,1 x 1 x 0,5	Quartzite	
BC-98	1 x 0,9 x 0,7	Quartzite	
BC-99	1,2 x 1,1 x 0,9	Sandstone	
BC-100	2,1 x 1,1 x 0,7	Limestone	
BC-101	1,7 x 1 x 0,7	Limestone	
BC-102	1,5 x 1,3 x 0,9	Limestone	
BC-103	1,4 x 1 x 1	Limestone	
BC-104	1,7 x 1 x 0,8	Limestone	
BC-105	1,5 x 0,8 x 0,8	Limestone	
BC-106	1,3 x 1 x 0,9	Limestone	
BC-107	1,5 x 1,1 x 0,8	non-carbonate	black
BC-108	1,8 x 1,2 x 0,2	non-carbonate	
BC-109	1,5 x 1,1 x 1	Dolomite	
BC-110	1,6 x 1 x 1	Dolomite	
BC-111	2,2 x 1 x 0,8	Dolomite	
BC-112	2,4 x 1 x 0,4	Dolomite	
BC-113	1,6 x 1 x 0,5	Dolomite	
BC-114	1,6 x 1,4 x 0,6	Dolomite	
BC-115	1,5 x 0,9 x 0,8	Dolomite	
BC-116	1,6 x 1,2 x 0,5	Dolomite	
BC-117	1,5 x 0,9 x 0,7	Dolomite	
BC-118	1,4 x 0,9 x 0,6	Dolomite	
BC-119	1,6 x 1,4 x 1	Granite	
PS72/393-3			
no stones			
PS72/396-3 (37 stones)			
BC-120	11 x 10 x 6	Limestone	from surface
BC-121	3 x 2,3 x 0,5	Limestone	from surface
BC-122	12 x 11 x 6	Sandstone	from middle
BC-123	6 x 3 x 2,4	Granite	
BC-124	6 x 2,5 x 2,2	Sandstone	
BC-125	3 x 2,7 x 1,5	Limestone	
BC-126	3,5 x 2 x 1,8	Sandstone	
BC-127	2,3 x 1,5 x 1,5	Limestone	

BC-128	2,5 x 1,6 x 1,1	Quartzite	
BC-129	2,3 x 1,1 x 1,2	Quartzite	
BC-130	1,6 x 1 x 0,8	Quartzite	
BC-131	1,2 x 1x 0,3	Quartzite	
BC-132	3 x 2,2 x 1,5	Sandstone	
BC-133	2 x 1,1 x 1	Sandstone	
BC-134	2 x 1,2 x 0,6	Sandstone	
BC-135	2 x 1 x 0,9	Sandstone	
BC-136	1,9 x 1,5 x 0,4	Sandstone	
BC-137	1,5 x 1 x 0,4	Sandstone	
BC-138	1,4 x 1,3 x 1,1	Limestone	
BC-139	1,7 x 1,2 x 0,9	Limestone	
BC-140	1,6 x 1,3 x 1,1	Limestone	
BC-141	1,7 x 1 x 0,8	non-carbonate	black
BC-142	2,5 x 1,8 x 1,4	Dolomite	
BC-143	2 x 2 x 1,3	Dolomite	
BC-144	2,3 x 2 x 0,8	Dolomite	
BC-145	2 x 1,3 x 0,7	Dolomite	
BC-146	2 x 1,5 x 1	Dolomite	
BC-147	1,6 x 1,2 x 0,8	Dolomite	
BC-148	2 x 1 x 0,7	Dolomite	
BC-149	1,5 x 1,1 x 0,8	Dolomite	
BC-150	1,5 x 1,1 x 1	Dolomite	
BC-151	1,3 x 1,2 x 0,9	Dolomite	
BC-152	1,6 x 0,9 x 0,7	Dolomite	
BC-153	1,5 x 1 x 0,8	Dolomite	
BC-154	1,3 x 1,2 x 1	Dolomite	
BC-155	1,2 x 1 x 0,7	Dolomite	
BC-156	1,1 x 1,1 x 0,6	Dolomite	
PS72/404-3 (32 stones)			
BC-157	2 x 1,8 x 1,2	Dolomite	from surface
BC-158	4 x 3,3 x 1,5	Dolomite	
BC-159	3,8 x 2,2 x 1	Dolomite	
BC-160	2,7 x 2 x 1	Dolomite	
BC-161	2,7 x 1,3 x 1,3	Dolomite	
BC-162	2,4 x 1,6 x 1	Dolomite	
BC-163	2 x 1,5 x 0,9	Dolomite	
BC-164	2 x 1,3 x 0,8	Dolomite	
BC-165	2,1 x 1,4 x 0,5	Dolomite	
BC-166	2,3 x 1 x 0,7	Dolomite	
BC-167	2,5 x 1,1 x 0,6	Dolomite	
BC-168	1,7 x 1 x 0,7	Dolomite	
BC-169	1,5 x 1,2 x 0,7	Dolomite	
BC-170	1,5 x 0,7 x 1,1	Dolomite	
BC-171	1,5 x 1,2 x 0,8	Dolomite	
BC-172	1,3 x 1,3 x 0,3	Dolomite	
BC-173	1,3 x 1 x 0,6	Dolomite	
BC-174	1,2 x 1 x 0,6	Dolomite	

BC-175	3 x 2 x 1,5	Limestone	
BC-176	2,8 x 1,8 x 0,8	Limestone	
BC-177	1,7 x 1,2 x 1,2	Limestone	
BC-178	1,5 x 0,8 x 1	Limestone	
BC-179	1,2 x 1 x 0,7	Limestone	
BC-180	2 x 1,5 x 0,3	Schist	
BC-181	1 x 0,7 x 0,8	non-carbonate	
BC-182	2 x 1,5 x 1,2	Granite	
BC-183	1,6 x 1,2 x 0,6	Granite	
BC-184	2 x 1,8 x 1	Quartzite	
BC-185	2 x 1,3 x 1	Quartzite	
BC-186	2,3 x 2 x 0,8	Sandstone	
BC-187	1,6 x 1,2 x 0,9	Sandstone	
BC-188	1,3 x 0,8 x 0,8	Sandstone	
PS72/408-3 (13 stones)			
BC-189	5 x 4,5 x 1,3	Limestone	from surface
BC-190	2 x 1,2 x 0,6	Limestone	
BC-191	1,7 x 1,2 x 0,6	Limestone	
BC-192	1,3 x 1,1 x 0,9	Limestone	
BC-193	2,5 x 1,4 x 0,6	Dolomite	
BC-194	2,1 x 1,7 x 1	Dolomite	
BC-195	1,6 x 1,2 x 0,6	Dolomite	
BC-196	1,3 x 1 x 1	Dolomite	
BC-197	1,7 x 1,1 x 0,4	Granite	
BC-198	1,7 x 1 x 0,9	Quartzite	
BC-199	1,3 x 1 x 0,8	Quartzite	
BC-200	1,2 x 1,1 x 0,7	Quartzite	
BC-201	1,8 x 0,9 x 0,3	Sandstone	
PS72/410-1 (37 stones)			
BC-202	6 x 4,5 x 2,5	Dolomite	
BC-203	3 x 1,8 x 2	Dolomite	
BC-204	3 x 1,7 x 1,3	Dolomite	
BC-205	1,9 x 1,3 x 1,4	Dolomite	
BC-206	2,3 x 1,4 x 0,7	Dolomite	
BC-207	2 x 1,3 x 0,7	Dolomite	
BC-208	2 x 1,5 x 1	Dolomite	
BC-209	2,5 x 1,2 x 0,3	Dolomite	
BC-210	1,5 x 1,2 x 0,7	Dolomite	
BC-211	1,8 x 1 x 0,6	Dolomite	
BC-212	1,6 x 1,2 x 0,7	Dolomite	
BC-213	1,6 x 1,2 x 0,5	Dolomite	
BC-214	1,2 x 1 x 0,5	Dolomite	
BC-215	1,1 x 1,2 x 0,5	Dolomite	
BC-216	1,7 x 1,2 x 1,1	Limestone	
BC-217	2,2 x 1,7 x 1	Limestone	
BC-218	1,6 x 1 x 0,6	Limestone	
BC-219	1,1 x 1 x 1	Limestone	
BC-220	1,2 x 1,1 x 0,5	Limestone	

BC-221	1,2 x 1 x 0,5	Limestone	
BC-222	1,2 x 1,2 x 0,8	Limestone	
BC-223	1 x 1 x 0,8	Limestone	
BC-224	5,5 x 4 x 3	Granite - Granodiorite	
BC-225	3,5 x 2,3 x 1,1	Granite - Granodiorite	
BC-226	2,3 x 1,3 x 0,9	Basalt	
BC-227	2,2 x 1,3 x 0,4	non-carbonate	
BC-228	1,8 x 1,3 x 0,7	non-carbonate	
BC-229	2,5 x 1,1 x 0,5	Chert	
BC-230	2,2 x 1,8 x 0,5	Quartzite	
BC-231	1,7 x 1,4 x 0,8	Quartzite	
BC-232	2,1 x 0,9 x 0,7	Quartzite	
BC-233	1,7 x 1,2 x 1	Sandstone	
BC-234	2,6 x 1,5 x 0,8	Sandstone	
BC-235	2 x 0,8 x 0,7	Sandstone	
BC-236	1,7 x 1 x 0,5	Sandstone	
BC-237	1,4 x 1 x 0,5	Sandstone	
BC-238	1,2 x 1 x 0,5	Sandstone	
PS72/413-3 (31 stone)			
BC-239	3 x 2,2 x 1,6	Limestone	from surface
BC-240	4,5 x 2,7 x 1,5	Dolomite	
BC-241	2,5 x 1,7 x 0,8	Dolomite	
BC-242	1,8 x 1,5 x 1,3	Dolomite	
BC-243	2,5 x 1,8 x 1,3	Dolomite	
BC-244	1,5 x 1,4 x 0,9	Dolomite	
BC-245	2 x 1,5 x 0,8	Dolomite	
BC-246	1,5 x 1,1 x 0,8	Dolomite	
BC-247	2,3 x 1 x 0,8	Dolomite	
BC-248	3 x 1,6 x 1,2	Dolomite	
BC-249	1,3 x 1 x 0,4	Dolomite	
BC-250	1,5 x 1,2 x 0,7	Dolomite	
BC-251	1,4 x 1 x 0,5	Dolomite	
BC-252	1,5 x 1,1 x 0,6	Dolomite	
BC-253	1,3 x 1 x 0,8	Dolomite	
BC-254	1,2 x 1,1 x 0,4	Dolomite	
BC-255	2 x 1,9 x 0,4	Limestone	
BC-256	2,1 x 1,8 x 1	Limestone	
BC-257	1,8 x 1,2 x 0,6	Limestone	
BC-258	1,8 x 1,2 x 0,8	Limestone	
BC-259	1,8 x 0,8 x 0,8	Limestone	
BC-260	2,2 x 1,2 x 0,8	Granite	
BC-261	4 x 2,3 x 0,5	Sandstone	
BC-262	2 x 1,6 x 0,3	Sandstone	
BC-263	2,2 x 1,4 x 0,3	Sandstone	
BC-264	1,7 x 1,5 x 0,7	Sandstone	
BC-265	1,7 x 0,8 x 0,7	Sandstone	
BC-266	1,5 x 1,2 x 0,3	Sandstone	
BC-267	1,7 x 1 x 0,5	Sandstone	

BC-268	1,2 x 1,1 x 0,4	Sandstone
BC-269	2,4 x 1,7 x 0,6	Schist
PS72/418-5 (15 stones)		
BC-270	5 x 2 x 0,6	Limestone
BC-271	1,3 x 0,7 x 0,8	Limestone
BC-272	2,3 x 1,3 x 0,9	Dolomite
BC-273	1,9 x 1 x 0,6	Dolomite
BC-274	1,5 x 1 x 0,7	Dolomite
BC-275	1,1 x 0,8 x 1	Dolomite
BC-276	2,2 x 1,7 x 0,7	Sandstone
BC-277	2 x 1,7 x 0,5	Sandstone
BC-278	2,1 x 1,4 x 0,8	Sandstone
BC-279	2 x 1,5 x 0,7	Sandstone
BC-280	1,7 x 1,5 x 0,5	Sandstone
BC-281	1,8 x 1,5 x 0,5	Sandstone
BC-282	1,5 x 1,1 x 0,4	Sandstone
BC-283	1,5 x 1,1 x 0,6	Sandstone
BC-284	1,3 x 1,1 x 0,7	Sandstone
PS72/422-3 (11 stones)		
BC-285	4 x 2 x 1,5	Limestone
BC-286	1,8 x 1,1 x 0,6	Limestone
BC-287	1,3 x 1 x 0,4	Limestone
BC-288	2,5 x 1,5 x 0,8	Dolomite
BC-289	1,7 x 1,2 x 1	Dolomite
BC-290	2 x 1 x 0,7	Dolomite
BC-291	1,2 x 1 x 1	Dolomite
BC-292	1,7 x 1,1 x 0,8	Quartzite
BC-293	2,4 x 1,4 x 1,1	Sandstone
BC-294	2,3 x 1,2 x 0,4	Sandstone
BC-295	1,6 x 1 x 0,3	Sandstone
PS72/430-3 (9 stones)		
BC-296	2,4 x 1,6 x 1,8	Quartzite
BC-297	1,3 x 1,2 x 0,3	Quartzite
BC-298	2,2 x 1,7 x 0,6	Sandstone
BC-299	2 x 1,5 x 1	Granite
BC-300	1,3 x 0,9 x 0,6	Granite - Diorite
BC-301	2 x 1,2 x 1	Dolomite
BC-302	1,5 x 1 x 0,5	Dolomite
BC-303	1,4 x 1,2 x 0,6	Dolomite
BC-304	2 x 1,4 x 1	Limestone
PS72/438-3 (2 stones)		
BC-305	1,6 x 0,8 x 0,8	Granite
BC-306	1,4 x 1 x 0,2	Schist
PS72/471-4 (3 stones)		
BC-307	2,2 x 1,8 x 1,5	non-carbonate
BC-308	4 x 2,7 x 0,3	non-carbonate
BC-309	3 x 1,5 x 0,8	non-carbonate

Stones from Gravity Corer

No	Interval, cm	Size, cm	Rock
PS72/287-3			
GC-1	18-19	2,5 x 1,3 x 1,2	Carbonate
GC-2	58-59	3,5 x 3 x 1,5	Carbonate
GC-3	316-317	3 x 2 x 1,4	Carbonate
GC-4	367-368	2 x 1,5 x 1,5	Carbonate
GC-5	381-384	3 x 3 x 2,5	Carbonate
GC-6	394-396	2,5 x 2 x 1,7	Carbonate
GC-7	398-399	1,5 x 1,5 x 1	Carbonate
GC-8	423-428	7,5 x 5 x 2	Carbonate
GC-9	430-433	3,5 x 3 x 1,5	Carbonate
GC-10	438-439	2 x 1,4 x 1	Carbonate
GC-11	439-440	1,3 x 1,1 x 1	Carbonate
GC-12	443-445	3 x 2 x 1,2	Carbonate
GC-13	450-452	3 x 2,5 x 1,5	Carbonate
GC-14	459-461	3 x 1,5 x 1,2	Carbonate
GC-15	Core Catcher	2,5 x 2 x 1,4	Carbonate
PS72/343-2			
GC-16	120	5,5 x 4,3 x 1,5	Sandstone
GC-17	314-316	3 x 1,8 x 0,6	Dolomite
GC-18	586	2,5 x 2 x 1,1	Dolomite
PS72/392-5			
GC-19	196-197	2,2 x 1,5 x 0,9	Dolomite
GC-20	281-282	2 x 1 x 0,4	non-carbonate
GC-21	289	1,4 x 1,1 x 0,6	Sandstone

Stones from Kastenlot

No	Interval, cm	Size, cm	Rock	Comments
PS72/291-2				
K-1	91-92	2 x 1,5 x 1,5	Dolomite	
K-2	146-148	2 x 1,5 x 1,5	Dolomite	"from ""pinkish"" layer"
PS72/340-5				
K-3	90-92	4,5 x 2,5x 2	Dolomite	
K-4	300-301	1,5 x 1,4 x 0,9	Limestone	upper part of the brown layer
K-5	415-416	1,5 x 1,2 x 0,7	Dolomite	
K-19	500	2,5 x 1,4 x 1,4	Dolomite	
K-20	500	5 x 3,5 x 3	Dolomite	
K-6	508	3,7 x 3,5 x 2	Limestone	"just above ""pinkish"" layer"
K-7	509-512	4,5 x 4 x 1,5	Dolomite	"in the ""pinkish"" layer"
K-8	511-512	2 x 1,3 x 0,7	non-carbonate	black
K-9	509-514	10,5 x 10 x 6,5	Dolomite	"in the ""pinkish"" layer"
K-10	509-514	8 x 6 x 5,5	Dolomite	"in the ""pinkish"" layer"
K-11	509-514	2 x 1,4 x 1	Dolomite	"in the ""pinkish"" layer"
K-12	509-514	3 x 2,5 x 2	Dolomite	"in the ""pinkish"" layer"
K-13	509-514	1,8 x 1,6 x 1,2	Dolomite	"in the ""pinkish"" layer"

K-14	514	6,5 x 6 x 1	Dolomite	"just below ""pinkish"" layer"
K-15	514-516	1,6 x 1,3 x 0,8	Dolomite	
K-16	514-516	1,1 x 1 x 0,9	Dolomite	
K-17	514-516	3 x 3 x 1,8	Quartzite	
K-18	573-575	2 x 1,4 x 1	Dolomite	
K-21	744-746	5,8 x 3,6 x 2,5	non-carbonate	coal (wood?) fragment
K-22	775	4 x 2,8 x 2	Dolomite	
K-23	807-809	2 x 1 x 1	Dolomite	
K-24	807-809	3 x 2 x 2	Dolomite	
K-25	807-809	6,5 x 6,5 x 2	Limestone	
K-26	807-809	2,5 x 1,8 x 1	Limestone	
K-27	Core catcher	2,2 x 1,3 x 1,2	Quartzite	
K-28	Core catcher	3 x 2,3 x 1	Quartzite	
K-29	Core catcher	5 x 2,8 x 2	Dolomite	
K-30	Core catcher	5,3 x 1,7 x 1,3	Dolomite	at the bottom
K-31	Core catcher	2,7 x 2,2 x 1	Dolomite	in sediment ""cap"" below CC
K-32	Core catcher	2 x 1,4 x 0,3	non-carbonate	imprint; in sed. "cap below CC
K-33	Core catcher	2 x 1,2 x 1	non-carbonate	black; in sed. "cap"below CC
K-34	Core catcher	2,2 x 1,5 x 1	Dolomite	in sediment ""cap"" below CC
K-35	Core catcher	1,8 x 1 x 1	Dolomite	in sediment ""cap"" below CC
PS72/341-5				
K-36	4-6	1,5 x 1,5 x 1,2	Dolomite	
K-37	150-151	2,5 x 2 x 1,7	Limestone	in upper part of brown layer
K-38	167-167	2,8 x 2 x 1,8	Dolomite	in bottom part of brown layer
K-39	169-170	2,5 x 1,8 x 1,2	Granite	
K-40	179-181	1,4 x 1 x 0,9	Dolomite	
PS72/396-5				
K-41	10-12	6 x 3 x 3,3	Dolomite	
K-42	11-12	1,8 x 1 x 1,1	Limestone	"in ""white"" layer"
K-43	12-13	2,5 x 2 x 1,7	Limestone	
K-44	15-18	8 x 6,5 x 3,5	Dolomite	in brown layer
K-45	29-30	2,5 x 2 x 1,3	Limestone	"in ""white"" layer"
K-46	31	2 x 1,4 x 1	Dolomite	"at boundary between ""white"" and ""pink"" layers"
K-47	109-111	3 x 2,6 x 2	Quartzite	
K-48	116-118	2,5 x 2 x 0,7	Sandstone	
K-49	129	5,5 x 4,5 x 1,5	Sandstone	
K-50	166	4 x 2,6 x 1,5	Sandstone	
K-51	166	1 x 1 x 0,7	Quartzite	
K-52	379-381	2,8 x 1,7 x 0,8	Sandstone	
K-53	530-532	3 x 1,5 x 1,2	non-carbonate	

K-54	587	3,3 x 1,8 x 1,2	Sandstone	
PS72/410-3				
K-55	75-77	6,7 x 3,7 x 3	Granite - Diorite	"above ""pinkish"" layer"
K-56	75-77	3,5 x 2 x 1,5	Dolomite	"above ""pinkish"" layer"
K-57	81-85	6 x 4,5 x 3	Dolomite	
K-58	85-90	5,5 x 3,7 x 3	Granite - Diorite	
K-59	130-131	1,8 x 1,4 x 1	Dolomite	
K-60	142-143	2,4 x 1,8 x 1,1	Chert	
K-61	145-147	3 x 1,8 x 1,5	Sandstone	
K-62	170-172	4,6 x 3,6 x 1,2	Dolomite	
K-63	172-174	4,5 x 2,5 x 2,8	Dolomite	
K-64	172-174	3,4 x 1,6 x 1,5	Sandstone	
K-65	174	3,5 x 1,9 x 1,3	Carbonate	
K-66	298	3,4 x 2 x 2,3	Dolomite	
K-67	300	2,5 x 1,6 x 0,8	Chert	
K-68	314	1,4 x 1,1 x 0,8	Limestone	black
K-69	395-396	2,7 x 2,3 x 2,8	Sandstone	in brown layer at the boundary with olive
K-70	479	2,8 x 1,7 x 0,5	Sandstone	
K-71	616-618	2,8 x 2,1 x 1,9	Dolomite	at the olive/brown boundary
K-72	697-698	2,1 x 0,8 x 0,9	non-carbonate	schist (?)
PS72/422-5				
K-73	7-9	1,6 x 1,3 x 0,9	non-carbonate	
K-78	99-101	2,7 x 1,7 x 1	Dolomite	
K-74	219	1,4 x 0,9 x 1,1	Dolomite	
K-75	257-260	6,5 x 3 x 3,5	Quartzite	
K-76	262-263	2 x 2 x 1,6	Quartzite	
K-77	263	10 x 7 x 3,5	Quartzite	
K-79	347	4,7 x 3,7 x 1,5	Sandstone	
K-80	361	4,5 x 2,5 x 1,5	Sandstone	
K-81	384	6 x 3,5 x 2	Dolomite	
K-82	417	1,9 x 1,5 x 0,8	Dolomite	
K-83	433-434	2,3 x 1,6 x 1	Granite - Diorite	
K-84	510	2,3 x 1,5 x 1	Dolomite	
K-85	516	3 x 2 x 1	Sandstone	black
K-86	610	1,6 x 1,5 x 0,8	Sandstone	
K-87	687	2 x 1 x 1	Dolomite	
K-88	700	1,5 x 1,4 x 1	Dolomite	
K-89	790	1,5 x 1,3 x 0,8	Sandstone	

A.4.4 SUMMARY PLOTS OF LOGGING DATA (F. NIESSEN, D. POGGEMANN, I. SCHULTE-LOH)

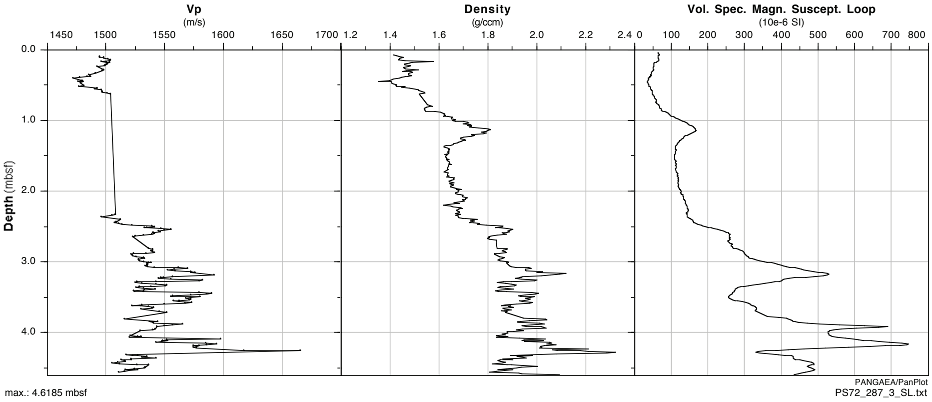

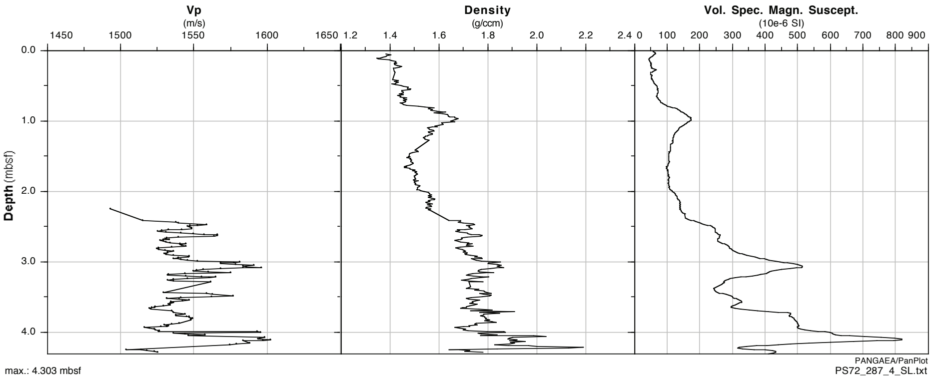

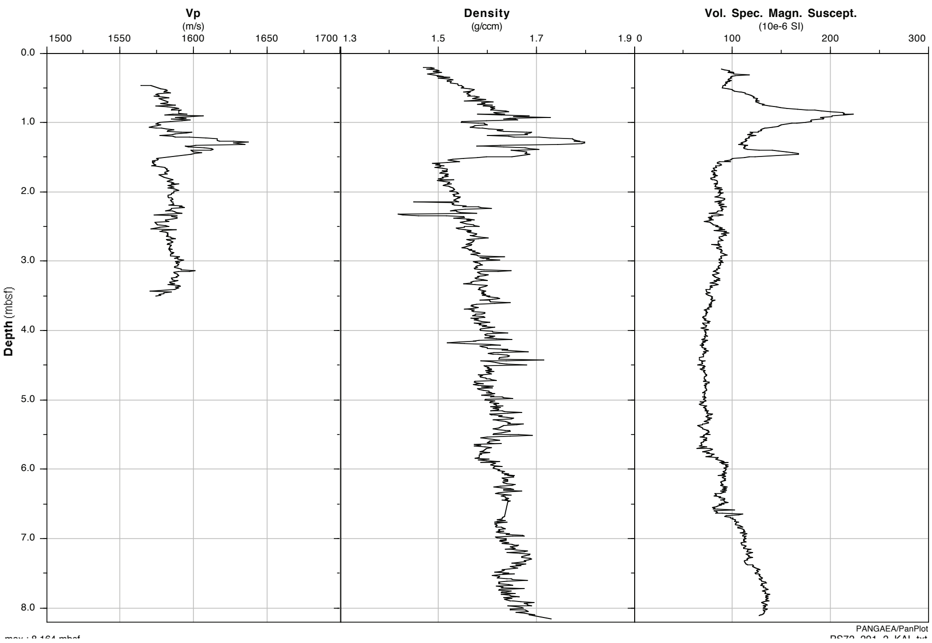

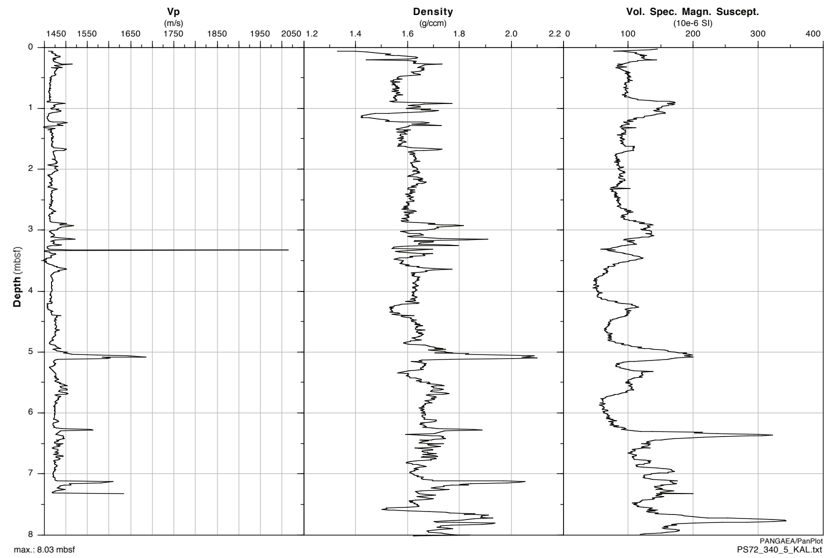
Vp
(m/s)
Density
(g/ccm)
Vol. Spec. Magn. Suscept.
(10e-6 SI)
Depth (mbsf)
max.: 8.03 mbsf
PANGAEA/PanPlot
PS72_340_5_KAL.txt

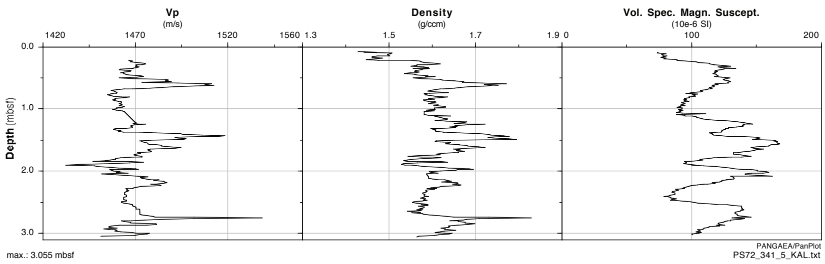
Vp
(m/s)
Density
(g/ccm)
Vol. Spec. Magn. Suscept.
(10e-6 SI)
Depth (mbsf)
max.: 3.055 mbsf
PANGAEA/PanPlot
PS72_341_5_KAL.txt

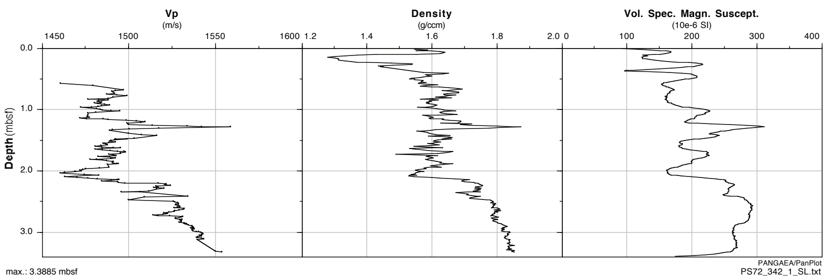
Vp
(m/s)
Density
(g/ccm)
Vol. Spec. Magn. Suscept.
(10e-6 SI)
Depth (mbsf)
max.: 3.3885 mbsf
PANGAEA/PanPlot
PS72_342_1_SL.txt

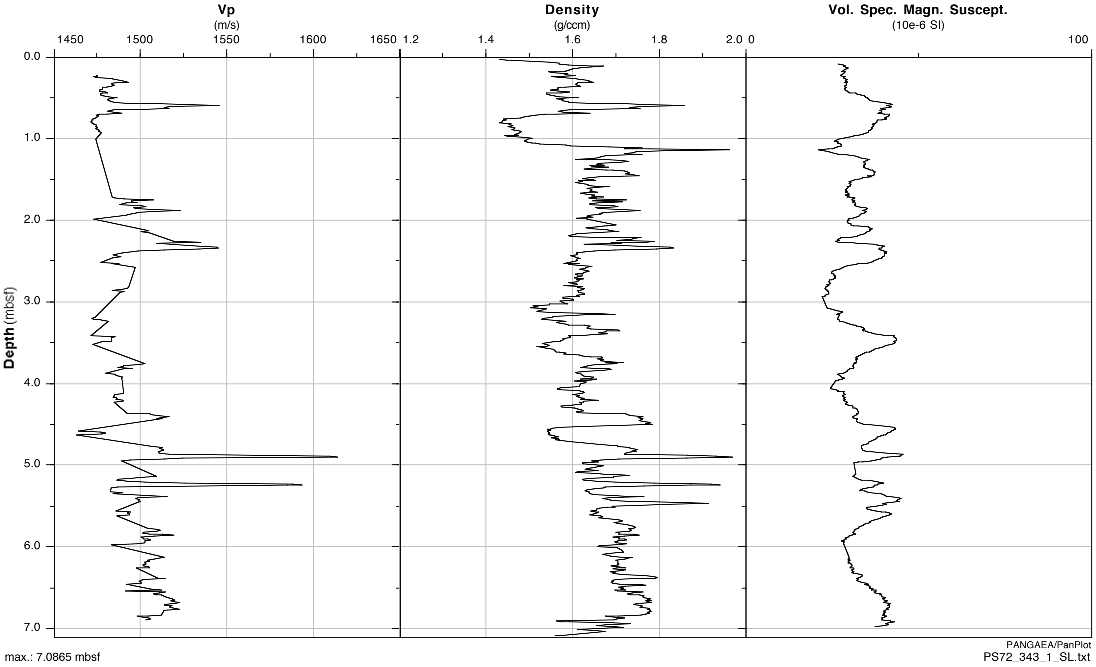
Vp
(m/s)
1450 1500 1550 1600 1650
Density
(g/ccm)
1.2 1.4 1.6 1.8 2.0
Vol. Spec. Magn. Suscept.
(10e-6 SI)
0 100
Depth (mbsf)
0.0 1.0 2.0 3.0 4.0 5.0 6.0 7.0
max.: 7.0865 mbsf
PANGAEA/PanPlot
PS72_343_1_SL.txt

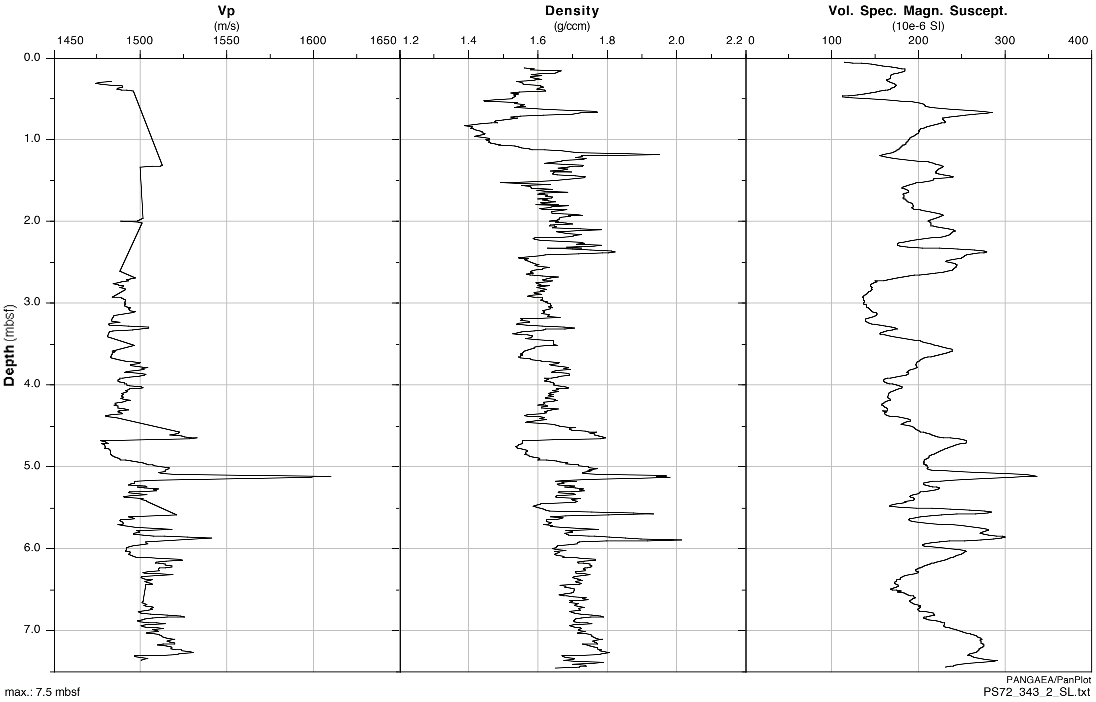
Vp
(m/s)
1450 1500 1550 1600 1650
Density
(g/ccm)
1.2 1.4 1.6 1.8 2.0 2.2
Vol. Spec. Magn. Suscept.
(10e-6 SI)
0 100 200 300 400
Depth (mbsf)
0.0 1.0 2.0 3.0 4.0 5.0 6.0 7.0
max.: 7.5 mbsf
PANGAEA/PanPlot
PS72_343_2_SL.txt

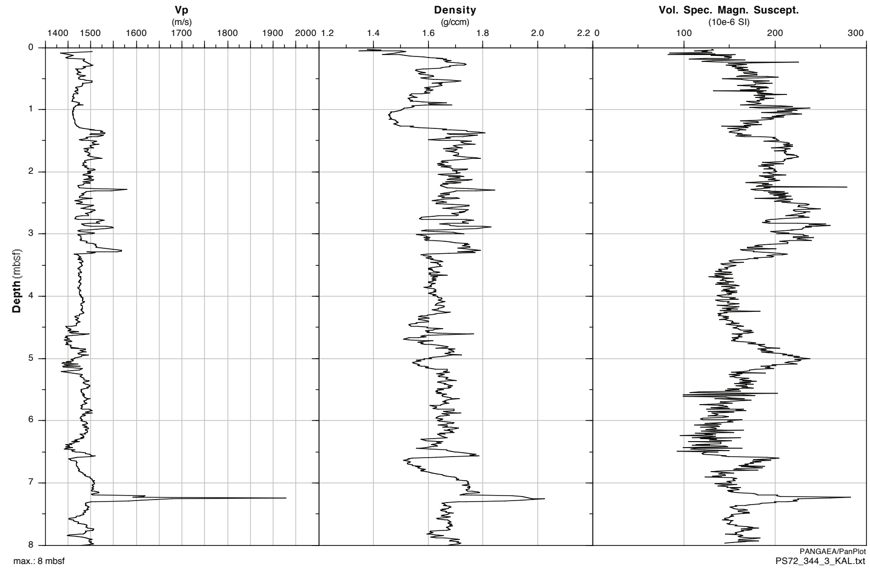
Vp
(m/s)
Density
(g/ccm)
Vol. Spec. Magn. Suscept.
(10e-6 SI)
Depth (mbsf)
max.: 8 mbsf
PANGAEA/PanPlot
PS72_344_3_KAL.txt

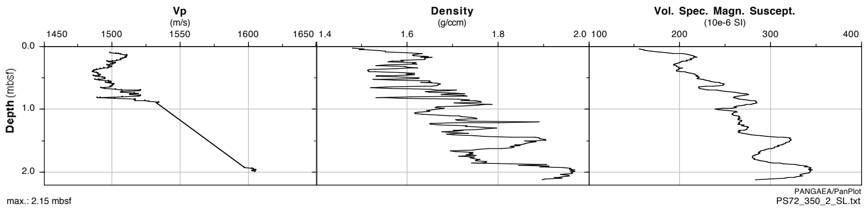
Vp
(m/s)
Density
(g/ccm)
Vol. Spec. Magn. Suscept.
(10e-6 SI)
Depth (mbsf)
max.: 2.15 mbsf
PANGAEA/PanPlot
PS72_350_2_SL.txt

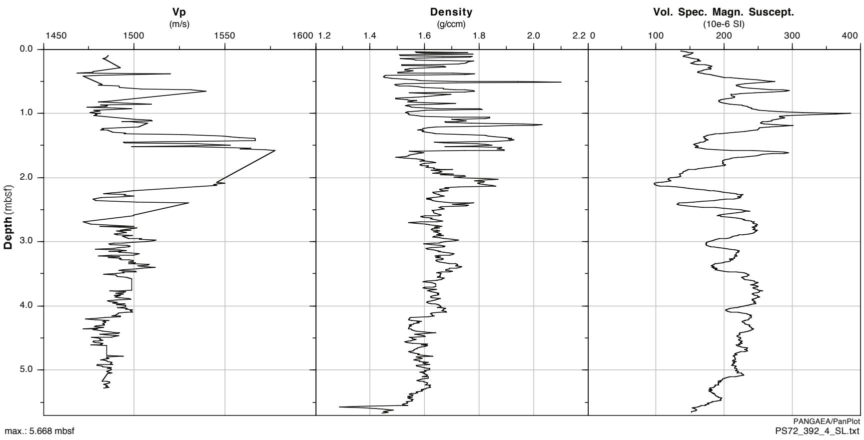
Vp
(m/s)
Density
(g/ccm)
Vol. Spec. Magn. Suscept.
(10e-6 SI)
Depth (mbsf)
max.: 5.668 mbsf
PANGAEA/PanPlot
PS72_392_4_SL.txt

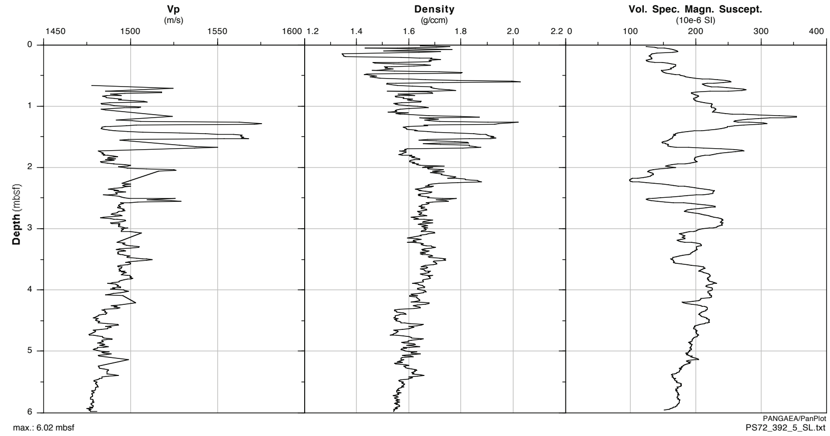

Vp
(m/s)
Density
(g/ccm)
Vol. Spec. Magn. Suscept.
(10e-6 SI)
Depth (mbsf)
max.: 6.02 mbsf
PANGAEA/PanPlot
PS72_392_5_SL.txt

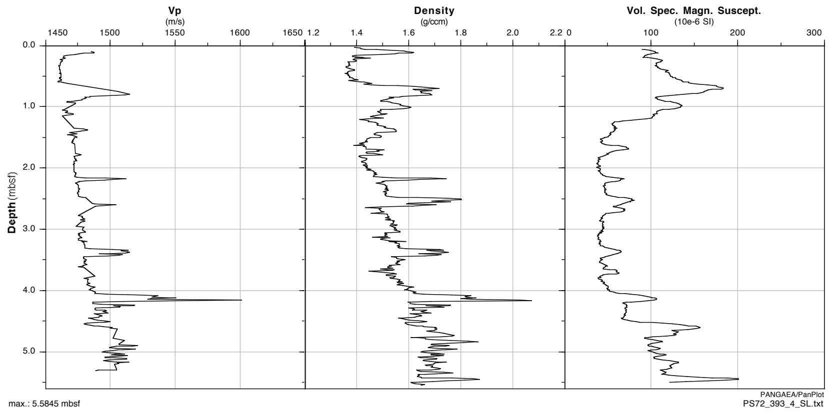

Vp
(m/s)
Density
(g/ccm)
Vol. Spec. Magn. Suscept.
(10e-6 SI)
Depth (mbsf)
max.: 5.5845 mbsf
PANGAEA/PanPlot
PS72_393_4_SL.txt

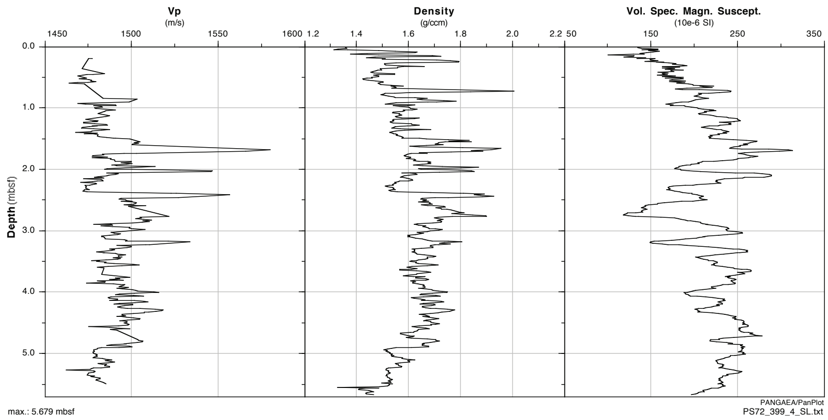

Vp
(m/s)
Density
(g/ccm)
Vol. Spec. Magn. Suscept.
(10e-6 SI)
Depth (mbsf)
max.: 5.679 mbsf
PANGAEA/PanPlot
PS72_399_4_SL.txt

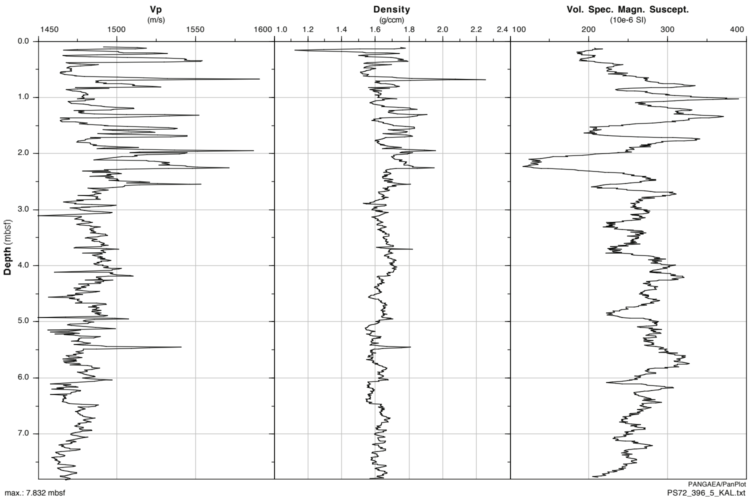
Vp
(m/s)
Density
(g/ccm)
Vol. Spec. Magn. Suscept.
(10e-6 SI)
Depth (mbsf)
PANGAEA/PanPlot
max.: 7.832 mbsf
PS72_396_5_KAL.txt

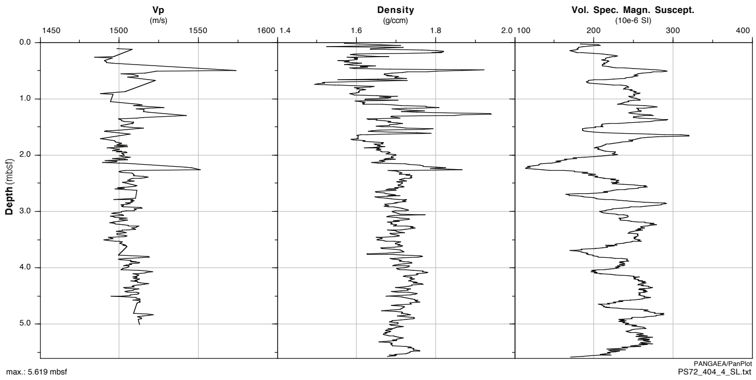
Vp
(m/s)
Density
(g/ccm)
Vol. Spec. Magn. Suscept.
(10e-6 SI)
Depth (mbsf)
PANGAEA/PanPlot
max.: 5.619 mbsf
PS72_404_4_SL.txt

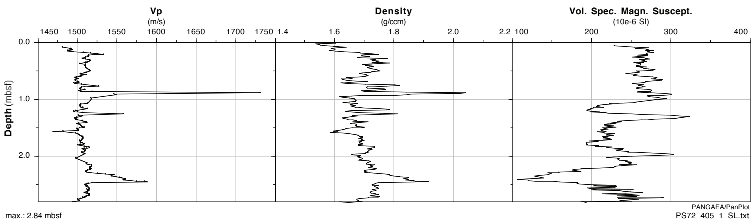
Vp
(m/s)
Density
(g/ccm)
Vol. Spec. Magn. Suscept.
(10e-6 SI)
Depth (mbsf)
PANGAEA/PanPlot
max.: 2.84 mbsf
PS72_405_1_SL.txt

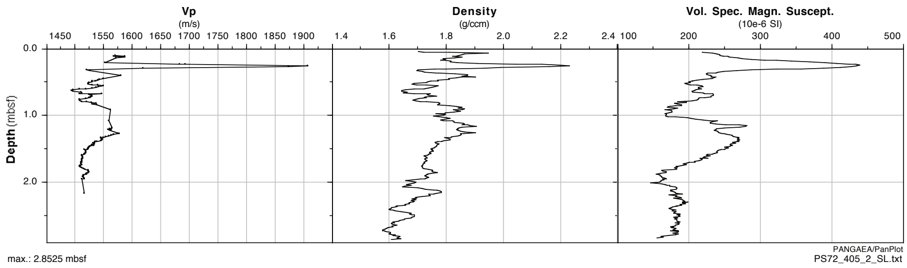
Vp
(m/s)
Density
(g/ccm)
Vol. Spec. Magn. Suscept.
(10e-6 SI)
Depth (mbsf)
max.: 2.8525 mbsf
PANGAEA/PanPlot
PS72_405_2_SL.txt

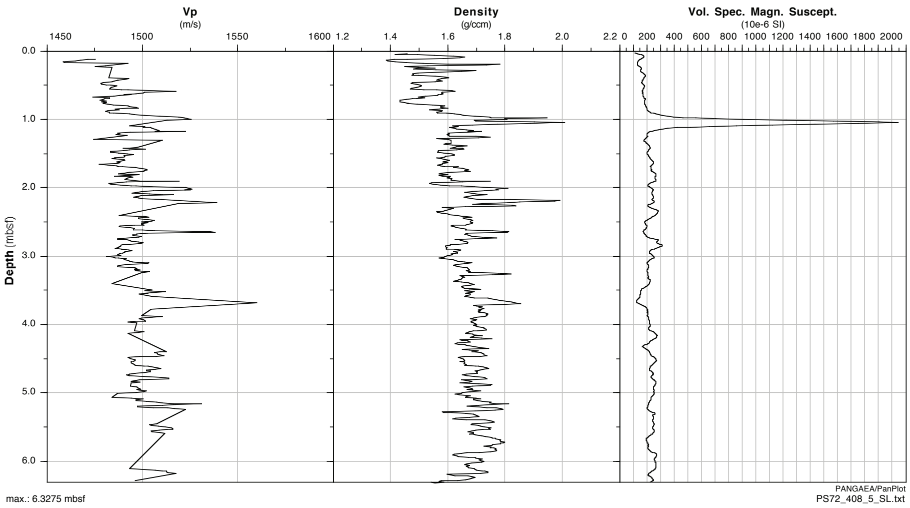
Vp
(m/s)
Density
(g/ccm)
Vol. Spec. Magn. Suscept.
(10e-6 SI)
Depth (mbsf)
max.: 6.3275 mbsf
PANGAEA/PanPlot
PS72_408_5_SL.txt

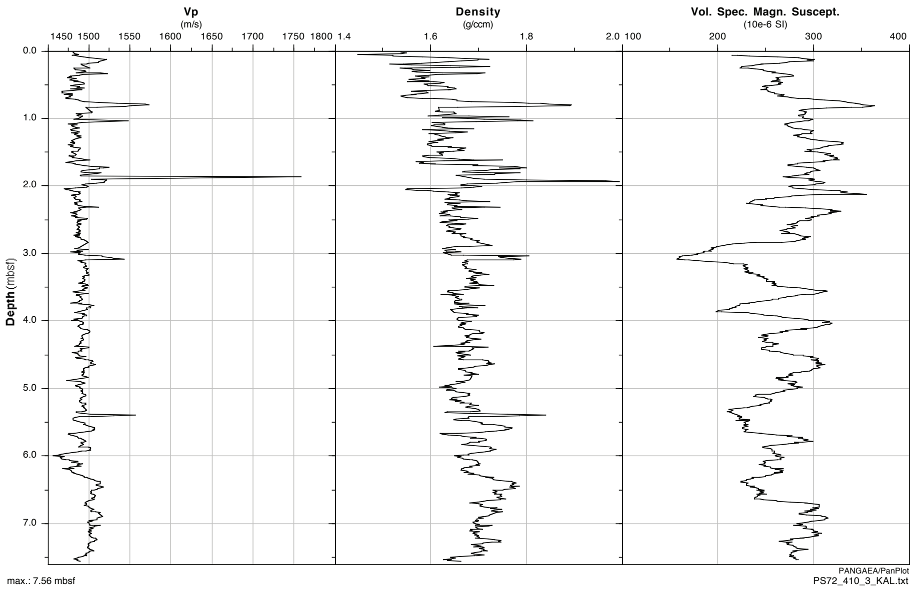
Vp
(m/s)
Density
(g/ccm)
Vol. Spec. Magn. Suscept.
(10e-6 SI)
Depth (mbsf)
max.: 7.56 mbsf
PANGAEA/PanPlot
PS72_410_3_KAL.txt

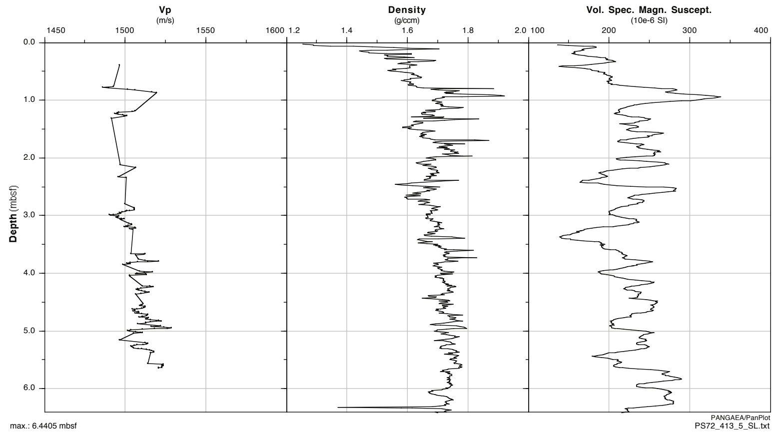
Vp
(m/s)
1450 1500 1550 1600
Density
(g/ccm)
1.2 1.4 1.6 1.8 2.0
Vol. Spec. Magn. Suscept.
(10e-6 SI)
100 200 300 400
Depth (mbsf)
0.0 1.0 2.0 3.0 4.0 5.0 6.0
max.: 6.4405 mbsf
PANGAEA/PanPlot
PS72_413_5_SL.txt

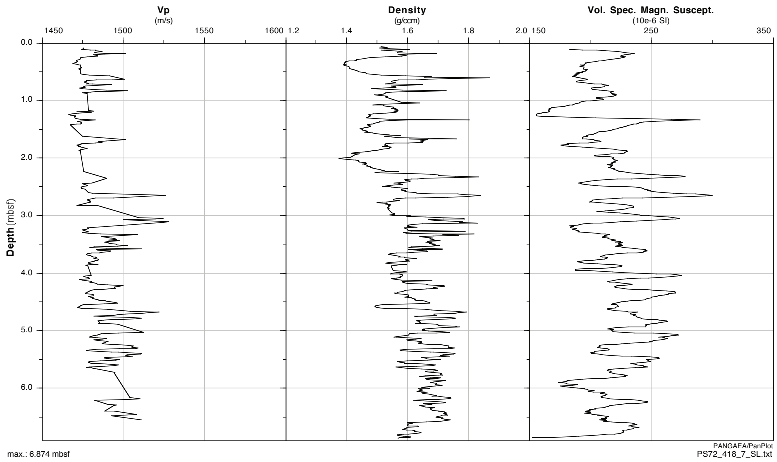
Vp
(m/s)
1450 1500 1550 1600
Density
(g/ccm)
1.2 1.4 1.6 1.8 2.0
Vol. Spec. Magn. Suscept.
(10e-6 SI)
150 250 350
Depth (mbsf)
0.0 1.0 2.0 3.0 4.0 5.0 6.0
max.: 6.874 mbsf
PANGAEA/PanPlot
PS72_418_7_SL.txt

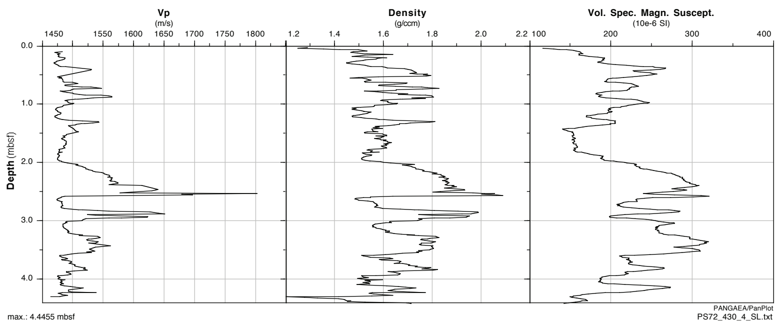
Vp
(m/s)
1450 1550 1600 1650 1700 1750 1800
Density
(g/ccm)
1.2 1.4 1.6 1.8 2.0 2.2
Vol. Spec. Magn. Suscept.
(10e-6 SI)
100 200 300 400
Depth (mbsf)
0.0 1.0 2.0 3.0 4.0
max.: 4.4455 mbsf
PANGAEA/PanPlot
PS72_430_4_SL.txt

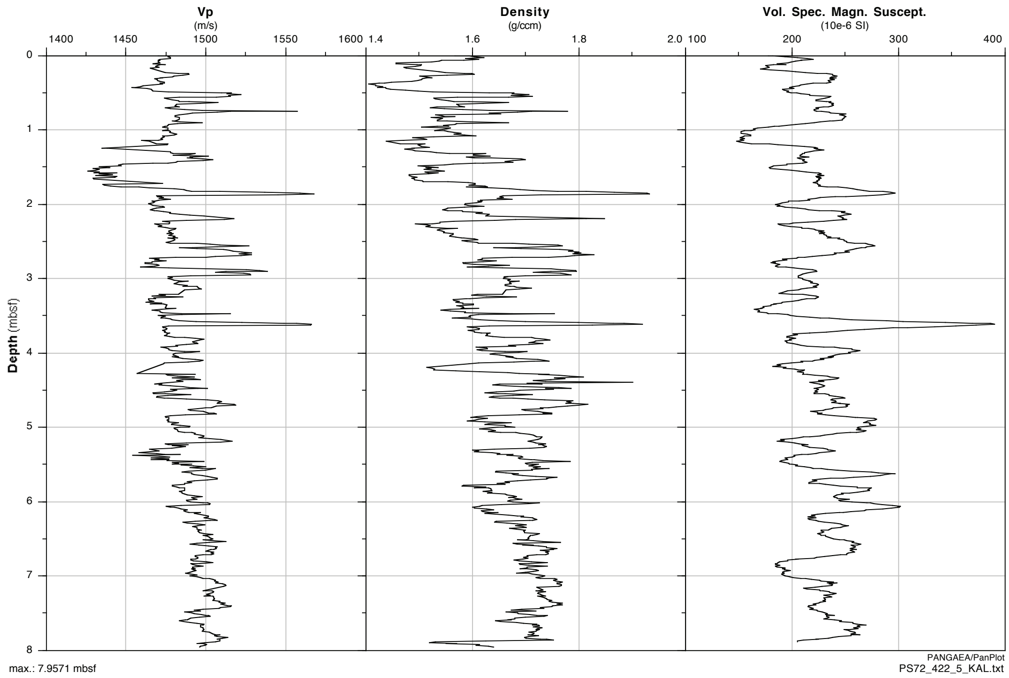
Vp
(m/s)
1400 1450 1500 1550 1600
Density
(g/ccm)
1.4 1.6 1.8 2.0
Vol. Spec. Magn. Suscept.
(10e-6 SI)
100 200 300 400
Depth (mbsf)
0 1 2 3 4 5 6 7 8
PANGAEA/PanPlot
max.: 7.9571 mbsf
PS72_422_5_KAL.txt

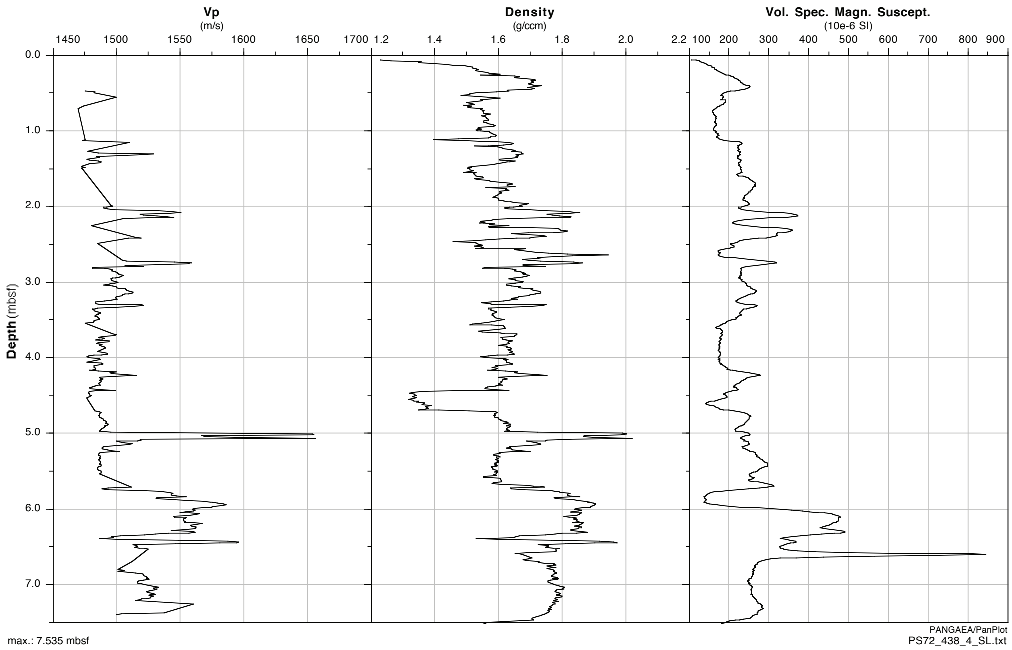
Vp
(m/s)
1450 1500 1550 1600 1650 1700
Density
(g/ccm)
1.2 1.4 1.6 1.8 2.0 2.2
Vol. Spec. Magn. Suscept.
(10e-6 SI)
100 200 300 400 500 600 700 800 900
Depth (mbsf)
0.0 1.0 2.0 3.0 4.0 5.0 6.0 7.0
PANGAEA/PanPlot
max.: 7.535 mbsf
PS72_438_4_SL.txt

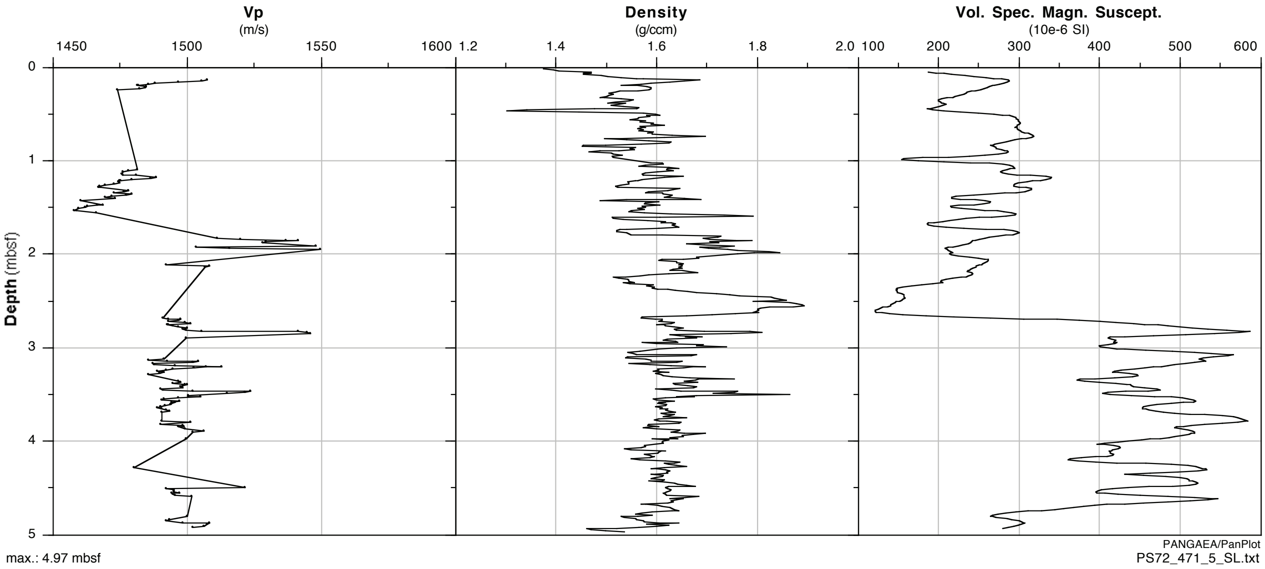
Vp
(m/s)
1450
1500
1550
1600
Density
(g/ccm)
1.2
1.4
1.6
1.8
2.0
Vol. Spec. Magn. Suscept.
(10e-6 SI)
100
200
300
400
500
600
Depth (mbsf)
0
1
2
3
4
5
max.: 4.97 mbsf
PANGAEA/PanPlot
PS72_471_5_SL.txt

A.5 SEABIRDS AND MARINE MAMMALS

greater shearwater cj

fulmar light cj

kittiwake cj

kittiwakes on iceberg 1 cj

kittiwakes on iceberg 2 cj

ivory gull cj

bowhead cj

fin whale cj

polar bear cj

polar bear + pup cj

ringed seal cj

A.6 STATION LIST

Station PS72	Date/Time	Latitude	Longitude	Elevation	Device	Comment
284-1	2008-08-13T16:23	62,9173	-28,5907	-1847	Profile sampling	end
284-1	2008-08-13T14:54	62,9172	-28,5951	-1846	Profile sampling	start
285-1	2008-08-19T16:35	72,3482	-64,8136	-2370	Expendable CTD	
286-1	2008-08-19T16:46	72,3653	-64,9036	-2376	Expendable CTD	
287-1	2008-08-21T12:58	74,266	-90,9856	-353	Boomerang-Grab	
287-2	2008-08-21T13:31	74,2657	-90,9844	-352	MultiCorer	
287-3	2008-08-21T14:16	74,266	-90,9852	-353	Gravity corer	
287-4	2008-08-21T15:11	74,266	-90,985	-352	Gravity corer	
288-1	2008-08-23T21:15	74,7854	-120,536	-485	Profile sampling	end
288-1	2008-08-23T19:36	74,7869	-120,4904	-487	Profile sampling	start
289-1	2008-08-25T13:00	75,1098	-136,5847	-3533	Giant box corer	
289-2	2008-08-25T14:52	75,1129	-136,5808	-3533	Kasten corer	
290-1	2008-08-25T17:45	75,1063	-137,0314	-3526	Multiple closing net	
290-2	2008-08-25T18:26	75,1082	-137,0209	-3525	CTD/Rosette	
291-1	2008-08-27T13:48	71,2692	-137,1802	-1548	Giant box corer	
291-2	2008-08-27T14:53	71,2697	-137,1803	-1549	Kasten corer	
292-1	2008-08-28T06:06	73,3008	-142,5922	-3648	Expendable CTD	
293-1	2008-08-28T09:03	73,605	-144,1458	-3712	Expendable CTD	
294-1	2008-08-28T12:06	73,9206	-145,7881	-3806	Expendable CTD	
295-1	2008-08-28T15:03	74,225	-147,41	-3835	Expendable CTD	
296-1	2008-08-28T18:04	74,511	-148,958	-3883	Expendable CTD	
297-1	2008-08-28T20:58	74,8059	-150,5686	-3904	Expendable CTD	
298-1	2008-08-29T00:02	75,1122	-152,2874	-3916	Expendable CTD	
299-1	2008-08-29T02:57	75,4142	-154,0135	-3920	Expendable CTD	
300-1	2008-08-29T05:56	75,7179	-155,787	-2862	Expendable CTD	
301-1	2008-08-29T09:01	76,0246	-157,6147	-609	Expendable CTD	
302-1	2008-08-29T12:06	76,2363	-159,6295	-2115	Expendable CTD	
303-1	2008-08-29T14:57	76,6043	-161,1806	-2182	Expendable CTD	
304-1	2008-08-29T18:00	76,8754	-162,8543	-1755	Expendable CTD	
305-1	2008-08-29T20:51	76,9138	-162,8437	-1747	Profile sampling	end
305-1	2008-08-29T19:20	76,9152	-162,8339	-1743	Profile sampling	start
306-1	2008-08-29T20:59	76,9097	-162,8406	-1635	Expendable CTD	
307-1	2008-08-29T23:47	77,0664	-164,121	-423	Expendable CTD	
308-1	2008-08-30T00:39	77,0872	-164,1464	-423	Multiple closing net	
308-2	2008-08-30T01:14	77,0924	-164,1459	-418	CTD/Rosette	
309-1	2008-08-30T03:03	77,2072	-164,9127	-432	Expendable CTD	
310-1	2008-09-04T05:00	77,5839	-171,5716	-2344	Seismic reflection profile	end
310-1	2008-08-30T04:18	77,2932	-165,214	-360	Seismic reflection profile	start
311-1	2008-08-30T05:58	77,3507	-165,8198	-728	Expendable CTD	
312-1	2008-08-30T09:02	77,4778	-166,7285	-706	Expendable CTD	
313-1	2008-08-30T12:00	77,6178	-167,6827	-476	Expendable CTD	
314-1	2008-08-30T15:23	77,7986	-168,7397	-666	Expendable CTD	end
314-1	2008-08-30T15:05	77,7825	-168,6442	-618	Expendable CTD	start
315-1	2008-08-30T18:02	77,9345	-169,5463	-1479	Expendable CTD	
316-1	2008-08-30T21:01	77,958	-170,622	-2406	Expendable CTD	
317-1	2008-08-30T23:57	78,0007	-171,8284	-2302	Expendable CTD	
318-1	2008-08-31T02:58	78,0039	-171,9366	-2300	Expendable CTD	
319-1	2008-08-31T05:59	78,0456	-173,1563	-2072	Expendable CTD	
320-1	2008-08-31T09:00	78,0985	-174,3531	-1921	Expendable CTD	
321-1	2008-08-31T11:58	78,1183	-175,6133	-1550	Expendable CTD	

Station PS72	Date/Time	Latitude	Longitude	Elevat-ion	Device	Comment
322-1	2008-08-31T15:00	78,1669	-176,8447	-957	Expendable CTD	
323-1	2008-08-31T15:03	78,1658	-176,8629	-955	Expendable CTD	
324-1	2008-08-31T17:56	78,2058	-177,9814	-1580	Expendable CTD	
325-1	2008-08-31T20:58	78,2306	-179,2105	-1094	Expendable CTD	
326-1	2008-08-31T23:58	78,2425	179,5604	-1770	Expendable CTD	
327-1	2008-09-01T02:46	78,3037	179,3134	-1802	Expendable CTD	
328-1	2008-09-01T06:07	78,118	178,7929	-1733	Expendable CTD	
329-1	2008-09-01T09:04	78,138	177,9724	-1764	Expendable CTD	
330-1	2008-09-01T12:04	78,1979	176,956	-1848	Expendable CTD	
331-1	2008-09-01T15:09	78,3229	176,0974	-1946	Expendable CTD	
332-1	2008-09-01T18:04	78,4031	175,0486	-1998	Expendable CTD	
333-1	2008-09-01T21:00	78,4049	173,9144	-1930	Expendable CTD	
334-1	2008-09-01T23:54	78,4385	172,9541	-1856	Expendable CTD	
335-1	2008-09-02T02:51	78,2978	172,7393	-1528	Expendable CTD	
336-1	2008-09-02T05:56	78,0792	173,0096	-1278	Expendable CTD	
337-1	2008-09-02T08:57	77,8285	172,9748	-1127	Expendable CTD	
338-1	2008-09-02T12:12	77,6	173,1378	-1109	Expendable CTD	
339-1	2008-09-04T01:28	77,5826	-172,9607	-2135	Boje	
340-1	2008-09-04T05:55	77,5763	-171,521	-2344	Multiple closing net	
340-2	2008-09-04T06:34	77,5804	-171,5317	-2342	CTD/Rosette	
340-3	2008-09-04T07:27	77,5864	-171,542	-2344	Giant box corer	
340-4	2008-09-04T08:43	77,5961	-171,5417	-2345	MultiCorer	
340-5	2008-09-04T10:08	77,6038	-171,4933	-2351	Kasten corer	
341-1	2008-09-04T19:13	77,5975	-176,1096	-1376	Multiple closing net	
341-2	2008-09-04T19:50	77,5998	-176,1093	-1371	CTD/Rosette	
341-3	2008-09-04T20:36	77,6046	-176,1111	-1372	Giant box corer	
341-4	2008-09-04T21:34	77,6134	-176,133	-1398	MultiCorer	
341-5	2008-09-04T22:48	77,5976	-176,1038	-1376	Kasten corer	
342-1	2008-09-05T02:10	77,6006	-177,344	-819	Gravity corer	
343-1	2008-09-05T09:54	77,3042	179,0526	-1226	Gravity corer	
343-2	2008-09-05T11:13	77,3055	179,0459	-1226	Gravity corer	
343-3	2008-09-05T12:12	77,306	179,0472	-1227	Giant box corer	
343-4	2008-09-05T13:08	77,3058	179,0474	-1227	MultiCorer	
344-1	2008-09-05T20:06	77,5997	174,5402	-1265	Giant box corer	
344-2	2008-09-05T21:04	77,6024	174,5441	-1264	MultiCorer	
344-3	2008-09-05T22:17	77,6081	174,5418	-1262	Kasten corer	
345-1	2008-09-05T23:33	77,5663	174,4395	-1250	Expendable CTD	
346-1	2008-09-06T01:04	77,317	174,1021	-1142	Expendable CTD	
347-1	2008-09-06T02:31	77,0688	173,7262	-882	Expendable CTD	
348-1	2008-09-06T03:53	76,8341	173,3774	-499	Expendable CTD	
349-1	2008-09-06T05:27	76,5623	172,9791	-345	Expendable CTD	
350-1	2008-09-06T21:47	74,6699	169,8393	-61	Multiple closing net	
350-2	2008-09-06T22:04	74,67	169,8384	-57	Gravity corer	
350-3	2008-09-06T22:35	74,67	169,8378	-61	Giant box corer	
351-1	2008-09-17T05:00	77,0662	-171,6981	-2318	Seismic reflection profile	end
351-1	2008-09-07T03:06	74,7605	171,2742	-67	Seismic reflection profile	start
352-1	2008-09-07T19:59	75,2915	176,4907	-270	Expendable CTD	
353-1	2008-09-07T22:54	75,3845	177,4245	-383	Expendable CTD	
354-1	2008-09-08T03:13	75,5243	178,8363	-733	Expendable CTD	
355-1	2008-09-08T04:56	75,577	179,3706	-906	Expendable CTD	
356-1	2008-09-08T07:59	75,6712	-179,6655	-1082	Expendable CTD	
357-1	2008-09-08T10:57	75,7669	-178,6787	-1179	Expendable CTD	
358-1	2008-09-08T14:00	75,8642	-177,672	-1178	Expendable CTD	

Station PS72	Date/Time	Latitude	Longitude	Elevation	Device	Comment
359-1	2008-09-08T17:00	75,9622	-176,6511	-1760	Expendable CTD	
360-1	2008-09-08T19:58	76,0741	-175,803	-2116	Expendable CTD	
361-1	2008-09-08T22:56	76,1518	-174,8001	-2253	Expendable CTD	
362-1	2008-09-09T01:58	76,2747	-173,8902	-2284	Expendable CTD	
362-2	2008-09-09T02:05	76,281	-173,8537	-2288	Expendable CTD	
363-1	2008-09-09T05:02	76,3196	-172,8356	-2289	Expendable CTD	
364-1	2008-09-09T07:59	76,3961	-171,8563	-2314	Expendable CTD	
365-1	2008-09-09T10:59	76,3253	-170,8868	-2257	Expendable CTD	
366-1	2008-09-09T14:05	76,3479	-169,7685	-2233	Expendable CTD	
367-1	2008-09-09T16:02	76,3327	-169,0686	-2137	Expendable CTD	
368-1	2008-09-09T18:02	76,316	-168,3458	-1805	Expendable CTD	
369-1	2008-09-09T19:57	76,3002	-167,6483	-1030	Expendable CTD	
370-1	2008-09-09T21:55	76,2833	-166,915	-369	Expendable CTD	
371-1	2008-09-09T23:56	76,2651	-166,148	-471	Expendable CTD	
372-1	2008-09-12T07:57	75,2257	-169,424	-271	Expendable CTD	
373-1	2008-09-12T10:58	75,4254	-170,028	-547	Expendable CTD	
374-1	2008-09-12T14:02	75,6761	-170,3251	-1410	Expendable CTD	
375-1	2008-09-12T16:57	75,9132	-170,8137	-1327	Expendable CTD	
376-1	2008-09-12T19:59	76,1875	-171,2159	-2140	Expendable CTD	
377-1	2008-09-12T22:56	76,4179	-171,7843	-2313	Expendable CTD	
378-1	2008-09-13T21:59	76,443	179,7498	-1197	Expendable CTD	
379-1	2008-09-14T00:57	76,4488	178,599	-1222	Expendable CTD	
380-1	2008-09-14T04:58	76,3911	178,0556	-1200	Expendable CTD	
381-1	2008-09-14T08:01	76,2124	177,2218	-881	Expendable CTD	
382-1	2008-09-14T10:59	76,029	176,3789	-452	Expendable CTD	
383-1	2008-09-14T12:58	75,9101	175,8371	-338	Expendable CTD	
384-1	2008-09-16T03:01	76,4397	-179,5274	-1133	Expendable CTD	
385-1	2008-09-16T06:56	76,7958	-179,0212	-1186	Expendable CTD	
386-1	2008-09-16T11:18	77,0128	-178,8331	-1505	Expendable CTD	
387-1	2008-09-16T15:01	77,0133	-177,3493	-1440	Expendable CTD	
388-1	2008-09-16T18:57	77,0093	-175,7447	-1812	Expendable CTD	
389-1	2008-09-16T23:01	77,0048	-174,0164	-2179	Expendable CTD	
390-1	2008-09-17T03:01	77,0762	-172,4885	-2207	Expendable CTD	
391-1	2008-09-17T08:00	77,2739	-171,6576	-2316	Expendable CTD	
392-1	2008-09-18T13:32	80,465	-158,7619	-3652	Multiple closing net	
392-2	2008-09-18T15:22	80,4629	-158,6762	-3617	CTD/Rosette	
392-3	2008-09-18T14:50	80,4644	-158,6973	-3635	Hand net	
392-4	2008-09-18T18:41	80,4626	-158,8213	-3619	Gravity corer	
392-5	2008-09-18T21:03	80,4663	-158,8397	-3621	Gravity corer	
392-6	2008-09-18T22:59	80,4789	-158,8367	-3669	Giant box corer	
393-1	2008-09-19T05:35	80,7197	-155,4976	-3879	Multiple closing net	
393-2	2008-09-19T06:10	80,7183	-155,4991	-3877	CTD/Rosette	
393-3	2008-09-19T07:30	80,717	-155,5167	-3879	Giant box corer	
393-4	2008-09-19T09:24	80,7213	-155,5478	-3880	Gravity corer	
394-1	2008-09-19T18:07	80,7249	-160,0911	-3674	Expendable CTD	
395-1	2008-09-19T22:16	80,5739	-162,4323	-2739	Expendable CTD	
396-1	2008-09-19T22:43	80,576	-162,4251	-2740	Multiple closing net	
396-2	2008-09-20T00:17	80,5833	-162,4041	-2736	CTD/Rosette	
396-3	2008-09-20T01:58	80,5866	-162,3607	-2731	Giant box corer	
396-4	2008-09-20T03:20	80,5831	-162,3264	-2728	MultiCorer	
396-5	2008-09-20T04:42	80,5778	-162,3179	-2723	Kasten corer	
397-1	2008-09-20T07:13	80,5716	-162,4543	-2744	Seismic reflection profile	
398-1	2008-09-20T12:56	80,5989	-164,852	-3089	Expendable CTD	
399-1	2008-09-20T18:29	80,6359	-166,6844	-3375	Multiple closing net	

Station PS72	Date/Time	Latitude	Longitude	Elevation	Device	Comment
399-2	2008-09-20T19:04	80,6388	-166,702	-3376	CTD/Rosette	
399-3	2008-09-20T20:18	80,6457	-166,7375	-3377	Giant box corer	
399-4	2008-09-20T22:08	80,6579	-166,7762	-3375	Gravity corer	
400-1	2008-09-22T03:16	80,6342	-166,7505	-3376	Ice sample	end
400-1	2008-09-21T01:06	80,666	-166,6704	-3375	Ice sample	start
400-2	2008-09-21T22:19	80,6454	-166,7746	-3374	CTD/Rosette	
401-1	2008-09-22T10:40	80,599	-169,5302	-3385	Seismic reflection profile	end
401-1	2008-09-22T03:46	80,6232	-166,8829	-3377	Seismic reflection profile	start
402-1	2008-09-22T04:51	80,5948	-167,3957	-3378	Expendable CTD	
403-1	2008-09-22T10:23	80,5985	-169,5278	-3387	Expendable CTD	
404-1	2008-09-22T14:11	80,7573	-171,1563	-2184	Multiple closing net	
404-2	2008-09-22T14:48	80,757	-171,1558	-2183	CTD/Rosette	
404-3	2008-09-22T15:44	80,7561	-171,1639	-2181	Giant box corer	
404-4	2008-09-22T17:04	80,7542	-171,1622	-2183	Gravity corer	
405-1	2008-09-22T20:13	80,7017	-171,6288	-2861	Gravity corer	
405-2	2008-09-22T21:49	80,7068	-171,6435	-2723	Gravity corer	
406-1	2008-09-23T12:10	80,5345	-174,1026	-2927	Seismic reflection profile	end
406-1	2008-09-23T02:18	80,6128	-169,5331	-3386	Seismic reflection profile	start
407-1	2008-09-23T08:13	80,5795	-172,4907	-3373	Expendable CTD	
408-1	2008-09-23T14:04	80,5462	-174,6945	-2569	Multiple closing net	
408-2	2008-09-23T15:24	80,5481	-174,676	-2574	CTD/Rosette	
408-3	2008-09-23T16:59	80,5486	-174,669	-2576	Giant box corer	
408-4	2008-09-23T18:38	80,5498	-174,6821	-2578	MultiCorer	
408-5	2008-09-23T20:04	80,5533	-174,7045	-2586	Gravity corer	
409-1	2008-09-23T21:17	80,5479	-174,9034	-2485	Expendable CTD	
410-1	2008-09-23T23:20	80,5096	-175,7408	-1801	Giant box corer	
410-2	2008-09-24T00:33	80,5174	-175,7345	-1828	MultiCorer	
410-3	2008-09-24T01:40	80,5231	-175,7197	-1854	Kasten corer	
411-1	2008-09-24T05:07	80,4547	-176,5555	-2456	Expendable CTD	
412-1	2008-09-24T07:24	80,3561	-177,9053	-1732	Expendable CTD	
413-1	2008-09-24T10:04	80,3011	-178,5488	-1265	Multiple closing net	
413-2	2008-09-24T11:12	80,3117	-178,5546	-1311	CTD/Rosette	
413-3	2008-09-24T13:29	80,2779	-178,5151	-1263	Giant box corer	
413-4	2008-09-24T14:21	80,2839	-178,4999	-1267	MultiCorer	
413-5	2008-09-24T15:17	80,2888	-178,4836	-1274	Gravity corer	
414-1	2008-09-24T16:27	80,3027	-178,6029	-1307	Seismic reflection profile	
415-1	2008-09-24T23:20	80,3752	178,6427	-2053	Seismic reflection profile	end
415-1	2008-09-24T18:46	80,3537	-179,4127	-1734	Seismic reflection profile	start
416-1	2008-09-24T18:57	80,3558	-179,5227	-1761	Expendable CTD	
417-1	2008-09-24T22:32	80,3865	178,8826	-2035	Expendable CTD	
418-1	2008-09-25T00:14	80,3864	178,6572	-2080	Multiple closing net	
418-2	2008-09-25T01:15	80,3887	178,7084	-2051	CTD/Rosette	
418-3	2008-09-25T02:19	80,3896	178,7666	-2046	Giant box corer	
418-4	2008-09-25T03:11	80,3911	178,8005	-2047	Giant box corer	
418-5	2008-09-25T04:12	80,3934	178,8248	-2044	Giant box corer	
418-6	2008-09-25T05:12	80,3959	178,8451	-2043	MultiCorer	
418-7	2008-09-25T06:18	80,4003	178,8609	-2043	Gravity corer	
419-1	2008-09-25T14:34	80,5753	175,6321	-2613	Seismic reflection	end

Station PS72	Date/Time	Latitude	Longitude	Elevation	Device	Comment
					profile	
419-1	2008-09-25T08:13	80,4102	178,7972	-2052	Seismic reflection profile	start
420-1	2008-09-25T10:41	80,4763	177,6074	-2053	Expendable CTD	
421-1	2008-09-25T13:54	80,5553	175,9722	-2418	Expendable CTD	
422-1	2008-09-25T15:32	80,5663	175,737	-2569	Multiple closing net	
422-2	2008-09-25T17:01	80,5557	175,7424	-2556	CTD/Rosette	
422-3	2008-09-25T18:38	80,55	175,7464	-2546	Giant box corer	
422-4	2008-09-25T19:52	80,5468	175,7458	-2540	MultiCorer	
422-5	2008-09-25T21:08	80,5431	175,7448	-2530	Kasten corer	
423-1	2008-09-26T07:15	80,6087	172,1734	-2810	Seismic reflection profile	end
423-1	2008-09-25T23:33	80,5617	175,8408	-2512	Seismic reflection profile	start
424-1	2008-09-26T02:46	80,552	174,1711	-2760	Expendable CTD	
425-1	2008-09-26T02:53	80,5535	174,1101	-2763	Expendable CTD	
426-1	2008-09-26T06:59	80,587	172,2089	-2808	Expendable CTD	
427-1	2008-09-27T04:18	80,9996	165,0074	-2871	Seismic reflection profile	end
427-1	2008-09-26T14:25	80,6082	172,1969	-2811	Seismic reflection profile	start
428-1	2008-09-26T18:53	80,7298	169,9412	-2837	Expendable CTD	
429-1	2008-09-26T23:33	80,8746	167,5068	-2858	Expendable CTD	
430-1	2008-09-27T05:04	81,0017	164,9207	-2875	Multiple closing net	
430-2	2008-09-27T08:17	81,0256	164,7888	-2874	CTD/Rosette	end
430-2	2008-09-27T06:38	81,0112	164,8678	-2872	CTD/Rosette	start
430-3	2008-09-27T09:53	81,0465	164,7447	-2875	Giant box corer	
430-4	2008-09-27T11:23	81,0676	164,7269	-2875	Gravity corer	
431-1	2008-09-28T20:05	80,9808	147,9702	-2466	Seismic reflection profile	end
431-1	2008-09-27T13:39	81,006	164,9784	-2872	Seismic reflection profile	start
432-1	2008-09-27T17:30	81,0001	162,786	-2877	Expendable CTD	
433-1	2008-09-27T22:20	81,0002	160,0711	-2877	Expendable CTD	
434-1	2008-09-28T02:46	81,0001	157,5444	-2837	Expendable CTD	
435-1	2008-09-28T07:16	81,0009	154,9863	-2737	Expendable CTD	
436-1	2008-09-28T11:58	81,0002	152,4269	-2470	Expendable CTD	
437-1	2008-09-28T16:43	81,0002	149,7673	-2553	Expendable CTD	
438-1	2008-09-28T20:54	80,9789	147,9136	-2463	Multiple closing net	
438-2	2008-09-28T22:26	80,9808	147,9586	-2468	CTD/Rosette	
438-3	2008-09-29T00:00	80,9828	147,9957	-2472	Giant box corer	
438-4	2008-09-29T01:20	80,9825	148,0252	-2474	Gravity corer	
439-1	2008-09-29T09:24	81,0335	145,0046	-2046	Seismic reflection profile	end
439-1	2008-09-29T03:21	81,0066	148,0412	-2482	Seismic reflection profile	start
440-1	2008-09-29T05:06	80,9977	147,1703	-2338	Expendable CTD	
441-1	2008-09-29T07:24	80,9946	145,9895	-2173	Expendable CTD	
442-1	2008-09-29T10:14	81,0187	144,9653	-2051	Multiple closing net	
442-2	2008-09-29T10:47	81,0189	144,9894	-2034	Expendable CTD	
442-3	2008-09-29T11:40	81,018	145,0353	-2043	CTD/Rosette	
443-1	2008-09-29T14:55	81,0064	144,5361	-1890	Seismic reflection profile	end
443-1	2008-09-29T12:51	81,0062	145,0659	-2050	Seismic reflection profile	start

Station PS72	Date/Time	Latitude	Longitude	Elevation	Device	Comment
444-1	2008-09-29T15:04	81,0053	144,5451	-1894	Expendable CTD	
445-1	2008-09-29T16:32	80,999	144,0139	-1732	Expendable CTD	
445-2	2008-09-29T16:35	80,9983	144,0091	-1729	Expendable CTD	
446-1	2008-09-29T18:23	80,9826	143,5926	-1639	CTD/Rosette	
447-1	2008-09-29T22:41	80,9889	141,9939	-1613	Seismic reflection profile	end
447-1	2008-09-29T19:30	80,9676	143,5386	-1614	Seismic reflection profile	start
448-1	2008-09-29T20:26	80,9578	143,0665	-1468	Expendable CTD	
449-1	2008-09-29T21:37	80,9636	142,5542	-1496	Expendable CTD	
450-1	2008-09-29T22:13	80,9788	142,2434	-1489	Expendable CTD	
451-1	2008-09-29T23:52	80,9621	141,9771	-1663	Multiple closing net	
451-2	2008-09-30T01:17	80,9684	142,0769	-1623	CTD/Rosette	
452-1	2008-09-30T05:43	81,0618	140,6096	-1396	Seismic reflection profile	end
452-1	2008-09-30T02:38	80,9874	142,1495	-1539	Seismic reflection profile	start
453-1	2008-09-30T03:52	81,0003	141,4983	-1711	Expendable CTD	
454-1	2008-09-30T04:50	81,0468	141,0909	-1694	Expendable CTD	
455-1	2008-09-30T07:41	81,0479	140,5366	-1337	CTD/Rosette	
456-1	2008-09-30T11:35	80,9943	138,995	-1705	Seismic reflection profile	end
456-1	2008-09-30T08:41	81,0439	140,4691	-1323	Seismic reflection profile	start
457-1	2008-09-30T09:29	81,024	140,0521	-1430	Expendable CTD	
458-1	2008-09-30T10:31	81,0075	139,5211	-1539	Expendable CTD	
459-1	2008-09-30T12:27	80,9861	138,9951	-1700	Multiple closing net	
459-2	2008-09-30T13:41	80,9781	139,013	-1701	CTD/Rosette	
460-1	2008-09-30T20:12	81,006	137,4769	-2509	Seismic reflection profile	end
460-1	2008-09-30T14:59	80,9627	138,9991	-1729	Seismic reflection profile	start
461-1	2008-09-30T17:06	81,0763	138,5359	-1858	Expendable CTD	
461-2	2008-09-30T17:12	81,0813	138,4926	-1870	Expendable CTD	
462-1	2008-09-30T18:52	81,0212	138,0446	-2291	Expendable CTD	
463-1	2008-09-30T21:42	80,9997	137,4195	-2512	CTD/Rosette	
463-2	2008-09-30T23:04	80,9952	137,4862	-2494	Multiple closing net	
464-1	2008-10-01T04:24	80,9761	136,8703	-2672	Expendable CTD	
465-1	2008-10-01T07:05	81,0102	136,2561	-3010	Expendable CTD	
466-1	2008-10-01T08:35	81,0129	136,1047	-3039	CTD/Rosette	
467-1	2008-10-01T14:15	81,0792	134,3858	-3772	Seismic reflection profile	end
467-1	2008-10-01T10:36	81,0226	136,0518	-3046	Seismic reflection profile	start
468-1	2008-10-01T15:31	81,0696	134,0133	-3839	Expendable CTD	
469-1	2008-10-01T23:11	81,1391	129,8783	-3959	Expendable CTD	
470-1	2008-10-02T10:26	81,1253	124,9649	-3549	Expendable CTD	
471-1	2008-10-03T08:07	81,2265	121,2987	-4033	Ice sample	end
471-1	2008-10-03T00:00	81,2361	121,1946	-4220	Ice sample	start
471-2	2008-10-03T00:42	81,2364	121,213	-4241	Multiple closing net	
471-3	2008-10-03T02:53	81,2353	121,2662	-4215	CTD/Rosette	
471-4	2008-10-03T05:09	81,2322	121,3007	-4073	Giant box corer	
471-5	2008-10-03T07:08	81,2288	121,3062	-4039	Gravity corer	
472-1	2008-10-03T15:42	81,2026	121,521	-2474	Dredge, chain bag	end
472-1	2008-10-03T11:11	81,2127	121,4312	-3257	Dredge, chain bag	start

Station PS72	Date/Time	Latitude	Longitude	Elevation	Device	Comment
473-1	2008-10-04T03:27	80,3592	121,3171	-3476	Expendable CTD	
474-1	2008-10-04T11:19	79,6627	118,978	-3286	Expendable CTD	
475-1	2008-10-04T20:57	79,0036	118,0049	-2826	Expendable CTD	
476-1	2008-10-05T00:57	78,5442	117,7898	-2347	Expendable CTD	
476-2	2008-10-05T01:04	78,5396	117,7557	-2334	Expendable CTD	
477-1	2008-10-05T05:51	78,0288	116,8632	-1401	Expendable CTD	
478-1	2008-10-11T12:57	72,0048	14,7167	-1284	MultiCorer	
478-2	2008-10-11T13:46	72,0043	14,7188	-1287	MultiCorer	
478-3	2008-10-11T14:34	72,0045	14,7197	-1286	MultiCorer	
478-4	2008-10-11T15:24	72,0046	14,7195	-1289	MultiCorer	

Die "Berichte zur Polar- und Meeresforschung" (ISSN 1866-3192) werden beginnend mit dem Heft Nr. 569 (2008) ausschließlich elektronisch als Open-Access-Publikation herausgegeben. Ein Verzeichnis aller Hefte einschließlich der Druckausgaben (Heft 377-568) sowie der früheren **"Berichte zur Polarforschung** (Heft 1-376, von 1982 bis 2000) befindet sich im Internet in der Ablage des electronic Information Center des AWI (**ePIC**) unter der URL http://epic.awi.de. Durch Auswahl "Reports on Polar- and Marine Research" auf der rechten Seite des Fensters wird eine Liste der Publikationen in alphabetischer Reihenfolge (nach Autoren) innerhalb der absteigenden chronologischen Reihenfolge der Jahrgänge erzeugt.

To generate a list of all Reports past issues, use the following URL: http://epic.awi.de and select the right frame to browse "Reports on Polar and Marine Research". A chronological list in declining order, author names alphabetical, will be produced, and pdf-icons shown for open access download.

Verzeichnis der zuletzt erschienenen Hefte:

Heft-Nr. 584/2008 — "Russian-German Cooperation SYSTEM LAPTEV SEA: The Expedition Lena - New Siberian Islands 2007 during the International Polar Year 2007/2008", edited by Julia Boike, Dmitry Yu. Bolshiyanov, Lutz Schirrmeister and Sebastian Wetterich

Heft-Nr. 585/2009 — "Population dynamics of the surf clams *Donax hanleyanus* and *Mesodesma mactroides* from open-Atlantic beaches off Argentina", by Marko Herrmann

Heft-Nr. 586/2009 — "The Expedition of the Research Vessel 'Polarstern' to the Antarctic in 2006 (ANT-XXIII/7)", edited by Peter Lemke

Heft-Nr. 587/2009 — "The Expedition of the Research Vessel 'Maria S. Merian' to the Davis Strait and Baffin Bay in 2008 (MSM09/3), edited by Karsten Gohl, Bernd Schreckenberger, and Thomas Funck

Heft-Nr. 588/2009 — "Selected Contributions on Results of Climate Research in East Germany (the former GDR)", edited by Peter Hupfer and Klaus Dethloff

Heft-Nr. 589/2009 — "The Expedition of the Research Vessel 'Polarstern' to the Arctic in 2008 (ARK-XXIII/1)", edited by Gereon Budéus

Heft-Nr. 590/2009 — "The Expedition of the Research Vessel 'Polarstern' to the Arctic in 2008 (ARK-XXIII/2)", edited by Gerhard Kattner

Heft-Nr. 591/2009 — "The Expedition of the Research Vessel 'Polarstern' to the Antarctic in 2008 (ANT-XXIV/4)", edited by Andreas Macke

Heft-Nr. 592/2009 — "The Expedition of the Research Vessel 'Polarstern' to the Antarctic in 2007 (ANT-XXIV/1)", edited by Sigrid Schiel

Heft-Nr. 593/2009 — "The Campaign MELTEX with Research Aircraft 'POLAR 5' in the Arctic in 2008", edited by Gerit Birnbaum, Wolfgang Dierking, Jörg Hartmann, Christof Lüpkes, André Ehrlich, Thomas Garbrecht, and Manuel Sellmann

Heft-Nr. 594/2009 — "The Expedition of the Research Vessel 'Polarstern' to the Antarctic in 2008 (ANT-XXV/1)", edited by Gerhard Kattner and Boris Koch

Heft-Nr. 595/2009 — "The Expedition of the Research Vessel 'Polarstern' to the Antarctic in 2008/2009 (ANT-XXV/2)", edited by Olaf Boebel

Heft-Nr. 596/2009 — "Crustal evolution of the submarine plateaux of New Zealand and their tectonic reconstruction based on crustal balancing", by Jan Werner Gerhard Grobys

Heft-Nr. 597/2009 — "The Expedition of the Research Vessel "Polarstern" to the Arctic in 2008 (ARK-XXIII/3)", edited by Wilfried Jokat